FTD-MT-24-384-67

AD 684023

FOREIGN TECHNOLOGY DIVISION

THEORY OF SOLID FUEL ROCKET ENGINES

by

Ya. M. Shapiro, G. Yu. Mazing and N. Ye. Prudnikov

D D C
MAR 25 1969
D

Distribution of this document is unlimited. It may be released to the Clearinghouse, Department of Commerce, for sale to the general public.

Reproduced by the
CLEARINGHOUSE
for Federal Scientific & Technical
Information Springfield Va. 22151

274

FTD-MT- 24-384-67

EDITED MACHINE TRANSLATION

THEORY OF SOLID FUEL ROCKET ENGINES

By: Ya. M. Shapiro, G. Yu. Mazing and N. Ye. Prudnikov

English pages: 261

TM8500590

THIS TRANSLATION IS A RENDITION OF THE ORIGINAL FOREIGN TEXT WITHOUT ANY ANALYTICAL OR EDITORIAL COMMENT. STATEMENTS OR THEORIES ADVOCATED OR IMPLIED ARE THOSE OF THE SOURCE AND DO NOT NECESSARILY REFLECT THE POSITION OR OPINION OF THE FOREIGN TECHNOLOGY DIVISION.	PREPARED BY: TRANSLATION DIVISION FOREIGN TECHNOLOGY DIVISION WP-AFB, OHIO.

FTD-MT- 24-384-67

Date 26 Feb 19 68

ACCESSION for
NTIS WHITE SECTION
DDC BUFF SECTION
UNANNOUNCED
JUSTIFICATION
BY
DISTRIBUTION/AVAILABILITY CODES
DIST. AVAIL. and/or SPECIAL
1

This document is a machine translation of Russian text which has been processed by the AN/GSQ-16(XW-2) Machine Translator, owned and operated by the United States Air Force. The machine output has been post-edited to correct for major ambiguities of meaning, words missing from the machine's dictionary, and words out of the context of meaning. The sentence word order has been partially rearranged for readability. The content of this translation does not indicate editorial accuracy, nor does it indicate USAF approval or disapproval of the material translated.

BEST

AVAILABLE

COPY

Shapiro Ya. M., Mazing G. Yu., Prudnikov N. Ye.

TEORIYA RAKETNOGO DVIGATELYA NA TVERDOM TOPLIVYE

Voyennoye Izdatel'stvo
Ministerstva Oborony SSSR
Moskva — 1966

256 pages

FTD-HT-24-384-67

DATA HANDLING PAGE

01-ACCESSION NO. TM8500590	02-DOCUMENT LOC	20-TOPIC TAGS solid fuel, rocket engine, thrust chamber, gas flow, rocket technology, solid propellant engine, solid rocket propellant system, thermal oxidation
03-TITLE THEORY OF SOLID FUEL ROCKET ENGINES		
41-SUBJECT AREA 21		

42-AUTHOR/CO-AUTHORS SHAPIRO, YA. M.;/6MAZING, G. YU. PRUDNIKOV, N. YE.	10-DATE OF INFO -----66
43-SOURCE TEORIYA RAKETNOGO DVIGATELYA NA TVERDOM TOPLIVE. MOSCOW VOYENNOYE IZD-VO MINISTERSTVA OBORONY SSSR (RUSSIAN)	66-DOCUMENT NO. FTD-MT-24-384-67
	69-PROJECT NO. 6040104

63-SECURITY AND DOWNGRADING INFORMATION UNCL, 0		64-CONTROL MARKINGS NONE	97-HEADER CLASN UNCL
76-REEL/FRAME NO. 1884 0742	77-SUPERSEDES	78-CHANGES	40-GEOGRAPHICAL AREA US, UR	NO. OF PAGES 261
CONTRACT NO. 94-00	X REF ACC. NO. 65-AM7013009	PUBLISHING DATE	TYPE PRODUCT Translation	REVISION FREQ None
STEP NO. 02 UR/0000/66/000/000/0001/0256			ACCESSION NO. TM8500590	

ABSTRACT

This is a basic text on rocket fuels intended for specialists and engineers. Basic data is drawn from U. S. rocket technology. Covered in the text are: 1) basic fundamentals of rocket fuels, composition, caloricity; 2) progressive burn characteristics; 3) gas flow equations, pressure characteristics; 4) engine tuning; 5) heat shielding; and 6) thrust chamber and atmospheric dependences.

TABLE OF CONTENTS

Introduction v

Chapter I. Solid Rocket Fuels 1

§ 1.1. Basic Requirements for Solid Rocket Fuels and Their Classification 1
§ 1.2. Ballistite Fuels 3
§ 1.3. Combustible Substance of Solid Composite Rocket Fuels 6
§ 1.4. Oxidizers of Solid Composite Rocket Fuels 8
§ 1.5. Compositions of Composite Fuels 11
§ 1.6. Basic Power Characteristics of Solid Rocket Fuels .. 18
§ 1.7. Enthalpy Method of Calculation of Power Characteristics of Solid Rocket Fuels 20
§ 1.8. Calculation of Caloricity of Fuel by the Method of DePauw 26
§ 1.9. Example of Calculation of Power Characteristics of a Double-Base Solid Fuel 28

Literature 32

Chapter II. Charges Used in RDTT and Their Progression Characteristics 34

§ 2.1. General Characteristics of a Charge Form 34
§ 2.2. Single-Channel Unclad Cylindrical Grain Charge (Tubular Charge) 38
§ 2.3. Slot Charge with External Clad Surface 40
§ 2.4. Charge with Star-Shaped Channel Section Burning from Within 46
§ 2.5. A Charge Made from Two Fuels with Different Burn Rates 58

Literature 63

Chapter III. Working Characteristic of RDTT 64

§ 3.1. Parameters of Gas from RDTT Nozzle 64
§ 3.2. Change of Parameters of Gas Flow in Thrust Chamber . 71

§ 3.3. Reaction Force (Thrust) 74
§ 3.4. Pulse of Reactive Force. Unit Pulse 81
§ 3.5. Dependence of Unit Pulse on Form of Nozzle and Pressure in Engine Chamber 84
§ 3.6. Outflow of Gas Containing Solid Particles 88
§ 3.7. Calculation of Parameters of Outflow of Gases with the Aid of Tables of Gas Dynamic Functions 91

Literature 94

Chapter IV. Basic Problem of Internal Ballistics of RDTT 96

§ 4.1. Speed of Burning of Solid Rocket Fuels 96
§ 4.2. Influence of Speed of Gas Flow On Speed of Burning of Fuel 106
§ 4.3. Basic Equations of Internal Ballistics of RDTT 109
§ 4.4. Solution of Basic Problem of Internal Ballistics of RDTT When Parameters $\sigma(\psi)$, $\phi(\varkappa)$ and $\chi(\psi)$ are Constant 111
§ 4.5. Determination of Maximum (Limiting) Pressure 114
§ 4.6. Sensitivity of p_{max} to Parameter of Loading Pressure Stability 120
§ 4.7. Method of Construction of the Curve of Pressure for a Constant Value $B(\psi)$ 123
§ 4.8. Character of Growth of Pressure Curve Under Different Loading Conditions 129
§ 4.9. Determination of Pressure in the Chamber of an Engine with Variable Parameter $B(\psi)$ 130
§ 4.10. Outflow After Termination of Burning of Fuel 132
§ 4.11. Change of Temperature of Gases in the Chamber 135
§ 4.12. Unstable (Anomalous) Burning of Rocket Charges 142
§ 4.13. Vibration Burning 147
§ 4.14. Ignition of Rocket Charge 151

Literature 154

Chapter V. Tuning RDTT 157

§ 5.1. Scattering of Thrust Characteristic of RDTT and the Means of Decreasing It 157
§ 5.2. Influence of Initial Charge Temperature on Basic Ballistic Parameters of Uncontrolled RDTT 159
§ 5.3. Tuning the Nozzle of RDTT for Constant Pressure ... 166
§ 5.4. Tuning the Nozzle of RDTT for Constant Thrust 169
§ 5.5. Basic Diagrams of Devices for Change of Critical Section of a Nozzle 174

Literature 178

Chapter VI. Thermal Shielding of RDTT 179

§ 6.1. Transmission of Heat from Gas to Engine Wall 179
§ 6.2. Propagation of Heat in the Wall of an Engine 189
§ 6.3. Coefficient of Thermal Losses in a Rocket Chamber . 192
§ 6.4. Construction Materials for the Body of an RDTT 196
§ 6.5. Maximum Time of Work of an Engine Without Thermal Insulation 198

§ 6.6. Basic Types of Heat Shield Coverings Utilized in RDTT 201

§ 6.7. Design of Refractory Thermal Insulation Coverings (Passive Thermal Shielding) 206
§ 6.8. Design of a Sublimable Covering 212
§ 6.9. Design of Carbonizing Plastic Thermal Coverings ... 217
§ 6.10. Heat Shielding of the Nozzle of an RDTT 225

Literature 231

Chapter VII. Heat Exchange Between the Atmosphere and Rocket Before Starting the Engine 234

§ 7.1. Coefficient of Heat Transfer 234
§ 7.2. Temperature Field of the Charge 236
§ 7.3. Influence of Nonuniform Charge Temperature on Ballistic Characteristics of an RDTT 240
§ 7.4. Time of Equalization of the Temperature of the Charge and the Surrounding Medium 242
§ 7.5. Calculation of the Necessary Power of Electroheating of RDTT 250

Literature 254

Appendix 255

U. S. Board on Geographic Names Transliteration System 260

Designations of the Trigonometric Functions 261

The book contains basic information about fuels, charges and materials used in solid fuel rocket engines. In detail the internal ballistics of the engine and the method of design of basic charge types are given. Great attention is allotted to heat shielding and body and charge strength designs. We consider basic questions of test adjustment and operation of the engine.

The book can be a valuable aid for engineers working in the area of rocket technology, and specialists of related areas, and also for students of higher educational institutions.

Examples of calculations are given for hypothetical engines and are of an illustrative character.

Designs for body and charge strength will be given in the book "Fundamentals of Design of Solid Fuel Rockets" by the same authors.[1]

---

[1]This last paragraph appeared in manuscript after errata sheet.

INTRODUCTION

Huge successes in development of rocket technology during the last 10-15 years have made it possible to solve a series of the most complex problems of rocket propulsion and to reach such a noble goal, as conquest of space. The first artificial earth satellite, launched in the Soviet Union on 4 October 1957, announced the beginning of a new space era. Soviet astronauts were the first to lay space routes in the spaciousness of the universe.

Problems being solved by rocket technology are continuously being complicated. This requires development and improvement of all its directions.

According to the variety of solved problems and the width of range of use, solid fuel rocket engines [RDTT] (РДТТ) do not have an equal. It is used in antitank missiles, where the necessary thrust is calculated in several kilograms, and in intercontinental and space rockets, where the necessary thrust is in hundreds and thousands of tons. Basic characteristics of contemporary solid fuel rockets of different classes are given in table 1. RDTT are frequently used for auxiliary goals as a source of working substance for a power unit and liquid pressure feed system and as an effector of a control system etc..

Solid fuel rocket engines as compared to liquid fuel engines possess a whole series of merits. Basic are: – high reliability of action and constant readiness for launching; – simplicity and exploitation and, connected with this, simplicity of ground equipment and a smaller number of maintenance personnel; – possibility of prolonged storage in final equipped form; – smaller, as compared to other rocket engines, cost of manufacture; – possibility of providing a high thrust-to-weight ratio (use as a booster).

To deficiencies of an RDTT pertain: – essential dependence of value of thrust and pressure on initial temperature of charge; – complexity of programming of thrust and pulse control (cutoff of thrust); – high cost of solid fuel (as compared to cost of usual liquid fuels).

For a prolonged time the obstacles to use of an RDTT in guided rockets were its bad weight characteristics and small time of work. These deficiencies were connected with basic, for that time, construction schemes of the engine with a freely inserted charge. With such charging of the engine combustion products touch the body all over its internal surface, leading to intense heating of the body and a lowering of strength characteristics of the material. Ballistite fuels used at that time could stably burn only at relatively high pressures, which led to an overestimate of the design pressure according to which thickness of the wall of the engine was selected. All of this conditioned high values of weight factor α, which is the ratio of weight of construction to weight of fuel. For an engine with a freely inserted charge the value of this coefficient was 0.8-1.25.

The contemporary stage in development of RDTT is connected with the use of composite fuels. Basic properties of these fuels, determining their value for RDTT, are stable burning at relatively low pressures (30-40 kg/cm^2) and the possibility of charging the engine by direct filling in the body. A construction scheme of an engine with fastened charge has appeared. In such an engine the main part of the body surface during burning of the fuel is protected from thermal influence of gases by the whole thickness of the charge. In the new scheme it has been possible to use structural materials with high specific strength σ_B/γ, such as high-strength steel, titanium, aluminum alloys and plastics. Due to this it has been possible to lower the value of coefficient α to 0.1-0.08, and to increase the time of work of the engine to several tens of seconds. On account of new compositions of fuels the value of a unit pulse of RDTT were increased from 180-220 to 245-250 kgs/kg.

In parallel with the creation of new types of solid fuel rockets, theoretical design fundamentals of RDTT have been developed.

At present in domestic and foreign literature questions of general theory of RDTT, basis of their design and application have been widely illuminated.

The authors of the present book have set theirselves the problem of expounding in compressed form basic positions of the theory of RDTT, characteristics of these engines, and also questions of their operation.

The book is designed for engineers working in the area of rocket technology. It may also be useful for specialists working in related areas of technology, and for students of higher educational institutions.

Doctor of technical sciences, professor, deserved worker of science and technology of [RSFSR] (РСФСР) Ya. M. Shapiro wrote § 1.6-1.9 of Chapter I, § 2.1-2.3 of Chapter II, Chapter III, § 4.3-4.11 of Chapter IV.

Candidate of technical sciences, lecturer G. Yu. Mazing wrote § 2.4, 2.5 of Chapter II, § 4.1, 4.2, 4.12-4.14 of Chapter IV,

Basic characteristics of contemporary rockets with solid engines fuel.[1]

No. of order	Name of rocket	Designation and state of development	Type of motor installation	Fuel	Thrust, P, t	Weight, Q, t	Flying range, km	Gauge, m	Length, m
1	"Minuteman" Modification "B"	ICBM (USA)	3-stage rocket with RDTT	Polybutadiene ammonium perchlorate	-	31.3	10,200	2.1	16.9
2	"Titan" 3C	Strategic ballistic shell, USA, in development	5-section RDTT	Synthetic latex (acrylate and acrylonitrile of polybutadiene) + ammonium perchlorate	~318 P_{max} = = 540	125	-	~3.0	23
3	"Polaris" A-1	Ballistic missiles, underwater launching (USA)	1st and 2nd stages RDTT	1st stage, mixed 2nd stage, nitroplastic ballistic	1st stage - 45	13.7	1,200	1.37	8.3
	"Polaris" A-2				2nd stage - 9	14.5	2,800	1.37	8.3
	"Polaris" A-3	Flight tests			-	-	4,600	1.37	8.3
4	"Pershing"	Ballistic missile, tactical-strategic (USA)	1st and 2nd stages RDTT	-	-	6	up to 600	-	10
5	"Nike-Zeus"	Anti-missile for defense against ICBM of average power (USA)	3-stage antiaircraft guided missile with RDTT	-	~200 (booster engine)	9.1	1,600	~1.5	~20
6	"Vickers" "Vigilant"	Anti-tank shell	One RDTT with two thrust stages	-	-	0.012	1.6	0.114	0.9

[1]During composition of the table there were used: M. N. Goncarenko. Rocket and the antirocket problem, izd. DOSAAF, 1962; S. A. Peresada, Zenith guided rockets, edition MO USSR, 1961; "Missiles and Rokets", X, 1959; XV, 1961, VIII, X, XIII, 1963 A. Ye. Tatarchenko, Guided missiles and rockets, edition DOSAAF, 1962.

Chapters V, VI, VII.

Candidate of technical sciences, lecturer N. Ye. Prudnikov has written § 1.1-1.5 of Chapter I.

The authors extend their sincere gratitude to doctor of technical sciences, lecturer M. F. Dyunze, who made a series of useful remarks which were considered by the authors during preparation of the manuscript.

General editing of the book was carried out by Ya. M. Shapiro.

CHAPTER I

SOLID ROCKET FUELS

§ 1.1. Basic Requirements for Solid Rocket Fuels and Their Classification

The composition and quality of a solid rocket propellant to a considerable degree determine the construction and effectiveness of work of a solid fuel rocket engine [RDTT] (РДТТ), and also render a decisive influence on speed and range of a rocket with this engine.

The main requirements presented to a fuel can be formulated by examining the well-known formula for maximum speed of a rocket obtained in 1903 by K. E. Tsiolkovskiy:

$$v_{max} = v_e \ln\left(1 + \frac{\omega}{q}\right),$$

where v_{max} – maximum velocity of a single-stage rocket obtained neglecting atmospheric drag and forces of gravitation; v_e – effective exit velocity of gases from nozzle of engine; ω – propellant weight; q – weight of rocket construction.

The first group of requirements presented to a fuel pertains to power and thermodynamic properties of a fuel and its combustion products. The most important of them are the following:

– high calorific value (caloricity) of the fuel; a fuel with high caloricity make it possible to obtain a large effective exit velocity (unit pulse of an RDTT $I_1 = \frac{v_e}{g}$), and consequently high flight speed of the rocket;

– large specific gravity of fuel; at a given weight of fuel on account of the raised value of specific gravity it is possible to decrease dimensions and weight of the combustion chamber, and also all dimensions of the rocket, and to increase the ratio ω/q and speed of the rocket;

– small molecular weight of combustion products; a decrease of the mean molecular weight of combustion products μ and an increase of the gas constant $\left(R=\frac{R_0}{\mu}\right)$ leads to an increase in exit velocity of the gas; by increasing the content in combustion products of free hydrogen and other substances with a small molecular weight, it is possible to secure this goal;

– stable and regular burning under conditions of low pressures in the combustion chamber; in case of low operating pressures the weight of the combustion chamber drops significantly on account of a decrease of wall thickness; selection of operating pressure in the engine to a considerable measure is determined by fuel factors, its ability to burn at low pressures and at high speeds of gas along the burning surface of the charge; furthermore, the value of design pressure depends on stability of burning of fuel, on the value of possible pressure jumps, on growth of pressure with an increase of charge temperature.

The second group of requirements pertains to conditions of exploitation and to technology of manufacture of the fuel. The most important requirements of this group are:

– sensitivity of the solid fuel to mechanical and thermal pulses should ensure unfailing work of the engine at the time of ignition of the charge and safety in handling;

– physical and chemical properties of the solid fuel have to be stable in different conditions of prolonged storage;

– charges of solid fuel have to be uniform and monotonic in terms of their physical chemistry and ballistic properties;

– products of combustion of a solid fuel have to possess small toxicity and smokelessness during exhaust of gases from the nozzle of the engine;

– a solid fuel should be inexpensive and prepared from noncritical source materials; the technology of manufacture of a fuel should be simple, safe, and economical.

Solid fuels used in rocket technology, in accordance with their composition and physical structure, can be divided into two large classes:

– ballistite, or homogeneous, fuel;[1]

– composite, or heterogeneous, fuel.

Ballistite solid fuels obtained wide propagation in RDTT before the second world war.

During manufacture of ballistite fuels, the basic initial components are nitrates of cellulose, which are plasticized by different solvents which contain a large percentage of active oxygen. In subsequent accounts of fuel of such a form they will be

called ballistite solid fuels.

A new direction in development of rocket fuels, connected with the development of composite fuels, pertains to the period of time after the second world war. Composite fuels constitute a mechanical mixture of organic combustible and inorganic oxidizing substances. As combustible components of composite fuels there usually serve rubber and tar substances of a type of rubber, asphalt, bitumen, organic resin etc.. Such elastic materials of a mixed fuel are simultaneously binders which ensure homogeneity of the mixture and obtaining of a rocket charge with the necessary mechanical properties.

As oxidizers in composite fuels there are used inorganic salts of nitric and chloric acids, rich in oxygen (for example, nitrates and perchlorates of potassium and ammonium).

Mixture compositions consist of noncritical materials, which has essentially expanded the raw material base for production of rocket fuels. For composite fuels it is possible over a wide range to modify the fuel-oxidizer ratio for the purpose of improvement of power characteristics of the fuel.

This circumstance, and also the large specific gravity of composite fuels, their ability to burn at low pressures and simplicity of manufacture of charges (filling of fuel in the chamber of an engine) considerably expanded the possibility of increasing power and ballistic characteristics of RDTT.

§ 1.2. Ballistite Fuels

Ballistite solid fuels constitute homogeneous systems which are plasticized and consolidated nitrates of cellulose. Nitrocellulose is obtained by treatment of cellulose (cotton, cotton down, wood) by a mixture of nitric and sulfuric acids. Depending on conditions of the process there are obtained products of highest or lowest degree of nitration. Nitrates of cellulose with a nitrogen content of 12.0-13.5% is called pyroxylin, and compositions with a nitrogen content of 11.5-12.0%, colloxylin.

In the process of obtaining rocket fuel the formation of plastic and thermoplastic masses of uniform composition and physical chemical properties, i.e., the gelatination process, is ensured by one or another solvent (plasticizer).

One of the basic solvents used in production of ballistite fuels is nitroglycerine.

Nitroglycerine contains a considerable quantity of oxygen which oxidizes the combustible elements in the fuel. Since nitroglycerine is the basic substance in the fuel ensuring the process of burning, then its percentage determines the caloricity of the fuel. Compositions of ballistite solid fuels with a large percentage of nitroglycerine are characterized by high power properties. Thus, for example, the American fuel JPN, with a large content of nitroglycerine (43%), can ensure in RDTT a unit pulse within the limits

of 215-230 kgs/kg.

Besides nitroglycerine, in production of ballistite solid fuels as a solvent there is used nitrodiglycol, which possesses a better gelatinizing ability than nitroglycerine. However, fuels based on nitrodiglycol are characterized by low power factors.

For the purpose of control of power factors in compositions of fuels, solvents dinitrotoluene, nitroguanidine are added. Introduction into the composition of a fuel of nitroguanidine permits obtaining a fuel with low combustion temperature and high gas constant.

To ensure chemical stability of fuel to its composition one can introduce stabilizers which, not acting chemically on nitrates of cellulose and other components of the fuel, connect acid products forming during decomposition of the solid fuel and thereby prevent its progressive autocatalytic decomposition.

As stabilizers there are used diphenylamin and centralite (diethyldiphenyl urea), constituting a hard crystalline substances.

In the composition of a solid fuel there are included also technological additions: chalk, which decreases internal friction of the fuel mass; vaseline and transformer oil, which lower pressure during pressing and improve the process molding.

Finally, solid fuels, as a rule, contain a certain quantity of additives which lower temperatures of burning (dibutylphthalate), decrease burning rate (phlegmatizor camphor) and hygroscopicity (rosin), increase the oxygen balance (inorganic oxidizer).

Compositions and certain characteristics of rocket fuels of the ballistite type are given in Table 1.1.

Production of ballistite fuels starts from the process of solution and mixing of nitrocellulose, nitroglycerine and other ingredients, as a result of which a gelatinous substance will be formed. For giving the fuel the required form the fuel mass is passed through a die and pressed in charges [1]. Squeezed from the casting mould during motion of the plunger, the mass is clamped after the crosspiece of the die around a needle, ensuring formulization in the grain of the axial channel. The external profile of the grain and profile channel are determined by configuration of the needle and die. During pressing the process of gelatination of the fuel mass is finished.

The shown technological process of preparation of the solid fuel ensures high density and homogeneity of the charge structure.

Grains of ballistite fuel can be obtained also by the method of casting [1]. An example of such technology is the process of filling ballistite fuel in the engine of the third stage of the "Minuteman" rocket [10]. After putting a sticky covering on the internal surface of the combustion chamber, the engine is covered with dry grains of nitrocellulose in the form of regular cylinders (dimensions

Table 1.1. Compositions and certain characteristics of ballistite types of rocket fuels [1.3].

Components of solid fuel and characteristics	Ballistite JPN, %	Ballistite JP, %	Ballistite SD, %	Ballistite HES-4016 %	Cordite SC, %	Cordite F, %	Cordite MK-I, %	Cordite M. R., %	Composition ATO, %	Diglycolic powder, %	Composition of BASAF R-61, %	Nitroguanidine powder, %	Slowly burning nitroglycerine powder, %
Nitrocellulose	51,5	52,2	66	54	50	67	37 (13% N)	65,68 (13% N)	64,7 (12% N)	65 (11,3—11,7% N)	64,5 (12,2% N)	40 (11,8—11,9% N)	56,5 (12,2% N)
Nitroglycerine	43	43	25	43	41	22	58	25,53	—	—	—	—	28,0
Dinitroethyleneglycol	—	—	—	—	—	—	—	—	29,3	24—28	34	18	—
Dinitrotoluene	—	—	—	—	—	—	—	—	—	—	—	—	11,0
Nitroguanidine	—	—	—	—	—	—	—	—	—	—	2,2	30,0	—
Diethyl phthalate	3,25	3,5	—	—	—	—	5	—	—	—	—	—	—
Ethylphenylurethane	—	—	—	—	—	—	—	—	—	—	1,4	—	—
Ethyl centralite	1,0	1,25	8,0	3,0	9,0	5,0	—	—	5,0	3—5	—	1,2—4	4,5
Acardite	—	—	—	—	—	—	—	—	0,2	1—5	0,3	1,6—2	—
Potassium sulfate	1,25	—	—	—	—	2,0	—	—	—	1,0	—	1,0	—
Vaseline	—	—	—	—	—	3,0	—	—	—	1,0	—	—	—
Graphite	0,2	—	—	—	—	—	—	—	0,1	1,0	—	0,4	—
Oxides	—	—	—	—	—	—	—	—	0,9	0,5 MgO	0,25	0,3	—
Moisture	—	—	—	—	—	1,0	—	—	—	—	0,9	—	—
Other impurities	0,08	0,1	1	0,1	0,07	—	—	4,45	1,0	0,3	0,35	0,3	0,08
Density γ, kg/dm^3	1,62	1,6	1,59	1,58	1,6	1,58	1,59	1,6	1,56	1,57	1,59	1,6	—
Caloricity Q_m, kcal/kg	1230	1230	—	1260	965	880	970	980	—	—	880	—	880
Combustion temperature, T°K	2900	3160	2170	3090	2535	2340	—	—	—	—	2390	—	2080
Unit pulse I_1, kgs/kg	220	220	—	—	190	—	190	195	—	—	—	—	—
Burning rate in mm/s at p = 70 kg/cm^2, T=20°C	16,5	17	—	14,3	7,8	11,9	9	10,0	—	—	—	—	—
Exponent in law of burning ν	0,69	0,71	—	0,75	0,69	0,73	—	—	—	—	—	—	—
Coefficient of temperature sensitivity $\left[\frac{\partial \ln u}{\partial T}\right]_p$ or D, 1/°C	0,0038	0,005	—	0,041	—	—	—	—	—	—	—	—	—

0.6 × 0.6 mm), which with the aid of a turning attachment are distributed evenly over the walls. After charging, the engine is vacuum treated for 24 hours for removal of traces of moisture. Then through special pipelines the chamber is fed nitrogylycerine with additions which accelerate swelling of the grains. After that there is carried out a 16-day vulcanization of the charge, at a temperature of 48°C and under pressure of compressed air. The process of charging is finished by cooling of the charge for five days. After termination of the process of vulcanization they remove the rods, or cores, with the aid of which the internal channels or cavity of the charge is formed. In view of the well-developed technology and sufficient production capacity of industry, ballistite solid fuels, although they are considered at present less effective than composite fuels, continue to be widely used in solid fuel rocket engines [4].

§ 1.3. Combustible Substance of Solid Composite Rocket Fuels

Combustible binding substances used in composite rocket fuels are presented the following requirement:

– high calorific value in the process of the combustion reaction (per unit volume);

– presence in the combustible material of a high percentage of hydrogen and a low percentage of carbon; fulfillment of the given condition can influence the obtaining of a fuel with a greater unit pulse with a small amount of combustible material in the fuel;

– good binding qualities of the combustible with a relatively low binder content (10-25% total of fuel); this property of the combustible directly influences the necessary strength characteristics of the fuel;

– the critical temperature, at which the fuel becomes fragile whould be low and not exceed the lower limit of the operational temperature range.

Furthermore, during practical application, combustible binding substances have to be characterized by low pressure of vaporization in the liquid phase, high boiling point and low freezing point, and also must possess viscosity at low temperatures and be polymerized during heating 20-100°C or without heating (in the presence of catalysts).

All the enumerated requirements limit the family of combustible binding substances used in the technology of production of composite rocket fuels.

As combustible binding substances in solid rocket propellants organic materials in the form of high-molecular compounds are used: asphastcarbonic, phenol and cellulose resins, formaldehyde rubber, natural and synthetic rubbers, polyethylent etc.. Of the contemporary polymers which possess binding properties, in composite

fuels the most often used are epoxy, polyurethane and polyester resins, polysulfide rubbers, polyvinyls, polyamide, polybutadiene, polyisobutylene and different nitropolymers.

In solid fuels of the type Galsite (Table 1.4) as combustible binder asphalt resin or asphalt oil was used. Alphalt in fuel negatively affects its stability. These fuels possessed also a tendency to plastic deformations even during comparatively small temperature changes. In contrast to the shown composition, fuels on the basis of polysulfide rubbers (thiocols) possess good binding and physical properties. A deficiency of thiocol fuels is the presence in polysulfide of sulfur, which considerably increases the molecular weight of combustion products and thereby decreases the unit pulse (I_1 = 180-200 $\frac{kg\ s}{kg}$). Best characteristics distinguish a fuel based on polyurethane resins and rubbers, in which the unit pulse is higher than for thiocol fuels. Charges based on polyurethanes can be sufficiently elastic even with an 80-percent content of fillers (oxidizer, soot and others). Besides, elasticity of the charges is preserved at low temperatures.

On the basis of high-molecular hydrocarbons, fuels have been developed which possess great stability during prolonged storage and best mechanical characteristics at low temperatures. These fuels are characterized by higher power properties than thiocol fuels [5].

To high-calorie fuels pertain compositions based on butadiene polymer, constituting a synthetic rubber with properties close to natural rubber. Butadiene rubber is well mixed with powdery and liquid ingredients (fillers, accelerators, etc.). On the basis of these rubber polymers there have been created good fuels with very limited application of plasticizer to ensure necessary mechanical properties [6].

Of special interest among butadiene rubber binders is polybutadiene with a terminal carboxyl group. This binding substance is a more improved binder than usual binding substances with respect to ballistic properties and exceeds them with respect to mechanical properties, especially at low temperatures. It also ensures high charge density (specific gravity 1.83 g/cm^3).

In Table 1.2 are given characteristics of composite fuels based on high-energy fuels. These fuels contain perchlorate of ammonium as an oxidizer and powdered aluminum.

Fuels with a high percentage of oxidizer are characterized by high power properties. However such compositions of fuels possess bad casting properties. Therefore is observed tendency for development of combinations in which the combustible materials would contain a high percentage of active oxygen. For example, it is possible to mention a new binder – nitroazole [6], the basis of which is nitrocellulose. In compounds with a plasticizer (solvent) constituting a mixture of two substances, one of which is a weak explosive, nitrocellulose obtains the properties of rubber-like compounds. On the basis of nitroazole is possible the creation of a fuel with an optimum relationship between binder with additions of

Table 1.2. Characteristics of composite rocket fuels based on high-energy fuels [6].

Combustible binding substance	Spec. gr. kg/дm^3	Combustion temperature T°C	Burning rate at 70 [atm (gage)] mm/s	Unit pulse I_1, kgs/kg	
				At 70-1.0 atm	In vacuum[1]
Polybutadiene with terminal carboxyl group	1.83	3204	7.6-17.8	248-252	287-292
Polybutadiene acrylonitrile	1.74	2926	10.2-17.8	239-243	277-288
Polyurethane	1.77	3537	7.6-17.8	244-248	282-287

[1]With coefficient of expansion of nozzle 25:1.

aluminum and crystaline oxidizer (NH_4ClO_4) 40:60. Such a fuel will be characterized by high density and viscosity, and also good elasticity at low temperatures and high strength at raised temperatures.

§ 1.4. Oxidizers of Solid Composite Rocket Fuels

Hard oxidizers for composite rocket fuels are usually mineral substances in crystal form. Most frequently in production of composite fuels potassium and ammonium perchlorates are used, and also potassium, sodium and ammonium nitrates. In certain cases are used organic compounds such as ammonium picrate.

Oxidizers are presented the following basic requirings:

– high content of active oxygen not connected in the form of oxides during decomposition of the oxidizer;

– minimum exothermic effect of formation;

– stability of physical-chemical properties in rated temperature interval and small hygroscopicity;

– absence of toxicity and danger of explosion in production and exploitation, and also small corrosion activity in relation to materials of the engine;

– high thermal stability of oxidizer and compatibility of it with combustible substances in technology of production of the solid

fuel.

To satisfy the enumerated requirements is possible only by correct selection of mixture combinations ensuring the biggest heat emission in the process of burning with the smallest possible molecular weight of combustion products.

In Table 1.3 are given basic properties of inorganic oxidizers.

Ammonium perchlorate NH_4ClO_4 is the basis of contemporary mixture high-energy solid rocket propellants. The given oxidizer is distinguished by low cost, fully satisfactory manufacturability. Fuels on the basis of perchlorate of ammonium are characterized by a high unit pulse (220-250 $\frac{kg\ s}{kg}$).

With a large percentage of ammonium perchlorate in the fuel, gases emanating from the nozzle are smokeless, but in a humid atmosphere they will form a fog containing HCl. A deficiency of ammonium perchlorate is its low stability.

Great attention is given to the possiblility of use of perchlorate of lithium $LiClO_4$ which is a stabler component of fuel and contains more active oxygen (60.1%). This permits one to lower the percentage of perchlorate of lithium in a composite solid fuel to 75% instead of 80%. The given oxidizer is not poisonous and is not dangerous in handling.

The high cost of perchlorate of lithium and high molecular weight of combustion products somewhat limit the use of it as an oxidizer in solid fuel.

Potassium perchlorate $KClO_4$ was one of the first oxidizers which found wide application in composite fuels. It contains a high percentage of free oxygen, but ensures a comparatively small unit pulse (near 180-220 kgs/kg). Perchlorate of potassium at present is replaced by smokeless compositions of ammonium.

Fuels on the basis of nitrate of ammonium NH_4NO_3 satisfactorily burn at small pressures with low speeds of burning, but a unit pulse of these fuels is comparatively small. An advantage of nitrate of ammonium as a component of a solid fuel consists in its very low cost. However the given oxidizer possesses an inclination to phase transitions during a change of temperature, a symptom of which is its swelling and a possibility of the appearance of cracks in the solid fuel charge. Furthermore, nitrate of ammonium is very hygroscopic. For removal of these deficiencies in the composition of the fuel it is recommended to introduce a binding substance which is well polymerized with butadiene (polymer - combustible material) [10]. Viscosity and elasticity of such a substance ensure preservation of the form of a fuel charge made from a mixture of this fuel and nitrate of ammonium, and prevent the appearance in it of cracks during swelling of the oxidizer due to phase transitions.

Table 1.3. Basic properties of inorganic oxidizers [4, 5].

Oxidizer	Chemical formula	Molecular weight	Specific gravity g/cm³	Melting point °C	Heat of formation, kcal/mole	Total amount of oxygen in % weight	Quantity of free oxygen in % weight	Reaction and products of decomposition
Ammonium perchlorate	NH_4ClO_4	117,5	1,95	Decomposes	—69,4 — —78,3	54,4	34,2	$2NH_4ClO_4 \rightarrow N_2 + 2HCl + 3H_2O + 2,5O_2$
Ammonium nitrate	NH_4NO_3	80,05	1,725	170 decomposes	—87,3	60	19,9	$2NH_4NO_3 \rightarrow 4H_2O + 2N_2 + O_2$
Lithium nitrate	$LiNO_3$	68,95	2,88	255	—118,5	69,6	34,81	$4LiNO_3 \rightarrow 2Li_2O + 4NO + 3O_2$
Lithium perchlorate	$LiClO_4$	106,4	2,43	236	—106,13	60,15	60,1	$LiClO_4 \rightarrow LiCl + 2O_2$
Potassium perchlorate	$KClO_4$	138,55	2,52	610	—99,24	46,2	46,2	$KClO_4 \rightarrow KCl + 2O_2$
Potassium nitrate	KNO_3	101,1	2,11	334	—117,76	47,4	23,7	$4KNO_3 \rightarrow 2K_2O + 4NO + 3O_2$
Sodium nitrate	$NaNO_3$	85,01	2,26	307	—106,6	56,4	28,2	$4NaNO_3 \rightarrow 2Na_2O + 4NO + 3O_2$
Lithium nitrate	$LiNO_3$	68,95	2,38	—	—115,3	58,01	—	—
Nitrosyl perchlorate	$2NOClO_4$	—	—	—	—	—	62,1	—
Nitron perchlorate	NO_2ClO_4	—	—	—	—	—	66,7	—

Nitrate of lithium $LiNO_3$ has in its molecule (by weight) more oxygen than perchlorate of lithium, but this oxygen can not wholly be used during the reaction but remains bonded in nitrogen oxide.

Nitrate of lithium is a safe substance in handling and during exploitation.

Ammonium picrate $C_6H_2(NO_2)_3ONH_4$ is one of the few representatives of oxidizers of solid fuels related to the class of organic compounds. By using ammonium picrate in the compositions of fuels as a secondary component, one obtains an oxidizer with a low power factor.

At present there is studied the possibility of use of new oxidizers, perchlorates of nitron NO_2ClO_4 and nitrosyl $2NOClO_4$ [6], containing a great percentage of free oxygen.

To oxidizers possessing higher contents of oxygen and ensuring low molecular weight of combustion products pertain also acyl nitrate and urea nitrate.

§ 1.5. Compositions of Composite Fuels

In composite fuels the relative content of oxidizer and fuel can be changed over comparatively wide limits. However, even for them there exist limitations which prevent achievement of an optimum relationship of these basic components.

Data given in Table 1.4 show that mixed fuels rarely contain more than 80-85% oxidizer. This is explained by the fact that binding and physical properties, and also casting qualities of a solid fuel are completely determined by the combustible. Therefore it is desirable that fuel contain also a large enough quantity of combustible connecting crystal particles of oxidizer.

In Fig. 1.1 are represented calculated thermodynamic characteristics during isobaric burning of a composite fuel in a rocket chamber ($p_K = 70 \frac{kg}{cm^2}$).

An increase of the oxidizer content in the fuel up to the optimum relationship between oxidizer and combustible (stoichiometrical relationship) leads to a considerable increase of combustion temperature, whereas the unit pulse increases considerably slower. In connection with this it is possible to change the contents in the fuel of oxidizer and combustible to one or another side of the stoichiometrical relationship without changing essentially the value of a unit pulse. Thus, for example, the optimum relationship between oxidizers of the type of perchlorate of ammonium and organic fuel by which there is ensured a maximum of unit pulse, is 88:12 (Fig. 1.1). However even at a weight ratio of crystal oxidizer and binder combustible of 80:20, due to the low content of binder in the fuel mass it is not possible to obtain fuel charges of uniform composition with satisfactory physical properties.

Table 1.4. Composition and certain ballistic characteristics of typical composite fuels [4, 7].

Type of solid fuel	Components of solid fuel	% total weight	Specific gravity, g/cm^3	Unit pulse[1] kgs/kg	Combustion temperature °C	Burning rate in mm/s p = 70 atm, T° = 21°C	Exponent ν in law of burning rate	Coefficient of temperature sensitivity $\left[\frac{\partial \ln u}{\partial T}\right]_p$ $\frac{1}{°C}$	Remarks
Galcite Alt-161	I. Potassium perchlorate..	76	1.8	190	1800-2000	36-38	0.70	0.0014	Lower limit of pressure 70 kg/cm^2
	Asphalt oil or asphalt rubber.....	17							
	Lubricating oil.....	7							
	II. Potassium perchlorate..	73	1.77	180-190	2000	20	0.71	-	Lower limit of pressure 50 kg/cm^2
	Polymer combustible (aeroplex)...	27							
EJA[2]	I. Potassium perchlorate..	56	1.84	178	2000	17.5	0.74	-	Lower limit of pressure 25 kg/cm^2
	Nitrocellulose (12.6% N)....	21							
	Nitroglycerine....	13							
	Gas soot.....	9							
	Ethyl centralite...	1							
	II. Potassium perchlorate..	55	2.8	-	2000	45	0.45	-	-
	Nitrocellulose (12.6% N)....	21							
	Nitroglycerine....	13							
	Magnesium....	0.5							
	Magnesium oxide.....	0.5							
	Gas soot.....	9							
	Ethyl centralite...	1							

Table 1.4 (Continued)

Type of solid fuel	Components of solid fuel	% total weight	Specific gravity g/cm^3	Unit pulse kgs/kg	Combustion temperature °C	Burning rate in mm/s p = 70 atm, T° - 21°C	Exponent ν in law of burning rate	Coefficient of temperature sensitivity $\left[\frac{\partial u_m}{\partial T}\right]_p$, $\frac{1}{°C}$	Remarks
NDRS type EJA218B	Ammonium picrate.....	45	1.68-1.8	160-170	2000-2500	31-32	0.45	-	Grain obtain by casting
	Sodium nitrate.....	45							
	Thermosetting resin (phenylformaldehyde).....	10							
NDRS type EJA480	Ammonium picrate.....	46.6	1.8	180		6-25		-	Grain obtain by casting
	Sodium nitrate.....	46.6							
	Buramine rubber.....	5.2							
	Plastic.....	1.6							
	Ammonium picrate.....	54.6	1.77	200	1750	-	-	-	Fuel is molded under pressure
	Potassium nitrate.....	36.4							
	Calcium stearate....	3.6							
	Ethylcellulose...	5.4							
Fuel based on ammonium nitrate	I. Ammonium nitrate.....	83.0	-	-	1400	1.3	0.5	-	-
	Synthetic rubber.....	10.0							
	Gas soot....	2.0							
	Plasticizer.	2.0							
	Solidifiers.	0.4							
	Antioxidant.	0.3							
	Combustion catalyst....	2.3							

Table 1.4 (Continued)

Type of solid fuel	Components of solid fuel	% total weight	Specific gravity, g/cm^3	Unit pulse kgs/kg	Combustion temperature °C	Burning rate in mm/s p = 70 atm, T° = 21°C	Exponent ν in law of burning rate	Coefficient of temperature sensitivity $\left[\frac{\partial u_{max}}{\partial T}\right]_p \frac{1}{°C}$	Remarks
Fuel based on ammonium nitrate	II. Ammonium nitrate..... Aeroplex (combustible based on polyesters).	80 20	-	200	-	1.4	0.5	0.0025	Lower limit of pressure 1-7 kg/cm^2
	III. Ammonium nitrate..... Polyurethane (without high-energy additions)..	-	1.55	210	-	3	0.5	-	-
Fuel based on ammonium perchlorate GCRC	I. Ammonium perchlorate. Aeroplex (binder combustible based on polyesters).	65 35	1.62	210	2000-2500	7.6-22.8	0.5-0.6	0.0012-0.0024	
Type A	II. Ammonium perchlorate. Trinitrotoluene..... Liquid hydrocarbon of paraffin series..... Asphalt.....	50 25 12.5 12.5	1.7	200	2400	13.0	0.4	0.0014	Lower limit of pressure 1-14 kg/cm^2

Table 1.4 (Continued)

Type of solid fuel	Components of solid fuel	% total weight	Specific gravity, g/cm^3	Unit pulse kgs/kg	Combustion temperature °C	Burning rate in mm/s p = 70 atm, T° = 21°C	Exponent ν in law of burning rate	Coefficient of temperature sensitivity $\left[\frac{\partial u_{\text{ср}}}{\partial T}\right]_p \frac{1}{°C}$	Remarks
Arcite	III. Ammonium perchlorate.. Nitroglycerine.... Nitrocellulose.... Polyurethane..... Aluminum..... Magnesium oxide..... Nitrodiphenylamin.	-	1.75	238	-	5.6	-	0.0012-0.0024	
	IV. Ammonium perchlorate.. Polyvinyl chloride..... Plasticizer oil..... Aluminum.....	-	1.7	200	3100	2.5-25.4		0.0012-0.0024	

[1] Values of unit pulse are given for standard engine $\left(p = 70\ \frac{кг}{см^2};\ \frac{d_k}{d_{кр}} = 2{,}24\right)$.

[2] Prescription is intermediate between ballistite and mixture compositions.

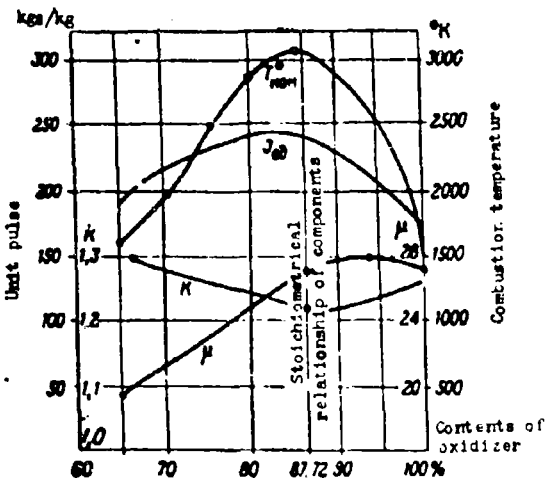

Fig. 1.1. Dependence of power factor on relative content of oxidizer.

At a given percentage of oxidizer it is possible to improve physical properties of the fuel, if one uses an oxidizer with large specific gravity, since mechanical properties are basically influenced not by the weight, but the volume part of oxidizer. In this respect ammonium salts yield to other oxidizers (Table 1.4).

Recently in solid fuels for the purpose of increasing unit pulse light metals have been introduced: aluminum, magnesium, zirconium, beryllium, boron and sodium. Application of powered metals as additions to a fuel is complicated by their inclination to spontaneous combustion, which creates a danger of premature ignition or uncontrolled burning in the process of production, operation and during starting of the engine. For decrease of their activity, particles of aluminum are passivated by incapsulation or covering aluminum particles with plastic. More promising is the use of aluminum as material for manufacture of capsules covering separate particles of solid combustible or oxidizer. This method will allow an increase in periods of fuel storage and creates the possibility of joint use and development of oxidizers and fuels which possess a high power potential.

Created composite rocket fuels ensure a unit impulse near 250 $\frac{kg\ s}{kg}$. In Table 1.5 are given comparative characteristics of composite and ballistite fuels.

In development are solid fuels based on perchlorate of ammonium with additions of beryllium, which will be able to ensure a unit pulse of ~260-265 $\frac{kg\ s}{kg}$ [13].

Table 1.5. Comparative characteristics of composite and ballistite fuels [9].

Fuel	Specific gravity δ g/cm^3	ν[1]	u_1[1] p_k = 70 kg/cm^2	Unit pulse I_1, kgs/kg
Mixture (ammonium perchlorate + polybutadiene with an addition of aluminum)	1.74	0.236	0.467	250
Ballistite (nitrocellulose and nitroglycerine, cast charge)	1.58	0.61 (when p_k = 56-116 kg/cm^2	0.45	219
Mixture (ammonium perchlorate + polyurethane	1.72	-	0.227	238
Ballistite (nitrocellulose and nitroglycerine, pressed charge)	1.55	-	0.46	216 (when p_k = 91 kg/cm^2)

[1] ν and u_1 – experimental constants in empirical formula $u = u_1 p^{\nu}$, expressing dependence of burning rate of solid fuel on pressure in combustion chamber.

Also studied is the possibility of an increase of unit pulse of a solid fuel to 270-275 $\frac{kg\ s}{kg}$ by addition to them of aluminum hydride and to 290-295 $\frac{kg\ s}{kg}$ by addition of beryllium hydride [11, 14]. It is noted that solid fuels can be created with a unit pulse to 340 $\frac{kg\ s}{kg}$. At the same time it is indicated that the majority of promising solid fuels with a unit pulse greater than 260 $\frac{kg\ s}{kg}$ are unstable, aggressive and toxic [8, 12].

A new direction in development of rocket technology is the development of high-calorie combined solid fuels [15].

During application of combined fuel it is assumed that oxidizer and combustible in the charge are separated. Different combinations are possible, from creation of two separate charges to a single layered charge [6], consisting of disk segments or concentric cylinders of combutible and oxidizer.

Depending on the nature of the binder-combustible substance, physical and power properties of composite fuels can be different. Between ballistic, physical and technological propellant properties there exists a defined interconnection. For example, if for a given system oxidizer-combustible one changes the distribution of dimensions of solid particles for the purpose of control of the burning rate, then one can attain such a structure with which the fuel will not be suitable for casting. If the density of loading of fuel is decreased for the purpose of safeguarding its ability to be cast or for improvement of mechanical properties, then unit pulse and density are changed.

§ 1.6. Basic Power Characteristics of Solid Rocket Fuels

The basic power factor of a solid rocket propellant is its caloricity or thermal energy liberated during its combustion. The full measure of this energy is that quantity of heat which will be liberated when cooling combustion products of the fuel from combustion temperature to absolute zero. Besides, one should consider that if one were to conduct a process of cooling of gases in such a manner that water vapor in combustion products were condensed, then there would be liberated more heat than when cooling without condensation of water vapor. For example, for ballistite powders this difference is 80-100 $\frac{\text{kcal}}{\text{kg}}$.

Usually, caloricity of a solid rocket propellant ($Q_{ж}$) is determined experimentally by burning it in a special calorimetric instrument and subsequent cooling of combustion products to 18°C (291°K); moreover, water vapor in combustion products is completely condensed.

For solid fuels of the ballistite type caloricity $Q_{ж}$ numerically is close to full caloricity of the fuel Q, corresponding to cooling of combustion products of the fuel to absolute zero. It is not difficult to see that

$$Q = \int_0^{T_0} c\,dT,$$

where T_0 – combustion temperature of fuel under conditions of experiment; c – heat capacity of 1 kg of combustion products of the fuel.

If one were to burn the fuel in a constant volume, then the maximum temperature of burning T_{0V}, where we obtain

$$Q = \int_0^{T_{0V}} c_V\,dT. \qquad (1.1)$$

where c_V – heat capacity of combustion products at constant volume.

Under conditions of the experiment in a bomb calorimeter with condensation of water vapor we obtain

$$Q_{ж} = \int_{291}^{T_{0V}} c_V\,dT + \Delta Q_{кон} = \int_{0}^{T_{0V}} c_V\,dT - \int_{0}^{291} c_V\,dT + \Delta Q_{кон} \qquad (1.2)$$

where $\Delta Q_{КОН}$ – heat of condensation of water of 1 kg of combustion products of the fuel.

Solving jointly equations (1.1) and (1.2) with respect to Q we obtain

$$Q = Q_{ж} + \int_{0}^{291} c_V\,dT - \Delta Q_{кон} \qquad (1.3)$$

Using expression (1.3), it is possible to calculate full caloricity of a solid rocket propellant with respect to value $Q_{ж}$. For an example of a calculation examined below, in 1 kg of products of combustion are contained 7.8 moles of water, and the heat of condensation of one mole of water is equal to 10.6 kcal/mole. Thus, $\Delta Q_{КОН} = 7.8 \times 10.6 = 82.5$ kcal/kg.

At the same time, internal energy of combustion products T = 291°K is equal to 86.6 kcal/kg. Thus, the difference between Q and $Q_{ж}$ is equal to 4.1 kcal/kg, or 0.6% of the value of caloricity of the fuel.

In view of the small value of the difference Q - $Q_{ж}$, caloricity of a solid fuel is usually characterized by the value of $Q_{ж}$.

During burning of a solid fuel in a thrust chamber, the average combustion temperature of the fuel is close to the combustion temperature at constant pressure. This temperature T_{0p} is determined from the expression

$$H_0 = \int_{0}^{T_{0p}} c_p\,dT = \tilde{c}_p T_{0p} \qquad (1.4)$$

where H_0 – initial heat content of combustion products of fuel;

$\tilde{c}_p$ – average heat capacity of these products at constant pressure in the interval of temperatures from 0 to T_{0p}.

During burning of a solid fuel in a constant volume, for example in a bomb calorimeter, on account of subsequent compression of gases

of burning components of the fuel an increase of temperature of gases occurs.

Temperature T_{0V} of combustion of a solid fuel at constant volume is determined from the expression

$$U_0 = \int_0^{T_{0V}} c_V \, dT = \tilde{c}_V T_{0V}, \tag{1.5}$$

where U_0 – initial internal energy of combustion products of fuel; $\tilde{c}_V$ – average heat capacity of these products at constant volume in the interval of temperatures from 0 to T_{0V}.

The difference between temperatures T_{0p} and T_{0V} corresponds to the energy expended on expansion of gases under conditions of burning of fuel at constant pressure (rocket chamber).

During combustion of a defined quantity of fuel the same energy is given off independent of whether burning occurs at constant volume or at constant pressure. Therefore $H_0 = U_0$, and from expressions (1.4) and (1.5) we obtain

$$\tilde{c}_V T_{0V} = \tilde{c}_p T_{0p}$$

or

$$\frac{T_{0V}}{T_{0p}} = \frac{\tilde{c}_V}{\tilde{c}_p} = \tilde{k},$$

where $\tilde{k}$ – mean value of adiabatic index for interval of temperatures from 0°K up to the combustion temperature.

§ 1.7. Enthalpy Method of Calculation of Power Characteristics of Solid Rocket Fuels

Combustion of solid rocket propellants in a thrust chamber occurs on account of the oxygen which is contained in the actual fuel. During combustion of ballistite solid fuels a process of intramolecular oxidation of separate components of the fuel occurs nitrates of celluloses and nitrates of polyatomic alchols (nitroglycerine, dinitroglycol). Components of fuel incapable of intramolecular oxidation in connection with a deficiency or absence in them of active oxygen borrow the oxygen necessary for oxidation from nitrates of celluloses and nitroglycerine.

The method of calculation of power factors is examined in an example of double-base (ballistite) fuel.

The burning reaction of a double-base fuel in general form can be recorded in the following way:

$$C_aH_bO_cN_d = xCO_2 + yCO + zH_2 + uH_2O + \frac{d}{2}N_2 \qquad (1.6)$$

where a, b, c, d – number of gram-atoms of corresponding elements in 1 kg of fuel; x, y, z, u, d/2 – number of gram-molecules of gases in combustion products of the fuel.

Special investigations [16] show that under conditions of burning of double-base solid fuel in a thrust chamber, the influence of dissociation on combustion temperature of the fuel is negligible. Under these conditions the equilibrium state of the gas mixture of CO_2, CO, H_2 and H_2O is determined by the composition of fuel and constant K_w of equilibrium of reaction of a water gas

$$CO_2 + H_2 \rightleftarrows CO + H_2O.$$

With an increase of temperature the reaction of water gas shifts to the right. The equilibrium state of combustion products does not depend on pressure, since the reaction of water gas occurs without a change of the number of moles. Therefore the constant of equilibrium of this reaction depends only on temperature.

In Table 1.6 are given values of the constant of equilibrium of water gas depending on temperature.

Table 1.6

T°K	300	600	800	1000	1200	1400	1600	1800	2000	2200	2400	2600	2800	3000
K_w	0	0,04	0,24	0,71	1,40	2,19	3,06	3,80	4,55	5,21	5,78	6,22	6,59	6,92

Here

$$K_w = \frac{[H_2O][CO]}{[H_2][CO_2]},$$

where $[H_2O]$, [CO] etc. – concentration of corresponding substances.

If one knows the temperature of gases, then their composition is determined by joint solution of equations of weight balance:

$$a = x + y;$$

$$c = 2x + y + u;$$

$$b = 2z + 2u$$

and of the equation of equilibrium of reaction of water gas

$$K_w = \frac{yu}{xz}.$$

Solution of the given system reduces to a solution of a quadratic equation with respect to the number of moles of CO_2 in products of combustion.

So we obtain

$$x = \frac{1}{2(K_w - 1)}\left\{-(K_w M + R + a) + \right.$$
$$\left. + \sqrt{(K_w M + R + a)^2 - 4(K_w - 1)aR}\right\}; \qquad (1.7)$$

$$\left.\begin{aligned} y &= a - x, \\ u &= c - a - x, \\ z &= \frac{b}{2} - u, \end{aligned}\right\} \qquad (1.8)$$

where

$$M = \frac{b}{2} - c + a;$$

$$R = c - a.$$

If one knows the composition of gases and their temperature, then by tables of heat content of gases one can determine heat content of 1 kg of combustion products of fuel by the formula

$$H = xH_{CO_2} + yH_{CO} + zH_{H_2} + uH_{H_2O} + \frac{d}{2}H_{N_2}, \qquad (1.9)$$

where $\underline{H}_{CO_2}$, $\underline{H}_{CO}$ etc. – heat content for each of the gases in kcal/mole.

Values of heat content of shown gases are given in Table 1.7.

The internal energy of combustion products at different temperatures can be determined from the expression

$$H = U + nrT,$$

where n – total number of moles of combustion products of fuel; r – gas constant of one mole equal to 1.986×10^{-3}.

By assigning a series of values of temperatures, it is possible for each of them to calculate composition of gases of combustion products, their heat content and internal energy, and construct curves $\underline{H} = f(T)$ and $U = \phi(T)$.

If we know the initial heat content $\underline{H}_0$ of combustion products

Table 1.7. Heat content of gases.

T°K	CO_2	CO	H_2O	H_2	N_2
0	0	0	0	0	0
100	0,68	0,68	0,80	0,45	0,68
200	1,44	1,40	1,60	0,96	1,40
300	2,26	2,09	2,39	1,57	2,09
400	3,19	2,77	3,20	2,23	2,78
500	4,22	3,50	4,00	3,06	3,50
600	5,33	4,20	4,88	4,05	4,20
800	7,70	5,70	6,66	5,04	5,67
1000	10,24	7,29	8,57	6,97	7,21
1200	13,00	8,86	10,53	8,42	8,79
1400	15,68	10,52	12,70	9,93	10,43
1600	18,43	12,22	14,89	11,47	12,02
1800	21,28	13,93	17,24	13,05	13,79
2000	24,17	15,65	19,63	14,68	15,51
2200	27,08	17,45	22,08	16,32	17,24
2400	30,02	19,12	24,57	18,02	18,97
2600	32,99	20,90	27,12	19,70	20,72
2800	35,98	22,68	29,70	21,46	22,48
3000	38,98	24,45	32,30	23,20	24,26

at the time of formation of gases during burning of the fuel, then from the graph $\underline{H} = f(T)$ can be found value T_{0p}, corresponding to value $\underline{H}_0$ (Fig. 1.2).

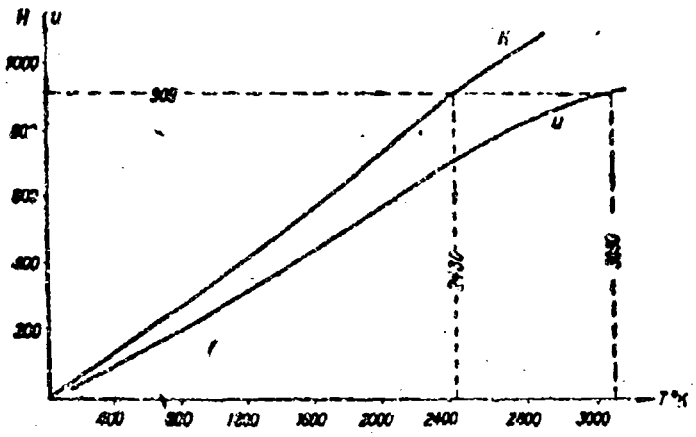

Fig. 1.2. Graph of calculated power characteristics of a fuel.

As noted above, the initial heat content and initial value of internal energy are equal to each other and are equal to caloricity of the fuel $Q_ж$. Therefore from the graph of $U = \phi(T)$ can be found temperature T_{0V}, corresponding to value $U_0 = \underline{H}_0 = Q$.

If caloricity of the fuel is unknown, it can be found by the DePauw method discussed below.

In the presence of curves H(T) and U(T) for any temperature we can determine true heat capacities and the adiabatic index from expressions:

$$c_p = \frac{dH}{dT}; \quad c_V = \frac{dU}{dT}; \quad k = \frac{c_p}{c_V}$$

by means of numerical differentiation of function H(T) and U(T).

If ΔT is a step of temperatures in the table of function H(T) and U(T), then the values of true heat capacities for temperature T_1 can be determined from expressions:

$$c_{p_i} = \frac{H(T_i + \Delta T) - H(T_i - \Delta T)}{2\Delta T}; \quad c_{v_i} = \frac{U(T_i + \Delta T) - U(T_i - \Delta T)}{2\Delta T}; \quad k_i = \frac{c_{p_i}}{c_{V_i}}. \qquad (1.10)$$

Average heat capacities in an arbitrary interval of temperatures $T_1 - T_2$ will be determined from expressions:

$$[c_p]_{T_1}^{T_2} = \frac{H(T_2) - H(T_1)}{T_2 - T_1};$$
$$[c_V]_{T_1}^{T_2} = \frac{U(T_2) - U(T_1)}{T_2 - T_1},$$

and accordingly is determined the mean value of the adiabatic index.

The force of fuel f_V is determined from expression

$$f_V = RT_{\omega},$$

where R = nr (r – universal gas constant).

Rocket technology usually uses the value of force of a fuel f_p, determined from expression

$$f_p = RT_{\omega p}$$

Values f_p and f_V are connected by the dependence

$$f_p = \frac{f_V}{k}.$$

The number of moles of powder gases n is determined in the process of calculation of the composition of products of burning. The number of moles of gases is not changed depending on their temperature and can be determined directly by the formula

$$n = a + \frac{b}{2} + \frac{d}{2}.$$

The volume of gases of products of burning under normal conditions (0°C and 760 mm Hg) is determined from the expression

$$w = 22{,}4n\left(\frac{\text{л}}{\text{кг}}\right).$$

The method of calculation examined above is based on the assumption that the composition of combustion products of a fuel is completely determined by the equilibrium of water gas and that dissociation of the gas can be disregarded. For high-calorie fuels it can be necessary to calculate basic reactions dissociation:

$$CO_2 \rightleftarrows CO + {}^1/_2O_2;$$
$$H_2O \rightleftarrows OH + {}^1/_2H_2;$$
$$H_2O \rightleftarrows H_2 + {}^1/_2O_2;$$
$$H_2 \rightleftarrows 2H;$$
$$N_2 + O_2 \rightleftarrows 2NO.$$

Calculation of the shown reactions considerably increases the labor of calculation. In work [16] a method is offered for calculation of the composition of combustion products of fuel, taking into account dissociations, with the aid of successive approximations, whereas the zero approximation is taken the result of the calculation which takes into account only equilibrium of the water gas according to formulas (1.7), (1.8). The essence of the method reduces to the following.

Let us assume that to the shown five reactions of dissociation correspond constants of equilibrium K_1-K_5 whose values in the function of temperature are given in tables. Then partial pressures of products of dissociation can be in the first approximation calculated by the formulas:

$$O_2 = \left(\frac{CO_2}{CO}K_1\right)^2; \quad OH = \frac{H_2O}{\sqrt{H_2}}K_2;$$
$$H = \sqrt{H_2K_4}; \quad NO = \sqrt{N_2O_2K_5}. \qquad (1.11)$$

in which chemical symbols designate partial pressures.

Here values CO_2, CO, H_2O, H_2 are taken from the calculations of the zero approximation (1.7), (1.8). Since the composition of gases was expressed in moles, then it is necessary preliminarily to produce a conversion of concentrations of gases into partial pressures p_i, assigning the value of $p = \sum p_i$ by the formula

$$p_i = p\frac{n_i}{n},$$

where n is the number of moles.

By calculating in the first approximation the composition of products of dissociation, we definitize the composition of basic components CO_2, CO, H_2, H_2O, N_2, whose amount in products of burning decreases. For this we definitize values M and R in formula (1.7) for calculation of CO_2. Proceeding from balance of material, we obtain:

$$R = R^\circ - (2O_2 + NO + OH);$$
$$M = M^\circ - \frac{1}{2}(H + OH) + (2O_2 + NO + OH), \qquad (1.12)$$

where

$$R^\circ = c - a = (CO_2 + H_2O)^\circ;$$
$$M^\circ = \frac{b}{2} - c + a = (H_2 - CO_2)^\circ.$$

Index (°) corresponds to the zero solution.

Further we calculate by formulas (1.7), (1.8) definitized values of partial pressures of basic gases CO_2, CO, H_2O, H_2. The corrected value of N_2 is found from expression

$$N_2 = N_2^\circ - \frac{1}{2}(NO + N).$$

Since during dissociation of basic components the number of moles is increased, then the sum of partial pressures of components will be increased and will be larger than assigned pressure in the chamber of the engine $p_{зад}$. In order to remove the shown divergence, we correct the value of partial pressures according to dependence

$$(p_i)_{корр} = p_i \frac{p_{зад}}{\sum p_i}.$$

At this point the first approximation is finished. If it is required to produce a second approximation, then the whole calculation is repeated, where the composition of basic components obtained in the first approximation is the initial point for the second approximation.

§ 1.8. Calculation of Caloricity of Fuel by the Method of DePauw

The principle of calculation of caloricity according to the method of DePauw consists of the fact that caloricity of a fuel is defined as the sum of the thermal effects created by participation in burning of fuel of its separate components.

We will designate by β_i a change of caloricity of a fuel caused by introduction in its composition of 1% of a given substance. Then according to DePauw

$$Q_{\text{ж}} = \sum n_i \beta_i$$

where n_i -- percentage of a corresponding fuel component.

The possibility of such a method of calculation is based on the following assumptions:

1. Independent of the value of $Q_{\text{ж}}$ an introduction in the fuel of 1% of a substance always causes a β kcal change in $Q_{\text{ж}}$.

2. Changes of caloricity of the fuel, caused by different components, are additive.

These assumptions are not theoretically flawless, since with a change of composition of fuel during introduction in it of one or another component, the composition of gases is changed differently, and consequently also the thermal effect of burning of the fuel.

Nevertheless the method of DePauw in application to double-base fuels leads to small errors, since the shift of equilibrium of water gas, during calculation, into liquid water gives a very small thermal effect.

This occurs as a result of an almost full compensation of thermal effects of processes:

$$CO_2 + H_2 \rightleftarrows CO + H_2O - 10{,}4 \text{ kcal}$$

and

$$H_2O_{\text{пар}} \rightleftarrows H_2O_{\text{ж}} + 10{,}6 \text{ kcal.}$$

Whenever introduction into a fuel of a defined component shifts equilibrium in the direction of formation of water, the lowering of thermal effect of burning of fuel by $10.4 \times \Delta n_{H_2O}$ kcal is almost completely compensated by the increased thermal effect of condensation of water by $10.6 \times \Delta n_{H_2O}$ kcal.

In Table 1.8 are given values of constants β according to DePauw.

Table 1.8

Designation of substance	Chemical formula	kcal	Remarks
Nitrocellulose	—	$1{,}3N-6{,}7$	N = contents of nitrogen in %
Nitroglycerine	$C_3H_5(ONO_2)_3$	+17,0	
Dinitrotoluene	$C_6H_3CH_3(NO_2)_2$	0	
Centralite	$CON_2(C_6H_5)_2(C_2H_5)_2$	−22,5	
Vaseline	$C_{20}H_{42}$	−32,5	
Magnesium oxide	MgO	0	

§ 1.9. Example of Calculation of Power Characteristics of a Double-Base Solid Fuel

We will examine a double-base fuel of the following composition:

Nitrocellulose N = 12.1%	56.1%
Nitroglycerine $C_3H_5(ONO_2)_3$	28.3%
Centralite $CON_2(C_2H_5)_2(C_6H_5)_2$	2.0%
Dinitrotoluene $C_6H_3CH_3(NO_2)_2$	12.1%
Vaseline $C_{20}H_{42}$	1.0%
Water H_2O	0.5%
Total	100%

The chemical formula of nitrocellulose can be composed by proceeding from the following dependences [16]:

$$C = 21{,}85 - 1{,}180\,(N\% - 12{,}75);$$
$$H = 27{,}32 - 2{,}690\,(N\% - 12{,}75);$$
$$O = 36{,}40 + 0{,}444\,(N\% - 12{,}75);$$
$$N = 9{,}10 + 0{,}722\,(N\% - 12{,}75),$$

where N% – percentage of nitrogen in nitrocellulose.

For N = 12.1% the formula of nitrocellulose has the form

$$C_{22,6}H_{29,1}O_{24,1}N_{6,4}.$$

Knowing the composition of the fuel, it is possible to compose a conditional formula of the fuel

$$C_aH_bO_cN_d,$$

where a, b, c, d – number of gram-atoms of corresponding elements in a conditional molecule of the fuel.

For example, in nitroglycerine, whose molecular weight is 227, there are three atoms of carbon. The relative content of nitroglycerine in fuel is 28.3%, or 283 g per 1 kg of fuel. Thus, the number of gram-atoms of carbon of nitroglycerine, referred to 1 kg fuel, is obtained equal to

$$a_1 = \frac{3 \cdot 283}{227} = 3{,}74.$$

Calculating the number of gram-atoms of carbon in all components of the fuel, and summarizing these values, we will obtain value $a = \sum a_i$. Similarly calculated are values b, c and d.

Results of calculations are given in Table 1.9.

Table 1.9

Component	Carbon a	Hydrogen b	Oxygen c	Nitrogen d
Nitrocellulose	12,65	16,29	20,21	4,81
Nitroglycerine	3,74	6,22	11,22	3,74
Centralite	1,22	1,43	0,07	0,14
Dinitrotoluene	4,63	3,97	2,65	1,32
Vaseline	0,76	1,57	—	—
Water	—	0,55	0,27	—
Total	23,00	30,03	34,42	10,01

We obtain the following conditional fuel formula

$$C_{23,0}H_{30,03}O_{34,42}N_{10,01}.$$

A check of correctness of the calculation is produced in the following way:

$$a \cdot 12 + b \cdot 1 + c \cdot 16 + d \cdot 14 = 1000.$$

The equation of fuel decomposition has the form

$$C_{23,0}H_{30,03}O_{34,4}N_{10,01} = xCO_2 + yCO + zH_2 + uH_2O + 5,00N_2.$$

Assigning a series of values of temperatures, we calculate by formulas (1.8) values x, y, z, u of gram-molecules of gases in combustion products of the fuel.

For example, for temperature T = 2400°K we obtain

$$A = \frac{K_w\left(\frac{b}{2} - c + a\right) + c}{2(K_w - 1)} = \frac{5,78(15,01 - 34,42 + 23,0) + 34,42}{2 \cdot 4,78} = 5,73;$$

$$x = -A + \sqrt{A^2 + \frac{a(c-a)}{K_w - 1}} = -57,3 + \sqrt{5,73^2 + \frac{23,0(34,42 - 23,0)}{4,78}} = 3,62;$$

$$y = a - x = 23,00 - 3,62 = 19,38;$$

$$u = c - a - x = 34,42 - 23,0 - 3,62 = 7,80;$$

$$z = \frac{b}{2} - u = 15,01 - 7,80 = 7,21.$$

Results of calculation for different temperatures are given in Table 1.10.

Table 1.10

T°K	2600	2800	2600	2400	2200	2000	1800	1600	1200	600	291
CO_2	3,32	3,40	3,50	3,62	3,80	4,04	4,35	4,77	6,28	9,36	11,18
CO	19,68	19,60	19,50	19,38	18,20	18,96	18,65	18,23	16,72	13,64	11,82
H_2O	8,10	8,02	7,92	7,80	7,62	7,38	7,06	6,62	5,14	2,06	0,24
H_2	6,92	7,00	7,10	7,21	7,30	7,63	7,96	8,36	9,87	12,95	14,78
N_2	5,00	5,00	5,00	5,00	5,00	5,00	5,00	5,00	5,00	5,00	5,00
n	43,02	43,02	43,02	43,02	43,02	43,02	43,02	43,02	43,02	43,02	43,02

By Table 1.7 for every gas at a corresponding temperature we determine heat content and multiply by the number of moles of a given gas in 1 kg of fuel.

The sum of heat content of all gases gives heat content of products of combustion of 1 kg fuel.

For temperature T = 2400°K, results of calculation are given in Table 1.11.

$$H = \sum n_i H_i = 897{,}7 \frac{\text{kcal}}{\text{kg}}.$$

Table 1.11

Gas	Number of moles n_i	Heat content H_i	$n_i H_i$
CO_2	3,62	30,02	108,5
CO	19,38	19,12	370,4
H_2O	7,80	24,57	194,5
H_2	7,21	18,02	129,5
N_2	5,0	18,97	94,8
Total . . .			897,7

Internal energy is calculated by the formula

$$U = H - RT = H - nrT = 897{,}7 - 43{,}02 \cdot 1{,}986 \cdot 10^{-3} \cdot 2400 = 691.$$

Average heat capacities in the interval of temperatures from 0 to 2400°K are equal to:

$$\tilde{c}_p = \frac{H}{T} = \frac{897}{2400} = 0{,}374; \qquad \tilde{c}_V = \frac{U}{T} = \frac{691}{2400} = 0{,}288; \qquad \tilde{K} = \frac{\tilde{c}_p}{\tilde{c}_V} = 1{,}297.$$

The mean value of heat capacities in a certain interval of temperatures ΔT are determined from expressions:

$$[c_p]_{\Delta T} = \frac{\Delta H}{\Delta T}; \quad [c_V]_{\Delta T} = \frac{\Delta U}{\Delta T}.$$

For example, for an interval of temperatures from 1000 to 2000°K, corresponding to average conditions of flow of gases from a thrust chamber:

$$[c_p]_{\Delta T} = \frac{730 - 337}{1000} = 3{,}93;$$
$$[c_V]_{\Delta T} = \frac{558 - 251}{1000} = 3{,}07;$$
$$K_{\Delta T} = 1{,}28.$$

Results of calculations for different temperatures are given in Table 1.12 and are shown on the graph (Fig. 1.2).

Table 1.12

T°K	3000	2400	2000	1600	1200	800	291
H	1157	898	730	568	410	264	82
RT	257	206	172	137	103	69	25
U	900	691	558	431	307	195	57
$\bar{c}_p$	0,386	0,374	0,365	0,355	0,342	0,330	0,282
$\bar{c}_V$	0,299	0,288	0,279	0,269	0,256	0,244	0,196
$\bar{K}$	1,286	1,297	1,307	1,318	1,333	1,350	1,438

If we know the caloricity of powder $Q_ж$, then, using the graph of function $H(T)$ at value $Q_ж = H_0$ we find the initial temperatures of burning at constant pressure, T_{0p}. Analogously, using the graph $U(T)$ at value $Q_ж = U_0$, we find initial temperatures of gases during burning of a fuel in a constant volume.

Calculation of $Q_ж$ is done according to DePauw.

For nitrocellulose at N = 12.1% coefficient

$$\beta = 1{,}3 \cdot 12{,}1 - 6{,}7 = 9{,}0.$$

Proceeding from the table of coefficients β according to DePauw and composition of fuel, we obtain

$$Q_n = 9{,}0 \cdot 56{,}1 + 17 \cdot 28{,}3 + 12{,}1 \cdot 0 - 22{,}5 \cdot 2 + 32{,}5 \cdot 1 = 909 \frac{\text{kcal}}{\text{kg}}.$$

Proceeding from this value of caloricity, we obtain

$$T_{\varphi p} = 2430^\circ \text{ K}; \quad T_{\varphi v} = 3050^\circ \text{ K}.$$

To power characteristics of a solid rocket propellant there also pertains the value of force of powder f_v, determined from expression

$$f_v = RT_{\varphi v},$$

in which the gas constant is expressed in mechanical units.

Besides, for the examined example we obtain

$$R = 427nr = 427 \cdot 43{,}02 \cdot 1{,}986 \cdot 10^{-3} = 0{,}848 \cdot 43{,}02 = 36{,}5,$$
$$f_v = 36{,}5 \cdot 3050 = 111500 \frac{\text{kg-m}}{\text{kg}}.$$

Analogously we obtain $f_p = 36.5 \times 2430 = 88800$ kg-m/kg,

$$K = 1{,}28.$$

Value f_p is called the derived force of powder.

The volume of gases is determined from expression

$$w = 22{,}4n = 22{,}4 \cdot 43{,}02 = 965 \frac{\text{l}}{\text{kg}}.$$

Literature

1. Barrer M., Zhomott A., Vebek B. F., Vandenkerkkhove Zh. Raketnyye dvigateli (Rocket engines). Oborongiz, 1962.

2. Budnikov M. A., Bystrov I. V., Levkovich N. A., Sirotinskiy V. F., Shekhter B. I. Vzryvchatyye veshchestva i porokha (Explosives and powder). Oborongiz, 1955.

3. Dolzhanskiy Yu. M., Kurov V. D. Osnovy proyektirovaniya porokhovykh raketnykh snaryadov (Design fundamentals of solid-propellant missiles). Oborongiz, 1961.

4. A. Zaehringer. Solid Propellant Rockets American Rocket Co. Michigan, 1958.

5. Paushkin Ya. M. Khimiya reaktivnykh topliv (Chemistry of propellants). Izd-vo AN SSSR, 1962.

6. Aeroplane No 2610.

7. Missiles and Rockets. 1957, T. 2, No 8, str. 67, 84. 1959, T. 5, No 2, str. 18. 1962, No 10, str. 36, 39, 40, 46.

8. Rabber Eydzh, 1958, VIII.

9. Missile Design and Development. 1960, vol. 6, No 9, p. 24-26.

10. "Aviation Week", 1963, vol. 79, No 2, p. 15; 1962, vol. 77, No 11, p. 162-167. "Aviation Age", 1963, vol. 59, T. 28, No 8, p. 112-116.

11. Chemical and Engineering News, 1963, vol. 41, No 39, p. 75.

12. Pirs L. "Voprosy raketnoy tekhniki", 1959, No 10, 62.

13. "Voprosy raketnoy tekhniki", 1961, No 5, 15, J. Crook. The Aeroplane and Austronautics, 98, No 2536, 650 (1960).

14. "Voprosy raketnoy tekhniki", 1959, No 28. R. Carpenter. ARS journal, 1960, 29, No 1, 8; 1961, 31, No 9, 1265-1272.

15. Progr in Astronaut and Rocketry, 1960, 1, 207-226.

16. Zel'dovich Ya. B., Rivin M. A., Frank-Kamenetskiy D. A. Impul's reaktivnoy sily porokhovykh raket (Pulse of reaction force of powder rockets). Oborongiz, 1963.

Footnote

[1]In foreign literature these fuels are called double-base.

CHAPTER II

CHARGES USED IN RDTT AND THEIR PROGRESSION CHARACTERISTICS

§ 2.1. General Characteristics of a Charge Form

The process of gas formation in a thrust chamber is ermined by the burning rate of the solid fuel, depending on its composition, and the burning surface of the charge, determined by its geometric parameters. During burning of a solid fuel of a given composition the pressure in the thrust chamber is mainly det mined by the ratio of surface of combustion to the area of the cri al section of the nozzle, but during constant critical section by the area of the burning surface of the charge. If the burning surface increases, then burning is called progressive (progressive charge form). Analogously, charges are of degressive form or of constant burning surface (neutral charge). The progression characteristic of a charge σ is the ratio of the burning surface of the charge S to the initial value of this surface S_0.

Selection of charge form should ensure the character of the change of pressure, and consequently of thrust in time in accordance with the required characteristics of the vehicle.

If a change of engine thrust over a wide range is not required by the flight dynamics of the object, then a considerable change of pressure of gases in the process of charge combustion is undesirable. In this case the upper limit of pressure is determined by strength characteristics of thrust chamber walls, and the lower limit by stability of charge combustion.

Besides, it is necessary to seek a small change of burning surface in the process of charge combustion. The shown requirements are satisfied by a charge made from unclad cylindrical grain with an internal channel. When cladding ends with an incombustible composition, the surface of burning of the grain remains strictly constant, since an increase of the burning surface of the internal channel is compensated by a reduction of the external burning surface of the grain. If ends are not clad, then the burning surface is weakly degressive.

The charge form should also ensure relatively complete filling by fuel of a given volume of the thrust chamber, characterized by the ratio of fuel weight ω to thrust chamber volume $W_{кам}$:

$$\Delta = \frac{\omega}{W_{кам}}.$$

During compact filling of the thrust chamber the density of filling approaches the density of the fuel. However this sharply drcreases the burning surface of the charge.

The degree charging of the volume of the chamber is sometimes characterized by the coefficient of filling of a cross section of the chamber

$$\varepsilon_0 = \frac{S_{T0}}{F_{кам}}, \tag{2.1}$$

where S_{T0} – initial area of cross section of charge; $F_{кам}$ – area of cross section of chamber.

During selection of the charge form it is necessary to consider that an increase of coefficient ε_0 is connected with a reduction in the area of free passage of gases and an increase of the flow rate of combustion products along the charge. This increases the danger of unstable erosion burning of the charge. During selection of dimensions of the internal channel one usually starts from the value of the parameter of Pobedonostsev (χ):

$$\chi = \frac{S_0}{F_{сооб}},$$

the maximum permissible value of which depends on composition of the fuel and pressure in the chamber.

Another important circumstance which must be considered during selection of the charge form is the thermal shielding of walls of the chamber which is ensured by application of charges fastened to the body of the engine. Here the external surface of the charge turns out to be clad and burning of the charge occurs only on the internal surface and the end. In certain cases even ends are clad. Jacketing of the external surface of the grain leads also to an increase of the density of filling (loading) on account of removal of the radial clearance between the external surface of the grain and the walls of the chamber. Maximum increase of density of loading is attained during use of a solid rod charge (without internal channel) which burns only from the end turned toward the nozzle (Fig. 2.1). However such charges are characterized by a small rate of gas formation and therefore can be used only for an engine with low thrust with a long burning time. A tubular grain with an externally clad surface and internal cylindrical channel (Fig. 2.2) is characterized by a high burning surface progression and a considerable growth of pressure in the process of burning of the charge. Therefore charges made from such grains have not found wide application. For compensation of the burning progression of a tubular grain with an external jacket the grain form is changed by introduction of degressively burning surfaces. For this, from the

end of the grain over a certain part of its length longitudinal cuts (slots) of narrow width (Fig. 2.3) are made. The additional surface formed by the slots burns degressively. By selection of the number of slots and their relative length it is possible to secure a small change of burning surface of the grain.

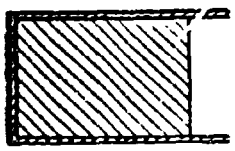

Fig. 2.1. Rod charge, burning from the end

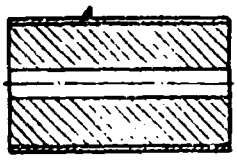

Fig. 2.2. Tubular grain with external jacket

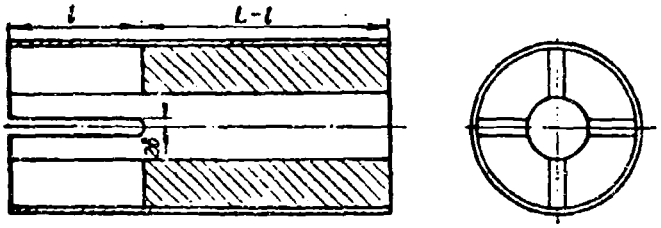

Fig. 2.3. Slot charge

Compensations of progression of the form of a tubular clad charge can be obtained also by giving part of the internal grain surface a conical form (Fig. 2.4).

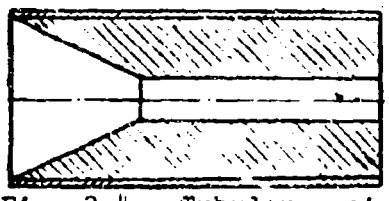

Fig. 2.4. Tubular grain with compensating cone

A small change of burning surface is attained also in externally clad grains with a star-shaped internal channel (Fig. 2.5), in multiport grains and in charges of "wagon wheel" configuration (Fig. 2.6).

A telescopic charge, consisting of a tubular grain, clad on the external surface and with an internal cylindrical rod (Fig. 2.7) with clad ends ensures constancy of the burning surface of a charge. However fixation of the internal rod presents well-known difficulties.

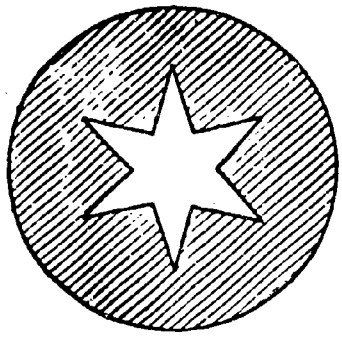

Fig. 2.5. Charge with star-shaped channel

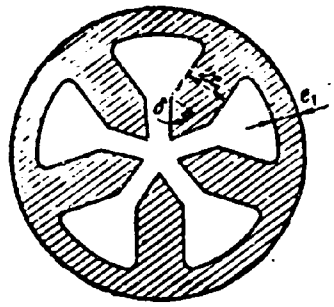

Fig. 2.6. Charge of "wagon wheel" configuration

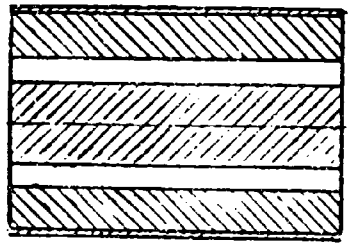

Fig. 2.7.
Telescopic Charge

Certain construction of charges, for example slot and star-shaped, are characterized by the presence of unburned fuel residues which appeared with a sharp pressure drop at the end of charge combustion. The presence of much unburned residue is undesirable, since this leads to a decrease of the total thrust pulse.

An important characteristic of a charge is its total burn time which depends on composition of the fuel and charge forrm. Charges intended for boosters and for antitank rockets are characterized by relatively great thrust and small burn time (on the order of fractions of a second or several seconds). Sustainers are characterized by a long burn time measured in tens of seconds.

In certain cases it can be necessary to select a charge which ensures a stepped thrust scheme. It is known that in surface-to-air rockets boosters of great thrust and sustainers of smaller thrust are used. Applications of a charge which ensures a stepped thrust characteristic permits eliminating the use of boosters.

A stepped thrust scheme can be ensured by filling the charge in the chamber in the form of concentric layers which burn at different rates. Here the internal rapidly burning layer ensures a thrust in booster conditions (Fig. 2.8). A stepped thrust scheme can be attained also by selection of a combined charge form. However

this decreases loading density.

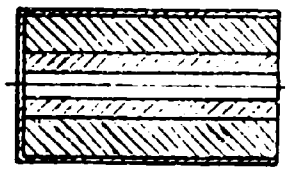

Fig. 2.8. A charge consisting of concentric fuel layers with different burn rates

Many of the forementioned requirements of a charge form are contradictory. The designer must look for a compromise solution which ensures the best technical characteristics of the vehicle.

Below are expounded methods of calculation of progression characteristics of certain types of charges.

§ 2.2. Single-Channel Unclad Cylindrical Grain Charge (Tubular Charge)

Let us consider the progression characteristic of an unclad cylindrical grain with internal channel.

We will begin with the relationships:

$$z=\frac{e}{e_1};\quad \sigma=\frac{S}{S_0};$$

$$\sigma_T=\frac{S_T}{S_{T0}};\quad \varphi=1-\frac{W}{W_0},$$

where e – variable thickness of burning layer; e_1 – maximum thickness of burning layer, $2e_1=R-r=\frac{D}{2}-r$ (R, r – external and internal radii of section of tube); S – total burning surface of tube; S_T – area of end of tube; W – volume of tube. Index 0 corresponds to the beginning of burn.

From elementary geometric notions we write:

$$S=2\pi[(R-e+r+e)(L-2e)+(R-e)^2-(r+e)^2];$$
$$S_0=2\pi[(R+r)L+R^2-r^2].$$

After division by L(R + r), substitution R - r = $2e_1$ and introduction of substitutions $\beta = \frac{2e_1}{L} = \frac{R-r}{L}$; $z = \frac{e}{e_1}$ we obtain

$$\sigma = \frac{S}{S_0} = 1 - \frac{2\beta z}{1+\beta}. \qquad (2.2)$$

The grain volume is determined from the expression:

$$W = \pi [(R-e)^2 - (r+e)^2] (L - 2e);$$
$$W_0 = \pi (R^2 - r^2) L,$$

whence it is easy to obtain:

$$\frac{W}{W_0} = (1-z)(1-\beta z);$$

$$\psi = 1 - \frac{W}{W_0} = (1+\beta) z - \beta z^2. \qquad (2.3)$$

Eliminating z from expressions (2.2) and (2.3), we obtain

$$\sigma = \sqrt{1 - \frac{4\beta}{(1+\beta)^2}\psi}.$$

Usually β is a value 0.03-0.05. Examining β as a value of first order of smallness and disregarding values of higher order of smallness, we will obtain

$$\sigma = 1 - 2\beta\psi. \qquad (2.4)$$

For example, when β = 0.05 and ψ = 1 we obtain a minimum value σ(1) = = 0.90 from expression (2.4) and σ(1) = 0.903 from expression (2.3). Obtained values of σ indicate that a charge made from a cylindrical unclad grain can be considered a charge of small degressiveness with linear a dependence of the progression characteristic σ on relative value of the burning charge ψ.

For the area of the end, proceeding from expressions:

$$S_T = \pi [(R-e)^2 - (r+e)^2];$$
$$S_{T0} = \pi (R^2 - r^2),$$

it is simple to obtain

$$\sigma_T = 1 - (1-\sigma)\frac{1+\beta}{2\beta},$$

or

$$\sigma_T = 1 - (1-\beta)\psi - \beta(1-3\beta)\psi^2.$$

Disregarding β^2 we obtain

$$\sigma_T = (1-\psi)(1+\beta\psi). \qquad (2.5)$$

For an end-clad grain the surface of burning is obtained constant:

$$S = S_0 = 2\pi(R+r)L; \quad \sigma(\psi) = 1.$$

In the case when a charge consists of several single-port grains, initital values of S_0 and S_{T0} are increased proportional to the number of grains, but values σ and σ_T, determined from expressions (2.4) and (2.5), remain constant.

§ 2.3. Slot Charge with External Clad Surface

We will examine a charge made from an externally clad surface cylindrical grain with an internal channel (Fig. 2.3). R and r – radii of external and internal cylinders, L – total length of grain. From one of the ends over length ℓ are cut slots of width 2δ. For determination of the progression characteristic of the charge σ we will examine separately the solid part of the grain and the part with cuts, which we will call the slotted part.

At an arbitrary thickness of the burning part of the charge e the length of the slotted part is increased by a value e. Considering that the "ceiling" of the slot takes the form of an arch, we will take the length of the slotted part equal to λe, where λ – the reduction factor determined below. Thus, for an arbitrary moment the length of the slotted part is equal to $\ell + \lambda e$, and the length of the solid part L is $\ell - \lambda e$.

Let us deduce the dependences which determine the progression characteristic of a slotted charge.

For the solid part of the grain.

Lateral burning surface

$$S_0^{\text{сп}} = 2\pi(r+e)(L-\ell-\lambda e).$$

Area of end

$$S_T^{\text{сп}} = \pi[R^2-(r+e)^2].$$

Total surface

$$S^{cn} = 2\pi(r+e)(L-l-\lambda e) + \pi[R^2-(r+e)^2]. \qquad (2.6)$$

Volume

$$W^{cn} = \pi[R^2-(r+e)^2](L-l-\lambda e). \qquad (2.7)$$

For the slotted part of the grain.

In Fig. 2.9 is shown a sector equal to 1/8 of the cross section of the slotted part. The solid line shows the initial perimeter of the section, and the dotted line the current perimeter, corresponding to combustion of thickness e of the charge. The current perimeter consists of arc AC and the segment of line CN. Let us connect points C and N by lines with the center of the section and note angles ϕ and α. Considering that

$$CN = R\cos\alpha - (r+e)\cos\varphi;$$
$$\widehat{AC} = (r+e)\left(\frac{\pi}{4}-\varphi\right),$$

we will obtain the full perimeter of the whole section

$$\Pi = 8\left[(r+e)\left(\frac{\pi}{4}-\varphi\right) + R\cos\alpha - (r+e)\cos\varphi\right],$$

where angles α and ϕ are found from the expressions:

$$\sin\alpha = \frac{\delta+e}{R};\ \sin\varphi = \frac{\delta+e}{r+e}. \qquad (2.8)$$

The arc part of the perimeter vanishes when angle ϕ, determined from expression (2.8), takes a value $\varphi \geqslant \frac{\pi}{4}$.

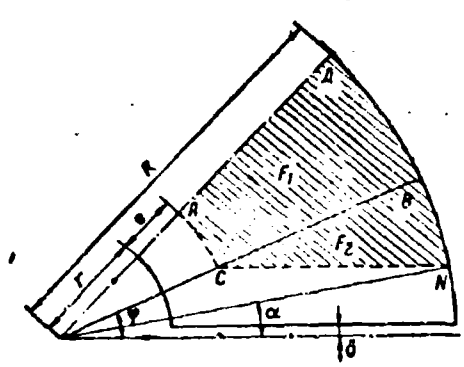

Fig. 2.9. Sector of slotted charge

The lateral burning surface is determined from expression

$$S_б^{сп} = 8\left[(r+e)\left(\frac{\pi}{4}-\varphi\right) + R\cos\alpha - (r+e)\cos\varphi\right](l+\lambda e).$$

The area of the end will be determined by including in it the area of the slot arch. Then

$$S_т^{сп} = S_т^{ка} = \pi[R^2 - (r+e)^2].$$

The total area of the slotted part is equal to

$$S^{сп} = 8\left[(r+e)\left(\frac{\pi}{4}-\varphi\right) + R\cos\alpha - (r+e)\cos\varphi\right](l+\lambda e) + \\ + \pi[R^2 - (r+e)^2]. \qquad (2.9)$$

In this expression when $\varphi \geqslant \frac{\pi}{4}$, which corresponds to disappearance of the arc part fo the perimeter, it is necessary to take $\varphi = \frac{\pi}{4}$.

The volume of the slotted part will be determined from expression

$$W^{сп} = 8(F_1 + F_2)(l+\lambda e),$$

where F_1 and F_2 – area of figures ADCB and CBN (Fig. 2.9).

$$F_1 = \left(\frac{\pi}{4} - \varphi\right)\frac{1}{2}[R^2 - (r+e)^2].$$

Area F_2 will be calculated by replacing arc BN by a chord:

$$F_2 = \frac{1}{2}CB \cdot CN \cdot \sin\varphi = \frac{1}{2}[R\cos\alpha - (r+e)\cos\varphi](R - r - e)\sin\varphi.$$

Thus,

$$W^{сп} = \{(\pi - 4\varphi)[R^2 - (r+e)^2] + 4[R\cos\alpha - \\ - (r+e)\cos\varphi](R - r - e)\sin\varphi\}(l+\lambda e). \qquad (2.10)$$

The total progression characteristic of the form of a slotted charge will be found from expression

$$S = S^{сп} + S^{ка} = 8\left[(r+e)\left(\frac{\pi}{4}-\varphi\right) + R\cos\alpha - (r+e)\cos\varphi\right] \times \\ \times (l+\lambda e) + 2\pi(r+e)(L - l - \lambda e) + 2\pi[R^2 - (r+e)^2]. \qquad (2.11)$$

The volume of the grain is determined from expression

$$W = W^{сп} + W^{ш} = \pi [R^2 - (r+e)^2](L - l - \lambda e) + \\ + ((\pi - 4\varphi)[R^2 - (r+e)^2] + 4[R\cos\alpha - (r+e)\cos\varphi] \times \\ \times (R - r - e)\sin\varphi)(l + \lambda e). \qquad (2.12)$$

Value S_0 and W_0, corresponding to the beginning of burning, are determined by substitution in expressions (2.11) and (2.12) of value $e = 0$.

Progression characteristics are determined from expressions:

$$\sigma = \frac{S}{S_0}; \quad \psi = 1 - \frac{W}{W_0},$$

which allow us to calculate the value of function $\sigma(\psi)$.

Since the area of the charge section is different in the solid and slotted part of the charge, then in this case it is impossible to determine the filling factor of the section of the chamber from expression (2.1).

By introducing the idea about the reduced initial area of the section of the charge determined from expressions $(S_{то})_{пр} = \frac{W_0}{L}$, we obtain the following expression for coefficient ε_0:

$$\varepsilon_0 = \frac{(S_{то})_{пр}}{F_k},$$

or finally

$$\varepsilon_0 = \frac{W_0}{LF_k}.$$

In conclusion we will examine the method of determination of the coefficient of reduction λ. During combustion of the thickness of the charge e the "ceiling" of the slot takes the form of an arch as shown in Fig. 2.10, where the dotted line corresponds to the current value e, and the solid line to the beginning of burning.

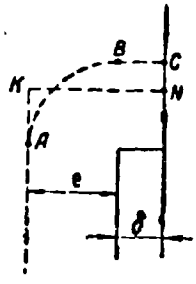

Fig. 2.10. Arch of "ceiling" of slot

The perimeter of the arch ABC is equal to $\delta + \frac{\pi e}{2} = \Pi_1$.

Let us replace real arch ABC by reduced arch AKN, whose height is equal to KA = λe, and the perimeter is equal to the perimeter of the real arch:

$$KA + KN = \lambda e + e + \delta = \Pi_2.$$

Equating $\Pi_1 = \Pi_2$, we obtain

$$\lambda e + e = \frac{\pi}{2} e,$$

whence

$$\lambda = \frac{\pi}{2} - 1 \approx 0{,}6.$$

We will examine an example of calculation of the progression characteristics of a slot charge with the following geometric parameters (dimensions in m):

$$R = 0{,}40;\ r = 0{,}12;\ L = 6{,}40;\ l = 2{,}13;\ \delta = 0{,}01.$$

Preliminarily we find boundary value e = e*, at which the arc part of the perimeter of the channel of the slot part vanishes. Value e* is from expression (2.8) when $\varphi = \frac{\pi}{4}$:

$$\sin\frac{\pi}{4} = \frac{\delta + e^*}{r + e^*},$$

whence e* = 0.26.

The maximum value of e is equal to $e_{max} = R - r = 0.28$.

Results of calculations are given in Table 2.1.

In Fig. 2.11 is given a graph of dependence $\sigma(\psi)$, from which it is clear that introduction of a degressively burning slotted part permits obtaining an insignificant change of the progression characteristic σ, where for the examined example $\sigma_{max} = 1.06$, $\sigma_{min} = 0.97$.

Coefficient ε_0 of filling of the section of the chamber by a charge is equal to

$$\varepsilon_0 = \frac{W_0}{LF_\text{п}} = \frac{W_0}{L\pi R^2} = \frac{2{,}88}{6{,}4\pi \cdot 0{,}4^2} = 0{,}895.$$

We note for comparison that for cylindrical clad charges freely packed in a chamber, we obtain $\varepsilon_0 \sim 0.7$.

Table 2.1

e	0	0,05	0,10	0,15	0,20	0,25	0,27	0,28
$\sin\varphi = (b+e):(r+e)$	0,083	0,353	0,500	0,593	0,657	0,710	0,710	0,710
φ°	4,8	20,6	30,0	36,4	41,1	45	45	45
$S_\varphi^{\text{пр}}$	6,20	5,34	4,38	3,37	2,18	0,49	0	0
$S_\varphi^{\text{сп}}$	3,22	4,52	5,81	7,07	8,35	9,83	10,15	10,30
$2S_\tau$	0,915	0,822	0,704	0,546	0,354	0,100	0,006	0
S	10,33	10,68	10,88	10,99	10,88	10,38	10,05	10,30
$W^{\text{пр}}$	0,93	0,65	0,41	0,22	0,084	0,034	0	0
$W^{\text{сп}}$	1,95	1,74	1,48	1,14	0,755	0,206	0,012	0
W	2,88	2,39	1,89	1,36	0,84	0,24	0,01	0
$\sigma = \frac{S}{S_0}$	1,000	1,032	1,051	1,065	1,051	1,005	0,973	0,995
$\psi = 1 - \frac{e}{e_0}$	0	0,172	0,172	0,347	0,530	0,710	0,916	1,00

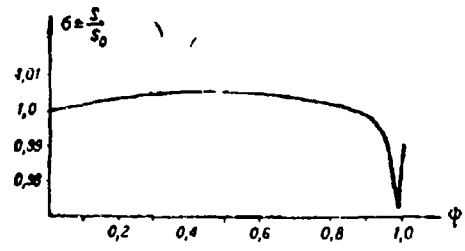

Fig. 2.11. Progression characteristic $\sigma(\psi)$

The character of change of the curve of progression burning $\sigma(\psi)$ in an essential measure depends on the relative length of slots $\frac{\ell}{L}$.. With an increase of this value, $\sigma(\psi)$ decrease. A close to unit value of $\sigma(\psi)$ corresponds to value $\frac{\ell}{L} \sim 0.3$.

§ 2.4 Charge with Star-Shaped Channel Section Burning from Within

During use of charges with a star-shaped channel section, reliable protection of walls of the chamber from the influence of hot gases is ensured, inasmuch as they come in contact with the internal surface of the chamber only at the actual end of burning.

The simplest form of such a charge is shown in Fig. 2.5. However it has not obtained practical application, since in regions of acute angles of the star a concentration of stresses appear which sharply increase receptivity of the charge to mechanical harm and lead to its cracking. In order to bring this undesirable phenomenon to a minimum, acute angles at summits must be rounded as shown in Fig. 2.12.

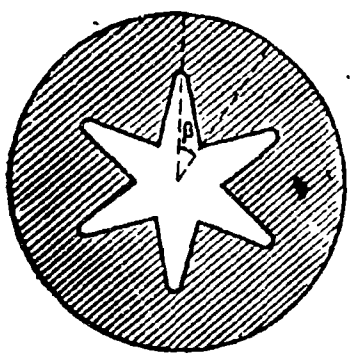

Fig. 2.12. Star-shaped charge with rounded angles

During the study of geometry of a charge with a star-shaped channel form it is possible to be limited to a consideration of one the sectors with a summit in the center and with the vertex angle $\beta = \frac{\pi}{n}$.

The cross section of the channel is constant over all its length.

The determining geometric parameters for a charge of such a form are:

Number of rays of star .....n

Relative thickness of burning arch .....$\bar{e}_1 = \frac{e_1}{D}$

Radius of curvature at summit of ray ... r, $\bar{r} = \frac{r}{D}$

Angle, subtending half of the initial arc of curvature .....α

Angle, subtending half of the arc of the sector during burning out of the charge by value e_1 ..ϕ_1

Vertex angle of forward charge ray .....θ

In general, burning of a charge with a star-shaped channel section can be divided into three phases (Fig. 2.13):

1. The burn front consists of an arc with radius r + e and a rectilinear section. Depending on selection of the initial geometric parameters, burning can be progressive, or with constant surface of burning (neutral) or degressive.

2. Rectilinear section vanishes. Burning occurs along the arc of radius r + e with decreasing angle ϕ. The end of this phase is designated by index 1.

3. Front of burning reaches walls of chamber. Burning takes on a sharply degressive character. Remainders of the charge burn at lowered pressure. Besides, on the pressure curve there appears a characteristic section of burn-down.

For the work process of engine only the first two phases of burning can be used.

The third phase, flowing with a sharp lowering of pressure, is accompanied by a fall of unit pulse, anomalies of burning, and therefore during selection of configuration of the charge it is necessary to see that the specific gravity of this phase in the process of burning is insignificant.

NOT REPRODUCIBLE

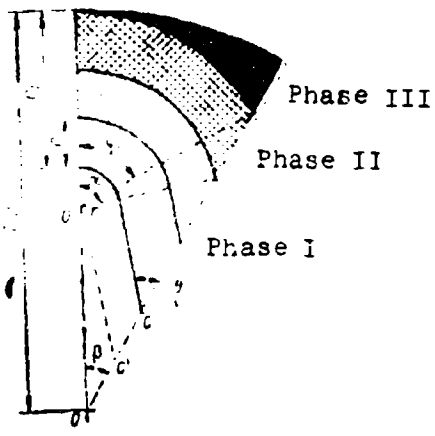

Fig. 2.13. Three phases of burning of charge

Degressive remainders of the charge actually are a supplement, to the passive weight of the rocket. In order to as far as possible reduce this increase, in the engine before filling of a composite fuel there are sometimes placed inserts of light material (foam plastic), corresponding in form and dimensions to degressive remainders of the charge [1].

Let us find the dependence of the perimeter of burning on thickness of the burning arch for the first phase (Fig. 2.14). For this we will conduct from point O_1 segment O_1C', parallel to the linear section of burning, and segment O_1F, perpendicular to ray OM. From the right triangle OO_1F we obtain

$$O_1F = OO_1 \sin\beta = \left(\frac{D}{2} - e_1 - r\right)\sin\beta.$$

From right triangle O_1FC' we find

$$O_1C' = \frac{O_1F}{\sin\theta} = \frac{\left(\frac{D}{2} - e_1 - r\right)\sin\beta}{\sin\theta}.$$

The length of the rectilinear burning section

$$BD = O_1C' - (r + e)\operatorname{ctg}\theta.$$

The initial value of the perimeter of burning

$$\Pi_0 = 2\pi(r\alpha + KC) = 2\pi\left[r\alpha + \frac{\left(\frac{D}{2} - e_1 - r\right)\sin\beta}{\sin\theta} - r\operatorname{ctg}\theta\right] \qquad (2.13)$$

or in a dimensionless expression

$$\bar{\Pi}_0 = \frac{\Pi_0}{D} = 2\pi\left[\bar{r}\alpha + \frac{(0{,}5 - \bar{e}_1 - \bar{r})\sin\beta}{\sin\theta} - \bar{r}\operatorname{ctg}\theta\right]. \qquad (2.14)$$

The current value of the perimeter of burning

$$\Pi = 2\pi\left[(r + e)\alpha + \frac{\left(\frac{D}{2} - e_1 - r\right)\sin\beta}{\sin\theta} - (r + e)\operatorname{ctg}\theta\right]. \qquad (2.15)$$

The relative change of the perimeter of burning in the first phase

$$\varphi_{\Pi_1} = \frac{\Pi}{\Pi_0}. \qquad (2.16)$$

We will examine, under what conditions in this phase of burning constancy of the perimeter of burning can be ensured. During a shift of the front of burning by value e a change of arc length will be αe. The length of the rectilinear section will be reduced by the value of segment e × ctg θ. The perimeter of burning for every

sector of the charge will be changed by value $\alpha e - e \times \operatorname{ctg} \theta$. Consequently, the condition of constancy of the perimeter of burning can be written as

$$\alpha = \operatorname{ctg} \theta. \tag{2.17}$$

From triangle OO_1C' $\angle OO_1C' = \theta - \beta$. Hence the sum of angles at summit O_1 can be written as

$$\alpha = \alpha + \frac{\pi}{2} + \theta - \beta.$$

Substituting value α from expression (2.17), we will obtain

$$\frac{\pi}{2} + \beta = \operatorname{ctg} \theta + \theta. \tag{2.18}$$

Or when $\beta = \frac{\pi}{n}$ we have

$$\frac{\pi}{2} + \frac{\pi}{n} = \operatorname{ctg} \theta + \theta. \tag{2.19}$$

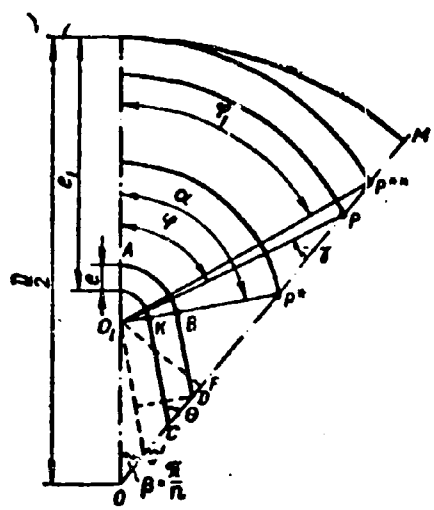

Fig. 2.14. Diagram for calculation of progression characteristic

From equation (2.19) we find value θ^*, single for every assigned number of rays of the star, ensuring constancy of the surface of burning in the first phase. These values of θ^* together with corresponding values of α^* from equation (2.17) are given in Table 2.2 [2].

Table 2.2

n	θ^*, deg	α^*, rad	δ^*, deg	n	θ^*, deg	α^*, rad	δ^*, deg
4	28,21	1,865	61,80	9	38,83	1,242	5,10 и 50
5	31,12	1,657	58,55	10	40,20	1,183	7,50 и 48,35
6	33,53	1,509	56,04	11	41,41	1,133	9,90 и 46,80
7	35,55	1,399	53,75	12	42,52	1,091	12,00 и 45,30
8	37,30	1,313	51,80				

The end of the first phase of burning (see triangle OO_1P^*) is determined by equality

$$\frac{O_1P^*}{O_1O} = \frac{e^* + r}{\frac{D}{2} - (e_1 + r)} = \frac{\sin\beta}{\cos\theta}.$$

Hence we find thickness of the arch burning toward the end of the first phase:

$$e^* = \left(\frac{D}{2} - e_1 - r\right)\frac{\sin\beta}{\cos\theta} - r. \qquad (2.20)$$

For the second phase of burning the perimeter is changed as is the length of arc $\phi(r + e)$, where angle ϕ at summit O_1 is equal to $\beta + \gamma$. Angle γ is determined from right triangle O_1PF, as arc sin $\left(\frac{O_1F}{O_1P}\right)$.

Consequently, for the second phase

$$\Pi = 2\pi(r + e)\left[\beta + \arcsin\frac{\left(\frac{D}{2} - r - e_1\right)\sin\beta}{r + e}\right]. \qquad (2.21)$$

At the beginning of the second phase

$$\Pi_{2,0} = 2\pi(r + e^*)\alpha. \qquad (2.22)$$

The change of the perimeter of burning in the second phase relative to the initial value for this phase will be

$$\sigma_{\Pi_2} = \frac{\Pi_2}{\Pi_{2,0}} = \frac{r+e}{r+e_1}\left[\frac{\beta}{\alpha} + \frac{1}{\alpha}\arcsin\frac{\left(\frac{D}{2}-r-e_1\right)\sin\beta}{r+e}\right]. \qquad (2.23)$$

In certain cases the second phase can be absent (Fig. 2.15). This occurs when

$$\alpha < \beta + \arcsin\frac{\left(\frac{D}{2}-r-e_1\right)\sin\beta}{r+e_1}. \qquad (2.24)$$

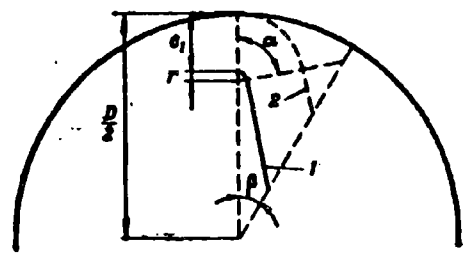

Fig. 2.15. Diagram for two phases of burning

For the end of the second phase the change of perimeter of burning relative to its value for the beginning of burning will be

$$\sigma_{\Pi} = \sigma_{\Pi_1} \cdot \sigma_{\Pi_2}. \qquad (2.25)$$

The ratio of area of the cross section of remainders after burn-out of charge by value e_1 to the initial area of the end of charge is called the remainder factor

$$\Lambda_{\Pi} = \frac{S_{\text{ост}}}{S_{\text{у}_0}} = \frac{\Lambda_{\text{к}}}{\varepsilon_0},$$

where

$$\Lambda_{\text{к}} = \frac{S_{\text{ост}}}{F_{\text{к}}}; \quad \varepsilon_0 = \frac{S_{\text{у}_0}}{F_{\text{к}}}.$$

The value of coefficient Λ_K, determined with respect to area of the chamber, is equal to [3]:

$$\Lambda_{\text{к}} = 1 - \frac{4\alpha}{\pi}\left[(\bar{r}+\bar{e}_1)^2\varphi_1 + (\bar{r}+\bar{e}_1)(0{,}5-\bar{r}-\bar{e}_1)\sin\varphi_1\right]. \qquad (2.26)$$

The coefficient of filling of a cross section of the chamber by the charge is expressed by the dependence [3]:

$$\epsilon_0 = 1 - \frac{4\alpha}{\pi}\left[\left(0{,}5 - \bar{e}_1 - \bar{r} + \frac{\bar{r}}{\cos\alpha}\right)^2 \frac{\sin\beta\cdot\cos\alpha}{\sin\theta} + \bar{r}^2(\alpha - \operatorname{tg}\alpha)\right]. \qquad (2.27)$$

The relative amount of the burning part of the charge with clad ends will be defined as

$$\phi = 1 - \frac{\epsilon}{\epsilon_0},$$

where $\epsilon = \frac{S_T}{F_\pi}$ – current value of ratio of area of end of charge to area of cross section of chamber.

Value ϵ is determined differently for the first and second phases of burning. For the first phase of burning, analogous to (2.27) we obtain

$$\epsilon = 1 - \frac{4\alpha}{\pi}\left[\left(0{,}5 - \bar{e}_1 - \bar{r} + \bar{e} + \frac{\bar{r} + \bar{e}}{\cos\alpha}\right)^2 \frac{\sin\beta\cos\alpha}{\sin\theta} + \right.$$
$$\left. + (\bar{r} + \bar{e})^2(\alpha - \operatorname{tg}\alpha)\right]. \qquad (2.28)$$

For the second phase of burning we obtain

$$\epsilon = 1 - \frac{4\alpha}{\pi}\left[(\bar{r} + \bar{e})^2\varphi + (\bar{r} + \bar{e})(0{,}5 - \bar{r} - \bar{e})\sin\varphi\right]. \qquad (2.29)$$

Using the first phase of burning formulas (2.28) and (2.15) and for the second phase of burning formulas (2.29) and (2.21), it is possible to construct dependence $\epsilon = f(\phi)$.

The relative change of full surface of burning of a charge during burn-out of the charge by value e_1 for the case of unclad ends will be:

$$\epsilon_g = \frac{2\pi\Pi_\varphi\varphi_g(L - 2e_1) + 2S_{\text{осн}}}{2\pi\Pi_\varphi L + 2S_{\text{осн}}}, \qquad (2.30)$$

or

$$\epsilon_g = \frac{\pi\Pi_\varphi\varphi_g(L - 2\bar{e}_1) + \frac{\pi}{4}\Lambda_\pi}{\pi\Pi_\varphi L + \frac{\pi}{4}\epsilon_0}. \qquad (2.31)$$

For the case of clad ends

$$\epsilon_g = \epsilon_0.$$

When it is necessary to maintain a constant surface it is expedient to originate from dependence $\sigma = f(z)$ with neutral burning in the first phase (Fig. 2.16). Such a form of dependence is ensured when $\sigma = \sigma^*$.

As calculations show [3], for every value n there exists a single geometric variant ensuring constancy of the surface of burning in both phases.

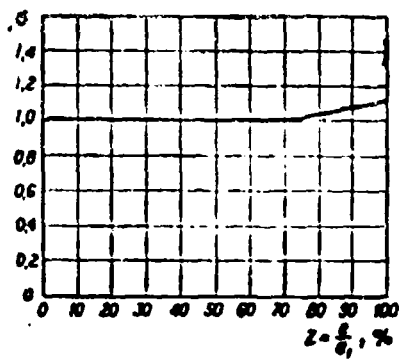

Fig. 2.16. Simplified dependence $\sigma(z)$

Basic characteristics of these variants are given in Table 2.3.

Table 2.3

Characteristics	$\sigma_s = 1,0$			$\sigma_s = 1,10$		
n	6	7	8	6	7	8
$\bar{\sigma}_1$	0,150	0,142	0,125	0,206	0,190	0,181
η_σ, %	82,4	75,5	67	86,5	79,6	75,7
A_σ, %	15	12,7	11,7	8,8	5,3	6,9

An essential deficiency of a charge with a star-shaped channel section is the great weight of degressively burning remainders. For variants with a constant burning surface their weight is 16-18%. The usefully utilized weight of the charge increases if one allows certain progressive burning in the second phase. In Table (2.3) are given characteristics of charges when $\sigma_S = 1.10$. From a comparison of data it follows that an increase of allowed progression sharply lowers the weight of degressively burning remainders, and also leads to an increase in thickness of the burning arch and density of loading.

In Fig 2.17 it is shown how basic characteristics of the examined type of charge change with an increase in the number of rays of the star with preservation of constancy of the perimeter of burning in the first phase. From the graph it is clear that with an increase in the number of rays of the star there is a drop in the coefficient of filling of the chamber with fuel, and an increase of surface progression. Simultaneously the coefficient of remainder Λ_K descends. For practice, most interesting are charges with number of rays n = 6, 7, 8, for which constancy of the surface of burning is ensured with a relatively high thickness of the burning arch and an acceptable value of ε_0.

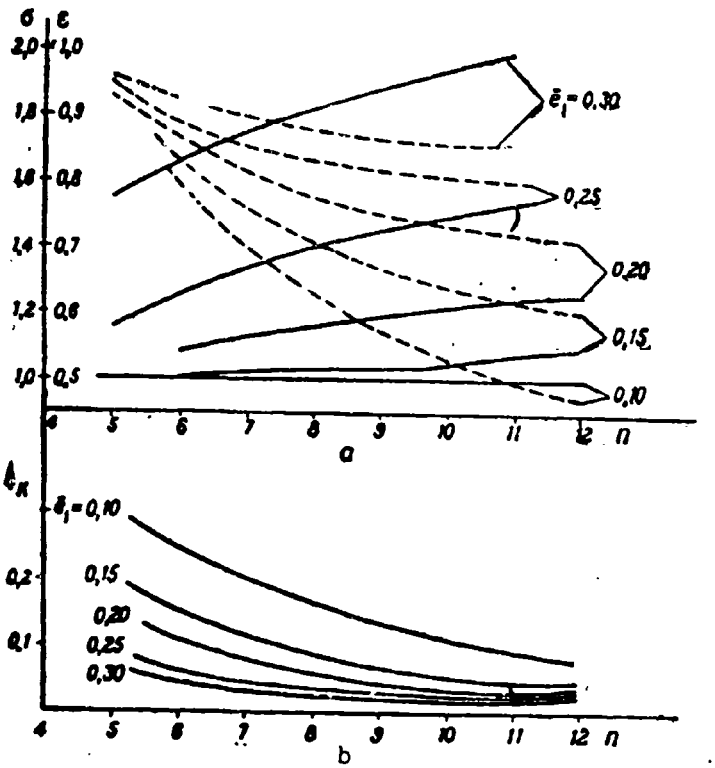

Fig. 2.17. Dependence of charge characteristics on number of rays

In Fig. 2.18 basic characteristics of a charge of given type are represented depending on relative thickness of the burning arch. As follows from the graph, constancy or a change in minimum limits of the surface of burning for a given type of charge can be ensured only during relative thickness of an arch not more than $\bar{\varepsilon}_1$ = 0.15-0.20.

The simplest modification of the examined charge form is represented in Fig. 2.19. Here between internal flanges are sections of a cylindrical surface.

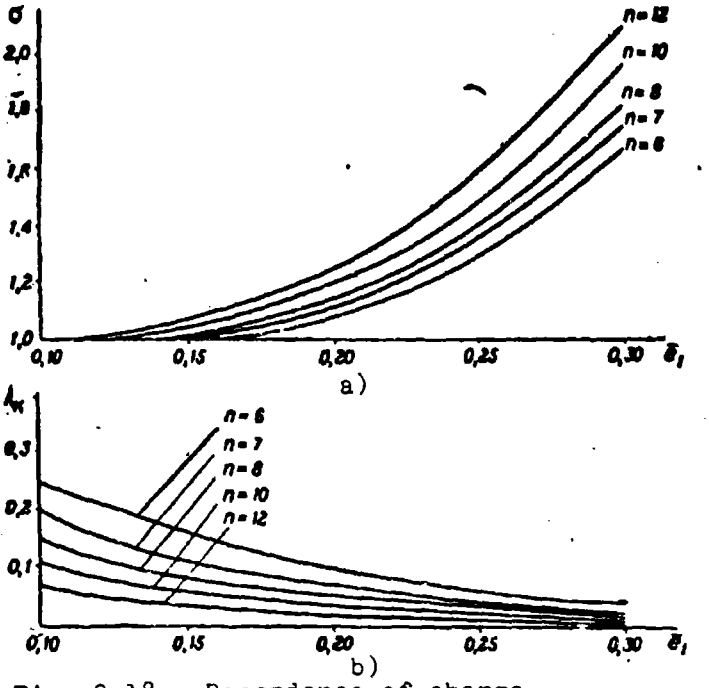

Fig. 2.18. Dependence of charge characteristics on relative thickness of a burning arch $\bar{e}_1$.

For internal flanges with rounding the dependences given above remain in force with the only distinction that angle β must be calculated as $\eta \frac{\pi}{n}$, where η – part on forward section of sector $\beta' = \frac{\pi}{n}$.

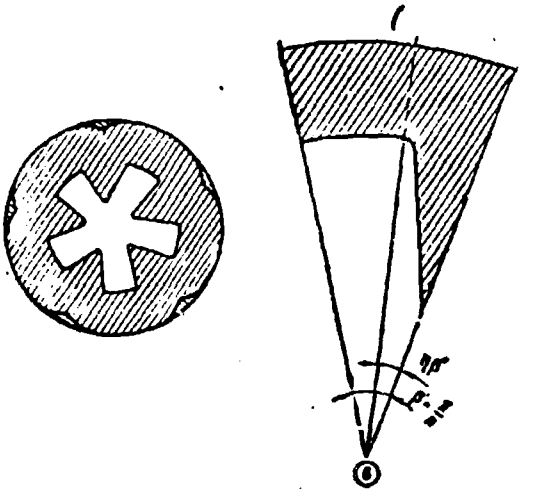

Fig. 2.19. Modified form of a charge with a star-shaped channel section.

The basic dependences for this charge take the form

$$\varepsilon_0 = 1 - \frac{4n}{\pi}\left[\left(0{,}5 - \bar{e}_1 - \bar{r} + \frac{\quad}{\cos\alpha}\right)^2 \frac{\sin\eta\frac{\pi}{n}\cos\alpha}{\sin\theta} + \right.$$
$$\left. + \bar{r}^2(\alpha - \operatorname{tg}\alpha)\right] - (1 - 2\bar{e}_1)^2(1 - \eta).$$

The initial value of the perimeter is

$$\Pi_0 = 2n\left\{\frac{\pi}{n}(0{,}5 - \bar{e}_1)(1 - \eta) + \bar{r}(\alpha - \operatorname{ctg}\theta) + \right.$$
$$\left. + \frac{(0{,}5 - \bar{e}_1 - \bar{r})\sin\eta\frac{\pi}{n}}{\sin\theta}\right\}.$$

The current value of the perimeter on the first phase of burning is

$$\bar{\Pi} = 2n\left\{\frac{\pi}{n}(0{,}5 - \bar{e}_1 + \bar{e})(1 - \eta) + (\bar{r} + \bar{e})\alpha + \right.$$
$$\left. + \frac{(0{,}5 - \bar{e}_1 - \bar{r})\sin\eta\frac{\pi}{n}}{\sin\theta} - (\bar{r} + \bar{e})\operatorname{ctg}\theta\right\}.$$

The condition of constancy of the perimeter of burning in the first phase preserves the former form (2.19); consequently, during calculation we can use the data of the Table (2.2).

The end of first phase occurs when the relative thickness of the burning layer is

$$\bar{e}^* = (0{,}5 - \bar{e}_1 - \bar{r})\frac{\sin\eta\frac{\pi}{n}}{\cos\theta} - \bar{r}.$$

Consequently, the duration of the first phase for such a modification will be less than for the initial variant.

For the second phase, a change of the perimeter of burning obeys the dependence:

$$\bar{\Pi} = 2n\left\{\left[(\bar{r} + \bar{e})\eta\frac{\pi}{n} + \arcsin\frac{(0{,}5 - \bar{e}_1 - \bar{r})\sin\eta\frac{\pi}{n}}{\bar{r} + \bar{e}}\right] + \right.$$
$$\left. + (0{,}5 - \bar{e}_1 + \bar{e})(1 - \eta)\frac{\pi}{n}\right\}.$$

The coefficient of remainder, determined with respect to the area of the chamber, is calculated by dependence (2.26).

With an identical number of rays n and equal thickness of the arch $\bar{e}_1$, the modified variant differs from the initial by a smaller coefficient of remainder. Simultaneously the coefficient of filling ε_0 descends. With a decrease of n thickness $\bar{e}^*$ descends and accordingly progression of burning in the second phase is increased. Due to this, according to a lowering of n the upper limit of the range, in which constancy of the surface of burning is ensured, is displaced in the direction of smaller values $\bar{e}_1$.

A change of the form of projections in the modified variant leads to a new type of charge, whose cross section reminds one of a wagon wheel (Fig. 2.6). Burning of such a charge also flows in three phases. A distinctive peculiarity of its burning is a sharp reduction of the surface of burning during transition to a second phase which can be used to ensure a stepped thrust scheme in flight. However when necessary, neutral burning of such a charge can be obtained. The values of angle δ^* ensuring constancy of the surface of burning are given in Table 2.2.

As analysis shows, for such a charge constancy of the surface of burning in combination with a relatively high coefficient of filling can be obtained only when n = 5. A graph for determination of basic parameters of the charge when n = 5 is shown in Fig. 2.20.

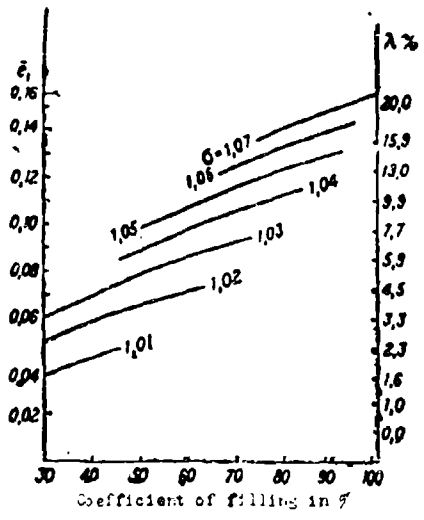

Fig. 2.20. Graph for determination of parameters of charge of the "wagon wheel" type

For charges of wheel-like form the possible values of $\bar{e}_1$ do not exceed 0.2, whereas for charges with a star-shaped channel $\bar{e}_1$ can reach 0.33.

Therefore, charges of wheel-like form are expediently used in and engine with a relatively short burn time.

The furthest development of the given type of charge is a wheel-like form with alternating long and short projections (Fig. 2.21). Different relationships of length and thickness of projections make it possible to ensure constancy of thrust, a two-stage change of thrust, or a three-step change of thrust.

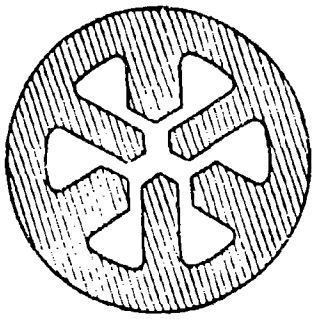

Fig. 2.21.
Modified form of
"wagon wheel"
charge

In conclusion one should note that application of casting technology of charging an engine permits obtaining charges with a channel which varies over its length in dimensions and form. This opens wide possibilities of changing progression characteristics of elementary geometric forms in a desirable direction.

§ 2.5. A Charge Made from Two Fuels with Different Burn Rates

When charging rocket engines with composite fuels it is possible to obtain charges consisting of two fuels with different burn rates.

The relation of burn rates is an additional parameter which expands the possibility of ensuring required burning behavior of a charge.

It is possible to separate two basic types of such charges.

1. The interface of the two fuels coincides with a certain intermediate position of the surface of burning. Here the process of burning of the charge is divided into periods during which only one of the fuels burn.

2. The interface of the two fuels never coincides with a surface of burning and simultaneous burning of both fuels occurs where the current relationship of their surfaces of burning is determined by the interface profile.

Charges of first type (Fig. 2.22) found application in single-chamber two-mode engines [4]. The burning process of the charge in such an engine includes a start period (use of rapidly burning fuel) and a sustainer period (use of fuel with slow burning rate). Calculation of the progression characteristics of such charges contains nothing new; for each of the periods of burning these

characteristics are calculated by usual dependences for basic forms of charges.

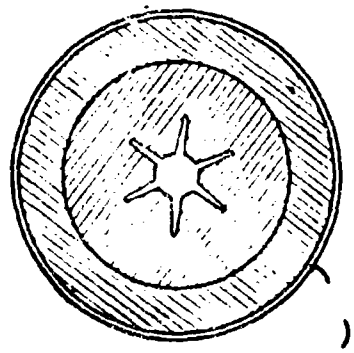

Fig. 2.22. Diagram of charge made from two consecutively burning fuels.

We will examine charges of the second type.

Let us consider the diagram of a charge in which fuel a with a greater burning rate is located in the central part, and fuel б with a smaller rate is on the periphery (Fig. 2.23).

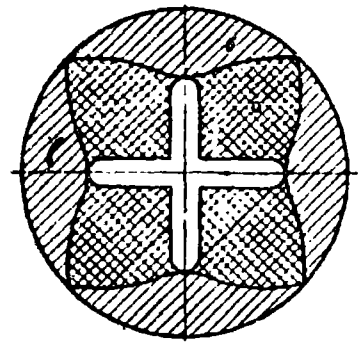

Fig. 2.23. Diagram of a charge made from two simultaneously burning fuels with different burn rates.

Such a charge, in contrast to the one examined in the preceding paragraph, permits obtaining the required law of change of the surface with any relative thickness of the burning arch. Here it becomes possible to ensure neutral burning for charges with a great relative thickness of the burning arch which are used in engines with a long operation time. Furthermore, by selecting the interface

profile of the two fuels it is possible to ensure that the surface of burning in the very last moment will coincide with the internal surface of the chamber, i.e., to avoid formation of degressive remainders. Charging of the engine in this case is produced in two procedures. During casting of the slowly burning fuel in the body there is placed a mandrel which occupies the volume of the internal channel and the rapidly burning fuel. After termination of charging the mandrel is removed and in its place there is set a second mandrel which ensures formation of the internal channel and charging of the engine with the rapidly burning fuel is produced [1]. In Fig. 2.24 there is a section of such a combined charge which is utilized in the second-stage engine of the "Minuteman" rocket [1].

REPRODUCIBILITY OF THE ORIGINAL PAGE IS POOR

Fig. 2.24. Charge of ballistic missile made from two fuels with different burn rates.

We will examine how the geometry of the combined charge is selected. Let us assume that the burning rate of fuel б equals u, and of fuel a equals $k_u u$.

We will consider that during a change of pressure in the engine the ratio of burn rates k_u is preserved constant. We will also consider that fuels a and b differ only by burn rates and have identical chemical composition and power characteristics. The problem consists of finding the form of interface of the two fuels which will ensure burning of the charge without degressive remainders. The set requirement is fulfilled if the burning front of fuel б at every arbitrary instant has a circular arc with center at point 0 radius R + e (Fig. 2.25). At that same instant the burn front of fuel a will stand from the initial position on a normal at distance $k_u e$. Consequently, the profile of the interface will be determined

by the intersection of circumferences of radius R + e and perimeters of burning of fuel a, constructed for the same instants. In general the perimeter of burning for fuel a will consist of a rectilinear section and an arc of radius $r + k_u e$.

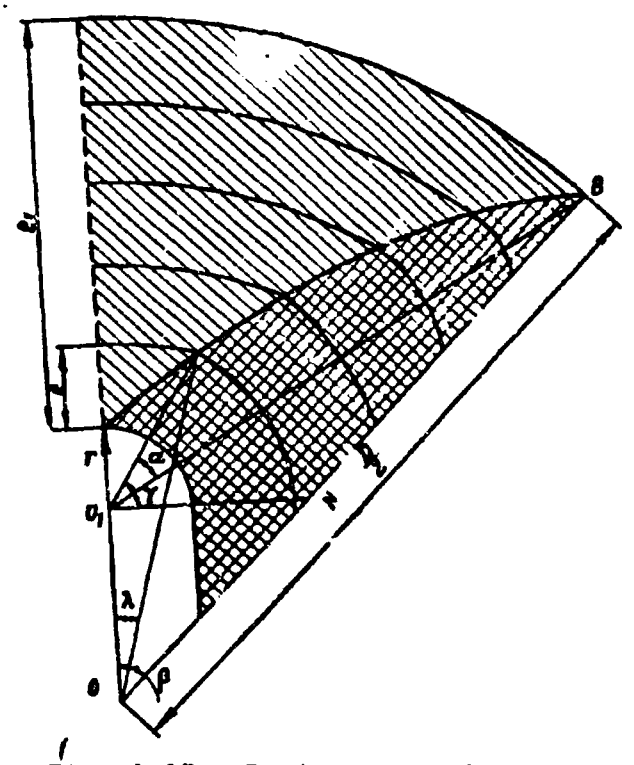

Fig. 2.25. Basic geometric parameters of a charge of two fuels.

In examining the progression characteristics of a combined charge it is expedient to introduce the idea of effective surface of burning

$$S_f = S_б + k_a S_a,$$

where $S_б$ and S_a – respectively surface of burning of fuels б and a.

Introduction of effective surface of burning permits considering internal ballistics of an engine with the use of usual dependences in terms of the burning rate of fuel б.

Applied to a two-dimensional problem we will obtain

$$\Pi_f = \Pi_б + k_u \Pi_a,$$

where Π_f – effective current value of perimeter of burning.

In a general case

$$\Pi_f = \left(\frac{D}{2} - e_1 + e\right)\lambda + (r + k_u e)\gamma + \left[\left(\frac{D}{2} - e_1 - r\right)\frac{\sin\beta}{\sin\theta} - (r + k_u e)\operatorname{ctg}\theta\right],$$

where

$$\lambda = \arccos\frac{\left(\frac{D}{2} - e_1 - r\right)^2 + \left(\frac{D}{2} - e_1 + e\right)^2 - (r + k_u e)^2}{2\left(\frac{D}{2} - e_1 + e\right)\left(\frac{D}{2} - e_1 - r\right)};$$

$$\gamma = \arccos\frac{\left(\frac{D}{2} - e_1 + e\right)\sin\lambda}{r + e};$$

e_1 – maximum thickness of burning arch of fuel б.

During burning of fuel a the same phases of burning are possible which are observed for a usual star. Here also are possible those cases when burning goes to an end with preservation of the rectilinear section.

If line O_1N intersects the curve of division of the two fuels, at a certain stage of burning the curvilinear section of burning of fuel a vanishes. One of the necessary conditions of neutral burning is intersection at one point on the surface of the chamber of the curve of division of the two fuels and ray O_1B. Here there should be fulfilled relationship

$$e_1 = \frac{O_1B - r}{k_u}.$$

The initial effective value of the perimeter of burning is calculated by formula (2.13) and then multiplied by k_u.

The coefficient of filling of the chamber is calculated by formula (2.27).

Analysis of characteristics of combined charges shows that an acceptable constancy of the effective surface (perimeter) burning is ensured at small values of n. Thus, for example, best constancy of surface ($\Delta S_f/S_{f0} = \pm 1\%$) is attained for n = 3 when k_u = 1.74, for n = 4 when k_u = 1.48. For n = 5, $\Delta S_f/S_{f0} = \pm 3\%$ is ensured when k_u = 1.32 [5].

For $n = 4$ during best constancy of the surface the allowable relative thickness of the burning arch when $\bar{r} = 0.05-0.25$ is accordingly $\bar{e}_1 = 0.46-0.29$.

A basic deficiency of combined charges is high sensitivity of progression characteristics to a change of the ratio of burning rates k_u. During deflection of k_u from computed values due to scattering of burning rates of fuels there occurs deflection from neutral burning and possibly the appearance of degressive remainders.

Literature

1. Mezhkontinental'yy ballisticheskiy snaryad "Minitmen" firmy "Boing" ("Minuteman" ICBM, Boeing). "Voprosy raketnoy tekhniki", 1963, No. 6.

2. Barrer, M., Zhomott, A., Vebek, B. F., Vandenkerkkhove Zh. Raketnyye dvigateli (Rocket engines). Oborongiz, 1962.

3. Stoun, M., Prakticheskiy matematicheskiy raschet konfigur konfiguratsii zaryada (Practical mathematical calculations of charge configuration). "Voprosy raketnoy tekhniki", 1958, No. 6.

4. Darvell, Kh. Dvukhrezhimnyye dvigateli na tverdom toplive (Two-mode solid fuel engines). "Voprosy raketnoy tekhniki", 1963, No. 5.

5. Barrere M., Larue, P. Fusées á propergol solide utilisant deux poudres ayant des vitesses de combustion differentes. Rech. aeronaut, 1962, No. 91.

C H A P T E R III

WORKING CHARACTERISTIC OF RDTT

§ 3.1. Parameters of Gas from RDTT Nozzle

During deviation of basic dependences for parameters of gas flow from a nozzle, one usually considers the process of outflow to be one dimensional and steady, where flow parameters are not changed as a function of time and are constant for every section perpendicular to the axis of the engine and nozzle. If, moreover, one does not consider the change of gas composition and its heat capacity along the flow, and also heat exchange with walls of the engine chamber and the nozzle, then from the equation of conservation of energy we obtain the following dependence for exit velocity of gases:

$$v = \sqrt{\frac{2gk}{k-1} RT_0 \left(1 - \pi^{\frac{k-1}{k}}\right)}, \tag{3.1}$$

where

$$\pi = \frac{p}{p_0},$$

p_0, T_0 – parameters of gas in chamber section in which it is possible to take speed of gases $v_0 = 0$; values p, v corresponds to an arbitrary flow section.

In reference to [RDTT] (РДТТ) conditions we will introduce the designation

$$f_p = RT_{0p}$$

where T_{0p} – combustion temperature of fuel at constant pressure in engine chamber; f_p – reduced force of powder.

For calculation of the lowering of temperature of gases due to heat transfer from gases to the body of the engine, we will introduce

in the expression (3.1) for exit velocity coefficient $\chi < 1$. Here we will obtain

$$v = \sqrt{\frac{2gk}{k-1}\chi f_p\left(1-\pi^{\frac{k-1}{k}}\right)}. \qquad (3.2)$$

The method of determination of coefficient χ will be examined in Chapter VI. Certain authors introduce before the root in the formula for computing exit velocity of gases an experimental "coefficient of speed." We will consider this coefficient included in parameter $\sqrt{\chi}$, which is determined or definitized by experiment.

For a one second mass flow rate of gases G through a certain section F of the nozzle we have the expression

$$G = gF\sqrt{\frac{2k}{k-1}p_0\rho_0\left(\pi^{\frac{2}{k}}-\pi^{\frac{k+1}{k}}\right)}. \qquad (3.3)$$

During steady motion of gases the flow rate per second in all sections of flow is identical. Therefore the least section of the nozzle corresponds to a maximum of the subradical expression (3.3). Besides

$$\pi_{кр} = \left(\frac{2}{k+1}\right)^{\frac{k}{k-1}} \qquad (3.4)$$

and expression (3.3) takes the form

$$G_{кр} = gF_{кр}\sqrt{\frac{2k}{k-1}p_0\rho_0}\left(\frac{2}{k+1}\right)^{\frac{1}{k-1}}. \qquad (3.5)$$

In reference to conditions of an RDTT engine it is convenient to give the last expression the form

$$G = \frac{\varphi A F_{кр} p_0}{\sqrt{\chi T_p}}, \qquad (3.6)$$

where

$$A = \left(\frac{2}{k+1}\right)^{\frac{1}{k-1}}\sqrt{\frac{2gk}{k+1}};$$

ϕ – coefficient which considers narrowing of the stream in critical section.

Values A for different values of the adiabatic index are given in Table 3.1. Considering constancy of flow rate per second along the nozzle from expressions (3.3) and (3.5) can be obtained ratio

$$\frac{F}{F_{кр}} = \frac{\left(\frac{2}{k+1}\right)^{\frac{1}{k-1}}\sqrt{\frac{k-1}{k+1}}}{\sqrt{\pi^{\frac{2}{k}}-\pi^{\frac{k+1}{k}}}}. \qquad (3.7)$$

Table 3.1

k	1,20	1,21	1,22	1,23	1,24	1,25	1,26	1,27	1,28	1,29	1,30
A	2,031	2,036	2,042	2,048	2,053	2,060	2,065	2,072	2,078	2,081	2,091

which sets the relationship between relative pressure $\pi = \frac{p}{p_0}$ and area of the nozzle section F. Instead of the ratio of areas $\frac{F}{F_{кр}}$ subsequently we will examine the ratio of diameters $\zeta = \frac{d}{d_{кр}}$.

Table 3.2. Subsonic region $\pi = f(k, \zeta)$.

ζ \ k	1,20	1,21	1,22	1,23	1,24	1,25	1,26	1,27	1,28	1,29	1,30
5,0	1,000	1,000	1,000	1,000	1,000	1,000	1,000	1,000	1,000	1,000	1,000
4,5	0,999	999	999	999	999	999	999	999	999	999	999
4,0	999	999	999	999	999	999	999	999	999	999	999
3,5	999	999	999	999	999	999	999	999	999	999	999
3,0	998	998	998	997	997	997	997	997	997	997	997
2,9	997	997	997	997	997	997	997	997	997	997	997
2,8	997	997	997	997	997	996	996	996	996	996	996
2,7	996	996	996	996	996	996	996	996	996	996	996
2,6	995	995	995	995	995	995	995	995	995	995	995
2,5	995	995	995	995	995	994	994	994	994	994	994
2,4	994	994	994	994	994	993	993	993	993	993	993
2,3	993	993	993	993	993	992	992	992	992	992	992
2,2	991	991	991	991	991	991	991	991	991	991	991
2,1	990	990	990	990	989	989	989	989	989	989	989
2,0	987	987	987	987	987	986	986	986	986	986	986
1,9	984	984	984	984	984	983	983	983	983	983	983
1,8	980	980	980	980	980	979	979	979	979	979	979
1,7	975	975	975	974	974	974	974	974	973	973	973
1,6	968	968	968	968	968	967	967	967	967	967	967
1,5	957	957	956	955	955	955	955	955	954	954	954
1,4	942	942	941	940	940	940	939	939	939	938	938
1,3	916	916	915	915	915	914	914	914	914	913	913
1,2	882	881	880	880	879	878	877	876	876	875	874
1,1	816	815	815	813	813	812	812	811	810	810	809

In Tables 3.2 and 3.3 are given dependences $\pi = f(\zeta)$ for different k. Table 3.2 corresponds to the narrowing part of the nozzle in which to a decrease of ζ there corresponds a decrease of pressure. In this part of the nozzle the flow is subsonic. Data of Table 3.3 correspond to the divergent section of the nozzle in which to a pressure drop corresponds an increase of nozzle section. In this part of the nozzle the flow is supersonic.

<u>Example</u>: From conditions $p_0 = 60 \frac{kg}{cm^2}$, $d_{кр} = 15$ cm, $d_a = 30$ cm we find for the outlet section $\zeta = 2$. When $k = 1.25$ by Table 3.3 we find $\pi = 0.0394$, whence $p_a = 0.0394 \cdot 60 = 2.3 \frac{kg}{cm^2}$.

For the same engine, examining in the narrowing part of the nozzle

Table 3.3. Supersonic region $\pi = f(k, \zeta)$.

ζ \ k	1,20	1,21	1,22	1,23	1,24	1,25	1,26	1,27	1,28	1,29	1,30
1,0	0,565	0,563	0,561	0,559	0,557	0,555	0,553	0,551	0,549	0,547	0,545
1,1	285	284	283	282	281	280	279	278	277	276	275
1,2	205	204	202	201	199	198	197	195	194	192	191
1,3	156	155	153	152	151	150	148	147	146	144	143
1,4	123	122	120	119	118	116	115	114	113	111	110
1,5	0,0992	0,0980	0,0969	0,0957	0,0945	0,0944	0,0922	0,0910	0,0898	0,0887	0,0875
1,6	810	800	791	781	772	762	753	744	734	724	715
1,7	680	671	662	653	644	635	626	617	608	599	590
1,8	580	571	563	554	546	538	529	520	512	504	495
1,9	498	490	482	475	466	459	451	443	436	428	420
2,0	428	421	414	408	401	394	387	380	374	367	360
2,1	375	368	362	355	349	342	336	330	323	316	310
2,2	330	324	318	312	306	300	293	287	281	275	269
2,3	291	286	280	275	269	264	259	253	248	242	237
2,4	259	254	249	245	240	235	230	225	221	216	211
2,5	232	228	223	219	214	210	206	201	197	192	188
2,6	209	205	201	197	192	188	184	180	176	172	168
2,7	189	185	181	177	173	170	166	162	158	154	150
2,8	179	168	165	162	158	154	151	148	144	140	137
2,9	156	153	149	146	143	140	137	134	130	127	124
3,0	142	139	136	133	130	128	125	122	119	116	113
3,1	130	127	124	122	119	116	113	110	108	105	102
3,2	120	117	115	112	109	106	104	101	0,00988	0,00961	0,00935
3,3	111	108	105	103	101	0,00981	0,00955	0,00929	0,00904	0,00878	0,00852
3,4	102	0,00995	0,00972	0,00947	0,00923	899	875	851	826	802	778
3,5	0,00945	922	899	876	853	830	807	726	704	682	660
3,6	880	858	836	814	793	772	750	731	707	689	667
3,7	818	797	777	757	736	716	696	676	656	635	616
3,8	702	743	724	704	685	665	647	628	608	589	570
3,9	715	696	678	659	641	622	604	586	567	548	530
4,0	670	652	635	617	600	582	565	546	530	512	495
4,1	627	610	594	577	560	544	527	510	493	477	460
4,2	588	572	556	541	525	509	493	477	462	446	430
4,3	552	537	522	508	493	478	464	449	434	420	405
4,4	520	506	492	477	463	449	435	421	406	392	378
4,5	490	477	463	450	436	424	410	396	384	370	357
4,6	460	447	435	422	410	398	385	373	360	348	335
4,7	435	423	412	400	388	376	365	353	341	330	318
4,8	415	403	392	380	369	358	346	334	323	312	300
4,9	395	384	372	361	350	338	327	316	305	293	282
5,0	380	369	358	347	336	325	314	303	292	281	270

the section where diameter d = 18 cm, we will obtain $\zeta = 1.2$ and by Table 3.2 we find $\pi = 0.878$, whence $p = 0.878 \cdot 60 = 52.5 \frac{kg}{cm^2}$.

The character of pressure distribution on the nozzle is shown in Fig. 3.1. In the same place a curve is given of change of flow rate of gases along the nozzle.

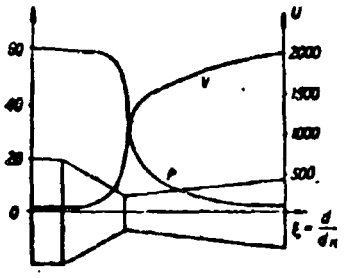

Fig. 3.1. Change of pressure and speed along nozzle.

The character of change of flow rate along the nozzle is easy to set by proceeding from dependence 3.2, considering relative pressure π as a function of ζ.

Here, by introducing designation

$$F_v(\zeta) = \sqrt{\frac{2gk}{k-1}\left(1 - \pi^{\frac{k-1}{k}}\right)}, \tag{3.8}$$

we obtain the expression for flow rate in such a form

$$v = \sqrt{\chi f_p} F_v(\zeta). \tag{3.9}$$

In Tables 3.4 and 3.5 are given values of function $F_v(\zeta)$ for values of adiabatic index k from 1.20 to 1.30. Table 3.4 corresponds to the subsonic region and permits calculating flow rate in different sections of the entrance cone of the nozzle. Table 3.5 corresponds to the supersonic region and permits determining flow rate of gases in the expanded part of the nozzle and, in particular, in its outlet section.

<u>Example</u>: For the example above, $k = 1.25$, $\zeta = 2$ we obtain for the supersonic zone $F_v(\zeta) = 6.85$. At value $\chi f_p = 90000 \frac{kg\text{-}m}{kg}$ we will obtain $v = 2050 \frac{m}{s}$. For the critical section ($\zeta = 1$) we will obtain $F_v(1) = 3.30$ whence $v_{кр} = 990 \frac{m}{s}$.

For a certain section of the narrowing part of the nozzle with

Table 3.4. Subsonic region $F_v(\zeta)$.

ζ \ h	1,20	1,21	1,22	1,23	1,24	1,25	1,26	1,27	1,28	1,29	1,30
5,0	0,0766	0,0766	0,0766	0,0766	0,0766	0,0766	0,0766	0,0766	0,0766	0,0766	0,0766
4,0	0,128	0,129	0,129	0,129	0,130	0,131	0,131	0,132	0,132	0,133	0,133
3,0	224	225	225	226	226	227	228	228	229	229	230
2,9	239	240	241	242	243	244	246	247	248	249	250
2,8	257	258	259	260	261	263	264	265	266	267	268
2,7	280	280	280	280	280	282	283	285	287	289	290
2,6	297	299	301	302	304	306	308	310	311	313	315
2,5	323	325	327	329	331	333	335	337	339	341	343
2,4	353	355	357	360	362	364	366	368	3,71	3,73	375
2,3	385	388	390	393	395	398	400	403	405	408	410
2,2	425	427	429	431	433	435	437	439	441	443	445
2,1	465	467	469	471	473	475	477	479	481	483	485
2,0	512	513	514	516	517	518	519	520	522	523	524
1,9	565	566	567	568	569	570	571	572	573	574	575
1,8	630	632	633	635	636	638	640	641	643	644	646
1,7	705	707	709	711	713	716	718	720	722	724	726
1,6	795	797	799	801	803	805	806	808	810	812	814
1,5	943	944	945	946	947	949	950	951	952	953	954
1,4	1,09	1,09	1,09	1,10	1,10	1,10	1,10	1,10	1,11	1,11	1,11
1,3	31	31	31	32	32	32	32	32	33	33	33
1,2	57	57	58	58	59	59	59	60	60	61	61
1,1	98	98	99	99	2,00	2,00	2,00	2,01	2,01	2,02	2,02

Table 3.5. Subsonic region $F_v(\zeta)$.

ζ \ h	1,20	1,21	1,22	1,23	1,24	1,25	1,26	1,27	1,28	1,29	1,30
1,0	3,27	3,28	3,28	3,29	3,29	3,30	3,31	3,31	3,32	3,32	3,33
1,1	4,82	4,81	4,79	4,78	4,76	4,75	4,74	4,72	4,71	4,69	4,68
1,2	5,23	5,23	5,22	5,22	5,22	5,22	5,21	5,21	5,21	5,20	5,20
1,3	60	60	59	59	88	58	57	57	56	56	55
1,4	89	88	88	87	57	86	85	85	84	84	83
1,5	6,14	6,13	6,12	6,11	6,10	6,10	6,09	6,08	6,07	6,06	6,05
1,6	35	34	33	31	30	29	28	27	25	24	23
1,7	53	52	50	49	47	46	44	43	41	40	38
1,8	70	68	66	65	63	61	59	57	56	54	52
1,9	81	79	78	76	75	73	71	70	68	67	65
2,0	94	92	90	88	86	85	83	81	79	77	75
2,1	7,05	7,03	7,01	6,99	97	95	93	91	89	87	85
2,2	15	7,1[illegible]	7,11	7,09	7,07	7,05	7,02	7,00	6,98	96	94
2,3	25	2[illegible]	20	18	15	13	11	7,08	7,06	7,03	7,01
2,4	33	31	28	26	23	21	18	16	13	11	0,8
2,5	7,41	38	36	33	31	28	25	23	20	18	15
2,6	48	45	43	40	37	35	32	29	26	24	21
2,7	55	52	49	46	43	41	38	35	32	29	26
2,8	62	59	56	53	50	47	43	40	37	34	31
2,9	68	65	62	58	55	52	49	46	42	39	36
3,0	73	70	66	63	60	57	53	50	47	43	40
3,1	79	76	73	69	66	62	59	55	52	48	45
3,2	84	81	77	74	70	67	63	60	56	53	49
3,3	89	85	82	78	75	71	67	64	60	57	53
3,4	93	89	86	82	79	75	71	68	64	61	57
3,5	98	94	91	87	83	80	76	72	68	65	61
3,6	8,02	7,98	94	91	87	83	79	75	72	68	64
3,7	06	8,02	7,98	94	90	87	83	79	75	71	67
3,8	09	05	8,01	7,97	93	90	86	82	78	74	70
3,9	13	09	05	8,01	7,97	93	89	85	81	77	73
4,0	16	12	08	03	8,00	96	91	87	83	79	75
4,1	20	16	12	07	03	7,99	95	90	86	82	78
4,2	23	19	14	10	06	8,02	7,97	93	89	84	80
4,3	27	23	18	14	09	05	8,00	96	91	87	82
4,4	29	25	20	16	11	07	03	7,98	94	89	85
4,5	32	28	23	19	14	10	05	8,01	96	92	87
4,6	35	30	26	21	17	12	07	8,03	7,98	94	89
4,7	38	33	20	24	19	15	10	05	8,00	96	91
4,8	40	35	30	26	21	16	11	06	02	97	92
4,9	42	37	32	28	23	18	13	08	03	7,99	94
5,0	44	39	34	30	25	20	15	10	06	8,01	7,96

the same relative section $\zeta = 2$ by Table 3.4 for the subsonic zone we will obtain $F_v(\zeta) = 0.518$ and $v = 155 \frac{m}{s}$.

The graph of change of flow rate of gases along the nozzle is shown in Fig. 3.1.

We will examine the influence of a change of external atmospheric pressure on distribution of pressure along the nozzle.

If the design pressure in the outlet section is larger than external pressure, then all characteristics of flow – pressure, speed, flow rate per second – do not depend on external pressure. This is explained by the fact that after the critical section there is a supersonic flow of gas, and therefore no disturbance of the flow spreading with the speed of sound can be transmitted in reverse direction to the flow. Expansion of the gas and a pressure drop from p_a to p_H occurs only outside the nozzle and is accompanied, as it were, by a buckling of the flow caused by the appearance of radial components of speed.

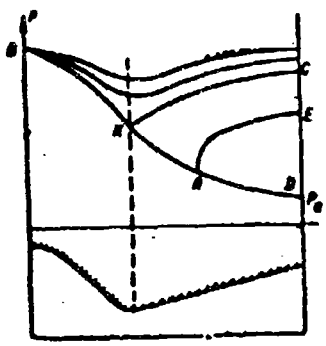

Fig. 3.2 Flow from nozzle with overexpansion.

Let us consider the case when the pressure drop $p_0 - p_a$ from the chamber to the outlet section is small and the flow of gases all over the nozzle is subsonic. In Fig. 3.2 to shown conditions correspond the curves which are located higher than curve BKC. On this curve point K corresponds to critical pressure determined by formula (3.4), and only this point corresponds to sonic speed of gas. The remaining points of curve BKC correspond to the subsonic region. In the examined case the distribution pressure along the flow, and consequently also flow rate and flow rate per second to an essential measure depend on external pressure.

In this case flow rate per second can be calculated by formula (3.3) and cannot be calculated by formula (3.5), since the latter is true only for supercritical outflow.

If external pressure p_H is larger than design pressure p_a corresponding to supersonic flow, but less than pressure corresponding to point C (Fig. 3.2), then one of the following two cases can take place.

1. Flow with overexpansion. Expansion of the gas occurs just as in the case when $p_H \leq p_a$, and is characterized by curve BKD. Moreover, since pressure in the outlet section is less than external ($p_a < p_H$), then directly after the nozzle there occurs an increase of pressure and compression of the stream with a system of oblique shock waves.

2. Flow with separation of flow from walls of nozzle. In the nozzle up to certain limits there occurs overexpansion of gases. Then due to breakaway of the boundary layer the oblique shock wave shifts from the outlet section to inside the nozzle (curve AE). With an increase of external pressure p_H the zone of breakaway of the boundary layer shifts from the outlet to the critical section. After the jump, pressure in the flow is increased. Conditions of breakaway of the boundary layer during flow with overexpansion is determined by experimental means. According to Sommerfield [1], for a nozzle with a half angle of conicity $\alpha \approx 15°$ and when $\frac{p_{KP}}{p_H} > 16$, separation of the boundary layer corresponds to condition $\frac{p_a}{p_H} < 0.4$.

§ 3.2 Change of Parameters of Gas Flow in Thrust Chamber

Let us consider the flow of gases in the chamber along the burning charge of the solid fuel. In the first approximation we will consider that burning of fuel and liberation of gases occurs evenly over the entire surface of the charge whose cross section is constant over the whole length. In this case it is possible to examine an idealized scheme when gases pass over the lateral surface of the engine chamber.

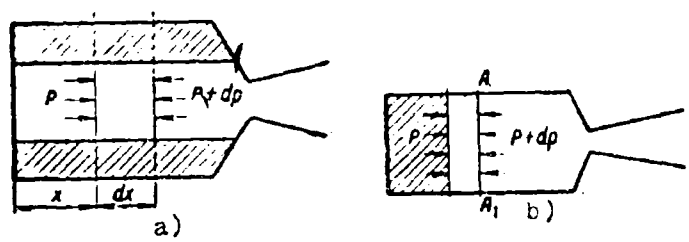

Fig. 3.3. Diagram of flow of gases in chamber; a) onset of gases from internal channel; b) onset of gases from bottom.

Let us designate by λ the mass of gas coming in one second from a unit of chamber length.

Let us consider an elementary volume of the chamber with length dx (Fig. 3.3a). During time dt over section x passes mass of gas $F\rho v dt$, and over section x + dx mass

$$F[\rho v + d(\rho v)]\,dt.$$

The difference of shown values should equal the quantity of gas which during time dt will be liberated from the wall of the chamber over an element length dx.

Thus
$$Fd(\rho v)\,dt = \lambda dx \cdot dt,$$

or
$$\rho dv + v d\rho = \frac{\lambda}{F} dx. \tag{3.10}$$

We will compose the equation of momentum for a mass of gas in element dx:

$$d(mv) = pF\,dt - (p + dp)F dt$$

or

$$m dv + v dm = -F dp\,dt.$$

With substitution

$$m = F\rho\,dx,$$
$$dm = \lambda\,dx \cdot dt,$$

we obtain

$$F dx \rho\,dv + v\lambda\,dx \cdot dt = -F dp \cdot dt. \tag{3.11}$$

Dividing by Fdt, considering that $\frac{dx}{dt} = v$, and replacing $\frac{\lambda}{F}$ dx from equation (3.10), we will obtain

$$\rho v dv + v(\rho dv + v d\rho) = -dp$$

or

$$2\rho v dv = -dp - v^2 d\rho = -dp\left(1 + \frac{v^2}{a^2}\right)$$

and finally

$$2\rho v dv = -dp\left(1 + \frac{v^2}{a^2}\right). \tag{3.12}$$

As we will see subsequently, speed of gases in the chamber of the engine is considerably less the local speed of sound. Considering in this case the gas as an incompressible liquid ($\rho = \rho_0$ = const), we obtain

$$dp = -2\rho_0 v dv.$$

Integrating along the engine chamber and considering that for the bottom $v_0 = 0$, we obtain

$$\Delta p = p_0 - p = \rho_0 v^2 = 2\frac{\rho_0 v^2}{2}, \tag{3.13}$$

i.e., the pressure drop along the charge of solid fuel equals the doubled impact pressure corresponding to speed of gases for the end of the charge turned towards the nozzle.

From expression (3.10), disregarding any change of density along the flow ($d\rho = 0$), we obtain

$$v = \frac{\lambda}{F\rho_0} x,$$

i.e., flow rate of gases in camera, the engine chamber is proportional to the distance of the examined section from the bottom of the chamber.

For the end of the charge turned toward the nozzle, we obtain

$$v_{max} = \frac{\lambda}{F\rho_0} L, \tag{3.14}$$

where L – length of charge.

Furthermore,

$$v_{max} F\rho_0 = \lambda L = \frac{G}{g},$$

since during stabilized flow the biggest flow rate per second of gases along the charge equals the flow rate per second through the critical section of the nozzle.

Thus, we have

$$v_{max} = \frac{G}{gF\rho_0} = \frac{Gf_p}{F\rho_0}.$$

Substituting the value of flow rate per second from expression (3.6), we will obtain

$$v_{max} = \varphi A \frac{F_{кр}}{F} \sqrt{Xf_p} \tag{3.15}$$

where F – free area of passage of gases along the charge of solid fuel.

Substituting in equation (3.13) value v_{max} from expression (3.15) and value ρ_0 from the state equation, we will obtain

$$\Delta p = -\rho_0 v^2_{max} = \frac{p_0}{gf_p} A^2 \left(\frac{F_{кр}}{F}\right)^2 f_p$$

or finally

$$\frac{\Delta p}{p_0} = -\frac{1}{g}\left(A\frac{F_{кр}}{F}\right)^2.$$

For example, when $\frac{F_{KD}}{F} = 0.3$ and $A = 2.06$, which corresponds to $k = 1.25$, we obtain

$$\frac{\Delta p}{p_0} = -\frac{1}{9{,}81}(2{,}06 \cdot 0{,}3)^2 = -0{,}039.$$

Pressure drops 4% along the charge.

Above we showed that during travel of gases in the chamber over the lateral wall or during burning of the charge from the lateral surface, the pressure drop along the charge is equal to double the impact pressure. It is not difficult to show that even in the case of burning of a clad charge from the end the pressure drop from the source of gas formation to the chamber is equal to double the impact pressure (Fig. 3.3b). Actually, we will examine a certain section of the chamber AA_1, close to the surface of burning, and we will apply the equation of momentum to the mass of gas between the surface of the solid fuel and this section.

The equation has the form

$$v\,dm = [pF - (p + dp)F]\,dt = -F\,dp\,dt;$$
$$v\frac{dm}{dt} = -F\,dp.$$

Considering that the flow rate per second of a mass of gas equals

$$\frac{dm}{dt} = \rho v F,$$

we obtain

$$\Delta p = -\rho v^2.$$

We see that even in this case the pressure drop equals double the impact pressure.

§ 3.3. Reaction Force (Thrust)

During flight of a rocket with a working engine the main vector of forces of pressure, effecting the rocket, is determined from expression

$$\bar{R} = \iint_S (p - p_н)\,\bar{n}\,dS, \qquad (3.16)$$

where $p - p_н$ – excess pressure in examined point of surface; $\bar{n}$ – unit vector of normal; S – total surface of rocket, consisting of external surface of rocket S_e and internal surface S_i of the chamber and nozzle of the engine.

Thus

$$\bar{R} = \iint_{S_e} (p - p_н)\bar{n}dS + \iint_{S_i} (p - p_н)\bar{n}dS = \bar{Q} + \bar{P}. \qquad (3.17)$$

The augend of (3.17) constitutes aerodynamic force, and the addend the reaction force.

Thus, the reaction force can be defined as the main vector of forces of excess pressure effecting the internal surface of the chamber and nozzle of the engine:

$$\bar{P} = \iint_{S_i} (p - p_н)\bar{n}dS. \qquad (3.18)$$

Let us note that in expressions (3.16) and (3.17) it would have been possible to write under the integral sign $p\bar{n}$ instead of $(p - p_н)\bar{n}$, since

$$\iint_{S} p_н\bar{n}dS = 0.$$

However, it is necessary to consider that in aerodynamics it is accepted to consider the excess above atmospheric pressure according to formula (3.16), and since in totality forces $\bar{Q}$ and $\bar{P}$ constitute the main vector of forces of pressure, even in the expression for reaction force it is necessary to consider excess pressure:

$$\bar{P} = \iint_{S_i} (p - p_н)\bar{n}dS = \iint_{S_i} p\bar{n}dS - p_н \iint_{S_i} \bar{n}dS. \qquad (3.19)$$

We will examine at first the addend of the right side of (3.19). If the chamber is supplied with a plug in the outlet section and is filled with gas, then internal forces of pressure will be balanced. If, however, one removes the plug, preserving constancy of pressure along the internal surface, then internal forces will be unbalanced by a value $-p_H F_a$, where F_a – area of nozzle exit section. Thus,

$$p_н \iint_{S_i} \bar{n}dS = -p_н F_a \bar{n}_a, \qquad (3.20)$$

where $\bar{n}_a$ is a unit vector of the external normal to the nozzle exit section.

Expression (3.19) takes the form

$$\bar{P} = \iint_{S_i} p\bar{n}dS + p_н F_a \bar{n}_a.$$

We will project the last expression on the axis of symmetry of the chamber and nozzle taking the positive direction of the axis against the flow. Here we obtain

$$P = \iint_{S_1} p \cos\alpha \, dS - p_a F_a; \tag{3.21}$$

where α — angle between normal to surface and axis of symmetry.

The integral in expression (3.21) will be calculated for the outlet cone of the nozzle, for the entrance cone, and for the engine chamber.

Indices will denote: 0 — bottom of chamber; 1 — beginning of entrance cone; к — critical section; a — outlet section.

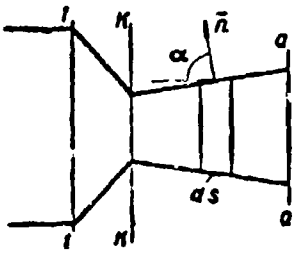

Fig. 3.4. Diagram of distribution of thrust along nozzle.

Let us consider the part from the outlet section F_a to critical section $F_{кр}$ (Fig. 3.4). By two sections, perpendicular to the axis, we will cut an elementary ring in the form of the frustum of a cone, the lateral surface of which is equal to dS. The projection of this surface on a plane perpendicular to the axis is equal to

$$dS \cdot \cos\alpha = -dF.$$

The "minus" sign indicates that growth of S corresponds to a decrease of F.

For the outlet cone of the nozzle the integral in expression (3.21) takes the form

$$\iint_{ak} p \cos\alpha \, dS = -\iint_{ak} p \, dF = -\iint_{ak} d(pF) + \iint_{ak} F \, dp. \tag{3.22}$$

From Bernoulli's equation we have

$$\rho v \, dv = -dp,$$

whence

$$F \, dp = -F \rho v \, dv = -\frac{G}{g} dv.$$

Expression (3.22) takes the form

$$\iint_{a\,c} p\cos\alpha\, dS = -p_c F_c + p_a F_a - \frac{G}{g} v_c + \frac{G}{g} v_a \qquad (3.23)$$

Analogously for the cone of the nozzle we have

$$\iint_{a\,1} p\cos\alpha\, dS = -p_1 F_1 + p_a F_a - \frac{G}{g} v_1 + \frac{G}{g} v_a \qquad (3.24)$$

Above we saw (3.13) that pressure for the bottom of the chamber exceeds the pressure at the entrance to the nozzle by a value of double the impact pressure

$$\Delta p = \rho v_1^2 = g\gamma F_1 v_1 \frac{v_1}{gF_1} = \frac{G}{g}\frac{v_1}{F_1}.$$

Thus, considering that $F_0 = F_1$, we have

$$p_1 F_1 + \frac{G}{g} v_1 = p_0 F_0$$

and expression (3.24) takes the form

$$\iint_{a\,1} p\cos\alpha\, dS = -p_0 F_0 + p_a F_a + \frac{G}{g} v_a \qquad (3.25)$$

For the bottom of the chamber we have a force of pressure

$$p_0 F_0 = P_{\text{дно}} \qquad (3.26)$$

Combining expressions (3.23), (3.25), (3.26), we obtain from (3.21)

$$P = \frac{G}{g} v_a + F_a (p_a - p_н). \qquad (3.27)$$

Expression (3.27) for reaction force is obtained by direct integration of forces of pressure over the internal surface of the chamber and nozzle.

From expression (3.27) it is clear that the biggest value of reaction force corresponds to flight of a rocket in a vacuum ($p_н = 0$). Moreover

$$P_{\text{вакуум}} = \frac{G}{g} v_a + F_a p_a$$

Certain authors say that the reaction force is the augend of the right side of formula (3.27), relating the addend to external forces.

The forementioned conclusion of the expression for reaction force indicates an inaccuracy of similar treatment, since both components in totality are equal to the value of the main vector of forces of pressure effecting the internal wall of the chamber and nozzle.

With well-known reason it would have been possible to relate to external forces only component $F_a p_H$ and to include it in the aerodynamic force. Besides, it is necessary to consider that in aerodynamics one calculates aerodynamic force by proceeding from the expression

$$\bar{Q} = \iint_{S_e} (p - p_H)\,\bar{n}\,dS = \iint_{S_e} p\bar{n}\,dS - p_H\bar{n}F_a,$$

where component $-p_H\bar{n}F_a$ is directed in the direction of motion.

If, however, one gives to aerodynamics a "foreign" (for an engine) component $p_H F_a$ directed against motion, then we will obtain

$$\bar{Q} = \iint_{S_e} p\bar{n}\,dS.$$

This means one must demand that aerodynamic professionals conduct the calculation of aerodynamic forces based not on excess, but on absolute pressures. It is doubtful whether this is practical.

Furthermore, in examining the work of an engine on a stand it would be necessary nevertheless to consider component $p_H F_a$.

Expressions (3.24) and (3.25) permit calculating not only the total quantity of reaction force, but also its separate components.

For example, add expressions (3.23) and (3.25), one can determine that part of the reaction force which was apportioned to the nozzle:

$$P_{сопло} = \frac{G}{g} v_e + p_e F_e - p_0 F_e \qquad (3.28)$$

Let us note that expression (3.28) can be positive or negative. In particular, it is possible to select such a nozzle and such operating conditions of the engine during which $P_{сопло} = 0$. Such a nozzle will not rush to be detached from the engine chamber.

<u>Example</u>: Let us consider the following conditions: $p_0 = 120\ \frac{kg}{cm^2}$; $d_a = 30$ cm; $d_k = 15$ cm; $f_p = 90{,}000$ m; $k = 1.25$; $F_a = 70.6\ cm^2$; diameter of chamber $D_{кам} = 50$ cm.

For the shown conditions we will obtain:

$$G = 14{,}5\ \frac{kg}{s};\quad v_a = 2050\ \frac{m}{s};\quad p_a = 4{,}7\ \frac{kg}{cm^2}.$$

Taking external atmospheric pressure $p_H = 1\ \frac{kg}{cm^2}$, by formula (3.27) we will obtain

$$P = \frac{G}{g} v_a + F_a (p_a - p_H) = \frac{14{,}5}{9{,}81} 2050 + 70{,}6 (4{,}7 - 1) = 3030 + 260 = 3290\ kg.$$

In this example augend $\frac{G}{g} v_a$ composes 92% of the total reaction force.

Let us determine the force effecting the nozzle by using formula (3.28). We have

$$F_c = 196\ cm^2,$$

$$P_{сопло} = \frac{G}{g} v_a + p_a F_a - p_c F_c = 3030 + 4{,}7 \cdot 70{,}6 - 120 \cdot 196 = -20\,160\ kg.$$

The "minus" sign indicates that force of pressure applied to the nozzle is directed in the direction of flow. By value it is 11.6% less than the force of pressure of gases on the bottom:

$$P_{дно} = p_c F_c = 120 \cdot 196 = 23\,520\ kg,$$

directed against the flow.

Let us consider under what conditions the main vector of forces of pressure applied to the nozzle is equal to zero. On the basis of expression (3.28) this condition takes the form

$$\frac{G}{g} v_a + F_a p_a - F_c p_c = 0.$$

Substituting values G and v_a from formulas (3.6) and (3.9), and also

$$F_a = \zeta^2 F_к,\quad p_a = \pi_a p_c,$$

we obtain

$$\varphi \frac{A}{g} F_v(\zeta) F_c p_c + \zeta^2 \pi_a F_к p_c - F_c p_c = 0,$$

whence we obtain the condition

$$\frac{F_c}{F_к} = \frac{\varphi A F_v(\zeta)}{g} + \zeta^2 \pi_a.$$

For the given example $\zeta = 2$; $\pi_a = 0.0394$; $F_v(\zeta) = 6.85$, consequently,

$$\frac{F_c}{F_к} = \frac{0{,}98 \cdot 2{,}06 \cdot 6{,}85}{9{,}81} + 4 \cdot 0{,}0394 = 1{,}43.$$

Thus, for the examined conditions, if the area of the cross section of the engine chamber in all exceeds by 43% the area of the critical section, and the area of outlet section exceeds area of last in four times ($\zeta^2 = 4$), then nozzle will be balanced.

During deviation of the expression for reaction force we originated from a stabilized flow process. Moreover speed, density, and consequently also momentum of gases in the chamber remain low. In reality the shown parameters of flow are changed, especially in the initial stage of work of the engine when a rise of pressure curve occurs. Let us give an appraisal of error allowable for disregarding the shown factor.

During a change of pressure in the engine chamber the temperature of gases and flow rate remain practically constant, and density is changed proportional to pressure. Momentum of gases in the chamber

$$K = mv_{cp} = \left(W_{кам} - \frac{\omega}{\delta}\right)\rho v_{cp}$$

where $W_{кам}$ – volume of chamber; δ – specific gravity of fuel; ω – its weight; $W_{кам} - \frac{\omega}{\delta}$ – volume of gases in chamber.

Considering that $\rho = \frac{p}{gf_p}$ and $W_{кам} = \frac{\omega}{\Delta}$, where Δ – density of loading of chamber with fuel, we obtain

$$K = \omega\left(\frac{1}{\Delta} - \frac{1}{\delta}\right)\frac{p}{gf_p}v_{cp}$$

If pressure in the chamber will be changed, then we will obtain

$$\Delta K = \frac{\omega v_{cp}}{gf_p}\left(\frac{1}{\Delta} - \frac{1}{\delta}\right)\Delta p.$$

We will compare the obtained expression with the basic value of momentum

$$K = \frac{G}{g}v_e\Delta t,$$

entering in the expression for reaction force

$$\varepsilon = \frac{\Delta K}{K} = \frac{\omega v_{cp}}{Gf_p v_e}\left(\frac{1}{\Delta} - \frac{1}{\delta}\right)\frac{\Delta p}{\Delta t}.$$

Examining the initial period of the rise of the pressure curve from zero p_{max}, we can write approximately

$$\frac{\Delta p}{\Delta t} \approx \frac{dp}{dt} \approx \frac{p_{max}}{t_1},$$

where t_1 corresponds to the moment of achievement of $p_{г\ x}$. Further,

$$\varepsilon = G_{cp}\tau,$$

where τ – full time of outflow.

Let us still take in the expression for ε

$$G = G_{cp}$$

Here we obtain

$$\varepsilon = \left(\frac{1}{\Delta} - \frac{1}{\delta}\right)\frac{\tau}{t_1}\cdot\frac{v_{cp}}{v_a}\cdot\frac{p_{max}}{f_p}.$$

For an appraisal of value ε it is possible to take:

$$\delta = 1\cdot 7\cdot 10^3\ \frac{kg}{m^3};\quad \Delta \approx 1{,}1\cdot 10^3\ \frac{kg}{m^3};\quad v_{cp} = 100\ \frac{m}{s};$$
$$v_a = 2000\ \frac{m}{s};\quad \frac{\tau}{t_1} \approx 20;\quad p_{max} \approx 120\cdot 10^4\ \frac{kg}{m^2};$$
$$f_p \approx 90000\ m.$$

Here we will obtain

$$\varepsilon = \left(\frac{1}{1100} - \frac{1}{1700}\right)20\cdot\frac{100}{2000}\cdot\frac{120\cdot 10^4}{90\,000} = 0{,}43\cdot 10^{-2}.$$

Thus, under shown conditions all change of momentum, and consequently also the reaction force due to deflection of conditions of work of the engine from stabilized, does not exceed 0.5%.

During deviation of expression (3.27) for reaction force we assumed the output flow of gases to be parallel to the axis of the chamber. In reality in conical nozzles the flow is divergent, and reaction force is determined by axial components of the exit velocity. It is not difficult to show [1], [2] that when accounting for the shown circumstance the expression for reaction force takes the form

$$P = \frac{1+\cos\alpha}{2}\left[\frac{G}{g}v_a + F_a(p_a - p_n)\right]. \qquad (3.29)$$

where α – half of the angle of conicity of the nozzle.

When $\alpha = 15°$ the correction factor $\frac{1+\cos\alpha}{2} \approx 0{,}983$.

§ 3.4. Pulse of Reactive Force. Unit Pulse

The total pulse of the reaction force during the time of work of

the engine is determined from the expression

$$I = I(\tau) = \int_0^{\tau} P\,dt,$$

where τ – full work time of engine.

It is not difficult to show that the total pulse of reaction force practically does not depend on the form of curve P(t). From expression (3.27) for reaction force we have

$$I = \frac{w_0}{g}\int_0^{\tau} G\,dt + F_a\int_0^{\tau} p_a\,dt - F_a p_a \tau. \qquad (3.30)$$

For the augend of the right side we obtain

$$\frac{w_0}{g}\int_0^{\tau} G\,dt = \frac{w_0 \omega}{g}.$$

For the addend we have

$$F_a\int_0^{\tau} p_a\,dt = F_a \varkappa_a \int_0^{\tau} p_0\,dt.$$

The last expression during calculation of dependence (3.6) for flow rate per second takes the form

$$F_a\int_0^{\tau} p_a\,dt = \frac{F_a}{F_{cp}}\cdot\frac{\sqrt{\gamma f_p}}{A}\varkappa_a\int_0^{\tau} G\,dt = \zeta^2\frac{\sqrt{\gamma f_p}\,\varkappa_a}{A}\omega.$$

Finally we obtain

$$I = \frac{w_0}{g}\omega + \zeta^2\frac{\varkappa_a \omega}{A}\sqrt{\gamma f_p} - p_a F_a \tau.$$

In the last expression the first two components depend neither on the form of curve P(t) nor on the duration of work of the engine. On the last factor depends only the last member, composing a small part of the value of reaction force.

A unit pulse of reaction force I_1 is the total pulse related to one kilogram of weight of fuel:

$$I_1 = \frac{I}{\omega} = \frac{w_0}{g} + \frac{\zeta^2 \varkappa_a}{A}\sqrt{\gamma f_p} - p_a F_a \frac{\tau}{\omega}. \qquad (3.31)$$

Considering that

$$\frac{\omega}{\tau} = G_{cp} = \frac{AF_{cp}(p_0)_{cp}}{\sqrt{\gamma f_p}},$$

and disregarding any change of p_0 in the last member, we will obtain

$$I_1 = \frac{v_e}{g} + \frac{C\varkappa_e}{A}\sqrt{\chi f_p} - \frac{p_n C}{p_0 A}\sqrt{\chi f_p}. \qquad (3.32)$$

The unit pulse is the most important power parameter characterizing effectiveness of a fuel during its use in the examined engine. In those cases when engines with a long time of burning of fuel are examined, it is frequently necessary to consider not only a change of pressure, but also a change of thermodynamic parameters of gases in the chamber, including temperature, adiabatic index, and force of fuel.

In these conditions instead of unit pulse it is more convenient to use the idea "specific thrust," defined as the ratio of thrust to flow rate per second:

$$P_{уд} = \frac{P}{G} = \frac{v_e}{g} + \frac{F_e}{G}(p_e - p_n). \qquad (3.33)$$

It is simple to see that

$$P_{уд} = I_1 = \frac{v_e}{g} + C\frac{\sqrt{\chi f_p}}{A}\left(\varkappa_e - \frac{p_n}{p_0}\right). \qquad (3.34)$$

however, it is necessary to consider that the unit pulse characterizes average effectiveness of fuel during the time of work of the engine, but specific thrust can be referred to a defined instant of work of the engine.

In view of the fact that the augend in expression (3.33) is the decisive one, it turns out to be convenient to take into consideration effective exit velocity, determined from expression

$$v_e = v_e + \frac{g}{G}F_e(p_e - p_n) = v_e - gC\frac{\sqrt{\chi f_p}}{A}\left(\varkappa_e - \frac{p_n}{p_0}\right). \qquad (3.35)$$

Moreover the expression for reaction force takes the form

$$P = \frac{G}{g}v_e \qquad (3.36)$$

and for a unit pulse

$$I_1 = \frac{v_e}{g}. \qquad (3.37)$$

For the example examined above we have:

$$v_e = 2050; \quad C = 14{,}5; \quad F_e = 70{,}6; \quad p_e = 4{,}7; \quad p_n = 1.$$

Moreover

$$\frac{g}{G} F_a (p_a - p_a) = \frac{9{,}81}{14{,}5} 70{,}6 (4{,}7 - 1) = 176;$$

$$v_e = 2050 + 176 = 2226;$$

$$I_1 = \frac{2226}{9{,}81} = 227 \ \frac{\text{кгс}}{\text{кг}}.$$

Effective exit velocity in the examined case exceeds speed v_a in the outlet by 8.5%.

§ 3.5. Dependence of Unit Pulse on Form of Nozzle and Pressure in Engine Chamber

The simplest type of nozzle used in rocket technology consists of a conically narrowing part with a half-cone angle within limits of 30-45° and an expanded part with the half angle close to 15°. The narrowing and divergent sections of the nozzle are connected by a toroidal annular unit whose radius of curvature is selected within the limits of 2-3 radii of the critical section.

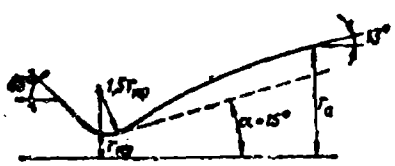

Fig. 3.5. Optimum shaped nozzle: ------ conical nozzle; ——— shaped nozzle $\frac{d_a}{d_{кр}} = 4.4$.

In certain cases shaping is used which ensures a decrease of losses in the nozzle and an increase of unit pulse. In Fig. 3.5 there is shown a shaped nozzle which ensures augmentation of thrust by 2% as compared to a conical nozzle [1]. By technological considerations it is more convenient to use conical nozzles. The basic characteristic of a nozzle is value $\zeta = \frac{d_a}{d_{кр}}$. The larger ζ, the bigger the pressure drop and growth of speed in the nozzle.

Let us consider the dependence of reaction force on the expansion ratio of gases in the nozzle, considering as variables the pressure in the chamber of the engine and the area of the critical section.

Remaining constant is the flow rate per second of gases. Differentiating the expression for reaction force

$$P = \frac{Gv_a}{g} + F_a (p_a - p_a)$$

with respect to p_a, we obtain

$$\frac{dP}{dp_a} = \frac{G}{g} \frac{dv_a}{dp_a} + F_a + (p_a - p_a) \frac{dF_a}{dp_a}. \qquad (3.38)$$

From equation $\rho v dv = -dp$ we have

$$\frac{dv_a}{dp_a} = -\frac{1}{\rho_a v_a}.$$

Considering that $G = g\rho_a v_a F_a$, we obtain

$$\frac{G}{g}\frac{dv_a}{dp_a} = -F_a$$

and expression (3.38) takes the form

$$\frac{dP}{dp_a} = (p_a - p_n)\frac{dF_a}{dp_a}.$$

Since $\frac{dF_a}{dp_a} \neq 0$, since with a change of area of cross section the pressure does not remain constant, then equating $\frac{dP}{dp_a}$ to zero, we will obtain condition

$$p_a = p_n.$$

We will estimate the sign of the second derivative

$$\frac{d^2P}{dp_a^2} = \frac{d^2F_a}{dp_a^2}(p_a - p_n) + \frac{dF_a}{dp_a}.$$

Setting $p_a = p_H$, we obtain

$$\frac{d^2P}{dp_a^2} = \frac{dF_a}{dp_a} < 0,$$

which corresponds to the condition of a maximum of the function Thus, the maximum thrust, and consequently also unit pulse, corresponds to that expansion of the nozzle with which pressure in the outlet section will equal external atmospheric pressure.

We will examine which nozzle fits this condition. Considering that

$$p_n = p_a = p_0\pi_a,$$

and taking $p_H = 1\ \frac{kg}{cm^2}$, we obtain $\pi_a = \frac{1}{p_0}$. For value $p_0 = 120\ \frac{kg}{cm^2}$ we obtain $\pi_a = 0.00835$ and by Table 3.3 we find

$$\zeta = \frac{d_a}{d_{cp}} \approx 3{,}5.$$

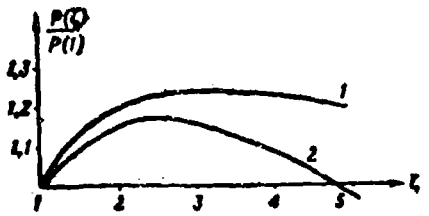

Fig. 3.6. Dependence of thrust on relative expansion of nozzle.

For value $p_0 = 60 \frac{kg}{cm^2}$ we obtain accordingly $\zeta = 2.7$.

Figure 3.6 gives curves of dependence $P(\zeta)$ for values $\frac{p_H}{p_0}: \frac{1}{130}$ – curve 1, and $\frac{1}{150}$ – curve 2.

Optimum value $\zeta = \frac{d_a}{d_{кр}}$ depends on ratio $\frac{p_H}{p_0}$ and is determined by Table 3.6.

Table 3.6.

$\zeta_{опт}$	2,0	2,5	3,0	3,5	4,0	4,5	5,0
$\frac{p_H}{p_0}$	0,039	0,021	0,013	0,008	0,006	0,004	0,003

From Fig. 3.6 it is clear that the maximum of function $P(\zeta)$ is not sharp. Furthermore, calculation of losses in the nozzle shifts the optimum in the direction of short nozzles, which is terms of weight. Therefore for the engine of first stages of rockets value ζ do not emerge from the limits 2-2.5. For the engine of second and third stages values ζ increase, which will agree with data of Table 3.6. Thus, for example, for the engine of the third stage of the "Minuteman" rocket $d_a = 375$ mm; $d_{кр} = 88$ mm, which corresponds to $\zeta = 4.7$.

With an increase of the angle of the conical nozzle losses of thrust are increased, induced by deflection of speeds of gas streams from an axial direction. From expression (3.29) it is clear that when the value of the half cone angle of a nozzle is $\alpha = 15°$, loss of thrust will be 1.7%. At the same time a decrease of the angle of the cone at a constant ratio $\zeta = \frac{d_a}{d_{кр}}$ leads to lengthening, and consequently also to loading of the nozzle. Within limits of values $\alpha = 10$-$25°$ the unit pulse weakly depends on angle α. Selection of the form of the nozzle is produced still taking into account technological factors.

Dependence of a unit pulse on pressure in the chamber is seen

from expression (3.32):

$$I_1 = \frac{w_0}{g} + \zeta \frac{\sqrt{\chi f_p}}{A} \pi_0 - \zeta \frac{\sqrt{\chi f_p}}{A} \frac{p_H}{p_0}.$$

During pressure in the chamber 100 $\frac{kg}{cm^2}$ and more, when dissociation of products of full combustion of the fuel is small, it is possible to take thermodynamic parameters of the gas in the chamber as not depending on pressure. Under these conditions the first two members of the right side of formula (3.32) do not depend on pressure in the chamber. The dependence of a unit pulse on pressure in the chamber, determined by the last member, for values: χf_p = 90,000 m; k = 1.25; ζ = 2; p_H = 1 $\frac{kg}{cm^2}$ is shown in Table 3.7.

Table 3.7.

p_0	60	80	100	120	140	160	180	200
$\Delta I_1 : (I_1)_{100}$	−1,7	−0,67	0	+0,44	+0,70	+0,97	+1,15	+1,28

During pressure in the chamber of p_0 = 100 $\frac{kg}{cm^2}$ we have

$$I_1 = \frac{2050}{9,81} + 4 \cdot \frac{\sqrt{90\,000}}{2,06} \cdot 0,0394 - 4 \cdot \frac{\sqrt{90\,000}}{2,06} \cdot \frac{1}{100} =$$
$$= 209 + 22,9 - 5,8 = 226,1 \ \frac{kg\,s}{kg}.$$

In Table 3.7 are given values of change ΔI_1, unit pulse in %, with respect to value I_1, corresponding to p_0 = 100 $\frac{kg}{cm^2}$.

From Table 3.7 is seen the small sensitivity of unit pulse to pressure in the chamber in the range of pressures close to p_0 = $\frac{kg}{cm^2}$. It is necessary, however, to note that with an increase of caloricity of the fuel temperature of gases in the chamber is increased. Besides, dissociation of products of full combustion CO_2 and H_2O, which leads to lowering of the unit pulse. With a lowering of pressure the degree of dissociation increases. Therefore, sensitivity of a unit pulse to a change of pressure in the chamber increases with an increase of caloricity of the fuel and with a decrease of pressure.

The dependence of a unit pulse of powders on different factors

is investigated in detail in work [3]. In this work it is shown that the dependence of unit pulse on caloricity of a powder is determined by an expression of the form $I_1 = AQ^{0.3}$.

§ 3.6. Outflow of Gas Containing Solid Particles

During burnout of certain solid fuels there is liberated a considerable quantity of solid particles removed by the gas flow. In those cases when dimensions of these particles are sufficiently small, it is possible to allow that temperature and speed of solid particles remain equal in conformity with temperature and speed of gases in the flow. The assumption about equality of speed and temperature in a mixed flow is justified approximately when diameters of particles are less than 10^{-3}-10^{-4} cm. Furthermore, it is possible to disregard specific volume of solid particles as compared to specific volume of gases, since the density of solid particles considerably exceeds the density of gases and, moreover, the weight part of solid particles is usually small.

Under the shown assumptions the influence of solid particles on characteristics of flow will be expressed only in change of heat capacities c_p, c_v, adiabatic index k and gas constant R of a mixed flow.

These parameters can be determined from the expressions [1]:

$$\bar{c}_p = (1-\varepsilon)c_p + \varepsilon c; \tag{3.39}$$

$$\bar{c}_v = (1-\varepsilon)c_v + \varepsilon c; \tag{3.40}$$

$$\bar{k} = \frac{\bar{c}_p}{\bar{c}_v};$$

$$\bar{c}_p - \bar{c}_v = A\bar{R} = A(1-\varepsilon)R,$$

where $\bar{c}_p$, $\bar{c}_v$, $\bar{k}$, $\bar{R}$ – parameters of mixed flow; ε – weight part of solid particles; c – specific heat of solid particles.

The process of expansion of a mixture of gases and solid particles can under shown conditions be considered adiabatic.

Proceeding from the equation of energy

$$A\frac{v^2}{2g} + \bar{c}_p T = A\frac{v_0^2}{2g} + \bar{c}_p T_0$$

and the adiabatic equation

$$\frac{p}{p_0} = \left(\frac{T}{T_0}\right)^{\frac{\bar{k}}{\bar{k}-1}}$$

and taking $v_0 = 0$, we obtain

$$v_a = \sqrt{\frac{2g\bar{k}}{\bar{k}-1}\bar{R}T_0\left[1-\left(\frac{p_a}{p_0}\right)^{\frac{\bar{k}-1}{\bar{k}}}\right]}.$$

Replacing

$$\bar{R}T_0 = (1-\varepsilon)RT_0 = (1-\varepsilon)f_p\chi,$$

we obtain

$$v_a = \sqrt{1-\varepsilon}\sqrt{\frac{2g\bar{k}}{\bar{k}-1}\chi f_p\left(1-\pi_a^{\frac{\bar{k}-1}{\bar{k}}}\right)},$$

or

$$v_a = \sqrt{1-\varepsilon}\, f_v(\zeta, \bar{k})\sqrt{\chi f_p}, \tag{3.41}$$

where function f_v is determined from Table 3.5 for output quantities $\bar{k}$ and $\zeta = \frac{d_a}{d_{кр}}$.

Analogously we obtain for flow rate per second

$$G = \frac{\bar{A}F_{кр}p_0}{\sqrt{1-\varepsilon}\sqrt{\chi f_p}}, \tag{3.42}$$

where

$$\bar{A} = A(\bar{k}) = \left(\frac{2}{\bar{k}+1}\right)^{\frac{1}{\bar{k}-1}}\sqrt{\frac{2g\bar{k}}{\bar{k}+1}}.$$

Value $\bar{A}$ can be determined from Table 3.1 from input value $\bar{k}$.

For reaction force we obtain

$$P = \frac{G}{g}v_a + F_a(p_a - p_н),$$

where G and v_a are determined by formulas (3.41) and (3.42), and value $p_a = \pi_a p_0$ is determined with the use of Table 3.3.

Specific thrust is determined from expression

$$I_1 = \frac{v_a}{g} + \frac{F_a}{G}(p_a - p_н).$$

Example: To determine parameters of flow for the above-examined conditions: $d_{кр} = 15$ cm; $\varepsilon = 2$; $k = 1.25$; $p_0 = 120 \frac{kg}{cm^2}$; $\chi f_p = 90{,}000$ m. For these conditions in the absence of solid particles we obtained $v_a = 2050 \frac{m}{s}$; $G = 14.5 \frac{kg}{s}$; $i = 3290$ kg; $l_1 = 227 \frac{kgs}{kg}$.

Let us now consider the case when at the same composition and temperature of gases the flow contains 10% solid particles ($\varepsilon = 0.1$). Let us take additionally $R = 36 \frac{m}{°C}$; heat capacity of solid particles $c = 0.35 \frac{kcal}{kg\ °C}$. Here we will obtain

$$c_v = \frac{AR}{k-1} = \frac{36}{427 \cdot 0{,}25} = 0{,}337;$$

$$c_p = kc_v = 1{,}25 \cdot 0{,}337 = 0{,}421.$$

By formulas (3.39), (3.40) we obtain

$$\bar{k} = \frac{(1-\varepsilon)c_p + \varepsilon c}{(1-\varepsilon)c_v + \varepsilon c} = \frac{0{,}9 \cdot 0{,}421 + 0{,}1 \cdot 0{,}35}{0{,}9 \cdot 0{,}337 + 0{,}1 \cdot 0{,}35} = 1{,}225.$$

We determine exit velocity v_a. Preliminarily by Table 3.5 we find:

$$f_v(\bar{k}, \varepsilon) = f_v(1{,}225;\ 2) = 6{,}89;$$

$$v_a = \sqrt{1-\varepsilon}\, f_v(\bar{k}, \varepsilon) \sqrt{\chi f_p} = \sqrt{0{,}9} \cdot 6{,}89 \cdot 300 = 1955 \frac{m}{s}.$$

We calculate flow rate per second; preliminarily by value $\bar{k} = 1.225$ we determine by Table 3.1, $\bar{A} = 2.045$, whence

$$G = \frac{AF_{кр}p_0}{\sqrt{1-\varepsilon}\sqrt{\chi f_p}} = \frac{2{,}045 \cdot 17{,}65 \cdot 120}{\sqrt{0{,}9}\sqrt{90\,000}} = 15{,}2 \frac{kg}{s}.$$

We determine pressure in the outlet section. Preliminarily by value $\bar{k} = 1.225$ we find by Table 3.3, $\pi_a = 0.411$, whence

$$p_a = p_0\pi_a = 120 \cdot 0{,}411 = 4{,}92 \frac{kg}{cm^2}.$$

We calculate reaction force

$$P = \frac{G}{g} v_a + F_a(p_a - p_н) = \frac{15{,}2}{9{,}81} 1955 + 70{,}6\,(4{,}92 - 1) = 3307 \text{ kg}.$$

We calculate unit pulse

$$I_1 = \frac{P}{G} = \frac{3307}{15{,}2} = 218 \frac{kcal}{kg}.$$

We compare parameters of flow in the presence and absence of solid particles in the flow.

	v_a	σ	ρ_a	P	λ
In form flow	2050	14,5	4,7	3290	227
Flow with solid particles $\varepsilon = 0,1$	1955	15,2	4,9	3307	218
difference in %	−4,6	+4,7	+2	+0,5	−4,0

From the given calculation it is clear that when $\varepsilon = 0.1$ the specific thrust decreases 4%. At the same time introduction of metallic additions in the fuel in the form of powder of aluminum or boron increases effectiveness of the fuel on account of an increase of its temperature of combustion and specific gravity. The question of the expediency of use of such fuels is decided by taking into account all the shown factors.

Furthermore, it is possible to nearly take exit velocity and specific thrust by varying proportionally $\sqrt{1-\varepsilon}$, and flow rate per second – inversely proportionally $\sqrt{1-\varepsilon}$. Reaction force remains practically constant.

§ 3.7. Calculation of Parameters of Outflow of Gases with the Aid of Tables of Gas Dynamic Functions

In the expression for speed of gas

$$v = \sqrt{\frac{2gk}{k-1} RT_0 \left(1 - \pi^{\frac{k-1}{k}}\right)},$$

considering that speed in the critical section

$$v_{кр} = a_{кр} = \sqrt{\frac{2gk}{k+1} RT_0}, \tag{3.43}$$

and introducing designation

$$\lambda = \frac{v}{a_{кр}},$$

we obtain

$$\lambda^2 = \left[1 - \pi^{\frac{k-1}{k}}\right] \frac{k+1}{k-1},$$

whence

$$\frac{\rho}{\rho_0} = \pi(\lambda) = \left[1 - \frac{k-1}{k+1}\lambda^2\right]^{\frac{k}{k-1}}. \tag{3.44}$$

For temperature and density we obtain accordingly:

$$\frac{T}{T_0} = \tau(\lambda) = 1 - \frac{k-1}{k+1}\lambda^2; \tag{3.45}$$

$$\frac{\rho}{\rho_0} = \varepsilon(\lambda) = \left[1 - \frac{k-1}{k+1}\lambda^2\right]^{\frac{1}{k-1}}. \tag{3.46}$$

The biggest value $\lambda = \lambda_{max}$ corresponds to infinite expansion of the stream into a vacuum.

Besides

$$\tau(\lambda_{max}) = 1 - \frac{k-1}{k+1}\lambda^2_{max},$$

whence

$$\lambda_{max} = \sqrt{\frac{k+1}{k-1}}. \tag{3.47}$$

Thus, the coefficient of speed λ is changed from $\lambda = 0$ to λ_{max} and is equal to one in the critical section.

When $k = 1.25$ $\lambda_{max} = 3$.

Functions $\pi(\lambda)$, $\tau(\lambda)$, and $\varepsilon(\lambda)$ monotonously decrease from one to zero during a change of λ from zero to λ_{max}.

Expression (3.7) by substitution of value $\pi(\lambda)$ from expression (3.44) can easily be reduced to the form

$$q(\lambda) = \frac{F_{кр}}{F} = \left(\frac{k+1}{2}\right)^{\frac{1}{k-1}} \lambda \left(1 - \frac{k-1}{k+1}\lambda^2\right)^{\frac{1}{k-1}}. \tag{3.48}$$

We will examine the expression for reaction force

$$P = \frac{Gv_a}{g} + F_a(p_a - p_н). \tag{3.49}$$

Throwing out index a, we obtain

$$P = \frac{Gv}{g} + pF - p_н F. \tag{3.50}$$

Further,

$$\frac{Gv}{g} = \rho F v \cdot v = \rho F a^2_{кр} \lambda^2.$$

Using value $a^2_{кр}$ from expression (3.43), we obtain

$$\frac{Gv}{g} = F\lambda^2 \rho \frac{2k}{k+1}\frac{p_0}{\rho_0} = F\lambda^2 \frac{2k}{k+1}\varepsilon(\lambda) p_0$$

or finally

$$\frac{Gv}{g} = Fp_0\lambda^2 \frac{2k}{k+1}\left[1-\frac{k-1}{k+1}\lambda^2\right]^{\frac{1}{k-1}}. \tag{3.51}$$

Let us further consider expression

$$pF = Fp_0\pi(\lambda) = Fp_0\left[1-\frac{k-1}{k+1}\lambda^2\right]^{\frac{k}{k-1}}. \tag{3.52}$$

Putting expression (3.51) and (3.52) in formula (3.50), we will obtain after conversions

$$P = Fp_0(1+\lambda^2)\left[1-\frac{k-1}{k+1}\lambda^2\right]^{\frac{1}{k-1}} - Fp_w. \tag{3.53}$$

Introducing into consideration function $f(\lambda)$, determined from expression

$$f(\lambda) = (1+\lambda^2)\left[1-\frac{k-1}{k+1}\lambda^2\right]^{\frac{1}{k-1}} = (1+\lambda^2)\,\varepsilon(\lambda),$$

and the coefficient of the nozzle σ_c, we obtain the expression for reaction force

$$P = \sigma_c F p_0 f(\lambda) - Fp_w, \tag{3.54}$$

where F and λ correspond to the outlet section.

Obtained functions:

$$\tau(\lambda) = 1-\frac{k-1}{k+1}\lambda^2 = \frac{T}{T_0};$$

$$\pi(\lambda) = [\tau(\lambda)]^{\frac{k}{k-1}} = \frac{p}{p_0};$$

$$\varepsilon(\lambda) = [\tau(\lambda)]^{\frac{1}{k-1}} = \frac{\rho}{\rho_0};$$

$$q(\lambda) = \left(\frac{k+1}{2}\right)^{\frac{1}{k-1}}\lambda\left[1-\frac{k-1}{k+1}\lambda^2\right]^{\frac{1}{k-1}} = \frac{F_{кр}}{F}.$$

$$f(\lambda) = (1+\lambda^2)\left[1-\frac{k-1}{k+1}\lambda^2\right]^{\frac{1}{k-1}} = \frac{P+Fp_w}{Fp_0}$$

are tabulated for different values k [4].

The order of calculation of parameters of flow with the aid of gas dynamic functions is as follows.

1. From thermodynamic calculation of power characteristics of gases in the chamber we determine values T_0, ρ_0, p_0, k, R, f_p.

2. We determine the critical speed of sound from expression

$$a_{кр} = \sqrt{\frac{2gk}{k+1}\chi f_p}$$

3. For the examined section, in particular for the outlet section, we calculate for given K

$$\frac{F_{кр}}{F} = q(\lambda)$$

and by the table of function $q(\lambda)$ by reverse interpolation we find λ.

4. We calculate

$$v = \lambda a_{кр}$$

5. On tables we find functions $\tau(\lambda)$, $\varepsilon(\lambda)$, $\pi(\lambda)$, $f(\lambda)$.

6. We calculate directly

$$T = T_0\tau(\lambda); \quad \rho = \rho_0\varepsilon(\lambda); \quad p = p_0\pi(\lambda).$$

7. We calculate thrust of the engine from expression

$$P = a_c F p_0 f(\lambda) - F p_н$$

8. We calculate flow rate per second from expression

$$G = \frac{\varphi A F_{кр} p_0}{\sqrt{\chi f_p}}.$$

where $A = \left(\frac{2}{k+1}\right)^{\frac{1}{k-1}}\sqrt{\frac{2gk}{k+1}}$ is determined on Table 3.1.

9. We calculate specific thrust from expression

$$P_{уд} = I_1 = \frac{P}{G}.$$

Literature

1. Barrer M., Zhomott A., Vebek B., Vandenkerkkhove Zh. Raketnyye dvigateli (Rocket engines). Oborongiz, 1962.

2. Alemasov V. Ye. Teoriya raketnykh dvigateley (Theory of rocket engines). Oborongiz, 1962.

3. Zel'dovich Ya. B., Ribin M. A., Frank-Kamenetskiy D. A. Impul's reaktivnoy sily porokhovykh raket (Pulse of reaction force of solid propellant rockets). Oborongiz, 1963.

4. Abramovich G. N. Prikladnaya gazovaya dinamika (Applied gas dynamics). Gostekhizdat, M., 1953.

C H A P T E R IV

BASIC PROBLEM OF INTERNAL BALLISTICS OF RDTT

§ 4.1. Speed of Burning of Solid Rocket Fuels

By burning rate of a solid rocket propellant we understand speed of displacement of the surface of burning in the length of the charge. Inasmuch as rocket fuels burn by parallel layers, the direction of the burning rate always coincides with the normal to the surface of burning. The product of burning rate and fuel density is the mass burning rate m, equal to the mass of gas forming per unit time from a unit area of the burning surface. Characteristic values of burning rates for different fuels are given in the tables of Chapter I.

Burning rates of contemporary rocket fuels under [RDTT] (РДТТ) oscillate within limits from 1 to 50 mm/s [1]. High speeds of burning are desirable for charges in unguided rocket missiles and boosters, and also for sustainer charges burning from the end surface. Small burning rates are necessary to ensure long work time of sustainers with charges which burn from within, in a radial direction.

The burning rate of a fuel is determined by its physical-chemical characteristics, pressure in the rocket chamber p, initial temperature T_H and speed v of the gas flow moving along the surface of burning.

Mathematically this dependence can be expressed so:

$$u = f(p)\eta(T_н)\varphi(v);$$

where functions f(p), $\eta(T_H)$ and $\varphi(v)$ are usually considered independent of one another.

They are determined by composition of the fuel and peculiarities of the technological process of its manufacture. For nitroglycerine ballistite fuels value u increases in proportion to the content of nitroglycerine. Of known influence are conditions of pressing [2]. For composite fuels u depends on the type of oxidizer and the degree of granulation of the oxidizer, and also on the presence of catalysts in the fuel.

As data of Table 1.3 show, of the most wide-spread oxidizers the maximum burning rate is ensured by potassium perchlorate and the minimum rate by ammonium nitrate, which is used for manufacture of slowly burning compositions.

Let us consider the dependence of burning rate on pressure, which in general form is written

$$u = f(p).$$

For ballistite fuels in a range of low pressures (to 30-80 kg/cm^2) the relationship between burning rate and pressure is expressed by formula

$$u = u_1 p^{\nu}, \tag{4.1}$$

which in internal ballistics called the exponential law of burning. With growth of pressure exponential dependence becomes linear:

$$u = A + Bp,$$

or

$$u = \bar{a}(1 + \bar{b}p). \tag{4.2}$$

The linear law of burning holds true for pressures from 40 to 200-300 kg/cm^2. In the interval of pressures from 30 kg/cm^2 to 150 kg/cm^2 during determination of burning rate with approximately identical accuracy it is possible to use either the exponential or the linear dependence. At high pressures in the binomial of the linear law it is possible to disregard value A, which transforms it into the monomial dependence utilized in internal ballistics of artillery armament:

$$u = u_1 p. \tag{4.3}$$

The dependence of burning rate of composite fuels on pressure usually is expressed by formulas of the same form as for ballistite fuels. Taken for separate intervals of pressure, they sufficiently exactly approximate the experimental curve. The universal expression of the law of burning for composite fuels will be examined below.

The value of exponent ν for contemporary rocket fuels changes within limits of 0.1-0.85. Higher values ν are characteristic for ballistite fuels (see Table 1.1). For composite fuels, the burning rate to a smaller degree depends on pressure.

It is necessary to indicate one of the probable deviations from the general dependence, the so-called "plateau" effect, observed

during burning of ballistite fuels with additions of different compounds of lead [4]. For such fuels the burning rate in a certain range of pressures does not depend on pressure ($\nu \to 0$).

Let us consider the equation of heat balance for the surface of burning of a solid fuel

$$\dot{m}c_T(T_s - T_H) = q_k + \dot{m}Q_r \qquad (4.4)$$

In the right part of equality stands the sum of quantities of heat supplied from the gas phase by means of convection q_k and liberated as a result of reactions in the solid phase from a unit surface area of burning per unit time. The left part of the equality represents the change of heat content of the mass of solid fuel, equal to m, during heating from initial temperature T_H to surface temperature T_s. Here c_T – specific heat of the solid fuel. The equation is based on the assumption that transmission of heat of the charge surface by radiation of the flame can be disregarded. Hence

$$\dot{m} = \frac{q_k}{c_T(T_s - T_H) - Q_r}. \qquad (4.5)$$

We will first examine the solution for a ballistite fuel.

During heating of a ballistite fuel thermal decomposition of its components occurs with formation of a gas mixture which contains combustible substances (formaldehyde and other complex organic compounds, oxide of carbon, hydrogen), oxidizers (mainly NO_2) and inert products.

The surface of burning adjoins a so-called zone of gasification, in which on account of restoration of NO_2 to NO oxidizing processes flow. These processes are accompanied by a great liberation of heat (nearly half the caloricity of the fuel) and growth of temperature of gases (up to 1100-1400°K).

After expenditure of reserves NO_2 formed during gasification of the fuel, oxidizing processes stop. In addition, there is not further temperature rise which in the limits of a certain region is preserved constant and equal to T_1. This region is called the preparatory or preardent zone. The subsequent stage of chemical activity is connected with accumulation in the gas mixture of active centers, which occurs all over the preparatory zone and leads to the appearance of a luminescent flame. In the zone of the luminescent flame burning of CO and H_2 occurs on account of restoration of NO to N_2. Here, temperature increases to a level corresponding to formation

of an equilibrium mixture of combustion products, i.e., to T_{op}.

At low pressures the width of the preparatory zone between zones of gasification and luminescent flame is measured in hundreds of micron. This excludes the influence of the luminescent flame on processes arising on the surface of the fuel.

Supply of heat to the surface of charge will be entirely determined by thermal conduction of the zone of gasification. The real profile of temperatures in the zone of gasification will be replaced by a linear characteristic coinciding with the tangent to the profile at point S (Fig. 4.1).

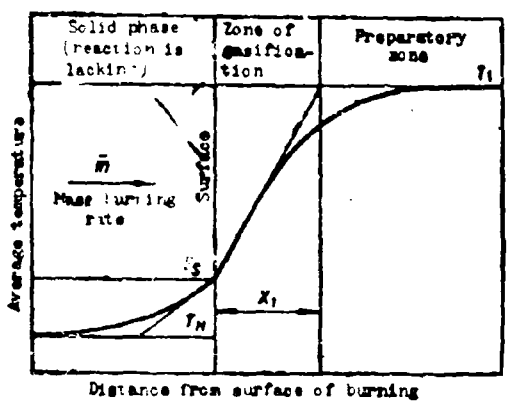

Fig. 4.1. Diagram of burning of ballistite fuel

Then during steady state thermal conduction

$$q_K = \lambda_r \frac{T_1 - T_S}{X_1},$$

where λ_r – coefficient of thermal conduction of gases; X_1 – gasification zone width.

Putting value q_K in equation (4.5), we obtain

$$\dot{m} = \lambda_r \frac{T_1 - T_S}{c_r\left(T_s - T_0 - \frac{Q_L}{c_r}\right) X_1}. \qquad (4.6)$$

The mass rate of decomposition of the solid phase is determined by the surface temperature T_S:

$$\dot{m}_S = \rho_T u = k_S e^{-\frac{E}{RT_S}},$$

ρ_T – density of fuel; u – burning rate; k_s – chemical constant; E – energy of activation; R – gas constant.

As analysis of an exact solution of this problem shows, during a change of pressure over a wide range, value T_s changes little. Thus, according to V. N. Vilyunov [5], for one of the fuels during a change of pressure from 10 to 70 kg/cm^2 the burning rate increases 3.5 times, whereas T_s is changed from 808 to 924°K, i.e., 14%. Such a high sensitivity of the speed of gas formation to a change of surface temperature is explained by location of the operating point of the process on the steep section of the S-shaped curve of the examined dependence. Practically, speed of gas formation is limited not by kinetics of chemical reactions, but by supply of heat to the surface of burning. This makes it possible, in the equation of heat balance for an approximate solution, to consider temperature T_s constant, taking its mean value for the pertinent range of pressures. After that, in expression (4.6) all values, with the exception of X_1, can be considered physical-chemical fuel constants. Designating their complex by F(T), we obtain

$$\dot{m} = \frac{F(T)}{X_1}. \tag{4.7}$$

For the zone of gasification oxidizing processess flowing on account of restoration of NO_2 to NO are characteristic. As a result of reactions in the zone of gasification a gas mixture containing combustible component CO and H_2 and large quantities of nitrogen oxide will be formed.

Gasification zone width can be defined as

$$X_1 = v\tau, \tag{4.8}$$

where $v = \frac{\dot{m}}{\rho_T}$ – speed of motion of gases formed normal to the surface of burning; ρ_T – density of gases; τ – time of completion of chemical reaction which is decisive for the zone of gasification.

$$\tau = \frac{c_{A_1} - c_{A_S}}{\left(\frac{dc_A}{dt}\right)_{cp}}, \tag{4.9}$$

where c_{A_1} and c_{A_S} – concentrations of substance A forming in the course of the reaction from substance D on borders of zone S – 1;

$\left(\frac{dc_A}{dt}\right)_{cp}$ – average chemical reaction rate.

According to laws of chemical kinetics the speed of the reaction of first order, in an elementary act of which one molecule participates, is equal to

$$\frac{dc_A}{dt} = K_1 c_D e^{-\frac{E}{RT}}. \tag{4.10}$$

The speed of the reaction of second order, an elementary act of which requires an encounter of two molecules of substance D, is equal to

$$\frac{dc_A}{dt} = K_2 c_D^2 e^{-\frac{E}{RT}}. \tag{4.11}$$

Here K_1 and K_2 – chemical constants.

Concentrations of reactants can be expressed as the product of relative concentration n and density of gases. Then for the reaction of first order:

$$\frac{dc_A}{dt} = \rho_r \frac{dn_A}{dt} = K_1 n_D \rho_r e^{-\frac{E}{RT}} = K_1 (1 - n_A) \rho_r e^{-\frac{E}{RT}}; \tag{4.12}$$

$$\tau = \frac{n_{A_1} - n_{A_S}}{\left[K_1 (1 - n_A) e^{-\frac{E}{RT}}\right]_{cp}}. \tag{4.13}$$

Inasmuch as in all cases, independently of pressure, value n changes within limits n_{A_S} and n_{A_1}, and temperature T within limits T_s' and T_1, time τ does not depend on pressure, i.e., $\tau(n, T) =$ $=$ const. Besides,

$$X_1 = \frac{\dot{m}}{\rho_r} \tau(n, T). \tag{4.14}$$

Putting expression (4.14) in expression (4.7), we obtain

$$\dot{m}^2 = \frac{F(T)}{\tau(n, T)} \rho_r. \tag{4.15}$$

Inasmuch as $\rho_r = \frac{p}{RT}$ in the case when for the zone of gasification the reaction of first order is decisive, we obtain

$$\dot{m} = \Phi_1(T, n)\, p^{0.5}, \tag{4.16}$$

where $\Phi_1(T, n)$ – complex determined by physical chemical propellant properties.

For a reaction of second order

$$\frac{dc_A}{dt} = \rho_r \frac{dn_A}{dt} = K_2 n_D^2 \rho_r^2 e^{-\frac{E}{RT}} = K_2 (1 - n_A)^2 \rho_r^2 e^{-\frac{E}{RT}}, \tag{4.17}$$

whence

$$\tau = \frac{n_{A_1} - n_{A_S}}{\left(K_2 n_D^2 e^{-\frac{E}{RT}}\right)_{cp} \rho_r} = \frac{n_{A_1} - n_{A_S}}{\left[K_2 (1 - n_A)^2 e^{-\frac{E}{RT}}\right]_{cp}} \frac{1}{\rho_r}; \tag{4.18}$$

$$X = \frac{\dot{m}}{\rho_r^2} \tau(n, T). \tag{4.19}$$

Putting expression (4.19) in expression (4.7) and solving consecutively with respect to $\dot{m}$ and X, we obtain:

$$\dot{m} = \Phi_2(T, n)\, p^{0.5} \tag{4.20}$$

$$X_1 = \frac{\Phi(T, n)}{p}. \tag{4.21}$$

Thus, in both cases an increase of pressure leads to reduction of the gasification zone width, and this in turn leads to an increase of heat supplied to the surface of burning from the gas phase. In view of the complexity of chemical processes flowing in the zone of gasification, it is very difficult to separate the decisive reaction. The order of the determining reaction is set by the relationship of rates of flowing reactions of different orders, which in general leads to dependence

$$\dot{m} = \Phi(T, n)\, p^{\nu}.$$

Initial equation (4.6) can be used for determination of the burning rate of a composite fuel. During heating of surface layers of a composite fuel thermal decomposition of the mineral oxidizer and binding substance occurs. The zone adjacent to the surface is filled by the flow of products of disintegration of fuel and oxidizer directed from the surface. During mixing of gaseous components processes of burning start. These processes are completed at a distance from the surface X_1 = 50-100 μm [17]. The zone in

which processes of mixing and burning occur is called the zone of granular diffusion burning. Within limits of the zone of burning, the temperature of gases continuously increases. Beyond its limits there is a constant temperature equal to T_0. Let us introduce average effective temperature of the surface of burning $\bar{T}_s$. Then according to the diagram (Fig. 4.2)

$$\dot{m} = \lambda_r \frac{T_0 - \bar{T}_s}{c_T\left(\bar{T}_s - T_0 - \frac{Q_s}{c_T}\right) x_1}. \tag{4.22}$$

During burning of a composite fuel two limiting cases are possible. At very low pressure the speed of process will be determined by speed of the burn reaction in the gas phase (kinetic) burning). At high pressures, when speed of chemical reactions is great, speed of the process will be determined by mixing of gaseous components, which corresponds to diffusion burning.

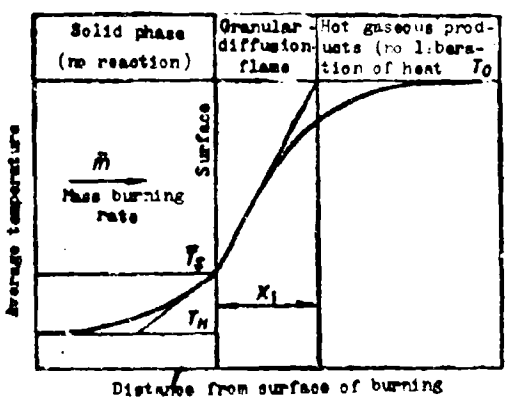

Fig. 4.2. Diagram of burning of composite fuel.

For the first case, derivation of the dependence coincides with the derivation for a ballistite fuel. Inasmuch as during burning of a composite fuel bimolecular reactions in the gas phase predominate, for this case formulas (4.19) and (4.20) hold true.

Let us consider the second case (diffusion burning). During decomposition of particles of oxidizer in the gas phase there will be an accumulation of decomposition products of dimension

$$d \approx \sqrt[3]{\frac{m_{ok}}{\rho_r}}, \tag{4.23}$$

where m_{OK} – mass of oxidizer particle.

The time of existence of such an accumulation can be considered

proportional to the area and cross section of the particle and inversely proportional to coefficient of diffusion D, which characterizes intensity of molecular diffusion of the two gaseous components

$$\tau \sim \frac{d^2}{D}.$$

If one disregards chemical reaction time and considers that the burning rate is determined only by time for mixing of components, distance X_1 will be defined as

$$X_{1D} \approx \frac{d^2}{D}\frac{\dot{m}}{\rho_T}. \tag{4.24}$$

Substituting value d from expression (4.23), we obtain

$$X_{1D} \approx \frac{m_{ox}^{0/3}\dot{m}}{\rho_T^{2/3}D}. \tag{4.25}$$

Putting expression (4.25) in expression (4.22) and solving the equation with respect to X_{1d}, we obtain

$$X_{1D} = \frac{m_{ox}^{1/3}\lambda_T^{1/3}(T_0 - T_S)^{1/3}}{\rho_T^{2/3}D^{1/3}c_T^{1/3}\left(T_S - T_0 - \frac{Q_S}{c_T}\right)^{1/3}}. \tag{4.26}$$

Inasmuch as

$$\rho \approx p,\ D \approx \frac{1}{p},$$

then

$$X_{1D} = \frac{\Phi_D(T)\, m_{ox}^{1/3}}{p^{1/3}}. \tag{4.27}$$

Putting expression (4.27) in expression (4.22), we obtain

$$\dot{m} = \lambda_T \frac{(T_0 - T_S)\, p^{1/3}}{c_T\left(T_S - T_0 - \frac{Q_S}{c_T}\right)\Phi_D(T)\, m_{ox}^{1/3}}, \tag{4.28}$$

or

$$\dot{m} = \frac{\Phi_{c_T}(T)\, p^{1/3}}{m_{ox}^{1/3}}. \tag{4.29}$$

In general, in a wide range of pressures, and also during partial mixing of components on the surface of burning, the burning rate of a composite fuel represents the total effect of diffusion and kinetic burning. Thickness of the zone of burning here can be expressed as

$$X_1 = Z_1 X_{1K} + Z_2 X_{1D}, \tag{4.30}$$

where Z_1 and Z_2 – coefficients expressing the share of participation of each of the forms of burning.

Substituting values X_{1K} and X_{1D} from expression (4.21) and (4.27), we obtain

$$X_1 = Z_1 \frac{\theta_K(T, n)}{p} + Z_2 \frac{\theta_D(T)\, m_{ox}^{2/3}}{p^{1/2}}. \tag{4.31}$$

Placing expression (4.31) in (4.22) and solving with respect to burning rate, we obtain

$$\frac{1}{u} = \rho_T \cdot \frac{c_T\left(\bar{T}_S - T_n - \frac{Q_g}{c_T}\right)}{\lambda_r(T_0 - \bar{T}_S)} \left[Z_1 \frac{\theta_K(T, n)}{p} + Z_2 \frac{\theta_D(T)}{p^{1/2}} m_{ox}^{1/3} \right],$$

or in general form

$$\frac{1}{u} = \frac{a}{p} + \frac{b}{p^{1/2}}. \tag{4.32}$$

Hence

$$u = \frac{p}{a + bp^{1/2}}. \tag{4.33}$$

Here coefficient a plays the role of a parameter of reaction time, and coefficient b – parameter of diffusion time. For an assigned composition of fuel with a rise of burning temperature (increase of content of oxidizer), coefficient a decreases. The value of coefficient b descends with a decrease of dimensions of particles. In Table 4.1 are given experimental values of these coefficients for fuel based on ammonium perchlorate and rubber P-13 [6].

As separate experiments show [6], formula (4.33) describes well the dependence of burning rate on pressure in the range from 1 to 100 kg/cm^2, when exponential and linear laws coincide with the experimental curve only on separate sections.

Table 4.1

Content of oxidizer, %	75	75	80	80
Average dimension of oxidizer particles μ	120	16	120	16
a	9,9	10,8	4,35	6,6
b	6,25	3,2	4,5	2,7

At values a and b shown in the table burning rate by formula (4.33) is expressed in cm/s if pressure is expressed in kg/cm^2.

Subsequently, during solution of problems of internal ballistics we will use the MKS system.

Besides, value a shown in Table 4.1 must be multiplied by 10^6, and value b – by 2.16×10^3.

§ 4.2. Influence of Speed of Gas Flow On Speed of Burning of Fuel

When the gas flows over the surface of the charge at high speed the burning rate of the fuel is increased. This phenomenon is observed during burning of long charges in an engine with a small area of passage for gases. The effect of increased burning rate of the charge at high speeds of flow of gases is in literature frequently called erosion burning. Such a term is unfortunate, inasmuch as the influence of the gas flow on intensity of gasification of the solid fuel has mainly a thermal character. Experimental determination of the increase of burning rate was conducted in two directions. The first of them is connected with burning of small flat samples (tablets) of fuels which are introduced on a special mandrel into a gas flow with known gas-dynamic parameters [7]. The second direction is based on burning of charges in a model engine with interruption of burning.

By producing measurements of fuel charges quenched at different instants, it is possible to establish how burning rate of a fuel changes with a change of chamber cross sections. In turn, the value of cross sections of the chamber jointly with pressure recorded on an oscillogram determines speed of gas flow in different sections over the length of the charge and in different instants. Measurements of quenched charges show that burning rate of a fuel increases over the length of the charge in the direction toward the nozzle, i.e., fuel charges burn nonuniformly over the length.

In Fig. 4.3 are given results of experiments in an engine with interruption of burning for a series of ballistite and composite fuels at $p = 67\ kg/cm^2$ [8]. Along the ordinates is the ratio of burning rate of a fuel at the examined speed of gas flow to speed of burning in the absence of flow:

$$\theta = \frac{u_p}{u_0},$$

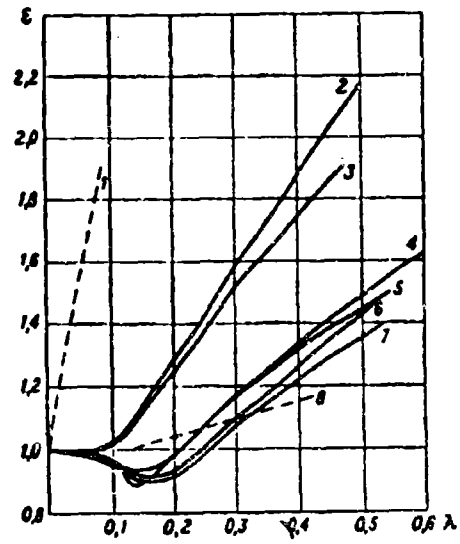

Fig. 4.3. Dependence of burning rate of solid fuel on flow rate of gases along surface of burning.

Along the abscissas are average values of dimensionless speed of gas flow over the length of a model chamber. Here curves 1 and 8 – composite fuels u - 0.24 and 2.18 cm/s, curves 2-7 – ballistite fuels u = 0.81; 0.86; 1.17; 1.20; 1.23; 1.29 accordingly. From the graph it follows that an increase of burning rate is observed starting with a certain threshold flow rate $\lambda_{пр}$. For speeds $\lambda > \lambda_{пр}$ burning rate is changed linearly in the first approximation, which permits the experimental dependence to be presented in the form

$$\varepsilon = 1 + k_{\lambda}(\lambda - \lambda_{пр}), \tag{4.34}$$

or

$$\varepsilon = 1 + k_{v}(v - v_{пр}). \tag{4.35}$$

According to source material [8], [9] the value of coefficients k_v and k_λ, called coefficients of erosion, is changed in inverse proportion to the burning rate of the fuel in a calm medium. The value of these coefficients is larger for fuels with a low combustion temperature and small for fuels with a high flame temperature. Separate data obtained at different pressures indicate the fact that value k_v descends with an increase of pressure in the engine. According to available data value k_v for all practical purposes does not depend on initial temperature of the charge.

For ballistite fuel of type JPN $v_{пр}$ = 180 m/s, and value k_v in the range v = 200-400 m/s can be accepted equal to 0.0022 s/m [9].

For the majority of composite fuels, characterized as compared to ballistite by higher flame temperatures and burning rates, the erosion effect appears considerably weaker.

Inasmuch as flow rate during assigned ratio $\frac{S_0}{F_{кр}}$ is simply determined by the parameter of Prof. Yu. A. Pobedonostsev $\varkappa = \frac{S_0}{F_{кр}}$, ratio ε can be expressed in a function of this parameter. For determination of $\varepsilon = \phi(x)$ for ballistite fuels with calorivity $Q_{ж}$ = = 800-900 kcal/kg, Ya. M. Shapiro offered dependence

$$\varphi(\varkappa) = 1 + 3{,}2 \cdot 10^{-3}(\varkappa - 100). \qquad (4.36)$$

This formula is accurate when $\varkappa \geqslant 100$. At smaller values $\varkappa$ one should take $\phi(x) = 1$. Known are empirical formulas which allow one to determine value ε for any section of the charge depending on the value of local velocity v.

Possibilities of contemporary computing technology allow development of such methods of calculation of intrachamber processes in RDTT which permit considering a spacial change of separate parameters. In this case the dependences for determination of a local change of burning rate obtain practical interest.

In general, during determination of ballistic parameters averaged over the chamber it is necessary to use dependences of type (4.35) and (4.36), expressing the integral effect of a change of burning rate over the length of the charge.

Let us consider causes of erosion burning.

The above stated burn scheme of a solid fuel is preserved even for conditions of flow around the surface of a charge by a gas flow until boundary zones - zone of gasification (ballistite fuel) and zone of granular diffusion burning (composite fuel) - are beyond the borders of the turbulent flow nucleus. Here distribution of temperature near the surface of the charge remains constant, and consequently, heat flow directed toward the surface of burning does not change. At a certain value of increased flow rate, borders of turbulent flow will shift to the depth of the shown zones. Turbulent heat transfer of reacting components is characterized by a higher intensity as compared to warm mass transfer, which is carried out in boundary zones by means of molecular diffusion and thermal conduction of gases. Therefore in the first approximation it is possible to consider that on the border of turbulent flow all processes of chemical interaction and mixings peculiar to boundary zones will be completed. Moreover, in the case of ballistite fuel, the border of turbulent flow should be at the temperature of the preparatory zone T_1, in case of a composite fuel - temperature of the flame T_0.

Thus, the influence of gas flow on burning rate of a fuel appears as a reduction of the depth of zone X_1, which at an assigned

difference of temperatures $T_1 - T_s$ (ballistite fuel) or $T_0 - \bar{T}_s$ (composite fuel) determines the value of the temperature gradient at the surface of the charge, and consequently also value of heat flow fed to the fuel.

Erosion conditions take place in an engine with high values of the parameter of loading κ on the initial stage of burning of the charge as long as the cross sections of the chamber are small. According to burning out of a charge a fast deceleration of the gas flow occurs and the erosion effect vanishes. The diagram of pressure in these cases carries a degressive character. Design pressure is determined by the height of soaring accompanying erosion burning, as a result of which engines are obtained heavy. In avoidance of this it is necessary to limit speed of the gas flow in the chamber, not allowing a considerable excess threshold value of speed. For a charge with constant area, all over its length, of free passage, lowering the speed of gas flow in the section turned toward the nozzle is inevitably connected with a decrease of density of loading of the engine. The optimum solution consists in creation of a charge with a free section increased in the direction of the nozzle. One of the variant solutions is a stepped charge, consisting of several charges with identical thickness of burning arch over the length of the chamber, but with areas of free passage, steps, increasing in the direction toward the nozzle. During manufacture of charges made from composite fuels it is possible to form a channel with continuous growth of section from nose cone to nozzle with the aid of a punch of special form.

§ 4.3. Basic Equations of Internal Ballistics of RDTT

We will start with the general dependence for the burning surface of a fuel

$$S = S_0 \sigma(\psi),$$

where ψ – relative amount of burning fuel; σ – function depending on form of solid fuel charge.

The burning rate of solid fuel at its normal temperature we determine from expression

$$u = f(p)\varphi(x),$$

where for a monomial exponential law $f(p) = u_1 p^{\nu}$, for a linear law $f(p) = A + Bp$ and for the universal law of burning $f(p) = \frac{p}{a + bp^{1/2}}$.

Function $\phi(x)$, characterizing the influence of flow rate of gases on burning rate of fuel, will be determined depending on the

parameter of Pobedonostsev:

$$\varkappa = \frac{S - S_T}{F_{\text{св}}}. \tag{4.37}$$

Since parameter $\varkappa$ is a function of ϕ, then it is possible to write the dependence for burning rate in the form

$$u = f(p)\varphi(\psi).$$

The expression for flow rate of gases per second we will write in the form

$$G = \frac{\varphi A F_{\text{кр}} p}{\sqrt{\chi T_p}}. \tag{4.38}$$

We throw out index 0 and write p instead of p_0, since subsequently we will examine only pressure in the chamber. Parameter χ determines the change of temperature of gases in the chamber on account of thermal losses. This parameter is changed in function ϕ approximately as a hyperbolic dependence (see § 6.3)

$$\chi = 1 - \frac{a}{1 + b\psi}. \tag{4.39}$$

The expression for a one-second flow of gases can be written in the form

$$\rho \frac{d\psi}{dt} = \delta S_{\text{св}}(\psi) f(p) \varphi(\varkappa), \tag{4.40}$$

where δ – density of fuel.

For flow rate per second of gases we have

$$\rho \frac{d\eta}{dt} = \frac{\varphi A F_{\text{кр}} p}{\sqrt{\chi T_p}}, \tag{4.41}$$

where η – relative amount of gases emanating towards instant t.

The weight quantity of gases in the chamber at the examined instant will be determined from expression

$$\rho(\psi - \eta + \gamma),$$

where $\gamma\omega$ – weight quantity of gases of igniter, which will remain in the chamber until the moment of ignition of its whole surface.

For an arbitrary instant the free volume in the chamber is equal to the initial free volume $\left(W_{кам}-\frac{\omega}{\delta}\right)$ plus volume $\frac{\omega\phi}{\delta}$ liberated from the burning part of the charge, minus covolume α of remaining gases.

The equation of the gas state takes the form

$$p=\frac{\chi f_{p}\omega(\psi-\eta+\gamma)}{W_{кам}-\frac{\omega}{\delta}(1-\psi)-\alpha\omega(\psi-\eta+\gamma)}.$$

Replacing $\frac{\omega}{W_{кам}}=\Delta$, where Δ – density of loading, we obtain

$$p=\frac{\chi f_{p}\Delta(\psi-\eta+\gamma)}{\frac{1}{\delta}-1+\psi+\alpha\Delta(\psi-\eta+\gamma)}. \qquad (4.42)$$

Integration of equations of input and expenditure of gases (4.40) and (4.41) jointly with the equation of state (4.42) permits determining ϕ, η and p and to obtaining the pressure curve in the function of time of burning p(t).

Value γ can be determined from the equation of state for initial moment

$$p_0\left(W_{кам}-\frac{\omega}{\delta}\right)=\chi f\gamma\omega,$$

where p_0 – initial pressure at the time of ignition of the charge of basic fuel; f – force of fuel of igniter charge.

In general, equations (4.40), (4.41) are not integrated analytically, and obtaining the pressure curve requires application of the method of numerical integration with the use of computers.

§ 4.4. Solution of Basic Problem of Internal Ballistics of RDTT When Parameters $\sigma(\psi)$, $\phi(\kappa)$ and $\chi(\psi)$ are Constant

We will examine the case, when for a given interval of time the dimensions of the charge of fuel and conditions of heat transfer will be changed insignificantly and in such a way that functions $\sigma(\psi)$, $\phi(\kappa)$ and $\chi(\psi)$ can be replaced by their mean values, which we subsequently for brevity will designate $\tilde{\sigma}$, $\tilde{\phi}$, $\tilde{\kappa}$.

Let us copy equations (4.40)-(4.42) in the following form:

$$\dot{\psi} = \frac{\delta S_0 \bar{\sigma} \bar{\varphi}}{\omega} f(p); \tag{4.43}$$

$$\dot{\eta} = \frac{\bar{\varphi} A F_{\text{кр}} p}{\omega \sqrt{\bar{\chi} f_p}}; \tag{4.44}$$

$$p = \frac{\bar{\chi} f_p \delta (\psi - \eta + \gamma)}{\frac{\delta}{\Delta} - 1 + \psi - \alpha\delta(\psi - \eta + \gamma)}. \tag{4.45}$$

We designate

$$x = \frac{\delta}{\Delta} - 1 + \psi = x_0 + \psi;$$
$$y = \psi - \eta + \gamma, \tag{4.46}$$

where $x_0 = \frac{\delta}{\Delta} - 1$.

Then

$$p = \frac{\bar{\chi} f_p \delta y}{x\left(1 - \alpha\frac{\delta y}{x}\right)}.$$

We will estimate component $\alpha\delta \frac{y}{x} \approx \alpha \frac{p}{\bar{\chi} f_p}$.

Considering $p = 100 \frac{\text{kg}}{\text{cm}^2} = 10^6 \frac{\text{kg}}{\text{m}^2}$, $\alpha = 10^{-3} \frac{\text{m}^3}{\text{kg}}$, $\bar{\chi} f_p = 75000$ м, we obtain $\frac{\alpha p}{\bar{\chi} f_p} \approx$ $\approx$ 0.013, which is approximately 1%, therefore subsequently we will disregard the covolume of gases. Equations (4.43)-(4.45) take the form:

$$\dot{x} = \frac{\delta S_0 \bar{\sigma} \bar{\varphi}}{\omega} f(p);$$
$$\dot{y} = \dot{x} - \frac{\varphi A F_{\text{кр}} p}{\omega \sqrt{\bar{\chi} f_p}};$$
$$p = \delta \bar{\chi} f_p \frac{y}{x}. \tag{4.47}$$

whence we obtain

$$\frac{dy}{dx} = 1 - N \frac{p}{f(p)}, \tag{4.48}$$

where

$$N = \frac{\varphi A F_{\text{кр}}}{\delta S_0 \bar{\sigma} \bar{\varphi} \sqrt{\bar{\chi} f_p}}. \tag{4.49}$$

Differentiating expression (4.47) with respect to x, we obtain

$$y'_x = \frac{p'_x x + p}{\delta \tilde{\chi} f_p}.$$

Placing it in expression (4.48) and separating variables, we obtain

$$\delta \tilde{\chi} f_p \frac{dx}{x} = \frac{dp}{1 - N\frac{p}{f(p)} - \frac{p}{\delta \tilde{\chi} f_p}}. \qquad (4.50)$$

We will estimate the last member in the denominator of the right side.

Considering

$$p = 100 \frac{\text{кг}}{\text{см}^2} = 10^6 \frac{\text{кг}}{\text{м}^2}, \ \tilde{\chi} f_p = 75000 \ \text{м}, \ \delta = 1600 \frac{\text{кг}}{\text{м}^3},$$

we obtain $\frac{p}{\delta \tilde{\chi} f_p} = 0{,}0083$, which is approximately 1% with respect to one. Disregarding this value, we obtain

$$\tilde{\chi} \delta f_p \frac{dx}{x} = \frac{dp}{1 - N\frac{p}{f(p)}}. \qquad (4.51)$$

Integrating in corresponding limits, we obtain

$$\tilde{\chi} \delta f_p \ln \frac{x}{x_0} = \Phi(N, p) - \Phi(N, p_0), \qquad (4.52)$$

where

$$\Phi(N, p) = \int_0^p \frac{dp}{1 - N\frac{p}{f(p)}}. \qquad (4.53)$$

Thus, under the shown assumptions a solution is obtained in general form for any form of function f(p), expressing the dependence of burning rate on pressure.

If function $\Phi(N, p)$ is tabulated, then, assigning value p, it is possible from expression (4.52) to determine value x and value ψ:

$$\psi = x + 1 - \frac{W_{\text{кам}}}{w} = x - x_\psi.$$

which determines the relative value of a burning charge of solid fuel. The method of calculation will be examined in § 4.7.

§ 4.5. Determination of Maximum (Limiting) Pressure

For determination of maximum pressure it is necessary to equate $\frac{dp}{d\psi}$ and $\frac{dp}{dx}$. From expression (4.51) we have

$$\frac{dp}{dx} = \frac{1}{x}\left[1 - N\frac{p}{f(p)}\right]\tilde{\gamma} f_p.$$

Equating $\frac{dp}{dx}$ to zero and considering that $\tilde{\gamma}$ is a finite quantity which varies from $x_0 = \frac{\delta}{\Delta} - 1$ to $x_1 = \frac{\delta}{\Delta}$, we will obtain the condition of maximum pressure from expression

$$N\frac{p_{max}}{f(p_{max})} = 1, \tag{4.54}$$

which is necessary to solve relative to p_{max}.

Let us see what value of x or ψ corresponds to p_{max}, determined from expression (4.54). If in expression (4.52) for $\ln\frac{x}{x_0}$ under the integral sign we place value $p = p_{max}$ from expression (4.54), then the denominator will turn into zero and the integrand expression will approach infinity. Here even the integral itself and consequently also $\frac{x}{x_0}$ will become infinite. Thus, the obtained value p_{max} corresponds to $x = \infty$ and we essentially have not maximum pressure $p_{пр}$ but ultimate pressure, which real pressure approaches asymptotically.

For determination of this pressure it is necessary to assign a form of function $f(p)$.

With the exponential law of change of pressure

$$f(p) = a_1 p^{\nu}$$

from expression (4.54) we obtain

$$p_{пр} = \left(\frac{a_1}{N}\right)^{\frac{1}{1-\nu}}. \tag{4.55}$$

With a linear law of burning

we obtain

$$f(p) = A + Bp$$

$$p_{np} = \frac{A}{N - B}. \tag{4.56}$$

And with law

$$f(p) = \frac{p}{a + bp^{1/2}}$$

we have

$$p_{np} = \left(\frac{1 - aN}{bN}\right)^{2/3}. \tag{4.57}$$

Let us note that formula (4.54) can be derived from simple physical prerequisites, if one considers the equality of income of gases to those expended.

Actually, in this case, equating expression (4.43) and (4.44), we obtain

$$\delta S_0 \tilde{\sigma} \tilde{\varphi} f(p) = \frac{\varphi A F_{\text{кр}} p}{\sqrt{\tilde{\varkappa} f_p}};$$

$$\frac{p}{f(p)} = \frac{\delta S_0 \tilde{\sigma} \tilde{\varphi} \sqrt{\tilde{\varkappa} f_p}}{\varphi A F_{\text{кр}}} = \frac{1}{N},$$

whence we obtain expression (4.54) just as formulas (4.55)-(4.57).

Example 1.

Let us define ultimate pressure in the chamber of a booster during the following characteristics of loading. The charge consists of seven cylindrical unclad charges of ballistite fuel.

Dimensions of the charge (in cm):

$$D = 5{,}6; \quad d = 1{,}1, \quad L = 77{,}5.$$

Critical throat diameter $d_{\text{кр}} = 5.6$ cm. Here $F_{\text{кр}} = 24.8$ cm^2.

Density of fuel $\delta = 1{,}6 \frac{\text{г}}{\text{см}^3} = 1600 \frac{\text{кг}}{\text{м}^3}$.

Initial surface of the charge is determined from expressions:

$$S_{бо} = 7\pi (D + d) L = 11400 \text{ см}^2;$$
$$S_{T0} = 7 \frac{\pi}{4} (D^2 - d^2) = 166 \text{ см}^2;$$
$$S_0 = S_{бо} + 2S_{T0} = 11730 \text{ см}^2.$$

Initial volume of the charge is determined from expression

$$W_0 = S_{T0} L = 1{,}66 \cdot 7{,}75 = 12{,}9 \text{ л}$$

Propellant weight

$$\omega = \delta W_0 = 1{,}6 \cdot 12{,}9 = 20{,}6 \text{ кг}$$

Progression characteristic $\sigma(\psi)$ is determined from expression

$$\sigma = 1 - 2\beta\psi, \tag{4.58}$$

where

$$\beta = \frac{D - d}{2L} = 0{,}029.$$

Moreover

$$S = S_0 \sigma(\psi).$$

A change of area of the end is determined from expression

$$S_T = S_{T0} \sigma_T(\psi) = S_{T0} (1 - \psi)(1 + \beta\psi). \tag{4.59}$$

The parameter κ of Pobedonostsev is determined from expression

$$\kappa = \frac{S - S_T}{F_{co}} = \frac{S - S_T}{F_{кам} - S_T}. \tag{4.60}$$

Internal diameter of the chamber $D_{кам}$ = 17.5 cm, where $F_{кам}$ = 240 cm^2. Parameter $\varphi(\kappa)$ will be determined from expression

$$\varphi(\kappa) = 1 + 3{,}2 \cdot 10^{-4} (\kappa - 100).$$

The coefficient of thermal losses we determine from expression (4.39)

$$\chi(\psi) = 1 - \frac{0{,}16}{1 + 2\psi}. \tag{4.61}$$

Force of the fuel f_p = 85,000 m (sic).

The adiabatic index for products of burning k = 1.25.

Dependence of burning rate on pressure is determined by expression

$$u = f(p) = \frac{p}{a + bp^{1/3}},$$

where

$$a = 7 \cdot 10^7; \quad b = 3{,}25 \cdot 10^9.$$

Here u is expressed in m/s and p in kg/m^2.

Parameter N, characterizing pressure in the chamber, is determined from expression (4.49)

$$N = \frac{\varphi A F_{кр}}{\delta S_\varphi(\psi)\,\varphi(\varkappa)\sqrt{\bar{X} f_p}} = \frac{N_0}{B(\psi)},$$

where

$$B(\psi) = \sigma(\psi)\,\varphi(\varkappa)\sqrt{\bar{X}}.$$

Besides, for adiabatic index k = 1.25 on Table 3.1 we find A = = 2.06.

Discharge coefficient ϕ we take equal to 0.98.

Besides, we obtain

$$N_0 = \frac{0{,}98 \cdot 2{,}06 \cdot 24{,}8}{1600 \cdot 11730\sqrt{85000}} = 0{,}916 \cdot 10^{-6}.$$

Value B(ψ), calculated by the formulas (4.58)-(4.61), are given in Table 4.2.

Table 4.2.

ψ	$\sigma(\psi)$	S_ψ	$\varkappa$	$\varphi(\varkappa)$	$\bar{X}$	$B(\psi)$
0	1,00	166	156	1,172	0,840	1,075
0,01	0,999	164	152	1,167	0,843	1,070
0,02	0,999	163	150	1,160	0,846	1,063
0,03	0,998	161	146	1,147	0,849	1,053
0,04	0,998	159	143	1,138	0,852	1,046
0,05	0,997	158	141	1,131	0,855	1,042
0,10	0,994	150	127	1,087	0,867	1,005
0,20	0,988	134	108	1,025	0,886	0,951
0,40	0,977	101	82	1	0,911	0,932
0,60	0,965	67	65	1	0,927	0,930
0,80	0,953	34	55	1	0,938	0,925
1,00	0,942	0	46	1	0,947	0,917

For an engine of examined type the rise of the pressure curve occurs for values ψ within limits 0–0.10.

Therefore for approximate determination of the highest pressure we take value $\psi_{cp} = 0.05$.

Here

$$N_{cp} = \frac{0{,}916 \cdot 10^{-6}}{1{,}012} = 0{,}879 \cdot 10^{-6};$$

$$p_{cp} = \left(\frac{1 - aN}{kV}\right)^{1/n} = \left(\frac{1 - 0{,}879 \cdot 10^{-6} \cdot 7 \cdot 10^{6}}{0{,}879 \cdot 10^{-6} \cdot 3{,}25 \cdot 10^{6}}\right)^{1/n} = 157 \cdot 10^{4}\ \mathrm{kg/m^2},$$

or

$$p_{cp} = 157\ \mathrm{kg/cm^2}.$$

Character of the rise of the pressure curve will be examined subsequently.

In Table 4.3 are given value $p_{пр}(\psi)$ calculated by proceding from values $B(\psi)$ in Table 4.2.

Table 4.3

ψ	0	0,01	0,02	0,03	0,04	0,05	0,07	0,10	0,20	0,50	0,80	1,00
$p_{пр}$, $\frac{kg}{cm^2}$	176	175	169	162	158	157	153	136	114	96	92	91

Example 2.

We will determine ultimate pressure in the chamber of an engine of a ballistic missile.

The charge consists of an externally clad cylindrical charge of composite fuel with internal channel and with longitudinal cuts (slot charge). Results of calculations of the progression characteristic are given in § 2.3.

Supplementary data:

$$\delta = 1750\ \frac{kg}{м^3};\quad f_p = 90\,000\ м;\quad k = 1{,}25;$$

$$D_{кам} = 0{,}814\ м;\quad d_{кр} = 0{,}193\ м;\quad F_{кр} = 0{,}0299\ м^2.$$

The dependence of burning rate on pressure will be determined by formula (4.33) at values $a = 1.05 \times 10^7$; $b = 1.3 \times 10^4$. Since walls of the chamber are isolated from the flow then coefficient χ of thermal losses in this case are less than in a booster chamber. Let us take for it expression

$$\chi(\psi) = 1 - \frac{0{,}05}{1 + 1{,}5\psi}.$$

Parameter $\phi(\kappa)$ we determine from dependence

$$\varphi(\kappa) = 1 + 3{,}2 \cdot 10^{-3}(\kappa - 100).$$

Values κ, $\phi(\kappa)$, χ and $B(\psi)$ are given in Table (4.4).

Table 4.4

ψ	0	0,01	0,02	0,03	0,04	0,06	0,10	0,20	0,40	0,60	1,00
κ	148	135	126	118	113	105	80	48	28	12	0
$\varphi(\kappa)$	1,153	1,112	1,083	1,058	1,042	1,016	1	1	1	1	1
χ	0,950	0,951	0,952	0,952	0,953	0,954	0,957	0,962	0,971	0,976	0,986
$B(\psi)$	1,125	1,100	1,075	1,058	1,042	1,030	1,012	1,018	1,047	1,035	0,960

The parameter of loading N will be determined from expression

$$N = \frac{N_0}{B(\psi)},$$

where

$$N_0 = \frac{\varphi A F_{\kappa\phi}}{\delta S_0 \sqrt{\chi_p}} = \frac{0{,}98 \cdot 2{,}06 \cdot 0{,}0299}{1750 \cdot 10{,}33 \sqrt{90000}} = 1{,}113 \cdot 10^{-4}.$$

$$N = \frac{1{,}113}{B(\psi)} 10^{-4}.$$

From Table 4.4 it is clear that minimum value $B(\psi) = 1.012$ corresponds to $\psi = 0.10$. This value $B(\psi)$ corresponds to minimum p_{np}, which we will find considering

$$N_{\psi=0{,}10} = \frac{1{,}113}{1{,}012} \cdot 10^{-4} = 1{,}10 \cdot 10^{-4};$$

then

$$p_{np} = \left(\frac{1 - aN}{bN}\right)^{0{,}4} = \left(\frac{1 - 1{,}10 \cdot 10^{-4} \cdot 1{,}05 \cdot 10^{7}}{1{,}10 \cdot 10^{-4} \cdot 1{,}3 \cdot 10^{4}}\right)^{0{,}4} = 48{,}5 \cdot 10^{4} \frac{kg}{m^2};$$

$$p_{np} = 48{,}5 \frac{kg}{cm^2} \approx 48 \frac{kg}{cm^2}.$$

Values $p_{пр}$ (ψ) are given in Table 4.5.

Table 4.5

ψ	0,02	0,05	0,10	0,20	0,50	0,75	1,00
$p_{пр}$	54	50	48	50	52	51	44

§ 4.6. Sensitivity of p_{max} to Parameter of Loading Pressure Stability

We will write the expression for the greatest pressure in the exponential law of burning

$$p_{max} = \left(\frac{u_1}{N}\right)^{\frac{1}{1-\nu}}. \tag{4.62}$$

We will examine the change of p_{max} during a small change of values in the expression for the parameter of loading N, for example, during a small change of the area of the critical section $F_{кр}$ or surface of fuel S_0. Logarithmizing and differentiating both parts of equality (4.62) and replacing differentials by increments, we obtain

$$\frac{\Delta p_{max}}{p_{max}} = \frac{1}{1-\nu}\left(\frac{\Delta u_1}{u_1} - \frac{\Delta N}{N}\right).$$

Analogously from the expression for N we obtain

$$\frac{\Delta N}{N} = \frac{\Delta F_{кр}}{F_{кр}} - \frac{\Delta S_0}{S_0} - \frac{1}{2}\frac{\Delta f_p}{f_p}.$$

Thus, we obtain

$$\frac{\Delta p_{max}}{p_{max}} = \frac{1}{1-\nu}\left[\frac{\Delta u_1}{u_1} + \frac{\Delta S_0}{S_0} - \frac{\Delta F_{кр}}{F_{кр}} + \frac{1}{2}\frac{\Delta f_p}{f_p}\right]. \tag{4.63}$$

Taking $\nu = \frac{2}{3}$; $\frac{1}{1-\nu} = 3$, we obtain that a change of any parameter in N, by 1% changes maximum pressure 3%. The nearer ν is to one, even greater is the coefficient of $\frac{\Delta N}{N}$, consequently, even greater is sensitivity of pressure to parameters of loading. Let us see from a purely physical side why the process of burning cannot be stable when $\nu \geq 1$.

From expression (4.43), (4.44) when $f(p) = u_1 p^{\nu}$ it follows that the second input is proportional to p^{ν}, and consumption of gases is proportional to p. When $\nu < 1$ we obtain the picture depicted in Fig. 4.4.

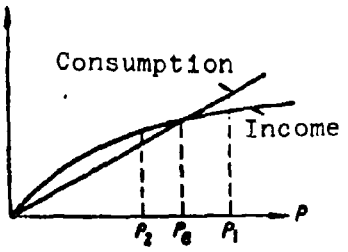

Fig. 4.4. Condition of stability of pressure in chamber.

The point of intersection of curves corresponds to a certain pressure p_e, at which income is equal to outflow. If for some cause pressure was $p_1 > p_e$, then consumption will be more than income and pressure will drop. If $p_2 < p_e$, then pressure will grow. Thus, equilibrium pressure will be stable.

If $\nu > 1$, then we will obtain the picture depicted in Fig. 4.5 (equilibrium pressure unstable). If the burning rate law is different than exponential, the question about stability of equilibrium pressure can be solved by comparison of graphs of income from consumption. For an analytic appraisal of sensitivity of pressure to parameters of loading it is possible for any function p(N) to write:

$$dp = p'(N)\,dN;$$
$$\frac{dp}{p} = \frac{Np'(N)}{p}\cdot\frac{dN}{N}$$

or, replacing differentials by increments:

$$\frac{\Delta p}{p} = \frac{Np'(N)}{p}\cdot\frac{\Delta N}{N}.$$

We will call the pressure index a function $\gamma(N)$, determined from expression

$$\gamma(N) = \frac{Np'(N)}{p}.$$

In this case we obtain dependence

$$\frac{\Delta p}{p} = \gamma\frac{\Delta N}{N},$$

connecting a relative change of pressure with a relative change of

the parameter of loading N. The less γ is, the less is sensitivity of pressure to conditions of loading.

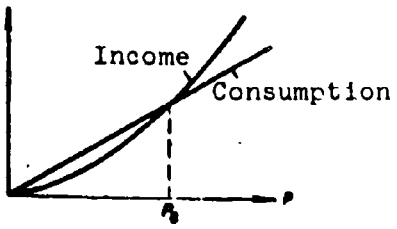

Fig. 4.5. Condition of unstable pressure in chamber.

In case of an exponential law of burning $\gamma = \frac{1}{1-\nu}$ is constant. For the binomial law from expression (4.56) we obtain

$$\gamma = \frac{N p_{ср}}{A}$$

or

$$\gamma = 1 + \frac{B}{A} p_{ср}$$

Thus, index of pressure γ increases with an increase of pressure. For the universal law we obtain

$$\gamma = \frac{3}{2} \frac{1}{1 - aN}$$

and taking into account expression (4.57)

$$\gamma = \frac{3}{2}\left(1 + \frac{a}{b p_{ср}^{1/2}}\right).$$

When

$$a = 5{,}6 \cdot 10^1, \quad b = 5 \cdot 10^3$$

we obtain

$$\frac{a}{b} = 1{,}12 \cdot 10^4,$$

$$\gamma = \frac{3}{2}\left(1 + \frac{1{,}12 \cdot 10^4}{p_{ср}^{1/2}}\right).$$

Thus, for the examined law of burning

$$f(p) = \frac{p}{a + b p^{1/2}}$$

with an increase of pressure, sensitivity of pressure to conditions of loading decreases.

For pressure $p_{ср} = 50 \frac{kg}{см^2} = 50 \cdot 10^4 \frac{kg}{м^2}$; $p_{ср}^{1/2} = 6{,}3 \cdot 10^3$ we obtain γ = 4.17.

For pressure $p_{ср} = 200 \frac{kg}{см^2} = 2 \cdot 10^6 \frac{kg}{м^2}$; $p^{1/2} = 1{,}59 \cdot 10^4$ we obtain γ = 2.56.

§ 4.7. Method of Construction of the Curve of Pressure for a Constant Value B(ψ)

Proceeding from constancy B(ψ), we obtained dependence (4.52):

$$\mathfrak{X} f_p \ln \frac{x}{x_0} = \Phi(N, p) - \Phi(N, p_0),$$

or

$$\mathfrak{X} f_p \ln \frac{x}{x_0} = \int_{p_0}^{p} \frac{dp}{1 - N \frac{p}{f(p)}}. \qquad (4.64)$$

We will originate from expression

$$f(p) = \frac{p}{a + bp^{1/2}}.$$

Here expression (4.64) takes the form:

$$\mathfrak{X} f_p \ln \frac{x}{x_0} = \int_{p_0}^{p} \frac{dp}{1 - N(a + bp^{1/2})},$$

or

$$\mathfrak{X} f_p \ln \frac{x}{x_0} = \frac{1}{1 - Na} \int_{p_0}^{p} \frac{dp}{1 - \frac{Nb}{1 - Na} p^{1/2}}.$$

But from expression (4.57) for $p_{пр}$ it follows that

$$\frac{1 - Na}{Nb} = p_{пр}^{1/2}.$$

Moreover, we have

$$\mathfrak{X} f_p \ln \frac{x}{x_0} = \frac{1}{1 - Na} \int_{p_0}^{p} \frac{dp}{1 - \left(\frac{p}{p_{пр}}\right)^{1/2}}.$$

Introducing designation

$$\Pi = \frac{p}{p_{пр}},$$

we obtain

$$\mathfrak{X} f_p \ln \frac{x}{x_0} = \frac{p_{пр}}{1 - Na} \int_{\Pi_0}^{\Pi} \frac{d\Pi}{1 - \Pi^{1/2}}. \qquad (4.65)$$

We are now free of parameter N under the sign of the integral and the latter can be calculated as a function of one variable Π.

Integrand $\frac{1}{1-\Pi^{1/3}}$ has a discontinuity at $\Pi = 1$ and has the form shown in Fig. 4.6.

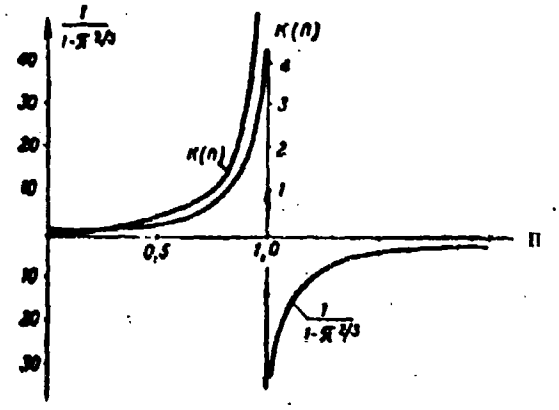

Fig. 4.6. Graph of function K(Π) utilized for construction of a pressure curve.

For conditions $p_0 < P_{пр}$; $\Pi_0 < 1$ (usually taking place in practice) it is possible to assign value Π, close to one, for example Π = 0.95 or Π = 0.98, and construction of the pressure curve if conducted up to this value of parameter Π. Introducing designation

$$K(\Pi) = \int_0^{\Pi} \frac{d\Pi}{1-\Pi^{1/3}},$$

we obtain expression (4.65) in the following form:

$$\ln \frac{x}{x_0} = \frac{p_{пр}}{\delta \chi / \rho (1 - N\alpha)} [K(\Pi) - K(\Pi_0)]. \qquad (4.66)$$

The last expression on the basis of formula (4.57) can be recorded in the form

$$\ln \frac{x}{x_0} = \frac{p_{пр} + \frac{a}{b} p_{пр}^{1/3}}{\delta \chi / \rho} [K(\Pi) - K(\Pi_0)]. \qquad (4.67)$$

Integral K(Π)with substitution $z = \Pi^{1/3}$ takes the form

$$K(\Pi) = 1{,}5 \left[\int_0^z \frac{z^2 dz}{1+z} + \int_0^z \frac{z^2 dz}{1-z} \right].$$

Integrals in brackets are found by elementary methods (substitution (substitution 1 + z = x; 1 - z = y).

Finally we obtain

$$K(\Pi) = \frac{3}{2} \ln \frac{1 + \Pi^{1/3}}{1 - \Pi^{1/3}} - 3\Pi^{1/3}. \tag{4.68}$$

Values of function $K(\Pi)$ are given in Table 4.6. Expression (4.67) permits setting the dependence of pressure p on x or on the relative value ψ of a burning fuel.

Table 4.6

Function $K(\Pi)$

Π	0,00	0,01	0,02	0,03	0,04	0,05	0,06	0,07	0,08	0,09
0,0	0	0,0103	0,0209	0,0319	0,0431	0,0545	0,0662	0,0781	0,0903	0,1027
0,1	0,1153	0,1282	0,1412	0,1546	0,1682	0,1820	0,1961	0,2103	0,2249	0,2397
0,2	0,2548	0,2701	0,2857	0,3016	0,3176	0,3342	0,3509	0,3679	0,3853	0,4029
0,3	0,4209	0,4391	0,4578	0,4767	0,4960	0,5157	0,5357	0,5562	0,5771	0,5982
0,4	0,6200	0,6421	0,6646	0,6876	0,7110	0,7351	0,7596	0,7845	0,8101	0,8362
0,5	0,8630	0,8903	0,9183	0,9469	0,9762	1,0062	1,0370	1,0686	1,1011	1,1344
0,6	1,1685	1,2036	1,2398	1,2770	1,3152	1,3547	1,3954	1,4374	1,4808	1,5256
0,7	1,5720	1,6202	1,6701	1,7219	1,7758	1,8319	1,8904	1,9516	2,0155	2,0826
0,8	2,1531	2,2274	2,3059	2,3890	2,4772	2,5714	2,6722	2,7807	2,8981	3,0260
0,9	3,1663	3,3216	3,4955	3,6903	3,9221	4,1918	4,5221	4,9482	5,5457	6,5432

The sequence of calculation is as follows.

1. By the method examined in § 4.5 we calculate the parameter of loading N and the biggest pressure $p_{пр}$.

2. Proceeding from characteristics of the igniter, we assign value p_0 and determine

$$\Pi_0 = \frac{p_0}{p_{пр}}.$$

3. Assigning several values Π

$$\Pi_0 < \Pi < 1,$$

we determine corresponding values $\frac{x}{x_0}$.

4. Proceeding from expression (4.46) for x, we find

$$\psi = \left(\frac{x}{x_0} - 1\right) x_0 = \left(\frac{x}{x_0} - 1\right)\left(\frac{\delta}{\Delta} - 1\right).$$

As a result of calculations carried out we obtain dependence $p(\psi)$.

If it is required to obtain dependence p(t), then it is

necessary to find dependence $\psi(t)$, proceeding from the equation of income of gases

$$\dot{\psi} = \frac{\alpha S_0 \bar{\sigma} \bar{\varphi}}{\omega} f(p),$$

whence at constancy of $\bar{\sigma}$ and $\bar{\varphi}$

$$t = \frac{\omega}{\alpha S_0 \bar{\sigma} \bar{\varphi}} \int_0^{\psi} \frac{d\psi}{f(p)}. \qquad (4.69)$$

For value

$$f(p) = \frac{p}{a + bp^{1/2}}$$

we have

$$t = \frac{\omega}{\alpha S_0 \bar{\sigma} \bar{\varphi}} \int_0^{\psi} \left(\frac{a}{p} + \frac{b}{p^{1/2}}\right) d\psi.$$

After obtaining dependence $p(\psi)$, as indicated above, the integral in expression (4.69) can be calculated by the method of numerical integration.

Let us consider a special case, when $p_0 > p_{пр}$; $\Pi_0 > 1$; this can take place during excessively great dispersion of the igniter, inasmuch as $p_{пр}$ depends on parameters of the basic fuel charge and does not depend on weight of the igniter. It is not difficult to see, that in this case with a growth of ψ pressure in the chamber will approach value $p = p_{пр}$, but approaching this value from above. During construction of the pressure curve it is necessary to consider that in this case $\Pi_0 > 1$, and since when $\Pi = 1$ the integrand has a discontinuity, then calculation can be produced only for values $\Pi > 1$.

Let us convert expression (4.65) into the form

$$8\chi f_p \ln \frac{x}{x_0} = \frac{p_{пр}}{1 - Na} \int_{\Pi}^{\Pi_0} \frac{d\Pi}{\Pi^{1/2} - 1}.$$

Previously used substitutions permit leading the last expression to the form

$$8\chi f_p \ln \frac{x}{x_0} = \frac{p_{пр}}{1 - Na} [L(\Pi_0) - L(\Pi)]. \qquad (4.70)$$

where $L(\Pi) = \frac{3}{2} \ln \frac{\Pi^{1/6} - 1}{\Pi^{1/6} + 1} + 3\Pi^{1/6}$.

Formula (4.70) permits constructing pressure curve $p(\psi)$ for the case when $p_0 > p_{пр}$.

Let us consider the case when dependence of the burning rate on pressure is expressed by formula

$$f(p) = n_1 p^{\nu}.$$

In this case expression (4.64) takes the form

$$\alpha \chi f_p \ln \frac{x}{x_0} = \int^{p} \frac{dp}{1 - \frac{N}{n_1} p^{1-\nu}}.$$

By introduction of substitution

$$p = \Pi p_{пр} = \Pi \left(\frac{n_1}{N}\right)^{\frac{1}{1-\nu}}$$

the last expression takes the form

$$\alpha \chi f_p \ln \frac{x}{x_0} = p_{пр} \int_{\Pi_0}^{\Pi} \frac{d\Pi}{1 - \Pi^{1-\nu}}.$$

Finally we obtain

$$\ln \frac{x}{x_0} = \frac{p_{пр}}{\alpha \chi f_p} [M(\Pi, \nu) - M(\Pi_0, \nu)], \tag{4.71}$$

where

$$M(\Pi, \nu) = \int_0^{\Pi} \frac{d\Pi}{1 - \Pi^{1-\nu}}$$

At $\nu = \frac{1}{3}$ value $M\left(\Pi, \frac{1}{3}\right)$ coincides with the value of function $K(\Pi)$, introduced earlier.

At $\nu = \frac{1}{2}$ by substitution $\left(1 - \Pi^{\frac{1}{2}}\right) = z$ we can obtain

$$M\left(\Pi, \frac{1}{2}\right) = 2\left[\ln \frac{1}{1 - \Pi^{1/2}} - \Pi^{1/2}\right].$$

At $\nu = \frac{2}{3}$ analogously we obtain

$$M\left(\Pi, \frac{2}{3}\right) = 3\left[\frac{1}{1 - \Pi^{1/3}} - \Pi^{1/3} - \frac{1}{2}\Pi^{2/3}\right].$$

Example of construction of pressure curve during constant B (ψ).

For the condition of Example 1 § 4.5 we construct the initial section of curve p (ψ). Additionally we assign the following parameters:

$$W_{\text{сан}} = 22{,}0\ л;\quad p_0 = 50\ \frac{кг}{см^2};\quad \Pi_0 = \frac{50}{157} = 0{,}318.$$

Density of loading

$$\Delta = \frac{m}{W_{\text{сан}}} = \frac{20{,}6}{22{,}0} = 0{,}936\ \frac{кг}{л\cdot м^3} = 936\ \frac{кг}{м^3}.$$

We determine the initial value of parameter x:

$$x_0 = \frac{\delta}{\Delta} - 1 = \frac{1{,}6}{0{,}936} - 1 = 0{,}71.$$

We conduct the calculation using expression

$$\ln\frac{x}{x_0} = \frac{p_{\text{пр}}}{\delta X f_p (1 - Na)}\,[K(\Pi) - K(\Pi_0)]$$

or

$$\lg\frac{x}{x_0} = A\,[K(\Pi) - K(\Pi_0)],$$

where

$$A = \frac{p_{\text{пр}}}{2{,}303\cdot\delta X f_p (1 - Na)}.$$

According to the data of Example 1 § 4.5:

$$A = \frac{157\cdot 10^6}{2{,}303\cdot 1600\cdot 0{,}855\cdot 85000\,(1 - 0{,}879\cdot 10^{-3}\cdot 7\cdot 10^7)} = 0{,}0152.$$

Further calculations are shown in Table 4.7. Values K(П) are determined by Table 4.6.

Table 4.7

$K(\Pi_0) = 0{,}454$

П	0,318	0,5	0,6	0,7	0,8	0,9	0,95	0,98
$K(\Pi)$	0,454	0,890	1,204	1,620	2,227	3,332	4,192	5,546
$K(\Pi) - K(\Pi_0)$		0,436	0,750	1,166	1,773	2,868	3,738	5,092
$\lg\frac{x}{x_0} = 0{,}0152[K(\Pi) - K(\Pi_0)]$		0,0066	0,0114	0,0177	0,0263	0,0436	0,0568	0,0773
$x : x_0$		1,016	1,027	1,042	1,063	1,106	1,140	1,195
$\psi = \left(\frac{x}{x_0} - 1\right) x_0$		0,010	0,019	0,030	0,045	0,075	0,100	0,138
$p = \Pi p_{\text{пр}}$	50	79	94	110	125	141	149	154

§ 4.8. Character of Growth of Pressure Curve Under Different Loading Conditions

From the example examined in the preceding section it is clear that pressure very rapidly approaches a maximum and that when $\psi = 0.10$, i.e., when 10% of the charge is burned, pressure in the chamber will differ from the maximum by 5%. Let us see whether in all cases there occurs such a fast growth of the pressure curve. Above we saw that during constancy of the surface of burning (σ = const) and constancy $\phi(x)$ and $\chi(\psi)$ pressure does not have a maximum, but asymptotically approaches value $p_{пр}$, determined by the parameter of loading N. Therefore we will assign a defined value $\Pi = \frac{p}{p_{пр}}$, at which one may assume that practically the highest pressure is attained. This pressure will be noted by index *:

$$\Pi^* = \frac{p^*}{p_{пр}}.$$

Subsequently we will take $\Pi^* = 0.95$ and will look for that ψ^*, to which it corresponds. Let us see, what parameters ψ^* depends on. From expression (4.67) it follows that

$$\ln \frac{x^*}{x} = \frac{p_{пр} + \frac{a}{b} p_{пр}^{1-\nu}}{\chi b f_p} [K(\Pi^*) - K(\Pi_0)]. \tag{4.72}$$

Furthermore, from expression (4.46) for x it follows that

$$\psi = \left(\frac{x^*}{x_0} - 1\right)\left(\frac{b}{\Delta} - 1\right). \tag{4.73}$$

From expressions (4.72) and (4.73) it follows that at fixed Π^* value ψ^* increases with an increase of $p_{пр}$ and decreases with an increase of b, χf_p and Δ.

In Fig. 4.7 is given the obtained calculation of the graph of dependence $\psi^* = f(p_{пр}, \Delta)$ for a model engine. Calculations show that the influence of initial pressure on value ψ^* is insignificant. Since the engines of ballistic missiles are characterized by large densities of loading and small pressures, then values ψ^* are obtained approximately 0.01. This means that pressure in the chamber very rapidly approaches value $p_{пр}$, determined by dependences (4.55), (4.57) and these formulas can be used for plotting pressure curves $p(\psi)$.

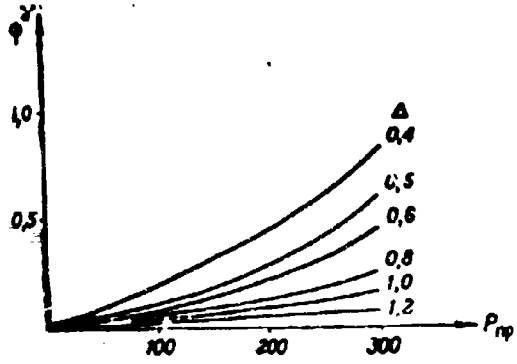

Fig. 4.7. Graph characterizing speed of approach of real pressure p to maximum $p_{пр}$.

§ 4.9. Determination of Pressure in the Chamber of an Engine with Variable Parameter $B(\psi)$

In § 4.7 we examined the method of construction of a pressure curve at constant values of parameters σ, ϕ and χ. In a general case of a variable surface of burning and variables of condition of heat transfer it is necessary to consider the variable character of shown functions. The exact method of determination of dependence $p(\psi)$ or $p(t)$ requires numerical integration of equations (4.43)-(4.45) taking into account initial conditions $\psi_0 = 0$ and $p = p_0$. Below is examined the method of approximation of pressure curve $p(\psi)$ with variable $\sigma(\psi)$, $\phi(x)$ and $\chi(\psi)$ with use of the method expounded in § 4.7. For this we will divide the ascending branch of the pressure curve $p(\psi)$ into sections in such a way that for each of these sections it is possible to take $B(\psi)$ constant and average for the examined section. Besides, for the i-th section from ψ_{i-1} to ψ_i calculation formulas take the form

$$\ln \frac{x_i}{x_{i-1}} = \frac{\tilde{p}_{пр\,i}}{\tilde{\chi}_i \tilde{b} f_p (1 - \tilde{N}a)} [K(\Pi_i) - K(\Pi_{i-1})]. \qquad (4.74)$$

where values noted by the sign (∿), correspond to mean values of parameters $\sigma(\psi)$, $\phi(x)$, $\chi(\psi)$ on the section from ψ_{i-1} to ψ_i:

$$\tilde{N} = \frac{1}{2}[N(\psi_i) + N(\psi_{i-1})];$$

$$\tilde{\chi} = \frac{1}{2}[\chi(\psi_i) + \chi(\psi_{i-1})];$$

$$\tilde{p}_{пр\,i} = p_{пр}(\tilde{N}_i) = \left(\frac{1 - a\tilde{N}_i}{b\tilde{N}_i}\right)^{1/k};$$

$$x_i = x_0 + \psi_i,$$

where

$$x_0 = \frac{1}{\Delta} - 1.$$

Calculation formula (4.74) will take the form

$$K(\Pi_i) = K(\Pi_{i-1}) + D \lg \frac{x_i}{x_{i-1}},$$

where

$$D = \frac{2{,}3038 \bar{x}_i f_p (1 - \bar{N}_{i0})}{\bar{p}_{\text{пр}\,i}};$$

$$\bar{N}_i = \frac{N_i}{B(\psi_\phi)}.$$

The method of construction of the pressure curve with variable parameter $B(\psi)$ will be examined in reference to conditions of Example 1 § 4.5 and the example of construction of a pressure curve with constant $B(\psi)$ § 4.7.

Initial data: $f_p = 85000$ кг; $\delta = 1600 \frac{\text{кг}}{\text{м}^3}$; $x_0 = 0{,}71$; $N_0 = 0{,}916 \cdot 10^{-6}$; $a = 7 \cdot 10^{1}$; $b = 3{,}25 \cdot 10^{3}$; $\Pi_0 = \frac{p_0}{p_{\text{пр}0}} = \frac{50}{175} = 0{,}276$.

Values χ, $p_{\text{пр}}$ and $B(\psi)$ are given in Tables 4.2 and 4.3.

The sequence of calculations is shown in Table 4.8.

The result of calculations of curve $p(\psi)$ for the ascending section of curve $p(\psi)$ is shown in Fig. 4.8. A maximum of pressure corresponds to $\psi = 0.08$. On the same figure is shown curve $p_{\text{пр}}(\psi)$. From a consideration of graphs of Fig. 4.8 it is clear that after achievement of maximum pressure the curve practically coincides with curve $p_{\text{пр}}(\psi)$. For construction of curve $p(t)$ it is necessary to determine dependence $t(\psi)$ with the help of dependence (4.69).

The appearance of curve $p(t)$ is shown in Fig. 4.9.

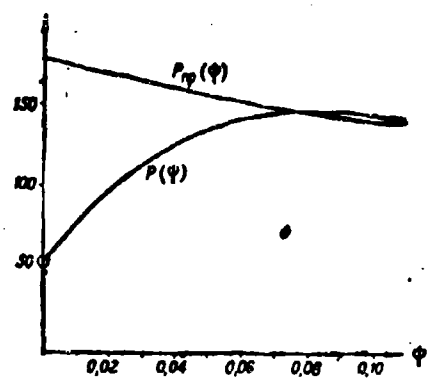

Fig. 4.8. Ascending section of curve $p(\psi)$

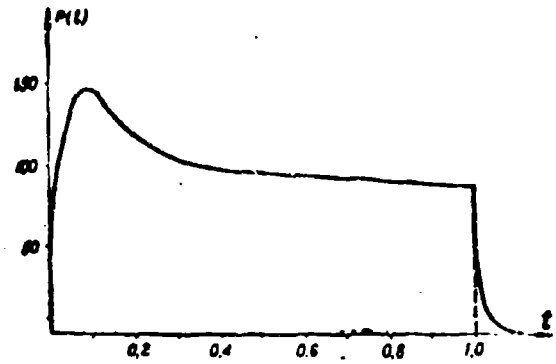

Fig. 4.9. Graph of curve $p(t)$ obtained by calculation

Table 4.8

1	ψ_{i-1}	0	0,01	0,02	0,03	0,04	0,05	0,07
2	ψ_i	0,01	0,02	0,03	0,04	0,05	0,07	0,10
3	$B(\psi_{cp})$	1,073	1,066	1,058	1,049	1,044	1,035	1,015
4	$\tilde{N} = N_0 : B(\psi_{cp})$	$0,855 \cdot 10^{-4}$	0,860	0,866	0,875	0,877	0,885	0,903
5	Na	0,598	0,602	0,606	0,613	0,614	0,620	0,631
6	$1 - \tilde{N}a$	0,402	0,398	0,394	0,387	0,386	0,380	0,369
7	$\tilde{\chi}$	0,841	0,844	0,847	0,850	0,853	0,858	0,863
8	$2,3038 f_p$	$3,13 \cdot 10^6$	3,13	3,13	3,13	3,13	3,13	3,13
9	$(6) \cdot (7) \cdot (8)$	$102,5 \cdot 10^6$	105,6	104,2	103,0	103,0	102,0	0,994
10	$\tilde{p}_{cp}$	$175 \cdot 10^6$	172	165	160	158	155	146
11	$(9) : (10) = D$	57,6	61,4	63,2	64,3	65,1	65,7	68,0
12	$\Pi_{i-1} = p_{i-1} : \tilde{p}_{cp}$	0,286	0,471	0,625	0,730	0,795	0,855	0,965
13	$x_i = x_0 + \psi_i$	0,72	0,73	0,74	0,75	0,76	0,78	0,81
14	$x_{i-1} = x_0 + \psi_{i-1}$	0,71	0,72	0,73	0,74	0,75	0,76	0,78
15	$x_i : x_{i-1}$	1,015	1,014	1,013	1,012	1,012	1,025	1,038
16	$\lg(x_i : x_{i-1})$	0,0065	0,0060	0,0056	0,0052	0,0052	0,0107	0,0162
17	$(11) \cdot (16) = D \lg(x_i : x_{i-1})$	0,374	0,368	0,354	0,334	0,338	0,703	1,100
18	$K(\Pi_{i-1})$	0,396	0,788	1,258	1,722	2,118	2,622	4,735
19	$(17) + (18) = K(\Pi_i)$	0,770	1,156	1,612	2,056	2,456	3,325	5,835
20	Π_i	0,464	0,596	0,708	0,786	0,838	0,910	0,984
21	$p_i = \Pi_i \tilde{p}_{cp}$	81	103	117	126	133	141	144

§ 4.10. Outflow After Termination of Burning of Fuel

Methods examined above permit constructing a pressure curve p(t) up to the end of burning of a fuel. For all the time of burning of the fuel combustion temperature in the chamber is taken constant, so that f_p = const.

After termination of burning of fuel pressure in the chamber of the engine rapidly drops. Besides, disregarding heat exchange with the chamber, it is possible to examine expansion of gases in the chamber as adiabatic. Upon completion of burning of a fuel, work of expansion of gases is accomplished at the expense of internal energy of gases, i.e., at the expense of a drop of their temperature. Let us consider the method of construction of pressure curve p(t) for the period of time from moment t_1 (termination of burning of fuel) to full outflow of gases.

After termination of burning of a fuel in the chamber there remains a certain weight quantity of gases Q_1 at pressure p_1. Value Q_1 will be found from the equation of the state of gases

$$Q_1 = \frac{p_1 W_{кам}}{U_p}. \qquad (4.75)$$

After termination of burning of a fuel the given force of gases of a fuel is impossible to consider constant, since adiabatic expansion of gases and a fall of temperature occurs. The expression for flow rate per second is conveniently given the form

$$Q = w\dot{\eta} = \frac{\varphi A F_{\text{кр}} p}{\sqrt{\mathcal{R}_p}} = \frac{\varphi A F_{\text{кр}} p}{\sqrt{pw}} = \varphi A F_{\text{кр}} \sqrt{\frac{p}{w}}, \tag{4.76}$$

where η, w – relative quantity of emanating gases and their specific volume.

Furthermore, total flow rate of gases from instant t_1 is equal to

$$w\eta = Q_1 - Q = Q_1 - \frac{W_{\text{кзн}}}{w},$$

where Q – weight quantity of gases in chamber for arbitrary instant t, and $\frac{1}{w}$ – weight density of gases. Consequently:

$$w\dot{\eta} = \frac{W_{\text{кзн}}}{w^2} \cdot \frac{dw}{dt}. \tag{4.77}$$

Equating expressions (4.76) and (4.77), we obtain

$$\varphi A F_{\text{кр}} \sqrt{\frac{p}{w}} = \frac{W_{\text{кзн}}}{w} \frac{dw}{dt},$$

whence

$$dt = \frac{W_{\text{кзн}} dw}{A F_{\text{кр}} \sqrt{p} w^{3/2}}. \tag{4.78}$$

Designating $z = \frac{p}{p_1}$, from the adiabatic equation we have:

$$w = w_1 \left(\frac{p}{p_1}\right)^{-\frac{1}{k}} = w_1 z^{-\frac{1}{k}};$$

$$dw = -\frac{w_1}{k} z^{-\frac{k+1}{k}} dz.$$

Putting w, dw and z in expression (4.78), we obtain

$$dt = -\frac{W_{\text{кзн}}}{k A F_{\text{кр}} \sqrt{p_1 w_1}} z^{-\frac{3k-1}{2k}} dz.$$

Taking the beginning reading of time from the moment of termination of burning of the fuel and integrating on the left from

zero to t, and on the right from one to z, we obtain

$$t = \frac{W_{\text{кам}}}{\varphi k A F_{\text{кр}} \sqrt{p_1 w_1}} \cdot \frac{2k}{k-1}\left(z^{-\frac{k-1}{2k}} - 1\right); \tag{4.79}$$

During replacement of $p_1 w_1 = \chi f_p$ and substitution

$$\frac{1}{B} = \frac{2W_{\text{кам}}}{\varphi A F_{\text{кр}} (k-1) \sqrt{\chi f_p}}, \tag{4.80}$$

expression (4.79) will take the form

$$Bt = \left(z^{-\frac{k-1}{2k}} - 1\right). \tag{4.81}$$

The obtained dependence is applicable when pressure in the chamber is higher than critical, since formula (4.76) for flow rate per second is true only in this case. It is necessary, however, to consider that subcritical outflow can take place when pressure in the chamber is low ($p \sim 2 \frac{\text{кг}}{\text{см}^2}$ when $p_{\text{н}} = 1\ \text{кг/см}^2$). Therefore, with sufficient practical accuracy it is possible to use dependence (4.81) for all the period of outflow of gases after termination of burning of the fuel. Values z = f(Bt) calculated by formula (4.81) are given in Table 4.9. Using this table, it is simple to construct the section of the pressure curve after termination of burning of the fuel.

Table 4.9

z	1,0	0,9	0,8	0,7	0,6	0,5	0,4	0,3	0,2	0,1
Bt	0	0,010	0,022	0,036	0,052	0,072	0,096	0,128	0,174	0,259
z	0,10	0,09	0,08	0,07	0,06	0,05	0,04	0,03	0,02	0,01
Bt	0,259	0,272	0,287	0,305	0,325	0,349	0,380	0,420	0,479	0,585

Let us consider conditions of the example given in § 4.9. We have $W_{\text{кам}} = 22{,}0\ \text{см}^3$; $F_{\text{кр}} = 24{,}8\ \text{см}^2$; $l_p = 85000\ \text{м}$. For the end of burning $\chi = 0{,}947$; $p = 91\ \frac{\text{кг}}{\text{см}^2}$

$$B = \frac{\varphi A F_{\text{кр}} (k-1) \sqrt{\chi f_p}}{2W_{\text{кам}}} =$$

$$= \frac{0{,}98 \cdot 2{,}06 \cdot 24{,}8 \cdot 10^{-4} \cdot 0{,}25 \sqrt{0{,}947 \cdot 85000}}{2 \cdot 22{,}0 \cdot 10^{-6}} = 0{,}806.$$

Assigning different values z, we determine Bt by Table 4.9. Dividing by B, we obtain corresponding values t. Results of calculations are given in Table 4.10 and are shown in Fig. 4.9 (final section).

Table 4.10

z	1	0,7	0,5	0,3	0,1	0,05	0,02
p	91	64	46	30	9	4,5	1,8
Bt	0	0,036	0,072	0,128	0,259	0,349	0,479
t	0	0,005	0,009	0,017	0,032	0,044	0,059

Let us consider what duration of free outflow of gases depends on. If in all cases we consider outflow completed at a fixed value, for example, at z = 0.02, then duration of free outflow will depend on parameter B, decreasing with its increase. From the expression for this parameter it is clear that duration of free outflow is proportional to value $\frac{W_{кам}}{F_{кр}}$.

For such an engine and fuel charges $W_{кам}$ is proportional to d^3, and $F_{кр} \to d^2$. Consequently, for such an engine duration of free outflow is proportional to the diameter of the chamber.

§ 4.11. Change of Temperature of Gases in the Chamber

During derivation of the equations which determine a change of pressure in the engine chamber, we originated from constancy of temperature of gases. Besides, temperature of gases $T_0 = T_{0p}$ was determined from the energy calculation of burning fuel at constant pressure proceeding from dependence.

$$Q_н = c_p T_{0p}$$

During burning of a fuel in a constant volume combustion temperature is determined from relationship

$$Q_н = c_v T_{0v},$$

whence it follows that

$$\frac{T_{0p}}{T_{0v}} = \frac{c_p}{c_v} = k$$

We considered thermal losses in the chamber by coefficient $\chi < 1$, determined from experiment or calculation. Thus, for an ideal process we considered temperature of gases to be constant. Such an assumption would be well founded in case of constant pressure in the chamber. However, in real conditions of variable pressure, temperature of gases does not have to remain constant. For determination of temperature of gases in the chamber it is necessary, besides the already used three equations – income, flow rate and state of gases – to compose an equation of energy balance.

Let us assume that in a certain time dt a weight quantity of $\omega d\psi$ burns and $\omega d\eta$ of gases flows out. During combustion of fuel, energy is liberated (in mechanical units)

$$dU = \frac{\omega d\psi \cdot Q_{\text{н}}}{A} = \frac{\omega c_v T_{0z}}{A} d\psi,$$

where $\frac{1}{A}$ – mechanical heat equivalent.

Considering that

$$c_v = \frac{AR}{k-1},$$

will obtain

$$dU = \frac{\omega}{k-1} RT_{0z} d\psi. \tag{4.82}$$

Energy dU is spent:

1. On internal energy of additional gases in the chamber

$$dU_1 = \omega (d\psi_c - d\eta_c) \frac{RT}{k-1}. \tag{4.83}$$

where T – variable temperature of gases in chamber.

2. On a change of internal energy of gases in the chamber, connected with a change of temperature of gases:

$$dU_2 = \omega (\psi - \eta + \gamma) \frac{C_v}{A} dT. \tag{4.84}$$

where γ – initial relative quantity of gases from igniter.

3. On losses of energy due to heat transfer from gases to walls of the chamber

$$dU_3 = \frac{q}{A}\,dt, \tag{4.85}$$

where $q = q(t)$ – heat flow per second from gases to walls of chamber.

4. On internal and kinetic energy removed by gases flowing out:

$$dU_4 = \frac{k}{k-1} RT\omega d\eta. \tag{4.86}$$

The expression for dU_4 emanates from the following considerations. During outflow of gases through the critical section, gases possess internal and kinetic energy. According to motion of gases along the nozzle, internal energy decreases, and kinetic energy increases. In the limiting case of outflow through an ideal infinitely divergent nozzle into a vacuum all internal energy is turned into kinetic. Besides, speed of gases

$$v_{max} = \sqrt{\frac{2gk}{k-1} RT},$$

where T – temperature of gases in chamber at examined moment of time.

Kinetic energy of emanating gases

$$\frac{\omega d\eta}{g} \cdot \frac{v_{max}^2}{2} = \omega \frac{k}{k-1} RT d\eta = dU_4.$$

If outflow occurs not through an infinitely divergent nozzle, then not all internal energy is turned into kinetic. However, the total quantity of removed energy dU_4 remains constant and is determined from expression (4.86). The equation of balance of energy is obtained in the following form:

$$dU = dU_1 + dU_2 + dU_3 + dU_4$$

or

$$\frac{RT\omega}{k-1}\omega d\psi = \omega(d\psi - d\eta)\frac{RT}{k-1} + \omega(\phi - \eta + \gamma)\frac{RdT}{k-1} + \\ + \frac{q}{A}dt + \frac{k}{k-1} RT\omega d\eta.$$

Dividing both parts of the equality by $\frac{\omega RT_{0v}}{k-1}$, considering that $AR=(k-1)c_v$, $c_vT_{0v}=Q_m$, and designating $\tau = \frac{T}{T_{0v}}$, we obtain

$$d\dot{\psi} = (d\psi - d\eta)\tau + (\psi - \eta + \gamma)\,d\tau + k\tau\,d\eta + \frac{q}{\omega Q_m}\,dt.$$

Dividing by dt, we obtain

$$\dot{\tau} = \frac{(1-\tau)\dot{\psi} - (k-1)\tau\dot{\eta} - \frac{q}{\omega Q_m}}{\psi - \eta + \gamma}. \tag{4.87}$$

If heat flow q(t) is known according to calculation data or experiment, then equation (4.87) jointly with equations of income and flow rate of gases:

$$\dot{\psi} = \frac{\delta S_{\omega}\varphi(\psi)\,\varphi(\pi)\,f(p)}{\omega}; \tag{4.88}$$

$$\dot{\eta} = \frac{\varphi A F_{\omega p} p}{\omega\sqrt{RT_{0v}\tau}} \tag{4.89}$$

and with the equation of state

$$p = \frac{\delta RT_{0v}\tau(\psi - \eta + \gamma)}{\frac{\delta}{\Delta} + 1 - \psi - \omega\delta(\psi - \psi + \gamma)} \tag{4.90}$$

permits determining values p, ψ, η, τ for arbitrary instant.

Subsequently we will not consider heat transfer from gases to walls. Let us consider special cases.

1. In case of burning of a fuel in a closed volume we obtain

$$\eta = 0;\quad \dot{\eta} = 0.$$

Equation (4.87) takes the form

$$\dot{\tau} = \frac{1-\tau}{\gamma + \psi}\dot{\psi}. \tag{4.91}$$

Integrating in corresponding limits, we obtain

$$(1-\tau) = \frac{1}{\gamma + \psi}(1 - \tau_0). \tag{4.92}$$

If at the initial moment temperature of gases in the bomb is to T_{0v}, then $\tau_0 = 1$, and from expression (4.92) it follows that $\tau = 1$, i.e., temperature of gases in the bomb all the time remains equal to the combustion temperature of the fuel T_{0v}. If at the initial moment temperature of gases in the bomb is less than T_{0v} (on amount of temperature of the air and gases of the igniter), then $\tau_0 < 1$ and the right side of the equality is positive. Consequently, $\tau < 1$. Since the right side continuously decreases, then τ continuously grows. Thus, in this case temperature in the bomb continuously grows, but remains less than T_{0v}. It is not difficult to see that if $\tau_0 > 1$, then τ decreases, but remains larger than one. Finally, if burning starts in a vacuum, then $\gamma = 0$ and always $\tau = 1$; $T = T_{0v}$.

2. Let us consider a stabilized process of outflow of gases in in the chamber, when $\dot{\psi} = \dot{\eta}$. In this case from equation (4.87) we obtain

$$\dot{\tau} = \frac{1-k\tau}{\psi-\eta+\tau}\dot{\psi}, \tag{4.93}$$

whence

$$\ln\frac{1-k\tau}{1-k\tau_0} = -k\int_0^{\psi}\frac{d\psi}{\psi-\eta+\tau}.$$

If in the initial moment $\tau_0 = \frac{1}{k}$, then $1 - k\tau_0 = 0$ and since the right side is finite, then there has to take place equality $k\tau = 1$

$$\tau = \frac{1}{k}; \quad T = \frac{T_{0v}}{k} = T_{0v}.$$

If $\tau_0 > \frac{1}{k}$; $k\tau_0 > 1$, then also $k\tau > 1$. Besides, since the right side is negative

$$\frac{k\tau-1}{k\tau_0-1} < 1 \text{ or } \tau < \tau_0$$

Thus, if $\tau_0 > \frac{1}{k}$, then τ decreases, remaining larger than $\frac{1}{k}$. Analogously it is possible to show that if $\tau_0 < \frac{1}{k}$, then τ grows, remaining less than $\frac{1}{k}$.

Thus, during a stationary process in the chamber, when income is equal to outflow and during absence of heat transfer to walls, the temperature of gases either is equal to $\frac{1}{k}$, continuously

approaches it from above or from below.

Let us consider a general case, when income is not equal to outflow and when pressure increases or drops. In this case $\dot{\psi} \neq \dot{n}$. For a certain finite interval of time we take $\dot{n} = n\dot{\psi}$, where n is a constant number. Equation (4.87) takes the following form:

$$\dot{\tau} = \frac{1-\tau-(k-1)m\tau}{\psi-\eta+\tau}\dot{\psi},$$

or

$$\dot{\tau} = \frac{1-m\tau}{\psi-\eta+\tau}\dot{\psi}, \tag{4.94}$$

where

$$m = 1 + n(k-1). \tag{4.95}$$

Comparing equations (4.94) and (4.93), we see that they differ only by the numerical value of the coefficient of τ. Consequently, we can conclude that during a nonstationary process in a chamber, at every given moment value τ approaches value $\frac{1}{m}$, and temperature of gases approaches $\frac{T_{0v}}{m}$.

Let us write the expression for m. From equations (4.88) and (4.89) it follows that

$$n = \frac{\dot{\eta}}{\dot{\psi}} = \frac{\varphi A F_{\text{кр}} p}{\delta S_0 \sigma(\psi)\varphi(\varkappa)\sqrt{RT_{0v}\tau/(p)}}. \tag{4.96}$$

It is possible to show that for determination of value m in formula (4.95) with an accuracy of 1% it is sufficient to determine value n with an accuracy of 5% and value τ in expression (4.96) with an accuracy of 10%. Under these conditions it is possible in in expression (4.96) to replace $RT_{0v}\tau$ by value $\chi RT_{0p} = \chi f_p$, which we took earlier. Besides, considering designation

$$N = \frac{\varphi A F_{\text{кр}}}{\delta S_0 \sigma(\psi)\varphi(\varkappa)\sqrt{\chi f_p}},$$

will obtain:

$$n = N\frac{p}{f(p)}$$

and

$$m = 1 + (k-1)N\frac{p}{f(p)}. \tag{4.97}$$

In case of an exponential function $f(p) = u_1 p^{\nu}$ we have

$$n = \frac{N}{u_1} p^{1-\nu}.$$

Considering the expression for $p_{пр}$

$$p_{пр} = \left(\frac{u_1}{N}\right)^{\frac{1}{1-\nu}},$$

whence

$$\frac{u_1}{N} = p_{пр}^{1-\nu};$$

we can write:

$$n = \left(\frac{p}{p_{пр}}\right)^{1-\nu}$$

and

$$m = 1 + (k-1)\left(\frac{p}{p_{пр}}\right)^{1-\nu}. \qquad (4.98)$$

Having the pressure curve calculated by the usual method at constant temperature in the chamber, it is possible from expression (4.97) or (4.98) to determine value $\frac{T_{0v}}{m}$, which temperature of gases in chamber approaches from above or from below. It is obvious that the biggest deviation of temperature of gases from isothermal, determined from expression $T = \frac{T_{0v}}{k} = T_{0p}$ can be expected in cases of the biggest deflection of the process in the chamber from stationary, when pressure in the chamber increases or drops rapidly. This occurs usually in the engine of antitank rocket missiles. In Table 4.11 are given results of calculation of temperature of gases in the chamber of conditional antitank missile by the method of numerical integration of equation (4.87)-(4.90) at value $k = 1.25$. In the same place are given values $\frac{1}{m}$, calculated by formula (4.98)

From a consideration of data of Table 4.11 we can make the following conclusions:

1. Under conditions of the examined problem, relative temperature τ differs from its value determined during a stationary process ($\tau = 0.8$) in a chamber by a value of up to 10%.

2. Exact values of temperature differ from their approximate

values $\tau = \frac{1}{m}$ by approximately 1% for the greater part of the period of burning of a charge.

3. For approximate calculations it is possible to originate from dependence $\tau = \frac{1}{m}$, where m is determined from dependence (4.97) or (4.98).

Table 4.11

φ	p $\frac{кг}{см^2}$	τ	$\frac{1}{m}$
0	75	0,885	0,891
0,1	260	0,847	0,842
0,2	347	0,832	0,824
0,3	392	0,822	0,815
0,4	410	0,814	0,809
0,5	415	0,809	0,807
0,6	415	0,806	0,803
0,7	410	0,804	0,803
0,8	390	0,804	0,803
0,9	362	0,797	0,784
0,95	310	0,781	0,750
1,00	185	0,736	0,683

§ 4.12. Unstable (Anomalous) Burning of Rocket Charges

The external criteria of anomalous burning are liberation of a large quantity of brown vapors of nitrogen dioxide and a pressure drop in the engine lower than the computed value determined by assigned parameters of loading.

Anomalous burning frequently appears in the form of intermittent burning, when after ignition of the charge and achievement of p_{max} there is observed a drop of pressure to atmospheric, followed by repeated soaring of pressure, changed by a drop, etc.. The number cycles oscillates from two to three to several tens. In all cases during anomalous burning a sharp lowering of the unit pulse is observed.

The value of the limiting maximum pressure in the engine $\left(p_{max}\right)_{min}$ lower than which anomalous burning is observed, is determined by propellent properties and consitions of loading. Ballistite fuels are characterized by high values $\left(p_{max}\right)_{min}$, which under favorable conditions of loading are near 20-40 kg/cm2. The upper figure pertains to fuels with caloricity ($Q_{ж}$ = 800-900 kcal/kg), the lower figure to fuels with high caloricity ($Q_{ж}$ = 1100-1230 kcal/kg) [2]. For composite fuels the border of stable burning is

lowered to several atmospheres.

Of the parameters of loading the decisive influence on stability of burning is rendered by parameter x, which in turn was recommended by Prof. Yu. A. Pobedonostsev as a criterion of stability of burning of fuel in an RDTT. As experiment shows, for every pressure there exists a limiting value x, higher than which burning becomes unstable. The character of dependence $(p_{max})_{min} = f(x_{пр})$ is represented in Fig. 4.10. From the graph it follows that with an increase of maximum pressure at the beginning of burning of a charge, allowable value x increases.

Fig. 4.10. Dependence of minimum allowable p_{max} on limiting value of parameter x.

Let us first consider the cause of unstable burning, connected with a low level of pressures in the engine under favorable conditions of loading $(x \ll x_{пр})$. The speed of chemical reactions flowing during the gas phase of burning, to a great degree depends on pressure. In the first place this pertains to reaction of interaction of oxides of nitrogen with H_2 and CO flowing in the ardent zone. During a lowering of pressure in the engine lower than a certain limit, the shown reactions are delayed so much that the time gases stay in the rocket chamber becomes insufficient for their completion. Products of combustion passing from the nozzle in this case contain considerable quantities of unreacted oxides of nitrogen (>20%), which, interacting with oxygen of the air, will form NO_2 (a gas of brown color). Inasmuch as these reactions need almost ha of the heat liberated during burning of the solid fuel, their incompleteness leads to a sharp fall of heat emission, and consequently also value RT_0, that involves a pressure drop in the engine lower than the rated value. Since with a pressure drop there occurs a lowering of speed of gasification, the pressure drop can become progressive and lead to full extinguishing of the charge.

The process of gasification of a fuel can even continue after a drop of pressure to atmospheric on account of the heat accumulated in the surface layer of the charge. With accumulation, in the

rocket chamber, of a sufficient quantity of products of gasification, and in the presence of an initiation source in the form of heated elements of the construction, a stormy reaction starts among these products. On account of liberated heat a sharp rise of pressure occurs.

With a rise of burning temperature (caloricity) of a solid fuel the speed of reactions flowing in the ardent zone increases, and fullness of the process of burning is attained at lower pressures. This explains the lowering of the value of ultimate pressure with a growth of caloricity of the fuel.

At values of the parameter of Pobedonostsev $\varkappa \geqslant \varkappa_{пр}$, unstable burning appears at higher pressures p_{max} than that which, according to the dependence of chemcial kinetics, conditions chemical incompleteness of combustion. For explanation of causes of the influence of $\varkappa$ on stability of burning of a solid fuel it is necessary to examine the connection between burning rate and thickness of the heated layer of the fuel. Distribution of excess temperature in the solid phase during stationary burning of fuel is described by equation

$$T - T_0 = (T_s - T_0) e^{-\frac{\zeta u}{a}}. \qquad (4.99)$$

where ζ – distance from surface of burning; $a = \frac{\lambda}{c\delta}$ – coefficient of temperature transfer of fuel.

Derivation of this dependence is given in § 6.8, Chapter VI. According to equation (4.99) the depth of heated layer is a conditional value, determined by a certain rated value of excess temperature ($T - T_H$):

$$\zeta_{пр} = \frac{a}{u} \ln \frac{T_s - T_0}{T - T_0}. \qquad (4.100)$$

Reserve of the quantity of heat accumulated in the surface layer of the charge 1 m^2 is

$$Q = \int_0^\infty (T - T_0)\delta c \, d\zeta = (T_s - T_0)\delta c \int_0^\infty e^{-\frac{\zeta u}{a}} d\zeta,$$

whence

$$Q = (T_s - T_0)\frac{\lambda}{u}. \qquad (4.101)$$

Consequently, during stationary burning to every value of burning rate there corresponds a temperature profile in the solid phase. For example, in Fig. 4.11 are given design temperature profiles in a charge made from ballistite fuel for different burning rates [9]. With deceleration of burning, the depth of heated layer is increased. Besides, the amount of heat accumulated in the surface layer of the charge also increases.

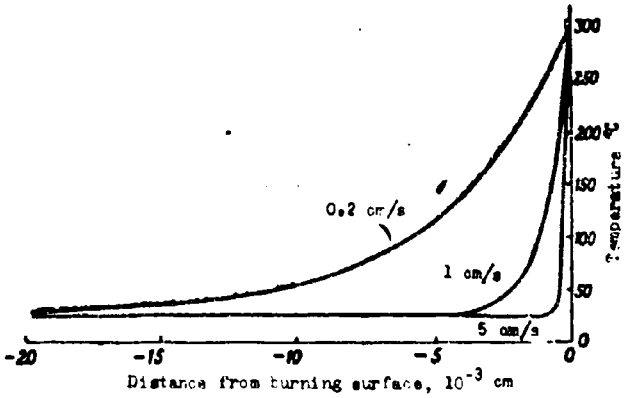

Fig. 4.11. Distribution of temperature in charge made from ballistite fuel for different burning rates (design data).

Consequently, a change of the temperature profile in a charge during a lowering of pressure in the engine is always connected with an expenditure of additional energy on heating of the thicker layer of fuel. If pressure descends slowly, the temperature profile follows pressure and is reconstructed in accordance with change of the stationary burning rate. During a fast pressure drop, reconstruction of the temperature profile lags. Due to this the burning rate at the initial moment descends to a larger degree than this would be caused by a pressure drop (see Fig. 4.12). Lowering of the burning rate can lead to unstable burning or even to extinguishing of the charge.

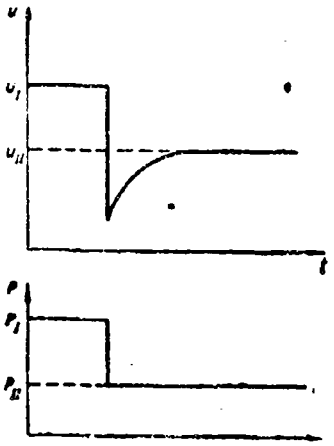

Fig. 4.12. Change of burning rate of a solid fuel during a sharp decrease of pressure.

As is shown in § 6.8, Chapter VI, the characteristic time of thermal relaxation of a system with a mobile interface of phases is the ratio a/u_c^2. It is possible to consider that transition to unstable burning as a result of a pressure drop will occur, if the time of the drop is less than the time of thermal relaxation

$$\tau < \tau_p^1.$$

Inasmuch as

$$\tau \sim \frac{1}{dp/dt}, \quad u_c^2 \sim p^{2\nu},$$

the condition of stability of burning can be presented in the form

$$\text{const} > \frac{1}{p^{2\nu}} \cdot \frac{dp}{dt}. \qquad (4.102)$$

In accordance with the given scheme, the influence of the parameter of Yu. A. Pobedonostsev on stability of burning of a rocket charge is explained by the fact that with an increase of x degressiveness of burning increases. At $x \approx x_{пр}$ speed of the pressure drop after the erosional peak of pressure attains the value at which inequality (4.102) changes its sign. According to in equality (4.102) the higher the pressure p_{max} preceding the decrease, even greater is degressiveness of burning, and consequently also higher x can be allowed without transition of burning of the charge into anomalous.

In practice stable burning of a charge is ensured by selection of the operating engine pressure $(p_{max} > (p_{max})_{min})$ and the parameter of loading $x < x_{пр}$.

But sometimes the goal is to extinguish the charge. Such a necessity appears during different investigations of working processes of RDTT. In this there is also one of the possible solution of control of firing distance of controlled ballistic missiles with RDTT with constant pitch angle at the end of the powered-flight trajectory. As an experiment shows, there exists a certain critical rate of pressure drop $(dp/dt)_{пр}$ which quarantees reliable extinguishing of the charge. The value of the critical rate of pressure in the chamber. It is necessary to note that the critical rate of pressure drop on the whole is an order higher

than value dp/dt at which unstable burning of the charge starts [11].

§ 4.13. Vibration Burning

In RDTT during certain conditions of burning there appear high frequency oscillations of pressure, accompanied by considerable deflections of the average burning rate of fuel from computed value. This phenomenon obtained in literature the name of vibration, or resonance burning. An external criterion of vibration burning is the appearance, on an oscillogram, of secondary peaks of pressure. The characteristic pressure curve for such a case during burning of a charge with a cylindrical channel and externally clad surface is shown in Fig. 4.13 [12]. According to indications of low-inertia transducers, 0.38 s after ignition of the charge, in the channel of the charge, there appeared oscillations of pressure with an amplitude of $\sim$0.07 kg/cm^2. Then these oscillations began to be strengthened, and at their maximum strengthening on the oscillogram sharp jumps of pressure appeared (to 74 kg/cm^2), exceeding 2.5 times the average pressure during stationary burning. With a weakening of oscillations, the process of burning returned to a steady state.

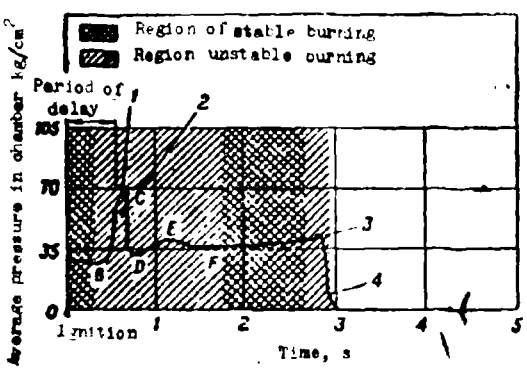

Fig. 4.13. Characteristic curve of change of pressure in RDTT during vibration burning.

Vibration burning is connected with strengthening of oscillations of pressure corresponding to one of the forms of natural oscillations of the column of gas in the internal cavity of the charge. The cause of an onset of oscillations is unclear. It is known that small oscillations are a usual phenomenon accompanying all types of flame.

As the experiment shows, in most cases tangential oscillations predominate. Frequencies of natural oscillations of a gas column ($\sim$1 to 10 kHz) during burning of a charge change in accordance with a change of geometry of the internal cavity of the charge. It is assumed the focuses of the appearance of vibration burning are located in places of antinodes of standing pressure waves, temperature and densities of gas. Inspection of the surface of charges after interruption of burning, performed after appearance of vibration burning [13], [14] leads to such a conclusion. On the surface of channels of charges in places of antinodes there are sections of maximum burning rate of the fuel. The surface in these places is covered by ripple, whose orientation makes it possible to judge

about the direction of oscillations (see Fig. 4.14 [13]).

Fig. 4.14. Ripple on surface of burning of ballistite fuel JPN after interrupted vibration burning. The ripple is oriented in a tangential direction.

GRAPHIC NOT REPRODUCIBLE

The probability of appearance of vibration burning in RDTT is connected with such parameters of loading as ratio $S_0/F_{кр}$ (assigned level of operating pressure in the engine), geometry of the charge, initial temperature of the charge and physical-chemical propellant properties.

As the experiment shows [12], for a charge of assigned geometry, according to a decrease of the critical section of the nozzle, in the beginning, inclination of the charge to vibration burning increases, then after achievement of a certain critical value of operating pressure it sharply drops. Thus is determined the lower bound of completely stable burning. This phenomenon is represented in Fig. 4.15 in the form of a graph $\Delta p/p_0 = f(S_0/F_{кр})$, where Δp – difference between height pressure during vibration burning and steady-state pressure in the chamber. For a charge made from a composite fuel on the basis of ammonium perchlorate, for which this graph is obtained, critical pressure equals approximately 20 kg/cm^2 [12].

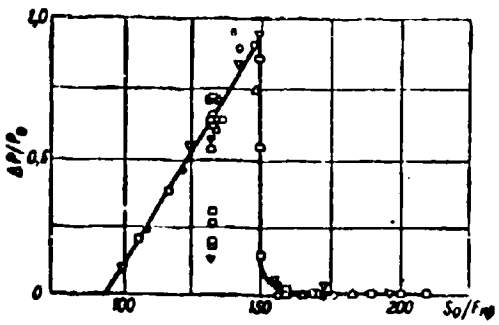

Fig. 4.15. Relative increase of pressure in RDTT during vibration burning depending on $S_0/F_{кр}$. Charge made from composite fuel based on ammonium perchlorate burning on the surface of a cylindrical channel.

Stability of burning favors a noncircular form of internal surface, hampering development of tangential oscillations. However for certain noncircular forms a channel (star-shaped profile) possibly the appearance of new types of oscillations is possible, for example, lateral oscillations in angles of the star [1].

Vibration burning is more frequently observed with relatively great lengths of the channel L/d. There exists for separate geometric forms a certain critical value L/d, determining transition from stable burning to vibration [12]. Vibration burning is more rarely observed for ballistite fuels with average caloricity $\sim 800\text{-}900\ \frac{\text{kcal}}{\text{kg}}$, and also for composite fuels based on potassium perchlorate, ammonium nitrate or ammonium picrate. According to certain data, for fuels based on ammonium perchlorate a tendency towards vibration burning drops with an increase of dimensions of oxidizer particles [13].

According to contemporary views on the nature of vibration burning, strengthening of weak oscillations in a gaseous environment occurs in the presence of defined phase connections between natural oscillations of this medium and a strengthening factor – oscillations of energy, inserted in the gaseous environment together with new input of gas from the surface of the charge. As was noted earlier, the rate of gas formation is determined by heat additions to the surface of burning from the zone of gasification. Oscillations in the gas phase, accompanied by a change of all gas-dynamic parameters, cuase oscillation of heat flow to the surface of the charge. The especially low thermal conduction of a solid fuel conditions localization of thermal vibrations in the surface layer of the charge. By this is determined high sensitivity of the surface of the charge to such oscillations of temperature and, connected with it, speed of gas formation. Speed of gas formation and, determined by it, energy entering the gas phase plays in the examined process a role of feedback. Between a change of speed of gas formation and a subsequent change of parameters of the gas flow in the internal cavity of the charge exists a certain break in time, a time lag. Delay is determined by the time necessary for completion of physical-chemical processes converting products of decomposition of the solid phase into end products of combustion. Factors favoring strengthening of oscillations are: high combustion temperature (caloricity) of the fuel, high heat of phase transition, high initial temperature of charge. Thus is explained the smaller inclination to vibration burning of fuels with low caloricity, and also fuels based on potassium perchlorate, for which the heat of decomposition is almost equal to zero. A more complex role is played by pressure, which, on the one hand, changes delay time, promoting a strengthening of oscillations, and on the other hand, increasing intensity of heat transfer, makes the process of burning less sensitive to oscillations of boundary parameters.

The harm of vibration burning is not exhausted by the possibility of destruction of the body of the engine at high pressure exceeding the computed value. Other possible consequences of vibration burning are:

– cracking of the fuel charge due to vibration loads;

– local burnouts of the body of the engine after vibration cracking of heat shielding;

– harmful influence of oscillatory loads on electronic equipment of the rocket;

– fatigue breakdown of separate subassemblies of construction;

– lowering of unit pulse.

For struggle with vibration burning at present there are used methods which have been set by empirical means during development of different types of RDTT. Let us consider these methods.

Distribution in the Internal Charge Cavity of Devices Made from Incombustible Materials

Depending on the form of a charge and construction of the engine such devices can be fulfilled in the form of partitions dividing the internal charge cavity into parts (Fig. 4.16a) [15], rods along axis of the channel (4.16b), perforated plates (4.16c). Such devices ensure acoustic "returning" of the cavity, disturbing conditions of the appearance of ordered acoustic oscillations.

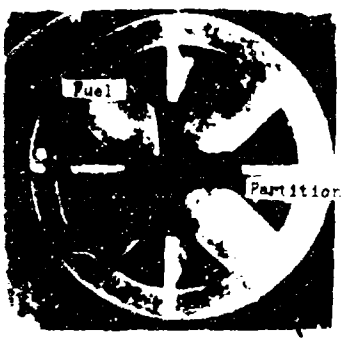

a)

b)

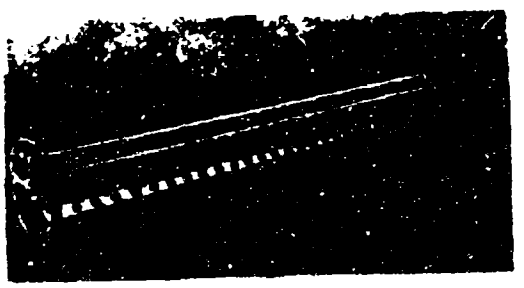

c)

GRAPHIC NOT REPRODUCIBLE

Fig. 4.16. Mechanical devices for removal of vibration burning: a) partition; b) rods; c) perforated plates.

Strengthening of Disordered Motion of Gases in the Cavity Charge

In tubular charges burning over the entire surface, this is attained by application of through radial drillings in the arch of a charge with a diameter $\leq 0.4d$ of the channel, located over the length of the charge in a helix. In charges of cross-like form this is ensured by apirally located clad sections on the external surface of the charge. The essence of this method consists in improvement of heat transfer to the surface of the charge on account of agitation of the main flow of gases. Besides, stability of heat transfer is increased, the dependence of it on oscillations of parameters of the thermal boundary layer descends [1].

Introduction of Damping Particles in the Gas Phase

As the experiment shows, introduction in the composition of fuel of additions which then will form in combustion products condensed particles of defined dimensions, ensures oscillation damping of the gas phase. This effect can be obtained during introduction in the composition of fuel of metals (aluminum, magnesium) which participate in burning (Fig. 4.17) [15].

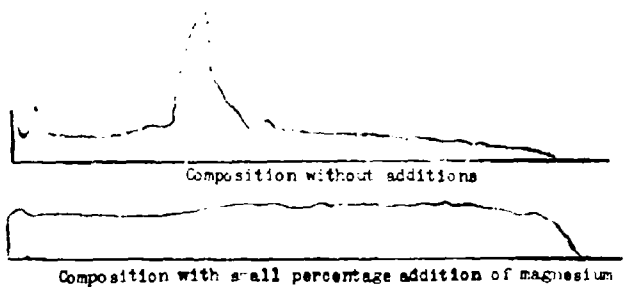

Fig. 4.17. Oscillograms showing stabilizing action of additions of metals.

§ 4.14. Ignition of Rocket Charge

Ignition is the initial stage of burning of a solid fuel. For ignition of a charge it is necessary to bring its surface layer to such temperature state with which heat emission on account of thermal decomposition of the solid phase starts to be stably developed. Along with the thermal pulse given to surface layers of the fuel, for normal ignition of a charge it is necessary to create in the rocket chamber a pressure which ensures stable burning of the fuel.

Transmission of heat to the surface of a charge during combustion of the igniter can be carried out by means of radiation, convection with products of combustion of the igniter flowing around the charge, and finally, by hot solid particles settling on the surface of the charge. In real conditions during ignition of a charge joint action of many factors appears, which prevents exposure of regularities of the actual process of ignition. For determination

of basic criteria of inflammability of fuels special sources of heat can be used which allow one to exactly measure the energy content given to the charge. Experiments on ignition of solid fuels with the aid of an arc reflective source [16] set the correspondence between assigned probability of ignition of one or another form of fuel and the quantity of established heat per unit surface of the charge. The minimum quantity of heat ensuring a 50-percent probability of ignition can be considered the threshold energy of ignition. It was found that for composite fuels based on ammonium perchlorate the threshold energy of ignition essentially decreases with growth of pressure to 5 kg/cm^2, after which it is changed insignificantly, being about 1 cal/cm^2. At pressures lower than 0.06 kg/cm^2 ignition becomes impossible: burning of the fuel is ceased together with irradiation. Threshold energy of ignition is changed with a growth of heat flow to the surface of the charge. The minimum threshold energy is ensured during a heat flow ~70-150 $kcal/m^2 \cdot s$ and composes approximately 1 kal/cm^2. During lowering of the hear flow the amount of heat tapped in the depth of the increases and threshold energy of ignition increases. For heat flows 10-20 $kcal/m^2 \cdot s$ it is approximately 3-2 kal/cm^2. Growth of the threshold energy with an increase of heat flow above the optimum value is connected with a decrease of time, and consequently also depth of heating. These experiments convincingly show that the temperature of the surface of a charge is not a criterion of inflammability. The criterion of inflammability must include along with the critical level of temperature of the surface the law of distribution of temperature in the surface layer of a fuel.

During feed to a fuel of a sufficient ignition thermal pulse, ignition of the fuel occurs with a certain delay in time, called delay time. Experiments on ignition of composite fuels based on ammonium perchlorate by means of hot gas generated in shock tube (p = 10-25 kg/cm^2, T_0 = 1200-1800° K, v = 50-100 m/s showed that ignition delay time of a charge is changed in inverse proportion to average thermal flow to the surface of the charge. To ensure delay within limits of 5-45 milliseconds the value of convection heat flow to the surface should be 1000-100 $kcal/m^2 \cdot s$ [17].

Inflammability of a fuel is essentially influenced by the initial temperature of the charge. The threshold energy of ignition with a lowering of the temperature of a charge increases linearly. For fuels based on ammonium perchlorate the temperature sensitivity of threshold energy is of approximately the same order as temperature sensitivity of the burning rate.

Inflammability of fuels essentially depends on their composition. Ballistite fuels ignite more easily than composite. Actual composite fuels are considerably distinguished in terms of inflammability: fuels based on ammonium nitrate do not ignite under conditions in which fuel based on ammonium perchlorate will ignite easily.

Ignition of rocket charges remains one of the least studied phenomena in the working process of RDTT. Therefore, selection of an igniter during development of a new engine is carried out usually by experimental means. Along with reliability of ignition and unfailing operation, the igniter of a rocket charge should satisfy the following requirements:

- minimum dimensions and weight;
- monotonic action;
- absence of pressure jumps;
- safeguard of minimum time of entry of engine into operation;
- possibility of prolonged storage.

As an igniter composition the most widely used in black powder. The high igniting ability of black powder is determined by its high content of heated solid particles in products of its combustion (up to 60% by weight), which conditions their high emissivity, and also intensity of contact heat transfer. Intensity of gas formation in known limits is regulated by grain value. Also used are pyrotechnic compositions based on metals (aluminum or magnesium) and mineral oxidizers (potassium perchlorate or nitrate). A deficiency of these compositions is oxidation of metals during prolonged storage.

We investigated the possibility of ignition of charges in RDTT by means of injection in the chamber of spontaneously inflammable liquids (chlorine trifluoride, bromine tri and pentafluoride). During settling of the liquid on the surface of the charge a chemical reaction starts between the injected substance and the fuel with liberation of heat sufficient for ignition of the charge. Thus it is possible to ensure ignition of the solid fuel at very low pressures (to 0.07 absolute atmosphere). However with wuch a method of ignition the delay time of ignition sharply increases (tens of times as compared to an igniter made from [DRP] (ДРП) – black propellant powder) and great jumps of pressure are observed [18].

The igniter composition is usually placed in a hermetic body made from plastic or metal. Ignition of the igniter composition in most cases is carried out by an electric detonator. Construction of the body should ensure sufficient strength of it during operation of the electric detonator, until the flame will embrace all the ignitor. However the body does not have to be so durable that destruction of it will occur with an explosion, since then the rocket charge can be damaged.

Insufficient mastery of processes of ignition and certain divergences in views on the mechanism of ignition of solid rocket fuels found reflection in a variety of empirical formulas which were offered by different researchers for calculation of weight of the igniter.

Let us give two characteristic dependences [10]:

$$\omega_p = \frac{qS_k}{Q_{\text{м.в}}};$$

$$\omega_p = 16\sqrt{\frac{S_k F_{\text{кр}}}{\Delta}}.$$

The starting point of the first dependence, proposed by Ya. M. Shapiro, is value q – quantity of heat per unit surface of the charge which quarantees reliable ignition. According to the recommendations of Ya. M. Shapiro q $\approx$ 7 kal/cm^2. In the denominator stands $Q_{\text{м.в}}$ – caloricity of igniter composition. Of the parameters of loading, here there enters only surface of burning of the charge. The second dependence includes also throat area and density of loading. These parameters were introduced in a calculation dependence for the purpose of calculation of pressure of ignition and duration of the influence of combustion products of the igniter. A basic deficiency of empirical dependences known at present is the fact that they are useful only in a narrow region corresponding to conditions of the experiment from which they are obtained.

A correct selection of weight of the igniter to a considerable degree determines the ballistic perfection of an engine. With a weak igniter, yield of the engine to operating conditions is protracted, a delay of ignition of the charge is possible. With excess weight of the igniter pressure peaks appear, threatening strength of the construction.

Literature

1. Barrer M., Zhomott A., Vebek B. F., Vandenkerkkhove Zh. Raketnyye dvigateli (Rocket engines) Oborongiz, 1962.

2. Uimpress R. N. Vnutrennyaya ballistika porokhovykh raket (Internal ballistics of solid-propellant rockets) Izd. inostr. lit., 1952.

3. Paushkin Ya. M. Khimiya reaktivnykh topliv (Chemistry of propellants) Izd. AN SSSR, 1962.

4. Preckel R. F. Plateau ballistics in nitrocellulose propellant. ARS, Journal, 1961, No. 9.

5. Vilyunov B. H. K matematicheskoy teorii statsionarnoy skorosti goreiya kondensirovannogo veshchestva (Mathematical theory of the stationary burning rate of a condensed substance) DAN SSSR, 1960, t. 136, No. 1.

6. Sammerfil'd M., Saterlend G. S., Uebb M. Dzh., Tabak Kh. Dzh., Kholl K. P. Mekhanizm goreniya topliv na perkhlorate ammoniya (Mechanism of burning of ammonium perchlorate fuels). "Issledovaniye raketnykh dvigateley na tverdom toplive". Sb. statey. Izd. inostr. lit., 1963.

7. Marklund T., Lake A. Experimental investigation of propellant erosion. ARS, Journal, 1960, No. 2.

8. Geron R. Problemy vnutrenney ballistiki RDTT (Problems of internal ballistics of RDTT) "Voprosty raketnoy tekhniki", 1963, No. 6.

9. Khuggett K. Goreniye tverdykh raketnykh topliv. (Burning of solid rocket propellants). Sbornik pod red. Yu. Kh. Shaulova. Izd. inostr. lit., 1959.

10. Serebryakov M. Ye. Vnutrennyaya ballistika stvol'nykh sistem i porokhovykh raket (Internal ballistics of trunk systems and solid propellant rockets) Oborongiz, 1952.

11. Siplach S. Vliyaniye bystrogo ponizheniya davleniya na goreniye tverdogo topliva (Influence of a rapid lowering of pressure on burning of a solid fuel) "Raketnaya tekhnika", 1961, No. 11.

12. Braunli V. G., Marbl F. Ye. Eksperimental'noye issledovaniye neustoychivogo goreniya v raketnykh dvigatelyakh na tverdom toplive (Experimental investigation of unstable burning in solid fuel rocket engines) "Issledovaniye raketnykh dvigateley na tverdom toplive" Sb. statey pod red. M. Sammerfil'da. Izd. inostr. lit., 1963

13. Prays Ye. V. Obzor eksperimental'nykh issledovaniy neustoychivogo goreniya tverdykh topliv (Survey of experimental investigations of unstable burning of solid fuels) Sb. statey pod red. M. Sammerfil'da. Izd. inostr. lit., 1963.

14. Landsbaum Ye. M., K'yubi U. S., Speyd F. U. Eksperimental'nyye issledovaniya neustoychivogo goreniya v raketnykh dvigatelyakh tverdogotopliva (Experimental investigations of unstable burning in solid propellant rocket engines) Sb. statey pod red. M. Sammerfil'da. Izd. inostr. lit., 1963.

15. Angelus T. A. Yavleniye neustoychivogo goreniya dvukh osnovnykh topliv. (Phenomenon of unstable burning of double-base fuels) "Issledovaniye raketnykh dvigateley na tverdom toplive". Sb. statey pod red. M. Sammerfil'da. Izd. inostr. lit., 1963.

16. Beer R. B., Fishman N. Vosplameneniye tverdogo topliva luchistoy energii vysokoy intensivnosti. (Ignition of solid fuel by radiant energy of high intensity) Sb. statey. Izd. inostr. lit., 1963.

17. Ber A. D., Rayan N. V., Solt D. A. Vosplameneniye topliva intensivnymi konvektivnymi teplovymi potokami (Ignition of fuel by an intense convection heat flow) Sb. statey pod red. M. Sammerfil'da. Izd. inostr. lit., 1963.

18. Siplach S., Allen D. Zazhiganiye tverdogo topliva v raketnykh dvigatelyakh posredstvom vpryska samovosplamenyayushchikhsya zhidkostey (Ignition of a solid fuel in a rocket engine by means of injection of spontaneously inflammable liquids) "Raketnaya tekhnika", 1961, No. 4.

Footnote

[1]The presentation about the order of magnitude of τ_p is given by the following calculation: n: for ballistite fuel JP at p = = 50 kg/cm^2, T_H = +21°C, u = 20 mm/s [2]; for ballistite fuels a = = 0.32 × 10^{-3} m^2/h = 0.89 × 10^{-7} m^2/s, whence

CHAPTER V

TUNING RDTT

§ 5.1. Scattering of Thrust Characteristics of RDTT and the Means of Decreasing It

Having logarithmized and differentiated the calculation dependences for pressure in the engine (4.55) and thrust (3.54), replacing differentials by finite increments of parameters, we obtain the formulas which connect a relative change of thrust characteristics of [RDTT] (РДТТ) with relative deflections of basic loading parameters:

$$\frac{\Delta p}{p} = \frac{1}{1-\nu}\left(\frac{\Delta u_1}{u_1} + \frac{\Delta S_0}{S_0} + \frac{1}{2}\frac{\Delta f_p}{f_p} - \frac{\Delta F_{кр}}{F_{кр}}\right); \tag{5.1}$$

$$\frac{\Delta P}{P} = \frac{\Delta p}{p} + \frac{\Delta f(\lambda_a)}{f(\lambda_a)}. \tag{5.2}$$

For time of burning, taking $e_1 = u_1 p^{\nu} \tau$, we obtain

$$\frac{\Delta \tau}{\tau} = \frac{\Delta e_1}{e_1} - \frac{1}{1-\nu}\frac{\Delta u_1}{u_1} - \frac{\nu}{1-\nu}\left[\frac{\Delta S_0}{S_0} + \frac{1}{2}\frac{\Delta f_p}{f_p} - \frac{\Delta F_{кр}}{F_{кр}}\right]. \tag{5.3}$$

According to dependences (5.1)-(5.3) the basic factors which determine inconstancy of thrust-time curves of an engine are: inconstancy of solid fuel combustion rate, scattering of its power characteristics difference of dimensions of charge and nozzle of engine within limits of allowances on their manufacture.

Of the enumerated factors the dominating role is played by inconstancy of the unit burning rate of the solid fuel. As was noted earlier, the unit burning rate of a solid fuel essentially depends on initial temperature of the charge, which in turn conditions the dependence on it of thrust parameters. For certain fuels used in rockets of the army of the United States, during a change of initial temperature of a charge by 50°C, thrust of the engine is changed 30%. For the ballistite fuels used in the Second World War, dependence of thrust on temperature of the charge was considerably

greater. Furthermore, at the same temperature in the same engine is observed velocity straggling of burning of charges due to different deflections from norms of the technological process during their manufacture and variations in chemical composition of the fuel. According to American data, change in chemical composition of fuel from lot to lot may cause a change of thrust of approximately 3%. For an engine equipped with charges made from one fuel lot there can be a thrust variation of approximately 2% [1].

Deflections of thrust parameters from their computed values can also be caused by accidental factors appearing in the process of work of the engine (increase of surface of burning due to the appearance of cracks in the charge, climax of the critical section of nozzle etc.).

The shown deficiencies of RDTT become especially unbearable during use of this engine in guided rockets. Inertial guidance systems of ballistic missiles present stringent requirements to constancy of engine thrust. During use of a liquid-fuel rocket engine constancy of thrust with an accuracy of 1% is comparatively simply ensured by control of feed of the liquid fuel into the combustion chamber. Creation of guidance systems which allow considerable changes of thrust, characteristic for unregulated RDTT, in the opinion of foreign specialists entails excessive complication of the system and increase of its cost with simultaneous lowering of its accuracy and reliability.

Thus, for certain types of rockets it becomes necessary to control RDTT to ensure required operating conditions and regulation of its thrust characteristics. Basic directions in the solution of this problem are:

- application of means of automatic control which continuously watch for a change of pressure in the engine or a change of acceleration of the rocket, and removal of deflections of these control parameters from program values by acting on the working process of the engine;

- prelaunch adjustment, or tuning.

Application of reliably working, compactly designed automatic dampers would appear to be the most promising and full solution of the examined problem. Only thus it is possible to be free from influence on thrust parameters of different accidental factors not subject to preliminary tuning. During the use of such systems it is possible also to change thrust of the engine in flight in accordance with an optimum solution of the problem of exterior ballistics. However development of means of automatic control of RDTT, as far as this is possible to judge by published data remains to emerged from the stage of long-term investigations.

According to the mechanism of influence of effectors on the working process of an engine, offered schemes of automatic control can be divided into three basic groups:

– adjustment by means of a change of the critical section of the nozzle;

– adjustment by change of the unit burning rate of the fuel (for example, on account of ultrasonic influences on the surface of burning);

– change of power factors (combustion temperature) by putting in the chamber additional components (water, hydrazine etc.).

Tuning, or prelaunch adjustment of RDTT, is the basic direction of regulation of thrust parameters of RDTT.

Tuning in a considerable measure removes the influence of the most essential causes of instability – dependence of burning rate on temperature of the charge, difference of burning rates for different fuel lots. Depending upon the set goal, we distinguish tuning of the engine for constancy of thrust and pressure. Adjustment of constancy of pressure is produced for the purpose of lowering design pressure, which determines thickness of walls of the body, in order to facilitate construction of the engine. The simplest means of tuning on RDTT is by a change of the throat area.

§ 5.2. Influence of Initial Charge Temperature on Basic Ballistic Parameters of Uncontrolled RDTT

The influence of the initial charge temperature on burning rate of a solid fuel appears mainly in a change of the speed coefficient u_1. This position is true in the case of the binmial linear law of burning $u = \bar{u}_1 (1 + \bar{b}p)$, so also for the exponential law $u = u_1 p^{\nu}$. Although the influence of temperature also has effect on a change of exponent ν and coefficient $\bar{b}$, however for existing rocket fuels in the working range of pressures this influence has a secondary value. Formulas which consider a change of burning rate with temperature carry a purely empirical character. The simplest of them is a dependence of the form [2].

$$u_{1T} = u_{1N} \frac{B}{B - (T - T_N)}, \tag{5.4}$$

where u_{1T} – burning rate at charge temperature T;[1] u_{1N} – burning rate at charge temperature T_N, taken for calculation; B – physical-chemical fuel constant.

---

[1]For simplification of designations in this chapter we drop index H.

From the analytic dependence (4.5) for burning rate it follows that at constancy of pressure (X_1 = const):

$$\frac{\dot{m}_T}{\dot{m}_N} = \frac{T_s - T_N - \frac{Q_s}{c_T}}{T_s - T - \frac{Q_s}{c_T}} \tag{5.5}$$

or

$$\frac{u_{1T}}{u_{1N}} = \frac{T_s - T_N - \frac{Q_s}{c_T}}{\left(T_s - T_N - \frac{Q_s}{c_T}\right) - T + T_N}. \tag{5.6}$$

Designating

$$B = T_s - \frac{Q_s}{c_T} - T_N,$$

we obtain

$$\frac{u_{1T}}{u_{1N}} = \frac{B}{B - (T - T_N)}. \tag{5.7}$$

Thus, by the analytical method we obtained a dependence which, coincides in structure with the empirical formula (5.4). Let us check the identity of value B entering formulas (5.4) and (5.7) in an example of fuel HES4016. For this fuel Q_s = 140 kcal/kg, c_T = = 0.35 kcal/kg °K [3]. Considering T_s = 874°K (mean value in range of pressures 10-70 kg/cm^2 according to [4]) and taking T_N = -40°C (233°K), we obtain

$$B = 874 - \frac{140}{0{,}35} - 233 = 241.$$

According to Table 1.1 for this fuel, experimental value B, corresponding to accepted T_N, is B = 1/D = 244. According to data of a strict analytic solution [4] value B for the given fuel during a change of pressure from 10 to 70 kg/cm^2 is changed within limits of 17%.

For simplification of calculations connected with tuning RDTT, it is more convenient to use another dependence [1]

$$u_{1T} = u_{1N} 2^{D(T - T_N)}, \tag{5.8}$$

where D is a constant, analogous to B.

Application of dependence (5.8) saves us from labor-consuming calculations connected with raising to a fractional power during use of the exponential law of burning, inasmuch as here there is used an exponential-tabular function, numerical values of which are given in all mathematical handbooks.

Selection of design temperature is determined by the specific character of the designed engine. For an engine designed for use in a wide range of emperatures, as T_N one can accept the minimum temperature of charge corresponding to the most unfavorable conditions of burning of the fuel, i.e., case which is calculated to ensure stability of burning of the charge.

In the given chapter for simplification of mathematical computations we also took $T_N = T_{min}$.

The distinction in selection of design temperature does not have any effect on the value of the exponential coefficient D, but leads to divergence of values u_{1N}. If one were to allow that to design temperature T_N^I there corresponds u_{1N}^I then, taking as design temperature T_N^{II}, we should in formula (5.8) take as the coefficient of burning rate

$$u_{1N}^{II} = u_{1N}^{I} e^{D(T_N^{II} - T_N^{I})}.$$

We will show that formulas (5.4) and (5.8), in spite of external distinctions, can be examined as mathematically identical expressions under the condition that in both dependences there is used the same value T_N. Decomposing the exponential factor of formula (5.8) into a series, we obtain

$$e^{D(T-T_N)} = 1 + \frac{D(T-T_N)}{1!} + \frac{D^2(T-T_N)^2}{2!} + \frac{D^3(T-T_N)^3}{3!} + \ldots$$

We will estimate the error inserted by rejecting terms of the expansion with a degree higher than one. The biggest value of error one should expect for fuels with a high temperature dependence, for example, for powder JPN (D = 0.0038). Assigning values $T - T_N = 90°C$ and D = 0.004, we obtain

$$e^{D(T-T_N)} = 1 + 0{,}36 + 0{,}064 + 0{,}00078 + \ldots$$

Consequently, already the value of the third term of the expansion is nearly 5% of the sum of the first two; the value of the fourth term of the expansion is less than one tenth percent of this sum. For composite fuels the value of the error will be considerably less. Consequently, considering the large scattering of the physical-chemical characteristics themselves, it is possible, being limited to the first two terms of the expansion, to write the approximate equality

$$e^{D(T-T_N)} \approx 1 + D(T - T_N).$$

Inasmuch as the second member of the sum in the right part of the equality is essentially less than one, according to rules of approximation calculus the right side can be converted so:

$$1+D(T-T_N)\approx\frac{1}{1-D(T-T_N)}=\frac{1/D}{1/D-(T-T_N)}.$$

Thus, as a result of conversion of the expression we obtain the formula

$$\frac{u_{1T}}{u_{1N}}=\frac{1/D}{1/D-(T-T_N)}.$$

Comparing it with formula (5.4), it is possible to write a dependence for transition from formula (5.4) to formula (5.8)

$$D=\frac{1}{B}. \qquad (5.9)$$

For appraisal of the temperature dependence, in literature they frequently use the temperature coefficient of the burning rate

$$\tau=\left[\frac{\partial \ln u}{\partial T}\right]_p. \qquad (5.10)$$

During determination of the temperature coefficient from formula (5.8) we obtain

$$\tau=D. \qquad (5.11)$$

Values τ, for different fuels are given in Table 1.1.

Initial temperature of the charge also influences the power characteristics of the fuel. For ballistite fuels, the heat capacity of which is approximately equal to heat capacity of products of burning, the change of combustion temperature is numerically equal to the change of initial temperature of the charge [5]:

$$T_{0(T)}=T_{0(N)}+T-T_N \qquad (5.12)$$

With a change of temperature of the charge from -50 to +50°C product RT_0 changes 3.5-4.5%, which corresponds to a change of I_1 by 1.5-2% [5]. Hence the dependence of a given force of the fuel on initial temperature is relatively weak.

By analogy with the temperature dependence for the burning rate, it is possible to record

$$f_{pT} = f_{pN} e^{2m(T-T_N)}. \tag{5.13}$$

Value m one can determine from relationship

$$\frac{T_{0(T)}}{T_{0(N)}} = e^{2m(T-T_N)},$$

whence

$$m = \frac{\ln (T_{0(T)}/T_{0(N)})}{2(T-T_N)}. \tag{5.14}$$

A direct result of the dependence of burning rate of a fuel on temperature of the charge is a change of operating pressure in the engine. If one were to use the dependence for the exponential law of burning of a fuel examined in Chapter IV, placing in it expressions (5.3) and (5.13), we would obtain

$$p = \left(\frac{u_{1N}^{\nu} S_0 \sqrt{f_{pN}}}{\varphi A F_{кр}}\right)^{\frac{1}{1-\nu}} e^{\frac{m+D}{1-\nu}(T-T_N)}. \tag{5.15}$$

The first cofactor expresses the value of pressure in the rocket chamber at design temperature

$$p_N = \left(\frac{u_{1N}^{\nu} S_0 \sqrt{f_{pN}}}{\varphi A F_{кр}}\right)^{\frac{1}{1-\nu}}. \tag{5.16}$$

Consequently:

$$p = p_N e^{\frac{m+D}{1-\nu}(T-T_N)}. \tag{5.17}$$

A relative change of pressue in an engine with fixed throat area will equal

$$\frac{p_T}{p_N} = e^{\frac{m+D}{1-\nu}(T-T_N)}. \tag{5.18}$$

From formula (5.18) it follows that a relative change of pressure with a charge temperature rise does not depend on loading parameters, but is determined by a relative change of burning rate and force of fuel on temperature, and also exponent ν. From formula (5.18) is follows also that at a fixed value of constants D and m pressure in the chamber at small values ν to a smaller degree depends on temperature of the charge. By this once again is confirmed the importance of safeguarding low values ν for developed fuels.

In connection with this one should note the ballistic advantages of fuels during whose burning there is observed a "plateau" effect. If operating pressure in an RDTT lies in the region of the "plateau," then, inasmuch as in this region $\nu \to 0$, dependence of engine parameters on temperature of the charge will be minimum.

Example 1: To estimate in what limits is changed pressure in an unregulated rocket engine in a range of temperatures from -40 to +50°C during use of fuels with high and low temperature dependence.

As a fuel with a high temperature dependence we will examine solid JPN ($D = 0.0038$, $\nu = 0.69$). As an average value characterizing the temperature dependence of composite fuels, we will take $D = 0.0014$ at $\nu = 0.4$.

For solid JPN on the basis of dependence (5.12) we obtain:

$$T_{\theta(+50)} = 3160 + 30 = 3190^\circ \text{ K};$$
$$T_{\theta(-40)} = 3160 - 60 = 3100^\circ \text{ K},$$

and from formula (5.14) we have

$$m = \frac{\ln(3190/3100)}{2 \cdot 90} = 0{,}00016.$$

According to source material [1] for certain composite fuels $m = 0.0002$. Considering the proximity of calculations of m for powder JPN, we will round it to 0.0002 and take this characteristic to be identical for fuels of both types.

For powder JPN

$$\frac{p_{+\theta}}{p_{-\theta}} = e^{\frac{0{,}0010}{1-0{,}69}\,90} = e^{1{,}16} = 3{,}19.$$

For a composite fuel

$$\frac{p_{+\theta}}{p_{-\theta}} = e^{\frac{0{,}0016}{1-0{,}40}\,90} = e^{0{,}24} = 1{,}27.$$

Example 2: To estimate the influence of index ν on maximum pressure in an unregulated engine. We consider composite fuels with equal temperature coefficients $D = 0.0014$, but with different indices $\nu = 0.7$ (fuel of type Alt-161) and $\nu = 0.4$ (fuel of type A from Table 1.4).

For a fuel with $\nu = 0.7$

$$\frac{p_{+\theta}}{p_{-\theta}} = e^{\frac{0{,}0016}{1-0{,}7}\,90} = e^{0{,}48} = 1{,}62.$$

As compared to the fuel for which $\nu = 0.4$ (see Example 1), for Alt-161 pressure at maximum temperature is 27% higher.

As characteristics of the dependence of pressure on temperature of the charge, sometimes we use derivative $\frac{\partial \ln p}{\partial T}$. As it follows from formula

$$\frac{\partial \ln p}{\partial T} = \frac{D+m}{1-\nu}. \tag{5.19}$$

With a change of pressure in the chamber there will be a change in the flow rate of combustion products and thrust of the engine. Engine thrust can be calculated by the formula

$$P = \sigma_c f(\lambda_a) p_0 F_a - p_a F_a = p_0 F_a \left[\sigma_c f(\lambda_a) - \frac{p_a}{p_0}\right].$$

A relative change of thrust at the expense of temperature will be

$$\frac{P_T}{P_N} = \frac{p_T}{p_N} \frac{\sigma_c f(\lambda_a) - p_a/p_T}{\sigma_c f(\lambda_a) - p_a/p_N}. \tag{5.20}$$

Considering the smallness of the second member of the difference, it is possible to consider that approximately

$$\frac{P_T}{P_N} \approx \frac{p_T}{p_N} = e^{\frac{m+D}{1-\nu}(T-T_N)}. \tag{5.21}$$

The linear burning rate of the fuel at temperature T will be defined as

$$u_T = u_{1T} p_T^{\nu} = u_{1N} e^{D(T-T_N)} p_N^{\nu} e^{\frac{m+D}{1-\nu}(T-T_N)\nu},$$

or

$$u_T = u_N e^{\frac{D+m\nu}{1-\nu}(T-T_N)}. \tag{5.22}$$

Time of burning of the charge at temperature T

$$\tau_T = \frac{\theta_1}{u_T}.$$

Relative change of time of burning of the charge

$$\frac{\tau_T}{\tau_N} = \frac{u_N}{u_T} = e^{-\frac{D+m\nu}{1-\nu}(T-T_N)}. \tag{5.23}$$

§ 5.3 Tuning the Nozzle of RDTT for Constant Pressure

Operating pressure in the engine should always remain within limits determined, on the one hand, by strength of the rocket chamber, and on the other hand, by stability of burning of a solid fuel. The variable area throat sections can be presented as the sum of a certain constant component, equal to the area of the throat section at design temperature of the charge $F_{крN}$ and variable of area $\tilde{F}_{кр}$. Designating

$$X = \frac{\tilde{F}_{кр}}{F_{крN}},$$

we obtain

$$F_{крT} = F_{крN}(1 + X). \tag{5.24}$$

Putting expression (5.24) in formula (5.15), we obtain

$$p_T = p_N \left[\frac{e^{(D+m)(T-T_N)}}{1+X}\right]^{\frac{1}{1-\nu}}. \tag{5.25}$$

So that pressure in the rocket chamber during a change of temperature of the charge will be preserved constant, it is necessary to fulfill condition

$$1 + X = e^{(D+m)(T-T_N)}. \tag{5.26}$$

From equation (5.26) can be found the required change of throat area, expressed in parts of area of it at design temperature. For the composite fuel examined in Example 1 of the preceding section, the change of throat area depending on temperature of the charge, calculated by formula (5.26), is represented in Fig. 5.1.

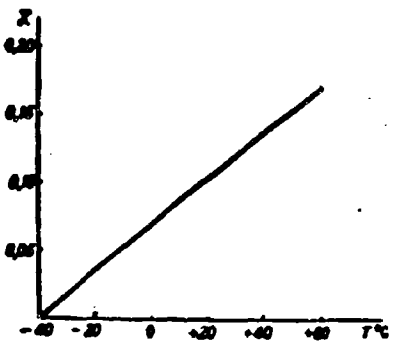

Fig. 5.1. Relative increase of throat area during tuning of engine for constant pressure (D + m = 0.0016).

The relative change of time of work of the engine, adjusted for constant pressure, equals

$$\frac{\tau_T}{\tau_N} = \frac{u_N}{u_T} = e^{-D(T-T_N)}. \qquad (5.27)$$

From a comparison of formulas (5.23) and (5.27) it follows that for a engine with constant pressure, time of work at even temperatures of the charge is larger, and maximum scattering of time with a change of temperature is less, than for an unregulated engine. Let us consider how during preservation of constant pressure, thrust is changed depending on temperature. We will consider that during adjustment of the throat the pressure recovery factor σ_c does not change. Then relative change of thrust at temperature T will be

$$\frac{P_T}{P_N} = \frac{\sigma_c f(\lambda_{aT}) - p_n/p}{\sigma_c f(\lambda_{aN}) - p_n/p}. \qquad (5.28)$$

Example: To calculate relative change of thrust for an engine adjustable for p = const = 50 kg/cm^2, with charge made from fuel of type JPN at temperature +50°C.

The necessary change of throat area

$$1 + X = e^{0,004 \cdot 90} = e^{0,36} = 1,43.$$

We will accept that at design temperature T_N = -40°C, $\frac{F_a}{F_{Kp}} = 4$, i.e., $q(\lambda_{aN}) = 0.25 \cdot f(\lambda_{aN}) = 0.3984$. At T = +50°C, $q(\lambda_{aT}) = 0.25 \cdot 1.43 = 0.358$. With this value $q(\lambda_{aT})$ we go to gas-dynamic tables and find at k = 1.25 the corresponding value of function $f(\lambda_{aT}) = 0.5438$. Taking $\sigma_c = 0.9$, we obtain

$$\frac{P_T}{P_N} = \frac{0,9 \cdot 0,5483 - \frac{1}{50}}{0,9 \cdot 0,3984 - \frac{1}{50}} = 1,395.$$

For a composite fuel of type A in analogous conditions we obtain:

$$1 + X = e^{0,0016 \cdot 90} = e^{0,144} = 1,155;$$
$$q(\lambda_{aT}) = 0,25 \cdot 1,155 = 0,289;$$
$$f(\lambda_{aT}) = 0,4536;$$
$$\frac{P_T}{P_N} = \frac{0,9 \cdot 0,4536 - \frac{1}{50}}{0,9 \cdot 0,3984 - \frac{1}{50}} = 1,135.$$

Thus, preservation of constant pressure by adjustment is connected with a considerable change of thrust. To avoid this is possible in that case when a change of F_{Kp} is carried out with

adjustable nozzles located at a right angle to the axis of the engine; besides, the given value of unit pulse, equal to the ratio of the pulse of axial thrust to combined weight of the charge, will with temperature of the charge drop inversely proportional to a change of the throat areas of the lateral nozzles

$$\frac{I_{1T}}{I_{1N}} = \frac{1}{1+X}.$$

Consequently, such a method of simultaneous adjustment for constant pressure and thrust is practically unacceptable. The only possible method of tuning an engine where the condition of constancy of pressure and thrust coincide, is prelaunch regulation of the engine.

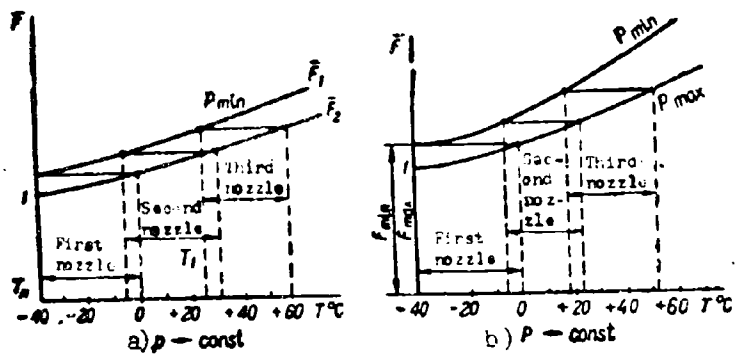

Fig. 5.2. Diagram of selection of sections of shift nozzles: a) during tuning of engine for constant pressure; b) during tuning for constant thrust.

In certain cases for rockets of the simplest construction instead of adjustment for constant pressure, it appears sufficient to limit its change by certain limits so that, on the one hand, pressure will never fall below level p_{min}, guaranteeing stable burning of the fuel, and on the other hand, will not rise higher than p_{max}, allowed by strength of the construction. This can be attained by step adjustment of the critical section by application of a set of shift nozzles. The diagram of selection of sections of shift nozzles and selection of a working range of temperatures for each of them is represented in Fig. 5.2a. Let us assume that the lower limit of pressure p_{min} at charge temperature T_N corresponds to the relative throat area taken for one. To ensure constancy of this pressure, a change of $(\bar{F}_{Kp})_{max}$ with temperature should follow dependence (5.26). According to this dependence is built curve $(\bar{F}_{Kp})_{max}$. Now let us construct the curve of change $(\bar{F}_{Kp})_{min}$, ensuring in the engine constant pressure p_{max}. The curve is

constructed by the same dependence (5.26) with the only distinction that the initial point of the curve, determined the scale of its ordinates, will correspond to a smaller critical section according to equality

$$\frac{(F_{\text{кр}N})_{\max}}{(F_{\text{кр}N})_{\min}} = \left(\frac{p_{\min}}{p_{\max}}\right)^{\frac{1}{1-n}}.$$

We will draw from the point corresponding to T_N on the upper curve $p = p_{\min}$ a horizontal segment $F_{\text{кр}} = \text{const}$ to the intersection with the lower curve. The point of intersection will determine the upper temperature limit of application of the first shift nozzle. The horizontal segment for the second nozzle again will start from curve $(\bar{F}_{\text{кр}})_{\max}$, but not from the point, corresponding to T_1, but from the one lying more to the left of it by 5-10°C, in order to ensure covering of the temperature ranges of the shift nozzles. A similar chart built in relative values for a defined fuel permits producing calculations for shift nozzles for any engine with this fuel. For this one needs the graphically found relative values $\bar{F}_{\text{кр}}$ multiplied by the absolute value of the throat area calculated for a given engine in terms of the value of minimum permissible pressure $p_{\min}$ at temperature T_N. With the help of the graph it is possible to solve the inverse problem, when one assigns the number of shift nozzles in the set and it is required to set the range of change of pressure in the engine during their use.

If one knows the deflection of the average (for a given fuel lot) unit burning rate Δu_{1N} from face value u_{1N}, the influence of this factor can also be compensated by a change of $F_{\text{кр}}$. For this it is necessary that the value of throat area calculated taking into account a change of temperature of the charge, be corrected by a factor

$$\varphi(u_1) = 1 \pm \frac{\Delta u_{1N}}{u_{1N}}.$$

We note that results of calculation by formulas (5.26), (5.27), and also by formulas (5.18), (5.21), (5.23) are determined by difference of temperatures $T - T_N$ and do not depend on value T_N. This permits present results of calculations in the form of graphs with a sliding scale $T - T_N$ which can be used at any value T_N.

§ 5.4. Tuning the Nozzle of RDTT for Constant Thrust

Will examine in the beginning the condition of constancy of thrust at different temperatures of the charge, when tuning is carried out by a change of throat area with constant area of the outlet section. This can be written in the following way:

$$[\sigma_{cT}/(\lambda_{aT})p_T - p_H]F_a = [\sigma_{cN}/(\lambda_{aN})p_N - p_H]F_a. \qquad (5.29)$$

where $\bar{\sigma}_{cT}$ and $\bar{\sigma}_{cN}$ – pressure recovery factors of nozzle during different installations of regulating device (throttle), corresponding to temperatures T and T_N, λ_{aT} and λ_{aN} – dimensionless speed in nozzle exit section, corresponding to these temperatures.

From equation (5.29) we obtain

$$\frac{p_T}{p_N} = \frac{\sigma_{cN}}{\sigma_{cT}} \frac{f(\lambda_{aN})}{f(\lambda_{aT})}. \tag{5.30}$$

Substituting expression p_T/p_N from (5.25), we obtain:

$$e^{\frac{D+m}{1-\nu}(T-T_N)} = (1+X)^{\frac{1}{1-\nu}} \frac{\sigma_{cN}}{\sigma_{cT}} \frac{f(\lambda_{aN})}{f(\lambda_{aT})}. \tag{5.31}$$

Logarithmizing (5.31), we solve the obtained equation with respect to temperature of the charge

$$T = T_N + \frac{1}{D+m} \ln(1+X) + \frac{1-\nu}{D+m} \ln\left[\frac{\sigma_{cN}}{\sigma_{cT}} \frac{f(\lambda_{aN})}{f(\lambda_{aT})}\right]. \tag{5.32}$$

If one were to assign value X, for a fuel with known characteristics D, m and ν it is possible to construct the dependence T = f(X). In order to use the dependence, it is necessary to set the connection between value X and a change of the gas-dynamic function $f(\lambda_a)$.

Since

$$q(\lambda_{aN}) = F_{\text{кр}N}/F_a;$$

$$q(\lambda_{aT}) = \frac{F_{\text{кр}T}}{F_a} = \frac{F_{\text{кр}N}(1+X)}{F_a},$$

$$q(\lambda_{aT}) = q(\lambda_{aN})(1+X). \tag{5.33}$$

Inasmuch as value $q(\lambda_{aN})$ is assumed assigned, dependence (5.33) permits one in terms of value X to determine value $q(\lambda_{aT})$, by which with the help of gas-dynamic tables [6] one can determine value $f(\lambda_{aT})$.

<u>Example</u>: Construct dependence T = f(x) for an engine adjusted for constant thrust in the range of temperatures T = -40 to +60°C.

Determine how pressure changes in the engine in the assigned range of temperatures.

Propellant properties: $\nu = 0.4$, D = 0.0014, m = 0.0002. Take: $T_N = -40°C$, $F_a/F_{\text{кр}N} = 6.25$, $\sigma_{cT} = \sigma_{cN}$.

The order of calculation is examined for one point X = 0.3:

$$q(\lambda_{aN}) = \frac{1}{6{,}25} = 0{,}16.$$

With this value, in tables of the gas-dynamic functions at k = 1.25, interpolating, we find:

$$f(\lambda_{aN}) = 0{,}2652.$$

$$q(\lambda_{aT}) = q(\lambda_{aN})(1 + X) = 0{,}16 \cdot 1{,}3 = 0{,}208.$$

By tables of gas-dynamic functions we find: $f(\lambda_{aT}) = 0.3373$;

$$T = -40^\circ + \frac{1}{0{,}0016} \ln 1{,}3 + \frac{0{,}6}{0{,}0016} \ln \frac{0{,}2652}{0{,}3373} = +33{,}3^\circ\,\mathrm{C}.$$

Calculating for other values X, we obtain the dependence represented on the graph (Fig. 5.3, curve 1) and in Table 5.1.

Table 5.1

T °C	−40	−12,4	+12,9	+33,3	+55
X	0	0,1	0,2	0,3	0,4
p_T/p_N	1	0,92	0,85	0,79	0,74

The relative change of pressure is calculated by the formula

$$\frac{p_T}{p_N} = \left[\frac{e^{(D+m)(T-T_N)}}{1+X}\right]^{\frac{1}{1-\nu}}.$$

On Fig. 5.4 are given values X calculated at D + m = 0.002 for different values ν, and on Fig. 5.5, corresponding to it, ratio p_T/p_N.

For fuels with a high temperature dependence (high values D) during tuning of a nozzle for constant thrust, as follows from formula (5.32), the throat area must be changed in wider limits. In Fig. 5.3 curve 3 corresponds to results of calculations conducted for a fuel of type JPN (ν = 0.69, D = 0.0038). With an increase of D there increases also the pressure drop in the assigned range of temperatures, within whose limits constant thrust is ensured.

As follows from the graphs shown in Fig. 5.3 and 5.4, an increase of ν should be examined as a contributory factor ensuring the effect of adjustment during small changes of the cross section of the nozzle and operating pressure in the engine.

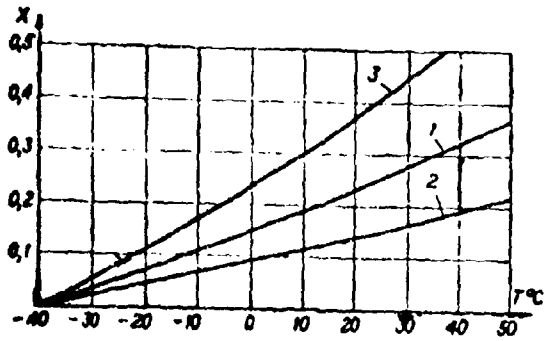

Fig. 5.3. Dependence of relative increase of throat area on temperature of charge when tuning on RDTT for constant thrust:
1 – when ν = 0.4, D + m = 0.0015;
2 – when ν = 0.7, D + m = 0.0016;
3 – when ν = 0.69, D + m = 0.0040.

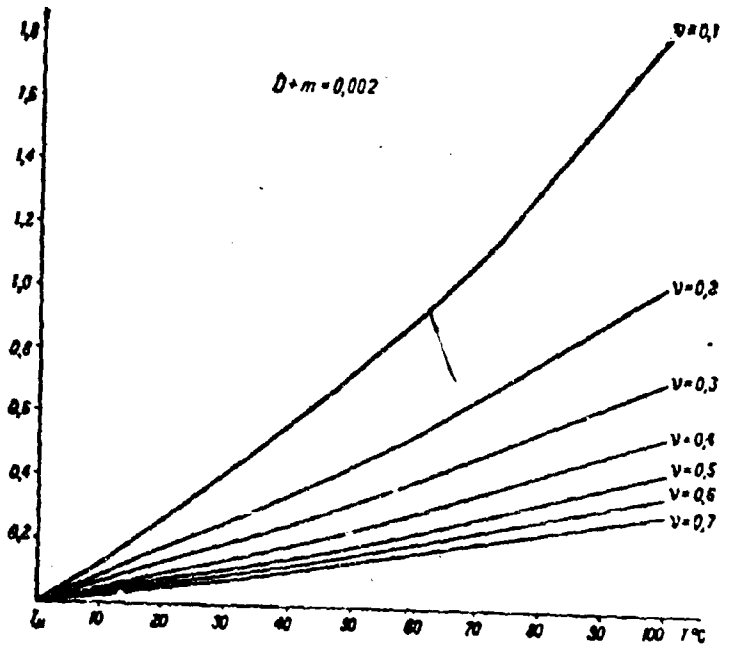

Fig. 5.4. Dependence of relative increase of throat area on temperature of charge when tuning an RDTT for constant thrust for different values ν when D + m = 0.002.

In certain cases we are limited by application of shift nozzles or application of launcher adapters to nozzles, ensuring constancy of thrust of the engine within limits of allowed scattering of thrust $P_{max} - P_{min}$.

If one were to consider that for all shift nozzles the ratio $F_a/F_{кр}$ is preserved constant, the condition of constancy of thrust can be rewritten in the following form:

$$F_{крT}p_T = F_{крN}p_N. \qquad (5.34)$$

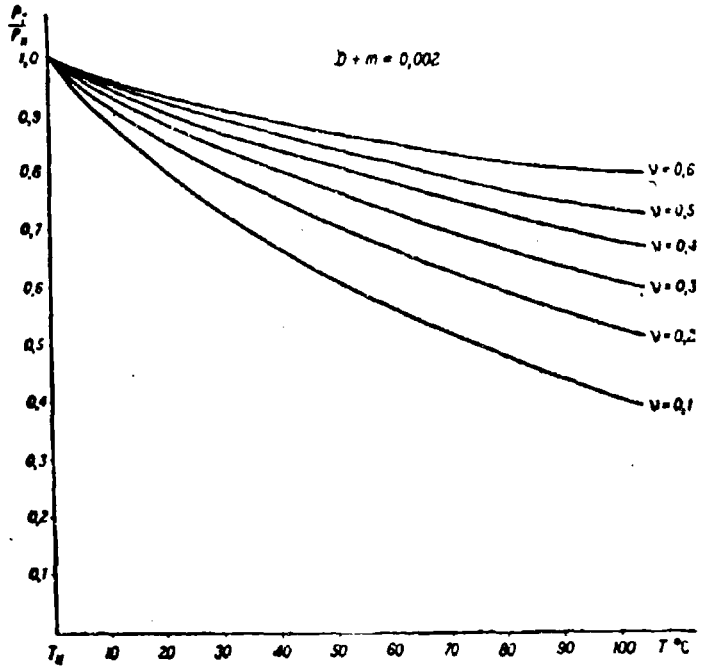

Fig. 5.5. Dependence of relative change of pressure on temperature of charge when tuning an RDTT for constant thrust (D + m = 0.002).

whence

$$\frac{p_T}{p_N} = \frac{F_{\text{кр}N}}{F_{\text{кр}T}} = \frac{1}{1+X}.$$

Substituting p_T/p_N from (5.25), we obtain

$$e^{\frac{D+m}{1-\nu}(T-T_N)} = (1+X)^{\frac{\nu}{1-\nu}}. \qquad (5.35)$$

Hence we will find the necessary change of critical section of the nozzle, ensuring constancy of thrust

$$1+X = e^{\frac{D+m}{\nu}(T-T_N)}. \qquad (5.36)$$

Let us assume that $(F_{\text{кр}N})_{\min}$ – throat area, ensuring at minimum temperature the minimum permissible value of thrust.

To ensure constancy of minimum value of thrust in the whole assigned range of temperatures, throat area should have been changed in accordance with dependence

$$(F_{\text{кр}})_{\min} = (F_{\text{кр}N})_{\min}(1 + X) = (F_{\text{кр}N})_{\min} e^{\frac{D+m}{\nu}(T-T_N)} \tag{5.37}$$

or in relative scale

$$(\bar{F}_{\text{кр}})_{\min} = \frac{(F_{\text{кр}})_{\min}}{(F_{\text{кр}N})_{\min}} = e^{\frac{D+m}{\nu}(T-T_N)}. \tag{5.38}$$

Accordingly, for maximum permissible value of thrust we obtain

$$(F_{\text{кр}})_{\max} = (F_{\text{кр}N})_{\max} e^{\frac{D+m}{\nu}(T-T_N)}. \tag{5.39}$$

If in the first approximation we consider thrust equal to $Fr(\zeta)pF_{\text{кр}}$, it is possible to use dependence

$$\frac{P_{\max}}{P_{\min}} = \frac{\rho_{\max}}{\rho_{\min}} \frac{(F_{\text{кр}})_{\max}}{(F_{\text{кр}})_{\min}}. \tag{5.40}$$

At temperature T_N

$$\frac{P_{\max}}{P_{\min}} = \left[\frac{(F_{\text{кр}N})_{\min}}{(F_{\text{кр}N})_{\max}}\right]^{\frac{1}{1-\nu}} \tag{5.41}$$

Putting equation (5.41) in equation (5.40), we obtain

$$\frac{(F_{\text{кр}N})_{\min}}{(F_{\text{кр}N})_{\max}} = \left(\frac{P_{\max}}{P_{\min}}\right)^{\frac{1-\nu}{\nu}}. \tag{5.42}$$

By dependence (5.42) is determined the relationship of ordinates of the graphs $(F_{\text{кр}})_{\max}$ and $(F_{\text{кр}})_{\min}$, in the scale of value $(F_{\text{кр}})_{\max}$ by dependences (5.37)-(5.39).

It is necessary to use such a graph (see Fig. 5.2b) just as the graph shown in Fig. 5.2a.

§ 5.5. Basic Diagrams of Devices for Change of Critical Section of a Nozzle

The simplest device for changing the critical section is a set of shift nozzles. For reduction of time on preparation of the engine for launch, sometimes instead of shift nozzles, nozzle launcher adapters are used (Fig. 5.6). To ensure exact correspondence of dimensions of inserts and the nozzle during manufacture of the inserts, final machining is done in combination with the nozzle for which they are designed [7].

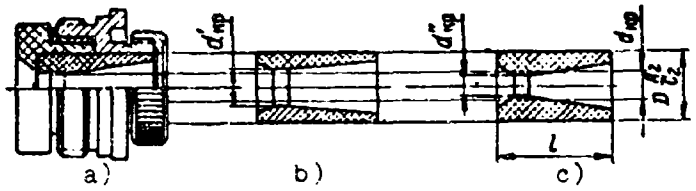

Fig. 5.6. Nozzle with launcher adapters: a) interseasonal insert (for average initial temperatures of the charge); b) summer insert; c) winter insert; $d_{кр}$, $d'_{кр}$, $d''_{кр}$ – diameters of critical sections of inserts a, b, c; $D(A_2/C_2)$ – landing diameter of insert assembly with nozzle body.

Smooth adjustment of the critical section of an engine nozzle in accordance with temperature of the charge is attained witht the use of a throttle (Fig. 5.7), which can be shifted along the axis of the nozzle. Placement of the throttle in the required position can be produced manually or with the aid of a mechanical drive.

We know of a series of constructions of self-adjusting nozzles for which placement of the throttle in the position corresponding to a given charge temperature is produced automatically, without interference of maintenance personnel.

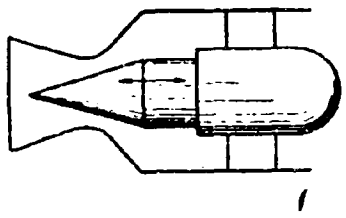

Fig. 5.7. Diagram of device for smooth change of critical section of nozzle.

In the diagram represented in Fig. 5.8 [8], shift of nozzle 3 relative to throttle 4 which is rigidly fixed in diaphragm 5, is ensured by a spiral bi-metallic spring 6. The spring consists of two bands of metal with quite different linear coefficients of thermal expansion. One of the ends of the spring is sealed in the body of the nozzle, the second can slip in the slot of the body of the engine. A change of ambient temperature leads to deformation of the spring. Here there appears a torque which, revolving the nozzle, shifts it by the thread to the required position. At the time of starting of the engine the axial component of forces of pressure of gases jams the nozzle in initial position, ensuring invariability of $F_{кр}$ during all the work of the engine. A deficiency of the scheme is the fact that tuning of the nozzle is produced actually in terms of temperature of the body of the engine, which can considerably differ from the average temperature of the charge.

NOT REPRODUCIBLE

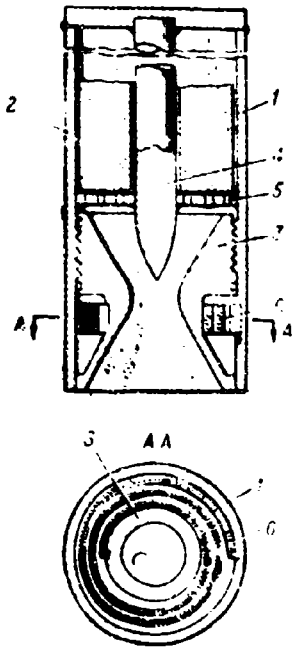

Fig. 5.8. Diagram of self-adjusting nozzle with a bimetallic spring: 1 — engine body, 2 — charge; 3 — nozzle; 4 — throttle; 5 — diaphragm; 6 — bimetallic spring.

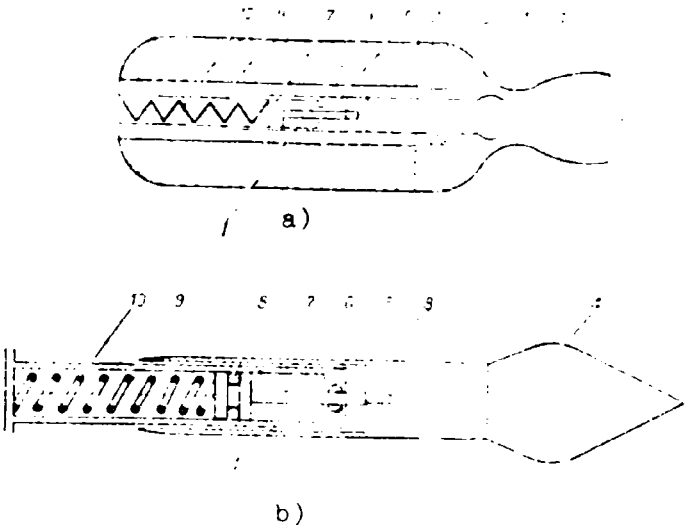

Fig. 5.9. Diagram self-tuning nozzle with pneumatic cylinder: a) general diagram of engine with self-tuning device; b) self-tuning system: 1 — body of engine; 2 — charge; 3 — centering diaphragm; 4 — throttle; 5 — mobile cylinder; 6 — rod; 7 — piston; 8 — sealing arrangement; 9 — fixed cylinder; 10 — return spr ng; f — volume filled by vapors of low-boiling liquid.

NOT REPRODUCIBLE

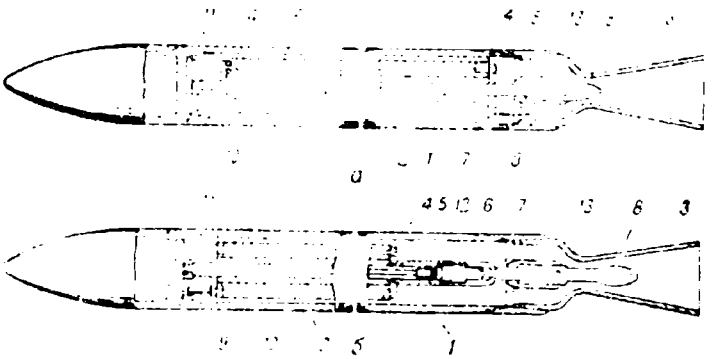

Fig. 5.10. Diagram of self-adjusting engine with throttle travelling on account of temperature lengthening of the charge: a) variant with direct shift of throttle; b) variant with reverse shift of throttle; 1 — body of engine; 2 — charge; 3 — nozzle; 4 — butt ring; 5 — diaphragm, 6 — directing cylinder; 7 — rod; 8 — throttle; 9 — pin; 10 — directing rod; 11 — crosspiece; 12 — igniter; 13 — bushing.

In the diagram shown in Fig. 5.9 [9], the mechanism of the throttle device consists of throttle 4, mobile cylinder 5 and rod 6 with piston 7, fixed cylinder 9 and return spring 10. Inside the fixed cylinder in the volume limited on the one hand by the front bottom of the cylinder and on the other hand by the piston is a low-boiling liquid. As such freon-12 and methyl chloride can be used. In avoidance of leakage of vapors of the liquid during storage of articles sealing devices 8 are used. With a change of temperature in the internal cavity of the engine vapor pressure of the liquid changes, and consequently also the pressure on piston 7 pressed by spring 10. With a temperature rise the pressure of vapors increases and the mobile system moves the throttle to the left. The throat section is then increased. With a lowering of temperature the process is carried out in the opposite direction.

At the time of starting of the engine during a sharp accretion of pressure there appears a difference in internal and external pressures having effect on the shell of the mobile cylinder. Excess external pressure produces a pressing of the thin-walled section of cylinder 5 and fastens it to fixed cylinder 9. Thus is ensured fixation of the mobile system, and consequently also placement of the throttle for the time of work of the engine.

In Fig. 5.10 [10] is a diagram in which placement of the throttle is produced by a change of charge length with temperature. This diagram was offered in the first place for engines in rockets of the class "air to air" and air to surface" utilized in a wide range of temperatures (from -60 to +60°C) under conditions where temperature of the charge can considerably differ from temperature of the ambient air. For different compositions of ballistite fuel, the linear coefficient of thermal expansion oscillates in the limits $\alpha = 1.2 \times 10^{-4}$ to $2.0 \cdot 10^{-4}$ 1/°C [11]. If as a mean value we take $\alpha = 1.6 \times 10^{-4}$ 1/°C, then in the range of temperatures from -60 to +60°C absolute lengthening of charges with lengths 1, 2 and 3 m will be accordingly 19.2; 38.4; 57.6 mm. Thus, linear shifts on account of temperature expansion of the charge turn out to be sufficient for the necessary shifts of the throttle.

Let us consider the basic structural elements of the variant shown in Fig. 5.10a. The rear end of the charge with butt ring 4 rests in diaphragm 5. The front end is free and can shift in an axial direction. From the front end of the charge through butt ring 4 and directing cylinder 6 by means of rod 7 passed through the channel of the charge, is connected throttle 8. The rod is prepared from an iron-nickel alloy with a low coefficient of thermal expansion. During axial lengthening the charge is centered on the one hand by pin 9 in diaphragm 5, on the other hand by directrix rod 10, rigidly fastened with crosspiece 11. In the recess of the directing rod is placed igniter 12 with an electric detonator, the wires from which through axial channels of the rod and throttle are led to the nozzle of the engine. The throttle is centered by diaphragm bushing 13. Lengthening of the charge with an increase of its average temperature leads to a shift of the throttle to the left and an increase in the critical section of nozzle. In the sealed volume in which the igniter is disposed, during operation of the electric detonator there

occurs a sharp increase of pressure, which leads to inflation of the thin-walled recess of the directing rod and wedging of the mobile parts.

In Fig. 5.10b the throttle is in the supersonic part of the nozzle. To ensure necessary shifts of the throttle, the mobile end of the charge faces the nozzle.

Literature

1. Geyts Dzh. and Pinto S. Regulirovaniye tyagi raketnykh dvigateley na tverdom toplive mekhanicheskimi sredstvami (Thrust control of solid fuel rocket engines by mechanical means). "Voprosy raketnoy tekhniki", 1960, No. 6.

2. Serebryakov M. Ye. Vnutrennyaya ballistika artilleriyskikh orudiy i porokhovykh raket (Internal ballistics of artillery and solid-propellant rockets). Oborongiz, 1962.

3. Gekkler R. Mekhanizm goreniya tverdykh raketnykh topliv. "Zhidkiye i tverdyye raketnyye topliva" (Mechanism of burning of solid rocket propellants. "Liquid and Solid Rocket Fuels"). Sb. perevodov pod red. prof. Yu. Kh. Shaulova. Izd. inostr. lig., 1959.

4. Vilyunov V. N. K matematicheskoy teorii statsionarnoy skorosti goreniya kondensirovannogo veshchestva (Mathematical theory of stationary burning rate of condensed substances). DAN SSSR, t. 136, No 1, 1960.

5. Zel'dovich Ya. V., Rivin M. A., Frank-Kamenetskiy D. A. Impul's reaktivnoy sily porokhovykh raket (Pulse of reaction force of solid-propellant rockets). Oborongiz, 1963.

6. Abramovich G. N. Prikladnaya gazovaya dinamika (Applied gas dynamics). Gosteortekhizdat, M., 1953.

7. Kurov V. D., Dolzhanskiy Yu. M. Osnovy proyektirovaniya porokhovykh snaryadov (Design fundamentals of powder missiles). Oborongiz, 1961.

8. Davies H. Temperature compensating Nozzle, US. Patent, No. 2909032, Oct. 20, 1959.

9. Long T. M. Temperature responsive Rocket Nozzle. US. Patent, No. 2870599, Jan. 27, 1959.

10. Brandenberqer E. M., Tanner E. Powder propellant Rocket Motors. US. Patent, No. 2957307, Oct. 25, 1960.

11. Barrer M., Zhomott A., Vebek B. F., Vandenkerkknove Zh. Raketnyye dvigateli (Rocket engines). Oborongiz, 1962.

12. Rozhkov V. V. Raketnyye dvigateli tverdogo topliva (Solid-propellant rocket engines). Voyenizdat. M., 1963.

C H A P T E R VI

THERMAL SHIELDING OF RDTT

§ 6.1. Transmission of Heat from Gas To Engine Wall

During burning of a fuel part of the heat from combustion products is transmitted to the body of the engine and the charge. The intensity of heat transfer is determined by the thermal state of basic elements of the construction: walls of the body, nozzle, gas-dynamic control equipment. Designing of these elements and calculation of their thermal shields are impossible without knowledge of basic laws of heat exchange. Calculation of thermal losses is necessary during the solution of the basic problem of internal ballistics of an [RDTT] (РДТТ) and during calculation of engine output performance. Transmission of heat from combustion products of the burning surface of the charge is the basic factor regulating the burning rate of a solid fuel.

To specific peculiarites of heat exchange in an RDTT one should relate high pressures and temperatures, high speed of gas flow especially in the nozzle. For heat exchange in the thrust chamber, characteristic is the considerable change of speed of the gas flow in terms of its length, as well as during work of the engine. This creates definite difficulties during use of calculation dependences which are known from the general theory of heat transfer.

The basic characteristic of heat exchange is specific heat flow q, constituting the quantity of heat transmitted per unit time through a unit surface, normal to the direction of propagation of the heat. In the theory of heat transfer the value of specific heat flow, from the gaseous environment to the surface of the solid is usually presented in the form proposed by Newton:

$$q = \alpha (T_0 - T_{c.в}), \tag{6.1}$$

where T_0 – determining temperature of gas flow, usually static temperature in the nucleus of the flow; $T_{c.в}$ – temperature of surface; α – coefficient of heat transfer.

Transmission of heat from combustion products of the solid fuel to elements of construction of the engine and to the surface of the charge is carried out by convection heat exchange and radiation. Inasmuch as these processes flow independent of one another, full heat flow to the surface can be examined as the sum of two heat flows, one of which is caused by convection (q_K), and the second – radiation ($q_Л$), taking in conformity with this the coefficient of heat transfer as $\alpha = \alpha_K + \alpha_Л$, where α_K and $\alpha_Л$ – coefficients of convection and radiation heat transfer.

Convection Heat Exchange

In thermotechnics, depending on the character of motion of a gas (free or forced) we distinguish two forms of convection heat exchange. In an RDTT the basic role is played by forced convection, connected with motion of the gas flow along the rocket chamber and nozzle. Free convection, caused by a shift of masses of gas with different densities and temperatures, can appear in separate places, where there are stagnant zones, for example, at the front bottom of the engine. During a simultaneous flow of both processes, calculation of convection heat flow is produced for the predominant form of convection.

Calculation methods of determination of the coefficient of convection heat transfer are based on the use of dependences:

a) during forced convection

$$Nu = f(Re, Pr); \tag{6.2}$$

b) during free convection

$$Nu = f(Gr, Pr). \tag{6.3}$$

In these dependences enter criteria of similarity: $Nu = \frac{\alpha_к d}{\lambda}$ – criterion of Nusselt; $Re = \frac{vd}{\nu}$ – criterion of Reynolds; $Pr = \frac{\nu c \gamma}{\lambda}$ – Prandtl number; $Gr = \frac{jd^3 \Delta T}{\nu^2 T_0}$ – Grashof number, where d – characteristic dimension; γ, c, ν, λ – specific gravity, specific heat, kinematic viscosity and coefficient of thermal conduction of gas, taken at the determining temperature; v – speed of gas flow; j – acceleration due to mass force (during bench tests j = g).

The expanded expressions of functional dependences (6.2) and (6.3) are set by experiment. For calculation of convection heat exchange during turbulent flow in long pipes, widely used is the dependence [1]:

$$Nu = 0{,}023 Re^{0.8} Pr^{0.4}. \tag{6.4}$$

This dependence has obtained application in the theory of rocket engines, although motion of a gas through a rocket engine essentially differ from motion in long straight channels with constant cross sections.

Several works are known for checking the fitness of dependence (6.4) for conditions of a rocket engine. For this in a liquid-fuel rocket engine measurements were produced of local heat flow over the length of the combustion chamber and nozzle. The value of heat flow was determined by the method of measurement of transient temperature of uncooled thick walls or by calorimetric means according to a change of heat content of the liquid during passage through a cooling section of small length of section of the engine. Greenfield [2] from experiments with a liquid-fuel rocket engine with liquid oxygen and ethyl alcohol obtained an empiracal formula for the coefficient of heat transfer, coordinated with dependence (6.4). Recently such investigations were conducted by Witte and Harper on an engine where as a fuel they used nitrogen tetroxide and hydrazine [3]. Their comparison of experimental data and that calculated by dependence (6.4) shows that calculation with sufficient practical accuracy will agree with experimental in all the length of the engine with the exclusion of a small section before the critical section of the nozzle. Heat flow measured on this section considerably (40-50%) exceeds that calculated by dependence (6.4). The authors explain this by the high gradients of pressures on the given section of nozzle which change the character of the boundary layer. These conclusions obviously, are completely applicable to nozzles of RDTT. For conditions of the rocket chamber of an RDTT the justice of dependence (6.4) is affirmed by the structure of the experimental formula which sets the connection between the quantity of heat transmitted to the wall of the chamber and the average specific flow rate of gas (6.20) [4].

Solving equation (6.4) with respect to the coefficient of heat transfer during forced convection, we obtain

$$\alpha_{\text{к}} = \frac{0{,}023}{g^{0.4}} \frac{(\gamma v)^{0.8}}{d^{0.2}} \frac{\lambda^{0.4} c_p^{0.4}}{\mu^{0.4}}. \qquad (6.5)$$

Uniting the coefficient of the constant and parameters determined by composition and temperature of combustion of the solid fuel (c_p, ν, λ), we obtain

$$\alpha_{\text{к}} = K_{\text{к}} \frac{(\gamma v)^{0.8}}{d^{0.2}}. \qquad (6.6)$$

As it follows from formula (6.6), during assigned characteristics of combustion products of fuel by a basic factor determining value α_K, there is a specific weight consumption $\overline{G} = \gamma v$, i.e., mass flow rate of gases, referred to a unit of area of the cross section of the engine: $\overline{G} = G/F$

Specific weight consumption constitutes the value which varies with length of the engine. On the section of the charge, where the area of the cross section is usually preserved constant by length,

accretion of value $\bar{G}$ in the direction to the nozzle is caused by an income of gases from the surface of burning of the charge. After the lower section of the charge, consumption of gases remains constant, and specific weight consumption is changed, as

$$\bar{G} = \frac{G}{F} = \sqrt{gk\left(\frac{2}{k+1}\right)^{\frac{k+1}{k-1}}} \frac{q(\lambda)p_0}{\sqrt{RT_0}}. \qquad (6.7)$$

The biggest value $\bar{G}$ corresponds to a maximum of the gas-dynamic function $q(\lambda) = 1$ when $\lambda = 1$ and is attained in the critical section of the nozzle. In this section is ensured the highest engine value α_K. According to expression (6.7) value $\bar{G}$ changes proportionally to pressure. Consequently:

$$\alpha_K = K_1 \frac{p^{0.8}}{d^{0.2}}. \qquad (6.6a)$$

For characteristic dimension d, entering in criteria Nu and Re, we usually take equivalent diameter

$$d = \frac{4F}{\Pi}, \qquad (6.8)$$

where F – area of cross section of gas flow, flowing around internal surface of engine; Π – perimeter of this section.

As follows from formula (6.6), value d weakly affects coefficient α_K. Putting expression (6.8) in formula (6.6), we obtain

$$\alpha_K = K_1 \frac{G^{0.8}\Pi^{0.2}}{4^{0.2}F}. \qquad (6.9)$$

For a freely inserted charge with burning on the external surface of grains and on the surface of channels

$$\Pi = \pi D_K + \Pi_{з.н}, \qquad (6.10)$$

where $\Pi_{з.н}$ – external perimeter of grains.

The area of free passage for gases in formula (6.9) for this case is taken equal to

$$F = F_0 = \frac{\pi D_K^2}{4} - \sum F_T, \qquad (6.11)$$

where $\sum F_T$ – total area of facets of grains, including the area of channels.

Consumption in dependence (6.9) is determined on the external surface of burning of the charge.

Inasmuch as use of dependence (6.9) for calculation of local values of the coefficient of heat transfer in the nozzle on separate sections leads to considerable errors, attempt were started to definitize this dependence. Bartz [5] offered a formula which can be represented in the form

$$\alpha_{\text{г}} = 0{,}026 \frac{c_p^{0,4} \lambda^{0,6}}{\mu^{0,4} g^{0,4} d^{0,2}} (\bar{G})^{0,8} \left(\frac{d_{\text{кр}}}{b}\right)^{0,1} \sigma, \tag{6.12}$$

where b – radius of curvature of wall in examined section; σ – parameter which considers a change of properties of gas across the boundary layer, caused by a change of temperature.

$$\sigma = (\rho_f/\rho_0)^{0,8} \cdot (\mu_f/\mu_{00})^{0,2},$$

where ρ_f and μ_f – density and viscosity of a gas calculated at determining temperature; ρ_0 and μ_{00} – these are parameters caluclated accordingly at static temperature of the gas and at stagnation temperature.

As determining temperature in formula (6.12) is accepted the value which we find from condition

$$T_f = 0{,}5\,(T_0 - T_{\text{с.в}}) + 0{,}22 Pr^{1/3} (T_\infty - T_{\text{с.в}}).$$

For calculation of the coefficient of heat transfer during free convection D. A. Frank-Kamenetskiy recommendes the dependence [6]

$$Nu = \sqrt[4]{Gr}, \tag{6.13}$$

whence after elementary transformations

$$\alpha_{\text{н}} = 0{,}32\lambda \sqrt[4]{\frac{l}{d}\left(\frac{p_0}{\mu R T_0}\right)^3}. \tag{6.14}$$

Radiant Heat Exchange in RDTT

The value of a radiant heat flow is determined by the formula

$$q_{\text{л}} = \varepsilon_{\text{ст.в}} \cdot \varepsilon_{\text{г}} \cdot 4{,}96 \left[\left(\frac{T_0}{100}\right)^4 - \left(\frac{T_{\text{с.в}}}{100}\right)^4\right],$$

where $\varepsilon_{\text{г}}$ – effective degree of blackness of combustion products, the ratio of intensity of their radiation at a given temperature to

intensity of radiation of an ideal black body gram the same surface with that same temperature; $\varepsilon_{ст.э}$ – effective degree of blackness of the internal surface of the chamber.

The coefficient of heat transfer by radiation is defined as

$$\alpha_л = \frac{q_л}{T_0 - T_{с.э}} = \varepsilon_{ст.э} \cdot \varepsilon_г \cdot 4{,}96 \cdot 10^{-8} T_0^3 \frac{1 - \left(\frac{T_0}{T_{с.э}}\right)^4}{1 - \frac{T_0}{T_{с.э}}}. \qquad (6.15)$$

Radiation of products of combustion of a solid fuel is composed of radiation of a gas phase and of condensed particles.

Let us first consider radiation of the gas phase.

The basic peculiarities of radiation of gases in contrast to solids is selectivity of the radiation, i.e., radiation of energy only in defined narrow spectral bands, and the volumetric character of radiation. During passage of heat rays through a gas there occurs absorption of the transmitted rays of energy, which is stronger as the quantity of molecules encountered in the way of the ray increases. This finds expression in the formula for degree of blackness of a pure gas

$$\varepsilon = 1 - e^{-k_\lambda p S},$$

where k_λ – attenuation factor of ray in layer, reduced to pressure in 1 [atm(abs.)]; p – pressure of gas; S – effective thickness of radiating layer.

Thus, the degree of blackness of a pure gas is a function of two parameters: T_0 and pS.

Inasmuch as bi-atomic gases at the temperatures of a rocket chamber are for heat rays practically transparent; radiation of the gas phase is wholly determined by the content of triatomic gases CO_2 and H_2O.

For determination of the degree of blackness of these gases ε_{CO_2} and ε_{H_2O} in thermotechnics are used experimental graphs with two inputs T_0 and $p_{CO_2}S$ for carbon dioxide and with three inputs T_0, $p_{H_2O}S$ and p_0 for steam, where p_{CO_2} and p_{H_2O} – partial pressures of the gases.

Effective thickness of radiating layer S characterizes the peculiarity of radiation of a limited gas volume. For a cylindrical vessel with radiation of the lateral surface during a change of relative length of the cylinder ℓ/d from 1 to ∞ value S changes within limits from 0.6d to 0.9d [1].

Graphs are built for a pressure of 1 [atm(abs.)]. The region of use of these graphs of pressure can be expanded by introduction of

correction factors C_{CO_2} and C_{H_2O}, which are determined on graphs given in work [8]. The degree of blackness of the gas mixture is defined as

$$\varepsilon_г = \varepsilon_{CO_2} C_{CO_2} + \varepsilon_{H_2O} C_{H_2O} - \Delta\varepsilon_г \qquad (6.16)$$

where $\Delta\varepsilon_г$ – correction, considering covering of the spectra of steam and carbonic gas.

Calculation determination of $\varepsilon_г$ for conditions of a rocket engine with use of the shown graphs carries a tentative character. D. A. Frank-Kamenetskiy, estimating the role of radiant heat exchange in RDTT, thus considers a defined value of $\varepsilon_г$ as a lower limit [6]. As the effective blackness of a gas $\varepsilon_г$ he recommends taking the arithmetic mean of two limiting values

$$\varepsilon_г = \frac{\varepsilon_{г\,расч} + 1}{2}.$$

For combustion products of nitrocellulose with 12.5% N in a model engine ($S = 6.5 \cdot 10^{-2}$ m) he obtained

$$\varepsilon_г = \frac{0{,}56 + 1}{2} = 0{,}78.$$

Similar to this the effective degree of blackness of the wall is found as the arithmetic mean from the degree of blackness of the surface material, considering absorption of heat during a first hit of a ray on a wall, and one, which corresponds to full absorption of heat during multiple reflections from the internal surface of the chamber:

$$\varepsilon_{ст.\,э} = \frac{\varepsilon_{ст} + 1}{2}.$$

According to calculations conducted by D. A. Frank-Kamenetskiy, for an engine of small dimensions the coefficient of radiant heat exchange in the range of temperatures 1800-2700°K can be from 0.075 to 0.24 kcal/m^{2}s°K [6]. In work [4] the effective value of $\alpha_л$ was obtained by extrapolation of the experimental dependence of the total coefficient α on $(\bar{G}/g)^{0.8}$ to a value $\bar{G} = 0$. At the intersection of the graph with the ordinate axis a value $\alpha_л = 0.14$ kcal/m^{2}s°K was obtained, which corresponds to a temperature $T_0 \sim 2300$-2500°K. Frank-Kamenetskiy by calculation obtained for this interval of temperatures $\alpha_л = 0.15$-0.16. Thus, the computed value will agree with experimental data.

During burning of composite fuels with additions of metals in combustion products there appears a great quantity of condensed particles. If dimensions of particles are great as compared to a wave

of radiation of the gas phase, their participation in radiant heat exchange reduces to simple blocking of the passage of rays through the gases. In this case the degree of blackness of combustion products can be defined by the well-known dependence

$$\varepsilon_{\Gamma+T} = 1 - exp\{-[k_\Gamma(p_{CO_2} + p_{H_2O}) + cF_T]S\}. \qquad (6.17)$$

The addend in brackets which considers weakening of the ray on account of contents of condensed particles, is equal to the product of the number of particles per m^3 by the area of projection of the surface of particles normal to the direction of the ray.

If one were to consider that the content of the condensed phase in combustion products is 20% at specific gravity of the condensed phase 4000 kg/m^3, we obtain $c = 18 \cdot 10^4/\pi D^3 1/m^3$, where D – diameter of a particle. Taking $F_T = \pi D^2/4$, D = 50 μm = $5 \cdot 10^{-5}$ m when S = $6.5 \cdot 10^{-2}$ m, we obtain $cF_TS = 0.585$.

Preserving for the gas phase the value calculated by Frank-Kamenetskiy, $k_\Gamma(p_{CO_2} + p_{H_2O})\ S = 1.51$, we obtain

$$\varepsilon_{\Gamma+T} = 1 - exp[-(1{,}51 + 0{,}585)] = 0{,}88.$$

Thus, in this case on account of the contents of the condensed phase, the rated value of the degree of blackness of combustion products increased by 60%, and effective degree of blackness $\varepsilon_э = \frac{1 + 0{,}88}{2}$ by 20%.

With an increase of dimensions of an engine, combustion temperature of the fuel and contents of solid particles, the role of radiant heat exchange in RDTT increases.

A comparison of the intensity of basic forms of heat exchange in RDTT shows that the decisive role in transmission of heat from gases to the body of an engine belongs to forced convection. The share of radiant heat exchange needs 20-30% of the total quantity of heat fed to the body. Therefore, an analysis of the dependence of heat exchange in RDTT on different factors is usually conducted with the use of dependences for only forced convection.

In certain cases for application of simple calculation methods known from the theory of heat transfer, allowing one to obtain an approximate engineering solution, it is necessary to assign a constant, averaged in time, value α, which we will call the average effective value of the coefficient of heat transfer $\alpha_э$:

$$\alpha_э = \frac{\int_0^\tau \alpha(T_0 - T_{c.э})\,d\tau}{\int_0^\tau (T_0 - T_{c.э})\,d\tau}. \qquad (6.18)$$

The numerator of expression (6.18) constitutes the full quantity of heat Q_1 transferred to 1 m^2 of the wall of the engine.

Approximately, value Q_1 can be found by the equilibrium temperature of the wall T_p which is set after termination of work of the engine during equalization of temperature over the thickness of the wall:

$$Q_1 = (T_p - T_н)\gamma c\Delta,$$

where Δ – thickness of the engine wall.

The denominator of expression (6.18) is simple to calculate by the oscillogram of temperature of the internal surface of the wall. For a static engine with thick walls the denominator can in the first approximation be presented as

$$\int_0^\tau (T_0 - T_{с.в})\,dt = \tau(T_0 - \bar{T}_{с.в}),$$

where $\bar{T}_{с.в}$ – time average value of $T_{с.в}$.

Then approximate value $\alpha_э$ will be expressed as

$$\alpha_э = \frac{\gamma c\Delta(T_p - T_н)}{\tau(T_0 - \bar{T}_{с.в})}. \qquad (6.19)$$

In Fig. 6.1 values $\alpha_э$ calculated by dependence (6.19) for experimental data [4] are given. The experiments were conducted on an engine with a gauge from 51 to 298 mm with charges made from ballistite fuels JP and JPN. Values $\alpha_э$ are represented as a function of average specific consumption to the power 0.8. The linear character of this dependence confirms the rightfulness of use, for RDTT conditions, of formula (6.4).

According to the graph

$$\alpha_э = 0{,}14 + 0{,}00515\bar{U}_{ср}^{0,8}. \qquad (6.20)$$

The first member of this formula is the coefficient of radiant heat transfer, the second – coefficient of convection heat transfer. The formula can be used for calculation of α in an engine working on ballistite fuels. The time average value of specific weight consumption is determined from condition:

$$\bar{U}_{ср} = \frac{1}{\tau}\int_0^\tau \bar{U}\,dt. \qquad (6.21)$$

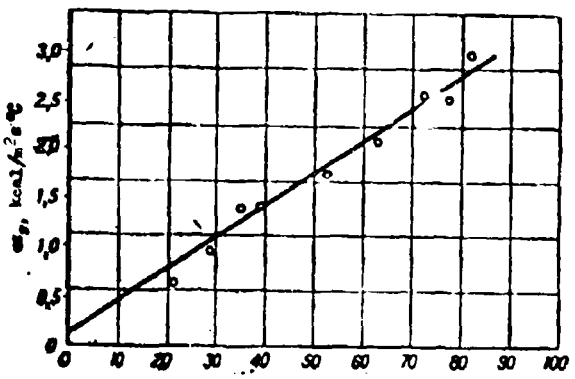

Fig. 6.1. Experimental dependence of $\alpha_э$ on $(\bar{G}/g)^{0.8}$.

The value of the integral can be obtained for any section of the engine on the basis of data of a ballistic calculation.

If during determination of the mean value of specific weight consumption of combustion products through an examined section of the engine one assumes that the area of the free section of the chamber, during a constant burning rate of the fuel, is changed linearly in time, then

$$\bar{\sigma}_{ср} = \frac{\sigma_0 \sigma_к}{\sigma_0 - \sigma_к} \ln \frac{\sigma_0}{\sigma_{ср}}. \qquad (6.22)$$

For a rocket chamber with freely inserted charge the most dangerous section for heating is that which coincides with the lower end of the charge. In this section the flow rate of gases attains a maximum value for a cylindrical section of a chamber. Therefore a check calculation of the chamber for strength, taking heating into account, should be conducted for this section.

Below as an illustration are computed values of coefficients of heat transfer, obtained for conditions of a model engine by D. A. Frank-Kamenetskiy [6]:

Table 6.1

α kcal/m^{2}s deg

		Beginning of burning	End of burning
Basic dimensions	$F_{кр}$ м$^2 \cdot 10^4$ Π м$\cdot 10^2$ d м$\cdot 10^2$	10,5 84,2 0,50	40,0 84,1 1,90
Beginning of chamber	$\alpha_к$ $\alpha = \alpha_к + \alpha_л$ α_0	0,139 0,334 0,295	0,111 0,278 0,295
End of chamber	$\alpha_к$ $\alpha = \alpha_к + \alpha_л$ α_0	1,220 1,390 0,688	0,334 0,500 0,688
Nozzle	α_0	2,810	2,810

§ 6.2. Propagation of Heat in the Wall of an Engine

During the study of heating of walls of the body of a rocket engine, the process of thermal conduction of the material is usually assumed to be one-dimensional. Distribution of temperature in the wall can be found by solving the heat-conduction equation

$$\frac{\partial T}{\partial t} = a\frac{\partial^2 T}{\partial x^2} \tag{6.23}$$

under the following boundary conditions:

$$t = 0 \qquad T(x, 0) = \text{const} = T_H; \tag{6.24}$$

$$x = 0 \qquad \alpha(T_0 - T_{c.B}) = -\lambda\left(\frac{\partial T}{\partial x}\right)_{x=0}; \tag{6.25}$$

$$x = \Delta \qquad \lambda\left(\frac{\partial T}{\partial x}\right)_{x=\Delta} = 0, \tag{6.26}$$

where T_H – initial temperature of the wall; $T_{C.B}$ – temperature on Δ – thickness of wall; λ, α – coefficients of heat and temperature transfer of the wall.

Equation (6.26) indicates that in most cases heat flow, directed into the surrounding medium, is negligible as compared to internal heat flow. In that case, when during flight of a rocket with great speeds it is necessary to consider aerodynamic heating, the boundary condition on the external surface is given in the form

$$\lambda\left(\frac{\partial T}{\partial x}\right)_{x=\Delta} = \alpha_A(T_{0_A} - T_{c.B}), \tag{6.27}$$

where T_{0_A} – stagnation temperature in an incident flow of air; α_A – coefficient of heat transfer during aerodynamic heating.

System of equations (6.23)-(6.26) is true for both a single-layer and for a multilayer wall, but with the only distinction that for a multilayer wall coefficients α and λ will have different values for separate layers.

The exact solution of this problem, taking into account the change in time of the coefficient of heat transfer and the change from temperature of values α and λ presents well-known difficulties.

The simplest method of solution is the use of an analog arrangement of a hydraulic or an electrical type. The action of such an arrangement is based on the community of mathematical dependences which describe processes of propagation of heat in a wall and overflowing of liquid in a system of capillaries, or electrical current in a system consisting of resistances and capacitances. In other words, analog

hydraulic and electrical models constitute a computer for solution of the problem of thermal conduction with a program of the solution already embodied in them.

Resolution of the problem of thermal conduction on electronic digital computers requires presentation of the heat-conduction equation in finite differences.

Below simplified methods of calculation are examined which allow one during minimum expenditures of time to estimate in the first approximation we expected temperature of a single-layer wall of an engine. Application of the simplified method of calculation is based on the following assumptions:

1. The coefficient of heat transfer from gases to wall of the engine is taken independent of time and equal to a certain effective value.

2. Basic heat-physical characteristics of the material of the wall (λ, c, γ) are assumed independent of temperature.

System of equations (6.23)-(6.26) can be represented in dimensionless form, if one crosses to new dimensionless variables and criteria:

$$\left.\begin{aligned} Bi &= \frac{\alpha\Delta}{\lambda} \text{ – Biot number} \\ Fo &= \frac{a\tau}{\Delta^2} \text{ – Fourier criterion} \\ \theta &= \frac{T_0 - T}{T_0 - T_{ж}} \text{ – temperature simplex} \end{aligned}\right\} \qquad (6.28)$$

$$\bar{x} = \frac{x}{\Delta}.$$

Then

$$\left.\begin{aligned} &\frac{\partial^2\theta}{\partial\bar{x}^2} = \frac{\partial\theta}{\partial Fo}; \\ &\left.\frac{\partial\theta}{\partial\bar{x}}\right|_{c0} = Bi\theta_{c0}; \\ &\left.\frac{\partial\theta}{\partial\bar{x}}\right|_{c0} = 0; \\ &\theta_{ж} = 1. \end{aligned}\right\} \qquad (6.29)$$

From the theory of heat transfer we know the solution of the problem of nonstationary thermal conduction for an unlimited plate with thickness 2Δ with equal distribution of temperature in the initial moment during bilateral heat exchange with environment, having temperature T_0. Inasmuch as the intensity of heat exchange with assigned coefficient of heat transfer α on both surfaces is identical, heating of the plate should be symmetric and heat flow through the

central plane of the plate should equal zero. Consequently, this solution should also be true for an unlimited plate of half thickness during one-sided heating and under the condition that heat removal from the other surface of the plate be absent.

The shown conditions correspond to formulation of the problem about heating of the wall of an RDTT. Thus, for calculation of the temperature field of the wall of an RDTT it is possible to use the ready solution of the classical problem of thermal conduction, which has the following form [9]:

$$\theta = \sum_{i=1}^{i=\infty} \frac{2\sin\Phi_i}{\Phi_i + \sin\Phi_i\cos\Phi_i}\cos(\Phi_i\bar{x})e^{-\Phi_i^2 Fo}. \tag{6.30}$$

Here Φ_i are consecutive values of roots (from i = 1 to ∞) of the transcendental equation:

$$Bi = \Phi_i \operatorname{tg}\Phi_i. \tag{6.31}$$

On the basis of dependence (6.30) tables of $\theta = f(Bi, Fo, \bar{x})$ [10], were calculated, allowing one for any instant to construct a distribution curve of temperature over the wall of the engine.

Good convergence of the infinite series in formula (6.30) makes it possible for determination of value θ, starting from certain values Fo, to use only one member of the series. The error induced by such a simplification when Fo > 0.3 is not more than 1%. Using the shown possibility, for calculation of heating of the wall of the engine we obtain the following the simplest dependences.

For the internal wall surface

$$\theta_{c.в} = Pe^{-\Phi_1^2 Fo}. \tag{6.32}$$

For the external wall surface

$$\theta_{c.н} = Ne^{-\Phi_1^2 Fo}. \tag{6.33}$$

On the average for all the mass of wall material

$$\theta_{cp} = Me^{-\Phi_1^2 Fo}. \tag{6.34}$$

In the exponent in all case we have Φ_1 – first root of the transcendental equation (6.31), which in turn determines the values of coefficients N, P and M:

$$N = \frac{2\sin\Phi_1}{\Phi_1 + \sin\Phi_1\cos\Phi_1};\quad P = \frac{2\sin\Phi_1}{\Phi_1 + \sin\Phi_1\cos\Phi_1}\cos\Phi_1;\quad M = \frac{2\sin\Phi_1}{\Phi_1 + \sin\Phi_1\cos\Phi_1}\,\frac{\sin\Phi_1}{\Phi_1}.$$

Value ϕ_1 and, determined by it, values N, P, M depend only on criterion Bi.

Numerical values of these coefficients are given in (The Machine Builder's Handbook,) V. 2, Mashgiz, 1962. For intermediate values of Bi the coefficients are found with the aid of simple linear interpolation. Formulas (6.32) and (6.33) can be used when Fo > 0.3. Formula (6.34) is applicable also at considerably smaller values of Fo, and when Bi > 0.5 – in all the region of Fo.

Calculating $\theta_{c.B}$, θ_{CM}, θ_{cp}, it is simple to determine the corresponding absolute values of temperature

$$T = T_0(1-\theta) + \theta T_w$$

§ 6.3. Coefficient of Thermal Losses in a Rocket Chamber

The general expression for determination of the coefficient of thermal losses in a rocket chamber has the form

$$\chi = 1 - \frac{\int_0^{F_{BH}} \alpha (T_0 - T_{c.B})\, dF}{YQ_H}, \qquad (6.35)$$

where Y – quantity of fuel burning per unit time; T_0 – temperature of combustion products; $T_{c.B}$ – temperature of internal surface of body touching gases; α – coefficient of heat transfer; F_{BH} – area of internal surface of the chamber.

Parameters α and $T_{c.B}$ are changed along the surface of the body touching gases, as well as in time, conditioning a time change of coefficient χ.

The character of the change of thermal losses in an RDTT and their total quantity are determined in the first place by such factors as the type of charge, relative surface area of the chamber touching gases, presence of thermal insulation coverings, temperature and composition of combustion products, character of motion of gases in the chamber.

The values of the coefficient of thermal losses and its determining dependences are essentially different for an engine with a freely inserted charge and for an engine with a fastened charge; therefore these two cases are examined separately.

Engine with Freely Inserted Charge

This case is characterized by the great surface area touching gases, and also by its constancy during burning of the charge. The basic part of thermal losses are apportioned to the cylindrical surface of the rocket chamber. This section, including from 80 to 97% of the internal surface of the engine, is washed by a gas flow with relatively high speeds. Therefore, calculation reduces to calculation of thermal losses on the cylindrical surface of the chamber. Thermal losses in bottoms and the diaphragm are accounted for by correction factor k_g.

Flow rate in an arbitrary section of the charge for calculation by formula (6.9) can be defined as

$$G(l)_{\text{п}} = \delta u \Pi_{\text{зп}} l, \tag{6.36}$$

where ℓ – length of the section of the charge above the given cross section; u – burning rate, averaged over the length of the charge.

Hence

$$\Pi_{\text{зп}} = \frac{G(l)_{\text{п}}}{\delta u l}. \tag{6.37}$$

In formula (6.9) the perimeter of the free section can be expressed as

$$\Pi_{\text{г}} = k_{\text{п}} \Pi_{\text{зп}}.$$

Putting expressions (6.36) and (6.37) in formula (6.9), we obtain

$$\alpha = \frac{K_{\text{г}} k_{\text{г}}}{d^{0.2}} \frac{G(l)_{\text{п}}}{F_{\text{г}}} \frac{k_{\text{п}}^{0.8}}{(\delta u l)^{0.2}}. \tag{6.38}$$

Although coefficient k_{Π} is a varialbe, averaging it in time, as follows from formula (6.38), does not have to lead to significant error.

The obtained dependence for α can be simplified if one considers that ratio G_H/F_H is equal to the mean value $\overline{G} = F_{CB}$ for all the free section of the chamber. The area of free passage for gases can be presented as

$$F_{\text{св}} = F_{\text{св.0}}(1 + b\psi). \tag{6.39}$$

where $F_{CB.0}$ – area of free passage at the beginning of burning;

$\phi = \frac{1}{1-\varepsilon}$ – coefficient which depends on initial filling of the chamber with fuel.

Taking into account expression (6.39) the formula for α obtains the form

$$\alpha = K_T \frac{G(l)}{(1+\psi)\, d^{0.2}\, p^{0.8}}. \qquad (6.40)$$

The difference of temperatures $T_0 - T_{C.B}$, if one were to use the average effective value of the coefficient of heat transfer for a given section of the chamber, according to equation (6.30) can be presented in the form:

$$T_0 - T_{c.B} = \sum_{n=1}^{\infty} A_i \exp\left(-\Phi_i^2 \frac{a}{\Delta^2} t\right),$$

where A_i and Φ_i – coefficients which are a function of $\alpha_э$.

The expanded expression for determination of χ obtains the form

$$\chi = 1 - \frac{1}{YQ_m} \frac{K_T \pi D_m}{(1+\psi)\, d^{0.2}} \int_0^l \Sigma A_i \exp\left(-\Phi_i^2 \frac{a}{\Delta^2} t\right) \frac{G(l)\, dl}{p^{0.8}}. \qquad (6.41)$$

The cumbersomeness of the obtained analytic solution limits the possibility of its practical use. However this dependence can be substantially simplified in reference to the limiting cases which have wide application in technology. Such limiting cases are: an engine with thermal insulation; an engine with a thick metal wall.

In the first case temperature on the internal surface of the chamber increases rapidly during operational output of the engine and then changes very little. Therefore, for the basic section of the pressure curve it is possible to consider $(T_0 - T_{C.B}) \approx$ constant.

In the second case (test engine) the temperature on the internal chamber surface during work of the engine remains low, composing a small part of value T_0, which permits averaging value $(T_0 - T_{C.B})$ in time.

In both cases dependence (6.41) will be converted to the form:

$$\chi = 1 - \frac{K_T}{YQ_m} \frac{\pi D_m (T_0 - T_{c.B})}{d^{0.2}(1+\psi)} \int_0^l \frac{G(l)}{p^{0.8}}\, dl. \qquad (6.42)$$

If one were to take $G(l) = G_{max}\frac{l}{L}$,

we obtain:

$$\chi = 1 - \frac{K_r}{Q_m}\frac{G_{max}}{1{,}8Y}\frac{F_{вн}}{(uL)^{0,1}}\frac{(T_0 - T_{c\,0})}{1 + b\psi}. \qquad (6.43)$$

Uniting the values which change in a narrow range, and the constants into one coefficient A, and also taking $Y \approx G$, we obtain

$$\chi = 1 - \frac{A}{1 + b\psi}. \qquad (6.43a)$$

An experimental study of thermal losses in an engine with a freely inserted charge was conducted by Ya. M. Shapiro.

Experiments were conducted on a test engine with interruption of burning at different instants. The quantity of heat accumulated by the body of the engine during the time of burning of the charge was determined in a calorimeter where the engine was placed immediately after interruption of burning. Determining thus the thermal losses for different times of burning of the charge, he obtained their dependence on time t and on ψ. This dependence Ya. M. Shapiro presented in the form

$$\chi = 1 - \frac{A}{1 + b\psi}. \qquad (6.44)$$

For conditions of conducted experiments

$$A = 0{,}30; \quad b = 5\,[12].$$

Thus, our earlier theoretical dependence in structure coincides with the empirical formula (6.44).

Engine with Fastened Charge

For an engine with a fastened charge burning on the surface of the figured channel and from ends, thermal losses in a rocket chamber will be determined by heat removal to the covering of the body in the prenozzle part and in the upper bottom. The value of thermal losses as compared to a engine with a freely inserted charge decreases sharply. During the use of heat shielding coverings the temperature of the internal surface of the chamber, touching hot gases, can in the first approximation be considered constant. The coefficient of heat transfer α, whose value is determined by forced motion of gases in the prenozzle volume or free convection in stagnant zones, is also preserved constant in time. The change of thermal losses during burning of a charge is conditioned by the growth of the heat exchange surface on account of burning of ends of the charge; the increase of surface can be expressed by the formula

$$F_{вн} = F_{вн\,0}(1 + b_1\psi). \qquad (6.45)$$

Consequently, in this case the dependence for χ takes the form

$$\chi = 1 - A(1 + b_1\psi). \tag{6.46}$$

An intermediate position is occupied by a slot charge. For it at climax of the slots along with an increase of the surface of heat transfer there will be observed a lowering of coefficient α on account of a decrease of specific weight consumption $\overline{G}$.

§ 6.4. Construction Materials for the Body of an RDTT

Inasmuch as for the body of an RDTT subject to the action of internal pressure the determining form of deformation is stretching, from the structural materials, used for its manufacture in the first place is required maximum specific strength σ_B/γ, where σ_B – temporary resistance of material to rupture. Of the other necessary qualities one should mention plasticity, good chemical stability under conditions of the environment during storage, manufacturability and good supply. Basic strength characteristics of construction materials for bodies of RDTT are given in Table 6.2.

Table 6.2

Material	Brand	Specific gravity, γ	Elastic modulus E, kg/cm^2	Specific strength σ_B/γ	Specific rigidity E/γ
Special steel for rocket chambers [13]	H-11	7.84	$2\cdot10^6$	25.5	2550
Special steel for rocket chambers [15]	D6AC	7.85	"	19.4	"
Aluminum alloy [18]	75ST	2.77		21.7	
Titanium alloy [15]	Ti-6Al-4V	4.5		28.1	
Fiberglass laminate on epoxy-phenolic resin [10]	ЭФ-32-301	1.7	$2.2\cdot10^5$	24.0	1300
Epoxy fiberglass (oriented for vessels under pressure) [16]		1.8		31.2	
Epoxy unidirectional fiberglass (theoretically accessible values) [16]		1.8		97.5	

At present the bodies of large engines in most cases are prepared from sheet alloy steel. According to American data [13], strength characteristics of utilized brands of steel lie in a narrow range, for which as average indices it is possible to take: $\sigma_s = 140$ kg/mm^2, $\sigma_B = 160$ kg/mm^2. The highest indices are possessed by steel H-11 ($\sigma_s = 183$ kg/mm^2, $\sigma_B = 200$ kg/mm^2). In the opinion of specialists, in the near future the strength of brands of steel used in rocket building may be increased to 280-300 kg/mm^2 [14]. However, according to a decrease of thickness of the wall of an engine on account of an increase of strength of the material, there is an increase in the danger of weakening of the construction due to concentration of stresses in places of accidental cuts and scratches.

Of other metals alloys of titanium attract special attention which in terms of specific strength exceed steel. Thus, for example, for titanium alloy Ti-6Al-4V at T = +20°C, $\sigma_B = 126$ kg/mm^2, $\sigma_s = 105$ kg/mm^2 and σ_B/γ is 45% higher than for steel [D6AS] (Д6АС). During manufacture from this alloy of the body of the RDTT of the second stage of the "Minuteman' rocket, its weight drops 30% as compared to the steel variant. Thickness of walls increases one and a half times, which increases rigidity of the construction and makes it less sensitive to cuts [15].

Recently in rocket building different types of reinforced plastics have obtained wide application, and also laminar compositional structures on their basis. The expediency of use of these materials for manufacture of bodies of RDTT is determined by their high specific strength and good heat-physical and technological properties. Reinforced plastics consist of a strengthening (reinforcing) filler and a polymerized binder. As reinforcing materials glass and quartz fiber, asbestos, and tissue from these fibers are used. At present it is possible to use as a reinforcing material artificial graphite fiber for increasing heat stability of the material. As a binder epoxy and phenolic resins are widely used. The biggest strength of material is attained usually with a weight ratio of filler and binder 70:30.

During manufacture of the body a method of winding is used. To the mandrel at a defined angle to its generator they reel out in several layers a fiberglass braid of a fibre impregnated with the binder compound. Then the article together with the mandrel is placed in a furnace and subjected to prolonged heating. Here occurs polymerization of the binder and the material of the article obtains the required mechanical qualities. So that the construction will be evenly durable, on account of the angle of the winding the necessary anisotropism of material in tangential and axial directions is ensured. According to reports of the foreign press, the plastic body of the first stage to the "Minuteman" rocket is 35% cheaper and 25% lighter than such a body made from high-quality steel, with yield points $\sigma_s = 152$ kg/mm^2 [16], [17].

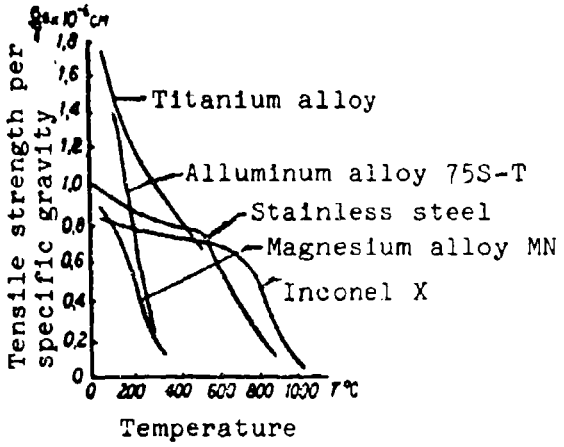

Fig. 6.2. Dependence of specific strength of certain characteristic materials on temperature.

A comparative appraisal of different materials in terms of their specific strength essentially depends on the temperature at which they are used. In Fig. 6.2 [18], [20] it is shown how with temperature value σ_B/γ changes for the most characteristic materials. A sharp fall of strength characteristics for aluminum alloys is observed at a temperature of over 150-200°C, for titanium alloys - over 400-450°C, for steel - over 650-750°C. Thus, strength possibilities of contemporary materials in full measure can be used only in engines with heat shielding of the body.

§ 6.5. Maximum Time of Work of an Engine Without Thermal Insulation

Let us consider the limits of possible use of an engine without thermal insulation and their dependence on different factors. Here we will consider the average temperature of the engine wall, and consequently also θ_{cp} to be assigned. Inasmuch as transcendental form in which the connection between temperature of the wall and parameters of heat exchange is expressed hampers such an analysis, we will convert formula (6.34) to a form which allows one to obtain an analytical dependence.

For values of criterion Bi, corresponding to conditions of an RDTT with a metallic body without thermal insulation, coefficient M changes very little. Thus, for example, in a range of Bi from 0 to 4 M is changed a total of 3.5%. Consequently, taking as its mean value M_{cp}, we allow an error in determination of θ_{cp} less than 2%. The tabular function $\Phi_1^2 = f(Bi)$ in the range of Bi which interests us can with an accuracy of 1% be approximated by the formula

$$\Phi_1^2 = 0{,}7Bi^{0{,}1}.$$

This permits converting dependence (6.34) so:

$$\theta_{cp} = M_{cp} exp(-0{,}7Bi^{0{,}1}Fo).$$

Logarithmizing, we obtain

$$Bi^{0.7} Fo = 3{,}29 (\lg M_{cp} - \lg \theta_{cp}).$$

Substituting the expanded expressions of Bi and Fo criteria, we have

$$\left(\frac{a}{\lambda}\right)^{0,7} \frac{a\tau}{\Delta^{1,3}} = 3{,}29 (\lg M_{cp} - \lg \theta_{cp}). \qquad (6.47)$$

The thickness of the wall necessary for the condition of strength can be in the first approximation calculated as

$$\Delta = \frac{\nu p_{max} d}{2\sigma_{BT}}, \qquad (6.48)$$

where σ_{BT} – tensile strength of material at assigned average temperature of the wall T_{cp}.

Putting in expression (6.47) dependence (6.48), the value of the coefficient of heat transfer (6.6a) and solving relative to τ, we obtain the maximum allowed time of work of the engine without thermal insulation

$$\tau = K_\tau \frac{p_{max}^{1,3}}{p^{0,56}} \frac{d^{1,44}}{\sigma_{BT}^{1,3}} \frac{\nu_\tau^{1,3}}{a} (\lg M_{cp} - \lg \theta_{cp}), \qquad (6.49)$$

where

$$K_\tau = 1{,}335 \frac{\lambda_\tau^{0,7}}{K_a^{0,7}}.$$

According to the obtained dependence at a given value θ_{cp}, and consequently at fixed value σ_{BT}, the basic factors determining maximum time of work of an engine are: engine gauge d, coefficient of temperature transfer of material of the body a, and pressure.

Formula (6.49) considers the distinction of design pressure p_{max} and operating pressure p, corresponding to the case for which the maximum time of work is determined. If these pressures coincide, for example, for an engine with a heated case or for an engine tuned for constant pressure, the formula takes the form

$$\tau = K_\tau p_{max}^{0,74} d^{1,44} \left(\frac{\nu}{\sigma_{BT}}\right)^{1,3} \frac{1}{a} (\lg M_{cp} - \lg \theta_{cp}). \qquad (6.50)$$

Thus, with an increase of design pressure when $\theta_{cp} = \theta_{зад}$, the allowed time of work of the engine increases. This is explained by the fact that although with growth of pressure the intensity of heat transfer from gases to the wall of the engine ($\alpha \sim p^{0.8}$) increases, the thickness of the wall, however, determined from conditions of strength, grows faster ($\sim p$), in consequence of which the heat

accumulating possibilities of the body of the engine are increased with a growth of pressure.

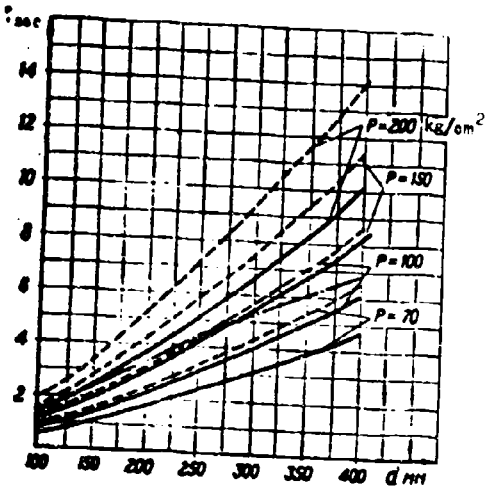

Fig. 6.3. Dependence of maximum time of work of an engine without heat shielding on gauge, operating pressure, and combustion temperature of the fuel T_0: - - - - T_0 = 2600°C; —— T_0 = 2000°C.

According to formula (6.50) the allowed time of work of an engine increases in proportion to gauge to the power 1.44. If during a change of gauge of the engine we preserve the geometric similarity of all its elements, then thickness of the burning arch, and consequently also time of work of the engine have to change in proportion to gauge to the first power. Consequently, during geometric modeling of an RDTT with growth of gauge, the time allowed by conditions of wall heating for work of an engine is increased faster than real time of work increases.

Computed values $\tau_{доп}$, obtained by us by formula (6.50) for different pressures and gauges, are represented in the form of graphs in Fig. 6.3. Calculations were conducted with the following initial data:

$$\varkappa_1 = 1{,}8;\ K_1 = 0{,}8\ 10^{-5};\ T_{пл} = 500°\,C;\ \sigma_{вт} = 2500\ kg/cm^2;$$
$$\lambda = 0{,}01\ kcal/ms\,°C;\ c = 0{,}14\,kcal/kg°C;\ \gamma = 7820\ kg/m^3.$$

As calculations show, the allowed time of work of an RDTT without a heat shield is extremely small: it is from several tenth fractions of a second to several seconds. With an increase of thickness of the wall of an engine along with a lowering of average temperature, there is an increase of temperature on the internal surface of the wall $T_{с.в}$. In certain cases during determination of the permissible time of work of an engine this factor becomes the limiting one. Thus in our calculations the determining role of this factor is revealed at T_0 = 2600°C at pressures over 100 kg/cm^2. The upper limit of possible use of an engine at T_0 = 2600°C, corresponding to $T_{с.в}$ = 0.9 $T_{пл}$, is drawn on graph 6.3 by a dot-dashed line.

§ 6.6. Basic Types of Heat Shield Coverings Utilized in RDTT

Thermal shielding of elements of the carrier construction from hot gases is ensured by coverings made from special materials, and also by a fuel charge fastened to the body of the engine.

The basic requirements of heat shield coverings are: reliability of the shielding of the carrier construction, minimum weight of the covering each 1 m^2 of protected surface, good adherence of the covering with the material of the carrier construction, sufficiently high resistances to vibration loads and mechanical and thermal shocks, ease of manufacture.

Protective coverings for RDTT known at present can be divided into passive and active heat shielding coverings.

Passive heat shielding is ensured by thermoresistant coverings made from materials which combine high melting points ($T_{пл} > T_0$) with low temperature transfer. Thickness of these coverings in the process of work should remain constant, therefore they have an additional requirement: sufficient resistance to erosion influences.

The basis of such coverings are refractory oxides (MgO, Al_2O_3, ZrO_2 and others), carbides, nitrides and borides of certain metals. A list of refractory materials is given in Table 6.3 [21], and physical properties of certain of these materials are given in Table 6.4 [20], [22], [23].

During the use of a glass-like binder one obtains two-component ceramic. In two-component compositions we sometimes and a fluring substance for the purpose of increasing the contents in a ceramic of fireproof material. Ceramic coatings are deposited in thin layers and can consist of a uniform material or alternating heterogeneous layers, each of which has its own special purpose.

Thus, for example, the external layer can consist of material with raised erosional stability, whereas internal layers will ensure high heat shielding qualities of the covering.

Wide application in rocket technology has been given to the method of flame spraying, which consists of the following. From a powder of fireproof material (silica, zirconium oxide, titanium oxide and others) a rod is formed which is placed in a high-temperature flame of a burner. The melted material is atomized and ejected on the preliminarily purified metallic surface. Adhering to the surface, the particles harden rapidly, forming protective layer. Such coverings made from refractory materials with sufficient thickness of the deposited layer can resist high heat flow. However due to porosity of the structure these coverings possess insufficient erosion stability. The adhesive strength of such coverings with the metal is low; this conditions their relatively low resistance to mechanical blows and vibration influences [21], [24].

Table 6 3. List of superrefractory materials (melting point over 2500°C).

Material	Melting point, °C
Elements:	
carbon	3500
molybdenum	2650
osmium	2700
rhenium	3170
tantalum	2850
tungsten	3370
Oxides:	
beryllium	2500
calcium	2550
hafnium	2800
magnesium	2800
thorium	2800
zirconium	2700
Borides:	
hafnium	3050
tungsten	2900
zirconium	2900
Carbides:	
hafnium	4150
molybdenum	2550
niobium	3500
silicon	2700
tantalum	4150
thorium	2800
titanium	3100
tungsten	2860
zirconium	3550
zirconium-tantalum	3900
Nitrides:	
boron	2750
hafnium	3300
scandium	2650
tantalum	3300
titanium	3200
zirconium	3000
Zirconates	
barium	2700
calcium	2660
strontium	2700
thorium	2800

Table 6.4

Material	Melting or decomposition point °C	Real specific gravity, kg/m^3	Apparent specific gravity, kg/m^3	Coefficient of linear expansion 10^6 1/°C	Coefficient of thermal conduction, $\frac{kcal}{ms°K} \cdot 10^3$	Specific heat kcal/kg°K
Aluminum oxide....	2015.7	3970	2950	8.1	0.62	0.27
Boron carbide.....	2449	2510	2510	4.5	0.413	–
Beryllium oxide...	2500	3020	2700	8.0	3.580	0.43
Zirconium dioxide.	2700	6270	4400	11.0	0.172	0.168
Magnesium oxide...	2800	3580	2500	14.3	0.825	0.187
Thorium oxide.....	2800	9690	7340	9.4	–	0.06
Boron nitride.....	2730	–	2210	0.77/7.51*	2.9	0.22
Silicon carbide...	2700	–	3170	25/1200	12.5/1	0.30
Titanium carbide..	3100	–	4900	–	1.86	0.21

*For anistropic materials, characteristics are given separately for longitudinal and transverse directions.

The biggest adhesive strength of a covering with a metallic surface is attained during the use of a plasma-arc torch, ensuring heating of the powdered material to a temperature of 10,000-12,000°C. Here deep diffusion embedding of the protective material in the layer of metal occurs.

One of the possible directions is creation of cermet coverings obtained during sintering of powders of the refractory material and metal, for example, Al_2O_3 and Cr [23].

An active thermal shield of a body is based on absorption of a considerable share of heat fed to the surface with destruction and removal of material of the covering. This heat is expended on phase transitions (fusion and evaporation, sublimation) and endothermal reactions (pyrolysis of organic substances) in the surface layer of the covering. Due to this the heat flow tapped in the depth of the material is small as compared to the flow fed to the wall. Coverings of such a type are frequently called ablating.

The term "ablation" is collective and embraces different cases of thermal decomposition and subsequent removal of a substance from the surface of a solid during heat exchange with a gas flow.

A specific requirement of such coverings is the greatest possible heat of ablation.

A basic advantage of ablating coverings is the possibility of using them at any combustion temperature of a solid fuel, whereas application of heat-resistant coatings is limited by the melting point of the covering material. Furthermore, as a rule, ablating coverings possess smaller specific gravity and higher mechanical characteristics.

Active heat shielding coverings are divided into coverings with surface and internal removal of the substance.

The first subgroup unites sublimable materials and certain polymers which are decomposed without formation of a carbonized layer [25], [26].

Sublimable coverings finding application in RDTT consist of mineral salts (sublimable material) and an organic binder. The material of the covering can be deposited on the surface of the article in a diluted state by brush, and also by atomization or casting. Characteristics of certain sublimable materials are given in Table 6.5 [22].

A covering of such a type is used in the RDTT the ballistic missile "Honest John" as heat insulation of the nozzle [26].

Of coverings of this subgroup one should also mention differnet types of rubber insulation. There are indications of the use of rubber coverings at a temperature of ~3900°C for 120 s [25]. Such coverings are used in the RDTT of the three-stage "Minuteman" rocket [27] for thermal shielding of the body and bottoms of the engine. The thickness of the rubber covering, depending on conditions of work, is changed from several millimeters to several centimeters. Thus, for

Table 6.5

Substance	Specific gravity, kg/m^3 10-3	Boiling point, °C	Heat of sublimation or dissociation, kcal/kg
Mg_3N_2	–	1500 (decomposition)...	2130
Si_3N_4	3.44	Sublimates.....	2800
AlN	3.26	2000 (sublimates).....	3720
NH_4F	1.315	Sublimates.....	1276
NH_4Cl	1.527	355 (sublimates).....	994
AlF_3	3.07	1270.....	905
SiS_2	–	Sublimates...	694
CdO	6.95	900-1000 (disintegration)	694
ZnO	5.61	1800 (sublimates).....	556

example, for the engine of the third stage of the "Minuteman" rocket the thickness of the layer of rubber on the nozzle cover attains 25 mm.

Coverings with internal removal of a substance consist of a nondestructible component (structure of the carrier) and a removable component which is a heat sink. Of coverings of such a type the most wide-spread are reinforced plastics. During their heating there is decomposition of the organic base with formation of gases diffusing to the surface and a relatively durable carbonized layer.

Reinforced plastic can be used in an RDTT as protective coverings and structural materials. If the RDTT body, made from reinforced plastic, does not have an additional covering, the surface layer of the plastic itself fulfills the role of an ablating covering. In the case when reinforced plastic fulfills only the function of a thermal insulation covering, it is possible to select an optimum composition which most fully corresponds to requirements of thermal shielding of the engine body. Coverings made from reinforced plastic are used in many samples. The thermal shield of the engine body of the anti-missile missile "Nike-Zeus," working for 80 s, is ensured by an internal lining made from fiberglass laminate. Coverings made from fiberglass laminate are used for shielding the lower part of the body of the engine of the first stage of the "Minuteman" rocket. The thickness of the plastic layer in place of bracing of the lower bottom attains 50 mm.

Of the other possible compositions of coverings with internal removal of a substance it is possible to indicate porous graphite and

tungsten, filled with a sublimable substance or polymers [22].

§6.7. Design of Refractory Thermal Insulation Coverings (Passive Thermal Shielding)

The character of distribution of temperature in an engine wall with a refractory thermal insulation covering is shown in Fig. 6.4. Here and subsequently the account of index M pertains to material of the carrier element of construction, index П – to the covering. In the thermal insulation layer a sharp fall of temperature is observed.

For determination of the temperature field of a two-layer wall we used the system of equations:

$$\left.\begin{aligned}
&a\frac{\partial^2 T}{\partial x^2}=\frac{\partial T}{\partial t};\\
&\Delta_п \geqslant x \geqslant 0,\ \lambda=\lambda_п,\ a=a_п=\frac{\lambda_п}{\gamma_п c_п};\\
&\Delta_п+\Delta_M \geqslant x > \Delta_п,\ \lambda=\lambda_M,\ a=a_M=\frac{\lambda_M}{\gamma_M c_M};\\
&x=0,\ -\lambda_п\frac{\partial T_п}{\partial x}=\alpha(T_г-T_{с.в});\\
&x=\Delta_п,\ \lambda_п\frac{\partial T_п}{\partial x}=\lambda_M\frac{\partial T_M}{\partial x};\\
&T_п=T_M;\\
&x=\Delta_п+\Delta_M,\ -\lambda_M\frac{\partial T_M}{\partial x}=0.
\end{aligned}\right\} \qquad (6.51)$$

An analytic solution of this system of equations leads to bulky calculation dependences whose use in engineering practice is difficult in view of the considerable labor-input of calculations [28]. A substantial simplification of these dependences is attained by examining limiting cases, which present the greatest practical interest. One of them is the case when temperature gradients in the protected material are insignificant. A similar phenomenon is observed when the carrier element of construction is made from metal, inasmuch as the coefficients of thermal conduction of a covering and metal usually differ by almost two order. This can be ensured also for a construction material with low thermal conduction at the expense of great thickness of the covering.

Solutions for this maximum case are given in works [28], [29], [30]. In work [30] the relative temperature of the boundary of covering and wall is represented in the form of a function of two parameters – the criterion of Fourier, enumerable for covering, and the compound criterion μ:

$$Fo=\frac{a_п\tau}{\Delta_п^2};$$

$$\mu=\frac{1}{Bi}+\frac{1}{M}+\frac{1}{BiM}.$$

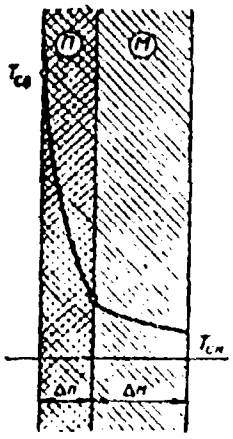

Fig. 6.4. Distribution of temperature in engine wall with a passive heat shield covering.

where Bi – criterion of Biot for the covering:

$$Bi = \frac{\alpha \Delta_п}{\lambda_п};$$

$$M = \frac{\gamma_п c_п \Delta_п}{\gamma_м c_м \Delta_м}.$$

The dependence for determination of temperature on the border of the covering and metal (it is the temperature of the wall) has the form

$$\theta = \frac{T_0 - T}{T_0 - T_н} = \sum_{i=1}^{\infty} \frac{2\mu e^{-F_0 \Phi_i^2} \sec \Phi_i^2}{1 + \mu + \mu \Phi_i^2}, \qquad (6.52)$$

where Φ_i – positive roots of the transcendental equation

$$\Phi_i \operatorname{tg} \Phi_i = \frac{1}{\mu}.$$

In Fig. 6.5. there is a graph of the dependence θ on Fo for values of μ from 0 to 50 [30]. Values of θ are given in logarithmic scale.

As can be seen from the graph, with the exception of a very limited region of small values Fo where $\theta \to 1$, not of practical interest, the dependence of the logarithm of θ on Fo when μ = const has a linear character. This indicates that the work of a heat-resistant thermal insulation covering almost wholly flows under conditions of regular thermal conditions (see Chapter VII).

With the aid of the graph it is easy to solve the inverse problem (check calculation): determination of the temperature of the protected material at assigned thickness and heat-physical characteristics of covering. However it is inconvenient for solution of the primary

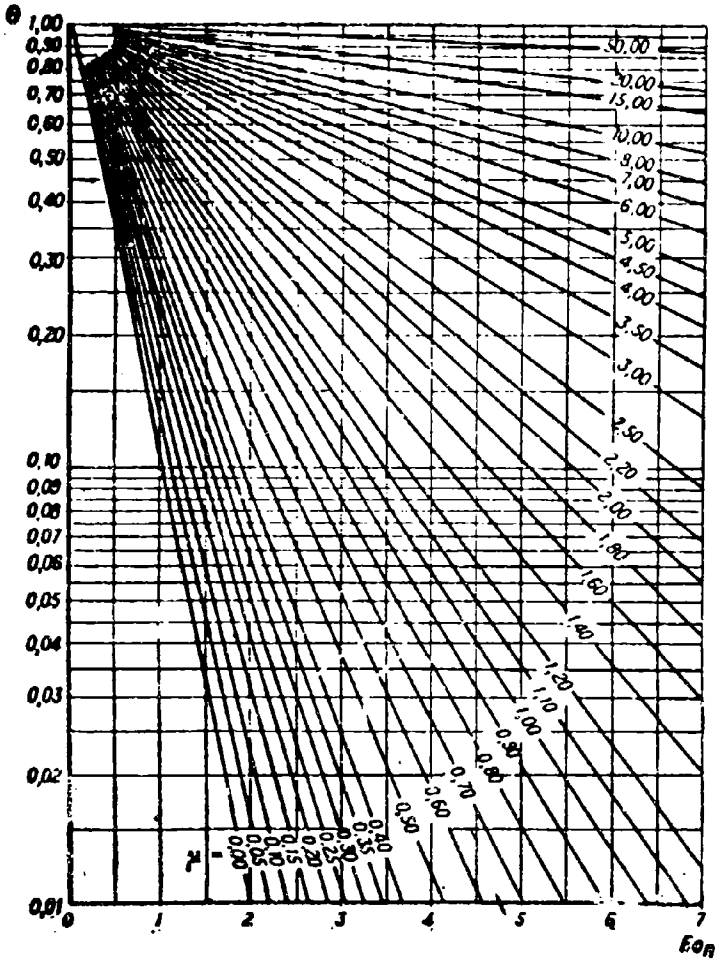

Fig. 6.5. Dependence of relative excess temperature on border of covering and metal on criterion $Fo_п$.

problem — detecting the thickness of the covering necessary for limitation of wall heating to the allowed temperature $T_{доп}$.

A simple solution of the primary problem is obtained if the solution represented by the graph is approximated by a dependence of the form

$$\lg \theta = \lg \theta_0 - \frac{A}{\mu + C} Fo, \qquad (6.53)$$

where A, C — approximation coefficients; $\lg \theta_0$ — approximation constant.

As analysis shows, when $A = 0.45$, $C = 0.40 \lg \theta_0 = 0.0212$, accuracy of the approximation in the region $\mu = 0.2$ to 20 is approximately 1-2%. When $\mu \to 0$ errors of approximation increase, remaining within the limits 10-12%.

Putting in dependence (6.53) the expanded expressions of Fo and μ we obtain an equation squared relative to $\Delta_П$. Solving it, we find

$$\Delta_П = -\frac{1}{2C}\left(\frac{\lambda_П}{a} + \frac{1}{\overline{M}}\right) + \sqrt{\frac{1}{4C^2}\left(\frac{\lambda_П}{a} + \frac{1}{\overline{M}}\right)^2 - \frac{1}{C}\left(\frac{\lambda_П}{a\overline{M}} + \frac{A a_П \tau}{\lg\theta - \lg\theta_0}\right)}, \qquad (6.54)$$

where

$$\overline{M} = \frac{\gamma_П c_П}{\gamma_M c_M \Delta_M}.$$

With an increase of temperature of the material of the wall its strength characteristics descend, but in accordance with this the necessary wall thickness determined from the condition strength of the rocket chamber increases. Simultaneously with an increase of the temperature limit to which heating of the wall is allowed, the necessary thickness of thermal insulation $\Delta_П$ decreases .

During calculation of a chamber for strength the thermal insulation, in view of its low strength characteristics is not taken into account.

Disregarding curvature of a two-layered chamber wall, the weight of one square meter can be determined as

$$Q_1 = \gamma_П \Delta_П + \gamma_M \Delta_M,$$

where $\Delta_П$ can be calculated by formula (6.54), and Δ_M is defined by the approximate dependence

$$\Delta_M = \frac{\eta p d}{2\sigma_{BT}},$$

where p – design pressure; η – safety factor; σ_{BT} – tensile strength taking into account temperature of the wall.

Among the infinite set of relationships of $\Delta_П$ and Δ_M satisfying the condition of engine body strength at assigned parameters of the process of heat transfer in the engine (T_0, α, τ), there exists one which ensures minimum weight of the construction. If from this optimum relationship it is displaced in the direction of decrease of thickness of the wall Δ_M, weight of the construction will increase on account of the considerable increase $\Delta_П$ necessary to ensure low

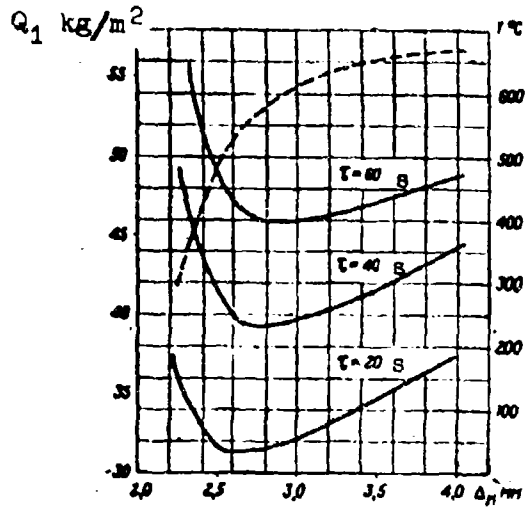

Fig. 6.6. Dependence of weight of 1 m^2 of wall of an RDTT body on allowed temperature of metal Δ_M – thickness of metal; —— weight 1 m^2 wall per wall Q_1; - - - - temperature of metal °C.

temperatures of the wall. With a decrease of Δ_M weight will increase on account of growth of Δ_M.

Clearness of the minimum of weight of the construction depends on conditions of the process, characteristics of covering and material of the body.

In Fig. 6.6 are graphs $Q_1 = f(\Delta_M)$, calculated for a steel wall with covering made from zirconium oxide at T_0 = 2000°C, α = 0.695 kcal/m^{2}s°C, for different times of work of the engine. Here the dotted line represents the dependence for temperature of the wall. Conditions of construction of the graph are expounded below.

As investigation show, for a series of combinations of metal with refractory covering a sharply expressed minimum of weight of the construction is observed and selection of optimum thickness can ensure a considerable gain in weight.

Example.

To find the optimum combination of thickness of a steel wall and covering made from zirconium oxide under assigned characteristics of materials and conditions heat transfer.

Given: $d = 300$ mm;
$p_{рег} = 125$ atm;
$\alpha = 0{,}695 \ \frac{\text{kcal}}{\text{ms}^\circ\text{K}}$;
$T_0 = 2000°$ C;
$T_н = +20°$ C;
$\tau = 40$ s.

Characteristics of wall material

$$\gamma_M = 7820 \text{ kg/m}^3 \qquad c_M = 0{,}140 \ \frac{\text{kcal}}{\text{kg}^\circ\text{K}}.$$

The dependence of tensile strength of the material on temperature is shown in graph 6.7 [20].

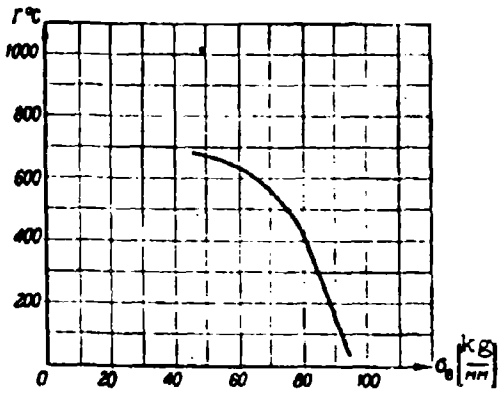

Fig. 6.7. Graph of dependence of tensile strength of heat-resistant steel on temperature.

Characteristics of covering material:

$$\gamma_п = 4400 \text{ kg/m}^3 \quad c_п = 0{,}168 \ \frac{\text{kcal}}{\text{kg}^\circ\text{K}} \quad \lambda_п = 0{,}172 \cdot 10^{-3} \ \frac{\text{kcal}}{\text{ms}^\circ\text{K}}$$

(see Table 6.4).

Let us assign several values of temperature of the wall $T_{доп}$ For each of them we determine $\Delta_п$, $\Delta_м$ and calculated Q_1. Let us consider the sequence of calculations for $T_{доп}$ = 500°C.

According to the graph, at T = 500°C, $\sigma_{вт}$ = 7400 kg/cm^2:

$$\Delta_м = \frac{125 \cdot 30}{2 \cdot 7400} = 0{,}253 \text{ см} = 2{,}53 \cdot 10^{-3} \text{ м};$$

$$\theta_{доп} = \frac{T_0 - T_{доп}}{T_0 - T_в} = \frac{2000 - 500}{2000 - 20} = 0{,}7575;$$

$$a_п = \frac{\lambda_п}{\gamma_п c_п} = \frac{0{,}172 \cdot 10^{-3}}{4400 \cdot 0{,}168} = 0{,}2305 \cdot 10^{-6} \ \frac{\text{м}^2}{\text{s}};$$

$$\frac{\lambda_п}{\alpha} = \frac{0{,}172 \cdot 10^{-3}}{0{,}695} = 0{,}248 \cdot 10^{-3} \text{ м};$$

$$\frac{1}{M} = \frac{\gamma_м c_м \Delta_м}{\gamma_п c_п} = \frac{7820 \cdot 0{,}140 \cdot 2{,}53 \cdot 10^{-3}}{4400 \cdot 0{,}168} = 3{,}74 \cdot 10^{-3} \text{ м};$$

$$\lg \theta - \lg \theta_0 = -0{,}1418;$$

$$\Delta_п = -\frac{1}{2 \cdot 0{,}4}(0{,}248 + 3{,}74) \cdot 10^{-3} + \sqrt{\frac{1}{0{,}64}(0{,}248 + 3{,}74)^2 \cdot 10^{-6} -}$$

$$-\frac{1}{0{,}4}\left(0{,}248 \cdot 3{,}74 \cdot 10^{-6} + \frac{0{,}45 \cdot 0{,}231 \cdot 10^{-6} \cdot 40}{0{,}1418}\right) = -4{,}99 \cdot 10^{-3} + 9{,}81 \cdot 10^{-3} =$$

$$= 4{,}82 \cdot 10^{-3} \text{ м};$$

$$Q_1 = \gamma_м \Delta_м + \gamma_п \Delta_п = 7820 \cdot 2{,}53 \cdot 10^{-3} + 4400 \cdot 4{,}82 \cdot 10^{-3} = 41{,}0 \text{ kg/m}^3$$

Table 6.6

$T_{доп}$, °C	300	400	500	550	600	675
σ_B, $\frac{kg}{cm^2}$	8500	8000	7500	7200	6500	4700
Δ_M 10^3, m	2,23	2,37	2,53	2,63	2,92	4,02
Δ_T 10^3, m	7,29	5,89	4,82	4,38	3,82	2,73
Q_L, $\frac{kg}{m^2}$	49,4	44,4	41,0	39,85	39,6	43,4

Results of analogous calculations for other temperatures are given in Table 6.6.

As it follows from graph 6.6, minimum weight is attained when Δ_M = 2.8 mm and composes 39.3 kg/m^2. As compared to the maximum variant $T_{доп}$ = 300°C at which σ_B still remains practically constant, the optimum variant ensures a 25% gain in weight of the construction.

Similarly built are two other graphs in Fig. 6.6.

§ 6.8. Design of a Sublimable Covering

Let us consider the case of stationary sublimation, when the surface of the sublimable covering shifts in the depth of the material with a constant linear speed u. Let us introduce a moving coordinate system, combining its origin with the surface of the covering, and the direction of the positive axis ζ with the direction of sublimation. The connection of the fixed and mobile coordinates is defined as

$$\zeta = x - ut.$$

We will present the heat-conduction equation for material of the covering in the moving coordinate system. Inasmuch as:

$$\frac{\partial \zeta}{\partial x} = 1; \quad \frac{\partial \zeta}{\partial t} = -u; \quad \frac{\partial^2 T}{\partial x^2} = \frac{\partial^2 T}{\partial \zeta^2}; \quad \frac{\partial T}{\partial t} = \frac{\partial T}{\partial \zeta}\frac{\partial \zeta}{\partial t} = -u\frac{\partial T}{\partial \zeta},$$

the heat-conduction equation will take the form

$$a\frac{\partial^2 T}{\partial \zeta^2} = -u\frac{\partial T}{\partial \zeta}. \qquad (6.55)$$

Introducing designation $\delta_T = \frac{a}{u}$ and taking into account that the distribution of temperature depends only on coordinate ζ, equation (6.55) can be presented in the form

$$\delta_T\frac{d^2T}{d\zeta^2} = -\frac{dT}{d\zeta}. \qquad (6.56)$$

Equation (6.56) has the general solution

$$T = -c_1 \delta_T e^{-\zeta/\delta_T} + c_2 \tag{6.57}$$

We will find the value of constants of integration:

when $\zeta = \infty$, $T = T_н$, $c_2 = T_н$;
when $\zeta = 0$, $T = T_s$, $c_1 = -(T_s - T_н)/\delta_T$.

After substitution of values c_1 and c_2 the equation of the temperature field in the covering takes the form

$$T - T_н = (T_s - T_н) e^{-\zeta/\delta_T}. \tag{6.58}$$

Let us note that for sublimable coverings the temperature of the surface T_s under any conditions of heat addition from the gas phase remains constant, equal to the temperature of sublimation of the covering material.

Let us estimate the depth of heating of the covering material during stationary sublimation, taking as a conditional border of heating the point in which temperature of the material is increased 20°. Let us take as initial data $\gamma = 2000$ kg/m^3, $c = 0.35$ kcal/kg°C. $T_s = 320$°C, $T_н = 20$°C, $\lambda = 0.667 \cdot 10^{-4}$ kcal/ms°C, $u = 0.4 \cdot 10^{-3}$ m/s, then

$$\zeta = \frac{\lambda}{\gamma c u}\left(-\ln \frac{T - T_н}{T_s - T_н}\right) = \frac{0{,}667 \cdot 10^{-4}}{2000 \cdot 0{,}4 \cdot 10^{-3} \cdot 0{,}35}\left(-\ln \frac{40 - 20}{320 - 20}\right) = 0{,}645 \cdot 10^{-3}\ м.$$

Thus, depth of heating is within limits of tenth fractions of a millimeter.

The temperature gradient at the covering surface

$$\left(\frac{\partial T}{\partial \zeta}\right)_s = -\frac{T_s - T_н}{\delta_T} = -\frac{\gamma c u}{\lambda}(T_s - T_н)$$

and, consequently, the flow of heat fed from the surface to the depth of the material, is equal to

$$q_2 = -\lambda\left(\frac{\partial T}{\partial \zeta}\right)_s = \gamma u c (T_s - T_н). \tag{6.59}$$

Heat flow q_1 fed to the surface of a sublimable covering, is calculated by the formula

$$q_1 = q_{10} - \eta_q \gamma u (I_0 - I_s). \tag{6.60}$$

where q_{10} – heat flow, calculated neglecting gas formation on surface of covering; I_s – enthalpy of sublimate at surface temperature, I_0 – enthalpy of sublimate at the temperature of the nucleus of the gas flow; η_q – experimental coefficient.

The second member standing in the right part considers weakening of the heat flow on account of absorption of heat by the sublimate moving toward it. Experimental coefficient η_q is ~0.8 for laminar flow and ~0.4 during turbulent flow of gases in the chamber [31].

Speed of stationary sublimation can be found from the equation of heat balance for the surface of sublimation:

$$q_1 = q_2 + \gamma u Q_s. \tag{6.61}$$

Putting in the equation of heat balance (6.61) the obtained expression for q_2 (6.59) and value q_1 from formula (6.60), we find:

$$u = \frac{q_{10}}{\gamma [Q_s + (T_s - T_n) c + \eta_q (I_0 - I_s)]}. \tag{6.62}$$

The thickness of layer sublimating during the time of work of the engine is equal to

$$\Delta_c = u\tau.$$

Calculation of organic coverings, decomposing during heat without formation of a carbonized layer is similar to calculation of a sublimable covering. The specific character of calculation of such a covering reduces to calculation of the dependence of mass speed of decomposition on temperature of the surface, which usually follows the law of Arrhenius [32]:

$$\dot{m}_s = \gamma u = K_m e^{-\frac{E}{2RT_s}}, \tag{6.63}$$

where E – activation energy; K_m – preexponential factor.

Putting expression (6.63) in the equation of heat balance for the surface of the covering, we obtain

$$\alpha_q (T_0 - T_s) - \eta_q (I_0 - I_s) = K_m e^{-\frac{E}{2RT_s}} [c (T_s - T_n) + Q_s]. \tag{6.64}$$

Expressing enthalpy as the product of temperature and average heat capacity of the gas, we obtain

$$(q_0 - \tau_0 \bar{c}_p)(T_0 - T_s) = K_a e^{-\frac{E}{RT_s}} [c(T_s - T_0) + Q_s]. \tag{6.65}$$

Solving the obtained equation by selection, one can determine the surface temperature T_s, and then by equation (6.63) one can find speed of ablation.

Inasmuch as the curve of the dependence of speed of decomposition of a plastic on temperature has a very steep climb (by analogy with burning of solid fuels), then it is possible to assume that in real conditions surface temperature of the covering during ablation oscillates in relatively narrow limits, and one can introduce in the calculation a certain mean value $\bar{T}_s$. In this case we return to calculation dependence (6.62).

Placing in dependence (6.62) the expanded value q_{10}, we will reduce all secondary values and those which are determined by characteristics of the material to coefficient K_a. Then

$$u \approx K_a (pv)^{0.8} \left(1 - \frac{T_s}{T_0}\right) T_0$$

The obtained formula permits one in the first approximation to estimate the dependence of speed of stationary ablation on basic parameters of internal ballistics: pressure p, speed of gas flow v and combustion temperature of the fuel T_0.

As examined by us, stationary ablation, strictly speaking, is the limit which the process of ablation approaches asymptotically, and the time for establishing a stationary process equal to infinity. However, in reality, after a short initial period, the process of ablation practically insignificantly differs from stationary. For an appraisal of this initial period we will examine the equation of the transient process of thermal conduction in the covering

$$a \frac{\partial^2 T}{\partial x^2} = \frac{\partial T}{\partial t} - u \frac{\partial T}{\partial x}. \tag{6.66}$$

We shall express this equation in dimensionless form, selecting corresponding scale units. As a time scale we will take a certain time τ, as a linear scale value a/u_c (u_c – speed of stationary ablation), as characteristic temperature, temperature on the surface of the covering during stationary ablation T_s. Then:

$$T = \bar{T} T_s; \quad l = \bar{l} \frac{a}{u_c}; \quad t = \bar{t}\tau; \quad u = \bar{u} u_c.$$

After substitution, equation (6.66) takes the form

$$\frac{u_c^2}{a}\frac{\partial^2 \bar{T}}{\partial \bar{\xi}^2} = \frac{1}{\tau}\frac{\partial \bar{T}}{\partial \bar{\tau}} - \frac{u_c^2}{a}\bar{u}\frac{\partial \bar{T}}{\partial \bar{\xi}}.$$

Dividing both parts of the equality by u_c^2/a, we obtain

$$\frac{\partial^2 \bar{T}}{\partial \bar{\xi}^2} = \frac{a}{u_c^2 \tau}\frac{\partial \bar{T}}{\partial \bar{\tau}} - \bar{u}\frac{\partial \bar{T}}{\partial \bar{\xi}}. \qquad (6.67)$$

Equation (6.67) will be converted to an equation for stationary process when $\bar{u} \to 1$, and $\frac{a}{u_c^2} \ll \tau$. Thus, value a/u_c^2 characterizes the time which is required to ensure a stationary distribution of temperature in the covering. Let us designate it by τ_p and call it time of thermal relaxation. The dependences derived for a stationary process become useful when $\tau \gg \tau_p$. As a rule, time of thermal relaxation for coverings is small and can be disregarded. Thus, in the example examined above

$$\tau_p = \frac{\lambda}{\gamma c u^2} = \frac{0{,}667 \cdot 10^{-4}}{2000 \cdot 0{,}35 \cdot 0{,}16 \cdot 10^{-4}} = 0{,}6 \text{ s}.$$

Let us note that the dependences derived above of thermal conduction in the solid phase during ablation and sublimation are useful for calculation of the distribution of temperature in a solid fuel during burning.

The minimum covering thickness necessary that temperature on the border of the covering and carrier elements of construction will not exceed an allowed value $T_{доп}$, in first the approximation will be defined as

$$\Delta = u\tau + \zeta = u\tau + \frac{a}{u}\left(-\ln\frac{T_{доп} - T_н}{T_s - T_н}\right). \qquad (6.68)$$

For a covering one should consider as optimum the material, the complex of physical-chemical characteristics of which ensures the least weight of the covering. Let us consider the simplest case, when available materials differ only in speed of ablation. With growth u there is an increase of thickness of the ablating layer, and a decrease of thickness of the heated layer. Differentiating expression (6.68) with respect to u and equating the derivative to zero, we find the optimum speed of ablation which ensures a minimum covering weight:

$$u_{опт} = \sqrt{\frac{a}{\tau}\left(-\ln\frac{T_{доп} - T_н}{T_s - T_н}\right)}. \qquad (6.69)$$

According to formula (6.69) value $u_{опт}$ descends with a decrease of temperature transfer of material and with an increase of time of work. For an engine with a relatively short time of work, a smaller covering weight is ensured at greater speeds of ablation.

§ 6.9. Design of Carbonizing Plastic Thermal Coverings

Under conditions of a rocket chamber during insufficient speed of the gas flow, solid remainders of thermal decomposition of the covering or plastic material of an organic-base body will form on the surface a porous carbonized layer whose thickness can attain several millimeters.

A diagram of heat-mass transfer for this case is represented in Fig. 6.8. Let us consider sequence of processes flowing here.

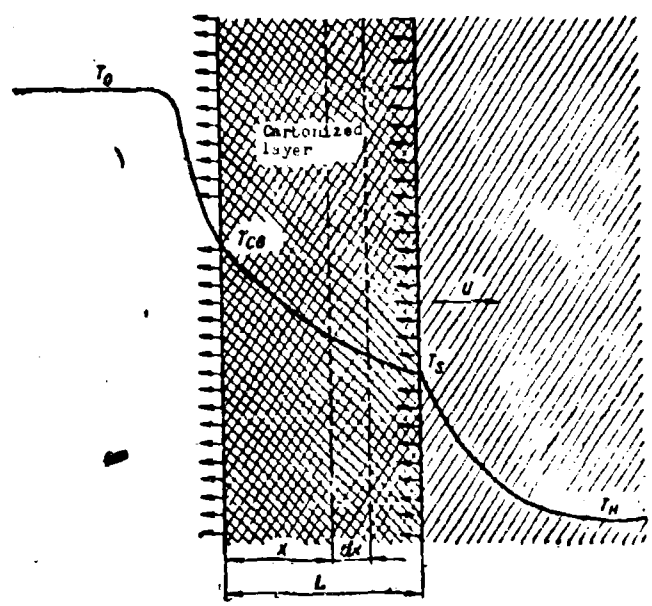

Fig. 6.8. Diagram of heat-mass transfer between gas flow and plastic covering in the presence of a carbonized layer.

During intense heating of the plastic thermal decomposition of the binding substance occurs (organic resins), known as a reaction of pyrolysis. A study of pyrolysis of plastics in tubular and arc reflective furnaces [33] has shown that products of disintegration consist of volatile substances and hard remainders in the form of a rigid nonuniform carbon compound, connected by the glass filler matrix. In a typical plastic from phenolic resin reinforced with glass fibre, the weight content of resin is 20-30%. As a result of pyrolysis approximately half of the resin (i.e., ~10-15% weight of all the material) is turned into gaseous products. During

decomposition of epoxy resins the yield of gaseous products is nearly 80% of the weight of resin. A typical composition of gaseous products of pyrolysis of phenolic resin is given in Table 6.7.

Table 6.7. [33]

Components	Molar, %
H_2	54
CO	12
CH_4	12
H_2O	12
Phenol	2.5
Cresol	2.5
Other gases (C_2H_4, C_3H_6, C_4H_8; toluene, benzene, xylene)	5

As it was established a solid remainder is a stable substance up to temperatures ~1600°K. At higher temperatures liberaties of CO is possible on account of carbon reduction of silicon oxide from the fibre.

The reaction of pyrolysis of the organic binder is endothermic. The thermal effect of the reaction for phenolic resin is Q_s = 300 kcal/kg [34]. In Table 6.8 are given computed values of Q_s for different polymers, checked by experiments on decomposition and burning of these polymers under conditions of convection heat exchange [34].

Table 6.8

Polymer	Q_s, $\frac{kcal}{mole}$	Q_s, $\frac{kcal}{kg}$
Polymethyl metacrylate $(C_5H_8O_2)_n$	13.0	130
Polystyrene $(C_4H_8)_n$	16.4	102
Polyisobutylene $(C_4H_8)_n$	12.6	92
Polybutadiene $(C_4H_6)_n$	17.9	82

Thus, for a sufficiently large quantity of polymers value Q_s is changed from -80 to -130 kcal/kg.

As results of experiments show [32], the mechanism of pyrolysis of the organic binder can be represented as a reaction of the first order with respect to the parent substance.

The speed of the monomolecular reaction, as a result of which relative weight of the undecomposed substance $G_{пл}$ continuously decreases, is determined by dependence

$$-\frac{dG_{пл}}{dt} = G_{пл} B e^{-E/RT}, \tag{6.70}$$

where E – activation energy; B – preexponential factor; T – temperature at a given point of the covering.

According to dependence (6.70) reactions of decomposition of the substance flow over all the heating region of the plastic. Due to this the content on undecomposed binder monotonously decreases, approaching zero as one approaches the border of the carbonized layer.

Derivation of calculation formulas for determination of the thickness of the carbonized layer on the basis of dependence (6.70), as this is done in work [32], is very complex. Without much error, the solution of the problem can be simplified by using the following considerations.

As it was shown by Ya. B. Zel'dovich and D. A. Frank-Kamenetskiy [35], under steep exponential dependence of the chemical reaction rate on temperature, the reaction basically flows in the region of the temperature of completion of the reaction.

In reference to our case this means that actually the reaction of pyrolysis of the organic substances is localized in the narrow zone on the border with the completely carbonized layer. This allows one to cross to the following simplified scheme of the process.

1. Decomposition of the organic binder occurs wholly on the interface of the undecomposed plastic and carbonized layer (pyrolysis front) at a certain temperature T_s.

2. Before the pyrolysis front only heating of the plastic on account of thermal conduction is observed.

The mass speed of decomposition of the material on the pyrolysis front will be expressed by the dependence

$$\dot{m}_s = K_s e^{-\frac{E}{2RT_s}}. \tag{6.71}$$

Similar simplifications are widely used during solution of problems in the theory of combustion. For appraisal of the error introduced by such a simplification in the solution of the given problem, calculations were made of mass flow rate by formula (6.71) for temperatures of the interface from reference [32]. From a

comparison of obtained data with results of calculations in [32] it follows that error in determination of $\dot{m}_s$ during transition to the simplified dependence (6.71) for assigned conditions does not exceed 5-6%.

The quantity of gases forming during pyrolysis per unit of time on a unit area of the pyrolysis front will be $\dot{m}_{s\chi}$, where χ – amount of material transformed into gases.

An insignificant amount of forming gases remains on place, filling pores formed in the material; the basic mass moves through pores of the carbonized layer to the surface of the wall. The mass flow rate of gases, taken over all the thickness of the porous layer as being constant, per unit area normal to the direction of motion of the gas will be

$$\chi \dot{m}_s \left(1 - \frac{\rho_r}{\rho_s}\right).$$

The expression in parentheses considers the quantity of gases remaining in zone of formation of filling of pores. For simplification of rotation we introduce the designation

$$\bar{\chi} = \chi \left(1 - \frac{\rho_r}{\rho_s}\right).$$

By porosity of carbonized layer ε we understand the ratio of volume of pores to the full volume of the material. The interesting product of effective density and specific heat for this layer can be presented as

$$(\rho c_p)_{ap} = (1 - \varepsilon)(\rho c)_{\tau o} + \varepsilon (\rho c_p)_{\tau \varepsilon \lambda}. \qquad (6.72)$$

For determination of the given value of the coefficient of thermal conduction of carbonized layer the following empirical dependence is recommended in work [32]:

$$\lambda_{ap} = (1 - \varepsilon)\lambda_{\tau o} + \varepsilon \lambda_{\tau \varepsilon \lambda}. \qquad (6.73)$$

Opposing transfer of the substance, heat flow from the surface is directed to the depth of the wall. Inasmuch as the value of voids (pores) is sufficiently small as compared to thickness of the carbonized layer, it is possible to consider that in any point of this layer local equality of temperatures of the solid remainder and gas penetrating through it is observed.

Proceeding from this, we will derive the heat-conduction equation for the carbonized layer. Let us separate in the carbonized layer an elementary section dx (Fig. 6.8), limited by control planes normal to

the directions of propagation of gas and heat flow. For the positive direction of coordinates we will take the direction of motion of the pyrolysis front. Into the examined element through a unit area on the left there enters per unit time on account of thermal conduction a quantity of heat

$$q_1 = -\lambda_{пр} \frac{\partial T}{\partial x}.$$

In the same time through the control surface from the right by means of thermal conduction there is removed a quantity of heat

$$q_2 = -\lambda \frac{\partial T}{\partial x} + \frac{\partial}{\partial x}\left(-\lambda \frac{\partial T}{\partial x}\right) dx.$$

Together with gases proceeding to the examined element from the right, a quantity of heat is introduced equal to

$$q_3 = c_t \dot{m}_S \bar{\chi}\left(T + \frac{\partial T}{\partial x} dx\right).$$

Gases emanating from the element through the left control surface carry off with them a quantity of heat equal to

$$q_4 = c_t \dot{m}_S \bar{\chi} T.$$

The change of heat content of the element for the same time is equal to

$$\Delta q = c_{пр} \rho_{пр} dx \frac{\partial T}{\partial t},$$

where $\rho_{пр}$ – given density of the layer taking into account the gas filling the pores; $c_{пр}$ – given heat capacity of the porous layer taking into account heat capacity of the gas.

Equation of heat balance of the separated element will be written as

$$\Delta q = q_1 - q_2 + q_3 - q_4,$$

or after substitution and reduction by dx

$$c_{пр} \rho_{пр} \frac{\partial T}{\partial t} = \lambda_{пр} \frac{\partial^2 T}{\partial x^2} + c_t \dot{m}_S \bar{\chi} \frac{\partial T}{\partial x}. \qquad (6.74)$$

Dividing both parts of the equality by $c_{пр}\rho_{пр}$, we obtain the heat-conduction equation of the carbonized layer

$$a_{пр}\frac{\partial^2 T}{\partial x^2} = \frac{\partial T}{\partial t} - \dot{m}_s \varkappa \frac{\partial T}{\partial x}, \qquad (6.75)$$

where $a_{пр} = \frac{\lambda_{пр}}{c_{пр}\rho_{пр}}$ – given coefficient of temperature transfer of the carbonized layer;

$$\varkappa = \bar{\chi}\frac{c_r}{c_{пр}\rho_{пр}}.$$

For solution of the obtained equation the boundary conditions are used:

a) on the pyrolysis front of the fiberglass

$$-\lambda_{пр}\left(\frac{\partial T}{\partial x}\right)_s = -\lambda_s\left(\frac{\partial T}{\partial x}\right)_s + \dot{m}_s \beta Q_s, \qquad (6.76)$$

where β – relative amount of binder in material.

b) on the internal surface of the wall

$$-\lambda_{пр}\left(\frac{\partial T}{\partial x}\right)_{св} = (\alpha - \eta_q \bar{\chi}\dot{m}_s c_r)(T_0 - T_{св}), \qquad (6.77)$$

where α – coefficient of heat transfer from gases to wall of the engine neglecting the blow of gases on the boundary layer.

System of equations (6.75), (6.76), (6.77) and (6.71), describing the process of carbonization of the covering, is solved on an electronic digital computer with the use of the finite-difference method or with the aid of analog devices.

During removal of carbonized material from the surface of the covering the system examined above should be augmented by an equation which describes the process of removal.

Let us consider the case of a stabilized process, when speed of removal of material from the surface equal to speed of advance of the pyrolysis front into the depth of the undecomposed plastic. The heat-conduction equation of the carbonized layer takes the form:

$$a_{пр}\frac{\partial^2 T}{\partial x^2} = -\dot{m}_s \varkappa \frac{\partial T}{\partial x}. \qquad (6.78)$$

In equation (6.76) the first member in the right part, which is heat flow fed from the pyrolysis front to the depth of the covering, during a stabilized process according to equation (6.59) is equal to

$$-\lambda_g\left(\frac{\partial T}{\partial x}\right)_s = \dot{m}_g c_{ga}(T_s - T_M).$$

Hence

$$-\lambda_{np}\left(\frac{\partial T}{\partial x}\right)_s = \dot{m}_g c_{ga}\left(T_s - T_M + \beta\frac{Q_g}{c_{ga}}\right). \tag{6.79}$$

We designate

$$T'_s = T_M - \beta\frac{Q_g}{c_{ga}}.$$

Consequently:

$$-\lambda_{np}\left(\frac{\partial T}{\partial x}\right)_s = \dot{m}_g c_{ga}(T_s - T'_s). \tag{6.80}$$

Passing from partial derivatives to full, inasmuch as the only variable is coordinate x, twice integrating equation (6.78), we obtain:

$$T = -\frac{1}{b}C_1 e^{-bx} + C_2 \tag{6.81}$$

where

$$b = \frac{\dot{m}_g c_{ga}}{a_{np}}.$$

We find the constant of integration.

At x = L

$$\left|\frac{dT}{dx}\right|_s = C_1 e^{-bL} = -\frac{\dot{m}_g c_{ga}}{\lambda_{np}}(T_s - T'_s). \tag{6.82}$$

Whence

$$C_1 = -\frac{\dot{m}_g c_{ga}}{\lambda_{np}}(T_s - T'_s)e^{bL}. \tag{6.83}$$

At x = 0

$$T = T_{ca} = -\frac{C_1}{b} + C_2 \tag{6.84}$$

Hence

$$C_2 = T_{cs} - \frac{c_{ns} a_{np}}{\lambda_{np}^{x}} (T_s - T_s') e^{bL}. \tag{6.85}$$

After substitution of constants of integration, the equation of the temperature field of the form:

$$T = T_{cs} - \frac{c_{ns} a_{np}}{\lambda_{np}^{x}} (T_s - T_s') e^{bL} (1 - e^{-bx}). \tag{6.86}$$

Considering x = L, T = T_s, we solve the obtained equation with respect to thickness of the carbonized layer:

$$L = \frac{a_{np}}{\dot{m}_s^{x}} \ln \left(1 + \frac{\lambda_{np}^{x}}{c_{ns} a_{np}} \frac{T_{cs} - T_s}{T_s - T_s'} \right). \tag{6.87}$$

Value T_{CB} will be determined from condition:

$$\left| \frac{dT}{dx} \right|_{cs} = C_1.$$

Putting in value C_1 and using boundary condition (6.77), we obtain:

$$(T_s - T_s') e^{bL} = \frac{1}{\dot{m}_s c_{ns}} (\alpha - \eta_q \dot{m}_s \bar{\chi} c_r)(T_0 - T_{cs}). \tag{6.88}$$

Inasmuch as according to equation (6.87)

$$e^{bL} = 1 + \frac{\lambda_{np}^{x}}{c_{ns} a_{np}} \frac{T_{cs} - T_s}{T_s - T_s'},$$

putting this value in equation (6.88) and solving the latter relative to T_{CB}, we obtain:

$$T_{cs} = \frac{T_0 \left(\frac{\alpha}{\dot{m}_s c_{ns}} - \frac{\eta_q \bar{\chi} c_r}{c_{ns}} \right) - T_s \left(1 - \frac{\lambda_{np}^{x}}{c_{ns} a_{np}} \right) + T_s'}{\frac{\alpha}{\dot{m}_s c_{ns}} - \frac{\eta_q \bar{\chi} c_r}{c_{ns}} + \frac{\lambda_{np}^{x}}{c_{ns} a_{np}}}. \tag{6.89}$$

Measurements of temperatures, performed by means of low-inertia thermocouples in a covering made from asbestos-phenol plastic during bench tests of RDTT, showed that in the range α = 4.9-5.9 kcal/m^{2}s temperature on the surface of the carbonized layer attains $T_{CB} \approx 1700°C$ and on the pyrolysis front $T_s \approx 600°C$ [36].

With growth of thickness of the carbonized layer, flow friction to the gas flow increases, moving through pores to the surface of the

covering. This also promotes gradual packing of the carbonized material near the surface due to deposition in pores of atomic carbon, given off during decomposition of gaseous hydrocarbons. Over the thickness of the carbonized layer considerable pressure drops appear which can attain several atmospheres. The value and sign of stresses in the carbonized material are determined by the relationship of forces of internal and external pressures:

$$\sigma = (p + \Delta p)\frac{n}{1-n} - p\frac{1}{1-n},$$

where p – external pressure (in gas flow); Δp – pressure drop in thickness of the carbonized layer; n – relative area of pores. At high external pressure (rocket chamber) in the material negative stresses (compression) will predominate. Under conditions at the outlet socket of the nozzle at low pressures in the flow, commensurable with value Δp, phenomena of breakaway of the carbonized layer are possible. Furthermore, in all cases of destruction of the carbonized layer, tangential frictional forces participate which effect the surface of the covering.

§ 6.10. Heat Shielding of the Nozzle of an RDTT

The nozzle is subject to the greatest heat stresses of the construction of an RDTT. In specially rugged conditions there are layers of material near the nozzle throat. Here are combined high intensity of heat transfer and strong mechanical influence of the gas flow on the surface of the nozzle. During prolonged action of these factors and insufficient stability of the material the high point of the critical section moves foreward accompanied by a chop of pressure and thrust of the engine, and in certain cases even damping of the charge. It follows from this that the basic requirement for the material and construction of a nozzle is safeguard of high heat-erosion stability.

In an engine with a short time of work, conditions of heating of the wall of the nozzle is knowingly nonstationary, and the temperature of the surface of metal in the region of the critical section remains considerably lower than the combustion temperature of the fuel.

It is considered that the nozzle for an engine with a short time of work is best prepared from a low-carbon steel, a noncritical material which possesses, as compared to heat-resistant steels, higher (2-3 times) heat conduction and due to this it ensures good erosion stability of nozzles.

For an engine with a long time of work the nozzle is usually assembly consisting of separate sections or components made from various materials. Since in such an engine the surface of the nozzle in the critical section in the process of work obtains a temperature close to stagnation temperature of the gas flow T_0, the nozzle throat is fulfilled in the form of an insert made from heat-resistant material with sufficient resistivity to thermal shock, chemical and mechanical influences.

These materials can be divided into three groups: 1) different forms of graphite, 2) heat-resistant metals, 3) ceramic materials.

Of the different forms of graphite, the most useful for manufacture of nozzle inserts is considered to be pyrolytic graphite or pyrographite [37]. Pyrolytic graphite differs from the usual kind by considerable thermal anisotropy: heat conduction of the material across layers of crystals can be 50-1000 times less than heat conduction along layers. At the same time pyrographite possesses the same high temperature of sublimation as usual graphite (~3500°C). Pyrographite possesses raised density (up to 2.22 g/cm^3) and high tensile strength at high temperatures, and also differs from usual graphite by greater stability to erosion and corrosion. Basic characteristics of pyrographite depending on temperatures are given in Table 6.9 [37].

For use of thermal insulation properties of pyrographite it is necessary that its layers be parallel to the flow of gases. A characteristic peculiarity of this variant is high temperature of the internal surface of the insert. After sharp accretion during the first seconds of work of the engine it then changes very little, remaining close to the temperature of combustion products. Due to the low heat conduction across layers in the thickness of the insert, very high temperature gradients appear (up to 700-800°C per 1 mm of thickness). This permits one in certain cases to combine an insert made from pyrographite with the carrier element of the construction made from light but not thermoresistant material (aluminum, plastic). In all cases the necessary thickness of the insert, guaranteeing its external surface temperature allowed for material of the carrier construction, may be calculated by the method expounded in § 6.7. Due to high thermal conduction of pyrographite in an axial direction, during heating there is a temperature equalization over the length of the insert, so that drops of temperature in the thickness of the insert for all cross sections turn out to be approximately identical. Therefore, inasmuch as the value of the coefficient of heat transfer versus length of the insert can change within considerable limits, calculation of heating of the insert should be conducted by proceeding from the average lengthwise value of α, examining a change of temperature in the material only in the transverse direction.

An essential deficiency of articles made from pyrographite is the presence of residual stresses which appear during cooling of the article after manufacture, which in unfavorable conditions can lead to destruction of insert.

Stability of graphite to erosion influences sharply increases upon introduction of silicon in its structure. This operation is called siliconizing of graphite [38], [39].

Heat-resistant metals for nozzle inserts possess high a melting point and high thermal conduction ($\lambda \approx 0.039$-0.025 kcal/ms°C). Of them the most wide-spread are molybdenum and tungsten (Table 6.3). These materials preserve high strength during heating, for example the tensile strength of molybdenum at 1100°C is 2100 kg/cm^2. A combination of high thermal conduction with good strength characteristics and a low linear coefficient of temperature lengthening

Table 6.9

Temperature °C	Coefficient of heat conduction, $\lambda \cdot 10^3$ kcal/ms°C		Specific heat, kcal/kg°C	Linear coefficient of temperature lengthening $1/°C \cdot 10^3$		Tensile strength, extension, kgf/mm²	
	a)	b)		a)	b)	a)	b)
21	89,0	0,447	0,23	0,05	0,09	4,92— 9,84	0,369
260	84,8	0,367	0,30	0,10	6,7	4,92— 9,84	0,323
537	70,3	0,330	0,38	0,25	13,4	4,92— 9,84	0,274
815	53,8	0,295	0,45	0,51	20,0	4,92— 9,84	0,218
1093	—	—	0,51	1,10	26,8	5,27—10,2	0,158
1649				2,8	40,0	5,98—11,6	0,088
2205				4,3	53,6	7,73—14,75	0,056
2761				6,6	67,0	8,43—23,9	0,140

a) in a longitudinal direction;
b) in a transverse direction.

(for Mo $\sim 5.4 \cdot 10^{-6}$ 1/°C) ensures high stability of these materials against thermal shock. However these metals are easily oxidized at raised temperatures, which hampers their use in the presence in combustion products of a solid fuel of chemically active components. During oxidation of molybdenum MoO_3, a volatile compound, which after formation immediately departs from the surface, in consequence of which the metal burns with a certain constant speed [23]. To ensure stability of metals against the influence of chemically active components it is considered expedient to apply coverings containing boron nitride, which is inclined to self-restoration at raised temperatures [24].

Of other deficiencies of materials of this group one should note their high specific gravity (for molybdenum – 10.2 g/cm³, for tungsten – 19.3 g/cm³).

At present constructions are known of nozzles with a tungsten covering, which is deposited on the surface of the base material in melted form with the aid of an electric arc [40].

Ceramic nozzle inserts, used at present, are not considered promising to to their fragility and sensitivity to thermal shock. An ideal solution, apparently, should consist in combining materials with high heat-resistance with metals which possessing great mechanical strength.

It is noted that as a basis for new fireproof compositions one can use carbides of hafnium and tantalum with a melting point of 4150°C [23].

With the growth of power characteristics of solid rocket propellants, accompanied by an increase of combustion temperature, presently known heat-resistant materials become less and less useful, because the melting point approaches the temperature of the gas flow. Furthermore, their ability to resist erosion drops in view of the steady growth of contents in gases of condensed particles and products

of dissociation with high chemical activity.

Preservation of the efficiency of nozzles in these conditions can be attained by application of external or internal cooling.

External cooling is ensured by a refrigerant, between the nozzle and its surrounding jacket. The nozzle is prepared from refractory material with high thermal conduction. As refrigerants metals with low melting and boiling points can be used. During work of the engine the refrigerant is melted and is brought to the boiling point. Vapor of the refrigerant emerges through special holes. After the beginning of boiling the temperature of the wall is preserved constant, equal to the boiling point of the refrigerant. Cooling of the nozzle is ensured by absorption of great quantities of heat during evaporation of the refrigerant. The allowed time of work of the nozzle is determined only by the presence of the necessary quantity of refrigerant.

In Table 6.10 are given heat-physical characteristics of fusible metals [11]. According to the table the most useful for the examined goal are aluminum, lithium and magnesium, for which an acceptable boiling point is combined with a very high heat of evaporation.

Table 6.10

Metals	Fusion		Boiling	
	specific heat, kcal/kg	temperature, °C	specific heat, kcal/kg	temperature, °C
Aluminum.....	9.3	658	2228	1800
Potassium.....	14.7	62.3	511.5	760
Lithium.....	32.8	186	2540	1200
Magnesium.....	70	651	2574	1100
Sodium.....	27.5	97.5	1015	880
Tin.....	14.4	231.8	271	2260
Lead.....	6.32	327.5	203	1620
Zinc.....	24.09	419.4	425	907

When selecting a refrigerant in terms of boiling point, it is necessary to take into account that with a lowering of temperature of the wall of the nozzle the quantity of heat transmitted to the wall increases and consequently also the necessary quantity of refrigerant. Furthermore, at a very low temperature of the wall of the nozzle, on it there can be condensed vapor of different mixtures to the fuel.

Liquid metals possess a very high thermal conduction, which ensures intense heat exchange on the external surface of the nozzle.

It is necessary to note that inasmuch as for liquid metals the values of the Prandtl number are very small (Pr = 0.005-0.03), heat conduction is a predominant factor in heat transfer from the wall to the liquid.

Effectiveness of such a method of heat shielding was proven by experiments with a nozzle made from molybdenum with wall thickness 1.5 mm during use of magnesium as a refrigerant. Walls of the nozzle, washed from within by a flow of gases with stagnation temperature T_0 = 3350°C for 60-80 s preserved a temperature equal to the boiling point of magnesium - 1100°C [41].

Internal cooling of the nozzle is carried out by feeding the refrigerant into the subsonic part of the nozzle. The shroud of colder gas forming at the wall, moving together with the basic flow, protects the surface of the critical section from thermal and chemical influences of products of combustion. The protective gas shroud can be created by products of ablation of the covering of the subsonic part of the nozzle [42]. Effectiveness of the heat shield will be determined by the mass speed of ablation and parameters of products of ablation. In work [43] results are given of tests of tungsten nozzle inserts during installation on the input in a nozzle of protective rings made from different ablating materials. Tests were conducted in an engine of gauge 305 mm working on a combined fuel with combustion temperature 3300°C. In Table 6.11 are indicated values of relative increase of the throat area due to climax when the duration of work of the engine in 17 s. Full absence of climax is obtained during use of a protective ring made from polyethylene a material with the highest speed of ablation. On the graph (Fig. 6.9) values are given of temperature on the internal surface of the nozzle insert, calculated by indications of two tungsten - tungsten-rhenium thermocouples, built in the insert at different distances from the internal surface.

Table 6.11

Material of protective ring	Increase of throat area, %
Polyethylene.....	0
Polyvinyl chloride + potassium sulfate.....	3.6
Graphite + phenolic resin.....	9.0
Without protective ring.....	9.8

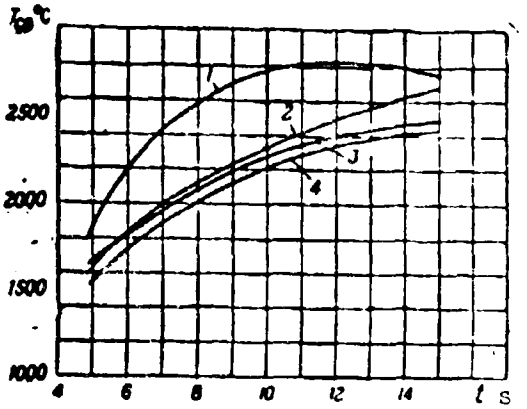

Fig. 6.9. Change of temperature on the internal surface of a tungsten insert in time: 1 – without protective ring; 2 – with ring made from graphite and phenolic resin; 3 – with ring made from polyvinyl chloride and potassium sulfate; 4 – with ring made from polyethylene.

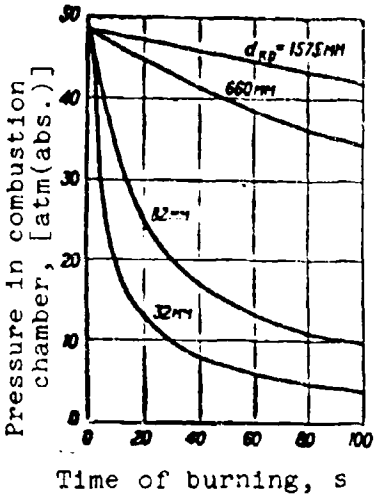

Fig. 6.10. Influence of critical throat diameter on change of pressure in an RDTT during climax of the nozzle.

In the opinion of certain researchers, one of the promising directions is application of nozzles with allowed climax of critical section made wholly from plastic [44]. As follows from Fig. 6.10 [45], the influence of climax of the critical section of a nozzle on pressure in the engine decreases according to growth of $d_{кр}$ and with a very large diameter it is relatively small. Furthermore, the influence of climax of the critical section can be compensated by an increase of the surface of burning (application of charges of progressive form). This makes possible the use of nozzles with allowed and precalculated climax in an engine with large diameters of critical sections of the nozzle. In the opinion of supporters of this direction, application of a one-piece plastic construction of a nozzle simplifies manufacture, control of the technological process and considerably increases reliability of work of the engine.

Literature

1. Mikheyev M. A. Osnovy teploperedachi (Fundamentals of heat transfer). Gosenergoizdat, M., 1949.

2. Greenfield S. J. Aeronaut. Sci, 18. 512, 1951.

3. Vitte A., Kharper E. Eksperimental'noye issledovaniye teplootdachi v soplakh raketnykh dvigateley (Experimental investigation of heat transfer in nozzles of rocket engines). "Raketnaya tekhnika", 1963, No. 6.

4. Uimpress R. N. Vnutrennyaya ballistika porokhovykh raket (Internal ballistics of solid-propellant rockets). Izd. inostr. lit., 1952.

5. Bartz, D. R. A simple equation for rapid estimation of rocket nozzle convective heat transfer coefficients. Jet Propulsion, 21, 1957.

6. Zel'dovich Ya. B., Rivin M. A., Frank-Kamenetskiy D. A. Impul's reaktivnoy sily porokhovykh raket (Reaction force pulse of solid-propellant rockets). Oborongiz, 1963.

7. Bakhtiozin R. A., Gorbis Z. R. Eksperimental'noye issledovaniye konvektivnoy teplootdachi zapylennykh potokov (Experimental investigation of convection heat transfer of powerded flows). Materialy Soveshchaniya po teplo-massoobmenu. Minsk, 1961.

8. Khottel' Kh. K. Inzhenernyye raschety luchistogo teploobmena (Engineering calculations of radiant heat exchange). "Turbulentnyye techeniya i teploperedacha". Sb. statey. Izd. inostr. lit., 1963.

9. Lykov A. V. Teoriya teploprovodnosti (Theory of heat conduction). Gostekhteorizdat, 1952.

10. Ivantsov G. P. Nagrev metalla (Metal heating). Metallurgizdat, M., 1948.

11. Spravochnik mashinostroitelya (Machine builder's handbook). T. 2. Mashgiz, M. 1956.

12. Serebryakov M. Ye. Vnutrennyaya ballistika stvol"nykh sistem i porokhovykh raket (Internal ballistics of trunk systems and solid-propellant rockets). Oborongiz, 1962.

13. High Strength steels for the missile industry. Published by the American Society for Metals, 1961.

14. Sherer R., Oppengeym R. Materialy, primenyaemyye v raketostroyenii (Materials used in rocket construction) "Voprosy raketnoy tekhniki", 1961, No. 9.

15. "Aviation Week", 1962, No. 9, 10. "Missiles and Rockets", 1961, vol. 8, No 8.

16. Plastmassy v raketnoy tekhnike (Plastics in rocket technology). "Voprosy raketnoy tekhniki", 1961, No. 7, 8.

17. "Interavia" 1962, No. 5101. "Aviation Week". 1962, No. 11.

18. Varrer M., Zhomott A., Vebek B. F., Vandenkerkkhove Zh. Raketnyye dvigateli (Rocket engines). Oborongiz, 1962.

19. Kiselev B. A. Stekloplasty – material budushchego (Fiberglass – material of the future). Izd-vo AN SSSR, 1959.

20. Besserer K. U. Inzhenernyy spravochnik po upravlyaemym snaryadam (Engineering reference book on guided missiles). Voyenizdat, 1962.

21. Guppert P. Novyye vidy keramicheskikh pokrytiy (New forms of ceramic coatings). "Voprosy raketnoy tekhniki", 1959, No. 7.

22. Barilett E. P. Thermal Protection of Rocket – Motor Structures. "Aerospace Engineering", 1963, No. 1.

23. Problemy vysokikh temperatur v aviatsionnykh konstruktsiyakh. Sb. statey (Problems of high temperatures in aviation constructions Collection of articles). Izd. inostr. lit., 1961.

24. Mekkel'burg E. Metallokeramicheskiye mnogosloynyye pokrytiya dlya raketnoy tekhniki (Cermet multilayer coverings for rocket technology). "Voprosy raketnoy tekhniki", 1962, No. 5.

25. "Missiles and Rockets", 1963, vol. 13, No. 1, 2, 5.

26. Yaffee M. Paint Gives Missiles Thermal Protection. "Aviation Week", 1959, No. 23.

27. Mezhkontinental'nyy ballisticheskiy snaryad "Minitmen" firmy "Boing". Obzor. (Intercontinental ballistic missile "Minuteman" of the "Boeing" firm Survey). "Boprosy raketnoy tekhniki", 1963, No. 6.

28. Yekhter M., Meyer E. Voprosy teploprovodnosti (Questions of thermal conduction). "Turbulentnyye techeniya i teploperedacha". Sb. statey. Izd. inostr. lit., 1963.

29. Zarubin V. S. Raschet nagreva dvukhsloynoy metallicheskoy plastiny (Calculation of heating of two-layered metallic plates). "Nekotoryye voprosy mekhaniki". Sb. statey pod red. prof. Feodos'eva B. I. Oborongiz, 1962.

30. Grover I. H., Holter W. H. Solution of the Transient Heat-Conduction Equation for an Insulated, Infinite Metal Slab. "Jet Propulsion", 1957, m. 27, No. 12.

31. Fledderman. Teploperedacha k poverkhnosti, podvergayushcheysya abiyatsii (Heat transfer to surface undergoing ablation). "Voprosy raketnoy tekhniki", 1960, No. 3.

32. Skala S., Gil'bert L. Teplovoye razrusheniye teplozashchignogo obuglivayushchegosya plastika pri giperzvukovykh poletakh (Heat distortion of heat shielding of carbonized plastic during hypersonic flights). "Raketnaya tekhnika", 1962, No. 6.

33. Bicher N., Rozensveyg R. Mekhanizm ablyatsii plastmass s neorganicheskim armirovaniyem (Mechanism of ablation of plastics with inorganic reinforcing). "Raketnaya tekhnika", 1961, No. 4.

34. Dushin Yu. A. Skorost' razlozheniya (goreniya) polimerov v vysokotemperaturnoy gazovoy srede (Speed of decomposition (burning) of polymers in a high-temperature gaseous environment). "Inzhenerno-fizicheskiy zhurnal", 1961, No. 10.

35. Zel'dovich Ya. B., Frank-Kamenetskiy D. A. Teoriya teplovogo rasprostraneniya plameni (Theory of thermal propagation of flames). "Zhurnal fizicheskoy khimii", t. XII vyp. 100, 1938.

36. High – Speed Thermocouples – Seabrook Hull. "Advanced Materials", 1960, No. 6.

37. Baratta F. Piroliznyy grafit i ego primeneniye (Pyrolysis of graphite and its application). "Raketnaya tekhnika", 1962, No. 1.

38. Yaffee M. Pyrolytic Graphite Sudied for Re-Entry. "Aviation Week", 1960, No. 4, p. 73.

39. Pyrographite May Cut Nose Cone Heat. "Aviation Week", 1959, No. 23, p. 71.

40. "Aviation Week", 1959, No. 13, p. 69.

41. "Missiles and Rockets", 1961, No. 10, p. 31.

42. Gustavson Dzh. Konferentsiya amerikanskogo raketnogo obshchestva po raketnym dvigatelyam na tverdom toplive (Conference of American rocket society for fuel rocket engines). "Voprosy raketnoy tekhniki", 1962, No. 11.

43. Makaleksander R., Donal'dson V., Robinson A. Sravneniye intensivnosti teploperedachi i erozii vo vremya raboty sopel s zashchitnymi kol'tsami i bez nikh (Comparison of intensity of heat transfer and erosion during work of nozzles with protective rings and without them). "Raketnaya tekhnika", 1962, No. 8.

44. Makelister L., Uolker A., Roy P. Razrabotka i razvitiye razrushayushchikhsya materialov dlya sopel raketnykh dvigateley (Design and development of destructible materials for nozzles of rocket engines). Ch. I. "Boprosy raketnoy tekhniki", 1964, No. 3.

45. Khorcher Kh., Mitchel B. Razrabotka razrushayushchikhsya materialov dlya sopel raketnykh dvigateley (Development of destructible materials for nozzles of rocket engines). Ch. II. "Boprosy raketnoy tekhniki", 1964, No. 3.

CHAPTER VII

HEAT EXCHANGE BETWEEN THE ATMOSPHERE AND ROCKET BEFORE STARTING THE ENGINE

During exploitation of rockets, and also during adjustment and tests of [RDTT] (РДТТ), cases are possible when the initial temperature of the rocket charge considerably differs from the temperature of the ambient air. Duration of the process of temperature balance is defined as the conditions of heat exchange between the surface of the rocket and the air and thermal conduction of the body of the rocket and the charge.

During investigation of heat exchange between the air and the charge we usually pursue the following target:

1. To determine the time necessary for establishing a temperature equilibrium.

2. To set the distribution of temperature in the charge for any intermediate instant if starting of the rocket is produced before establishing the temperature equilibrium.

Let us consider the possibility of an analytic solution of the problem on hand.

Subsequently for uniqueness cooling of the rocket charge is examined, however the expounded dependences with a change of sign can be used for calculation of heating of a cooled charge.

§ 7.1. Coefficient of Heat Transfer

The value of the heat flow per unit area of the external surface of a rocket engine is expressed by the formula

$$q = \alpha(T_{\text{п}} - T_{\text{A}}),$$

where T_A – temperature of ambient air; $T_п$ – temperature of engine surface; α – coefficient of heat transfer, which in turn can be

represented in the form

$$\alpha = \alpha_к + \alpha_p,$$

where $\alpha_к$ – coefficient of convection heat transfer; α_p – coefficient of heat transfer by radiation.

In calm air, transmission of heat to it from the rocket will be carried out by means of free convection. The coefficient of heat transfer from a cylindrical surface during free convection in thermotechnics is determined by the formula [1]

$$\alpha_к = \frac{22,7}{\sqrt{397 + 0,5(T_A + T_п)}} \sqrt[4]{\frac{T_п - T_A}{d_п}}, \qquad (7.1)$$

where $d_п$ – diameter of the article.

During motion of air, when transmission of heat is ensured by forced convection, the coefficient of convection heat transfer for transverse flow around the cylinder is determined from the criterial dependence [2]

$$Nu = CRe_f^n Pr^{1-n}, \qquad (7.2)$$

where $Nu = \frac{\alpha d_п}{\lambda_A}$ – criterion of Nusselt; Re_f – criterion of Reynolds; Pr_f – Prandtl number,

In formula (7.2) value C and n are selected depending on the interval in which is located value Re_f. Solving dependence (7.2) with respect to the coefficient of heat transfer, we obtain

$$\alpha = C\frac{\lambda_f}{d_п}\left(\frac{Wd_п}{\nu_f}\right)^n \cdot \left(\frac{\nu_f}{a_f}\right)^{1-n} = D\frac{W^n}{d^{1-n}} \text{ kcal/м}^2\text{ h °C},$$

where coefficient D includes physical parameters of the air λ_f, ν_f, a_f, determined at its average temperature near the cooled surface:

$$T_f = \frac{1}{2}(T_A + T_п).$$

The dependence of value D on T_f is relatively weak. Thus, during a change of T_f from 0 to 100°C value D when n = 0.6 is changed within limits of 8%. In the first approximation it is possible to consider that coefficient D does not depend on temperature and is determined only by value Re_f. Therefore for engineering calculations

in thermotechnics the following dependences are used [1]:

$$Wd_{\text{п}} < 0{,}8 \ \text{м}^2/\text{s}$$

$$\alpha_{\text{к}} = 3{,}475 \frac{W^{0{,}72}}{d_{\text{п}}^{0{,}28}} \ \text{kcal/m}^2\text{h} \ ^\circ\text{C} \qquad (7.3)$$

when

$$Wd_{\text{п}} > 0{,}8 \ \text{м}^2/\text{s}$$

$$\alpha_{\text{к}} = 3{,}645 \frac{W^{0{,}81}}{d_{\text{п}}^{0{,}19}} \ \text{kcal/m}^2\text{h} \ ^\circ\text{C} \qquad (7.4)$$

The coefficient of radiation heat transfer is calculated by the formula

$$\alpha_{\text{р}} = \frac{c}{T_{\text{п}} - T_{\text{A}}} \left[\left(\frac{T_{\text{п}}}{100} \right)^4 - \left(\frac{T_{\text{A}}}{100} \right)^4 \right] \ \text{kcal/m}^2\text{h} \ ^\circ\text{C} \qquad (7.5)$$

where c — radiation factor.

§ 7.2. Temperature Field of the Charge

The temperature field of a charge is determined by the solution of the differential heat-conduction equation of a solid fuel during assigned boundary conditions, which are initial distribution of temperature in the charge and the law of heat exchange between the body of the engine and the external surface of the charge.

In an engine with a fastened charge, transmission of heat from the charge to engine body is carried out by means of heat conduction. An exact solution can be obtained by the usual methods which are used for calculation of thermal conduction of multilayer articles. A simplified approach to the solution of this problem assumes two cases:

1. The body of the engine is made from material with a high thermal conduction as compared to the fuel.

2. Thermal conduction of the body is approximately the same as the fuel. Adhesive covering (armoring) in both cases is examined as one whole with the charge.

The first case corresponds to the use of such materials as steel, titanium, aluminum alloys with thermal conduction 50-100 times exceeding the thermal conduction of the solid fuel. With such distinction of coefficients λ, taking into account also the small thickness of the wall of the engine, it is possible to consider that the temperature on the surface of the charge is equal to the temperature on the surface of the body, and calculation of thermal conduction of the fuel must be conducted at the rated value of the coefficient of heat transfer on the surface of the body.

The second case can take place during manufacture of body from plastic. Certain sorts of plastics by their heat-physical properties approach solid fuels. Besides, for simplification of calculations it is possible to examine the body as one whole with the charge.

Transmission heat from a freely inserted charge to an engine body is carried out mainly by free convection in the air layer between the charge and body. In the theory of heat exchange, calculation of free convection in a limited space reduces to calculation of thermal conduction of its filling medium with a certain equivalent coefficient of thermal conduction

$$\lambda_{экв} = \lambda\varepsilon_к,$$

where λ – normal coefficient of thermal conduction of medium (air); ε_K – coefficient of convection.

Coefficient ε_K when GrPr < 1000 is taken equal to 1, and at higher values of this product it is calculated by the formula

$$\varepsilon_к = A_0 \delta_з^{1/4} \cdot (\Delta T)^{1/4},$$

where ΔT – differnce of temperatures of charge and body; δ_3 – value of clearance; A_0 – coefficient depending on temperature of air.

During a change of air temperature from 0 to +50°C value A_0 is changed from 20.0 to 16.0.

Thus, and in the case of an engine with freely inserted charge, solution of the problem reduces to calculation of thermal conduction of a multilayer article with assigned conditions of heat exchange on the surface.

However even for the simplest cases of a fastened charge, an analytic solution of the problem of nonstationary thermal conduction is possible only for such forms as a solid cylinder or a cylinder with a central cylindrical channel.

These forms to one or another degree are approximated by such types of fastened charges as slot, a charge with channel of star-shaped profile and large thickness of the burning arch, and others.

Let us consider the solution of the problem of nonstationary thermal conduction for a hollow cylinder with assigned dimensions – with external radius R_H and channel radius R_{BH} with constant initial temperature over all the mass of the fuel T_H, which at some instant would be transferred to the atmosphere with constant temperature T_A. We will consider that temperature in separate points of the charge depends only on radius and time. The system of equations for this

case takes the form:

$$\left.\begin{aligned}
&\frac{\partial T}{\partial t} = a\left(\frac{\partial^2 T}{\partial r^2} + \frac{1}{r}\frac{\partial T}{\partial r}\right); \quad R_{вн} < r < R_н;\\
&T(r, 0) = T_н;\\
&-\lambda\frac{\partial T(R_н, t)}{\partial r} = \alpha\left[T(R_н, t) - T_A\right];\\
&-\lambda\frac{\partial T(R_{вн}, t)}{\partial r} = 0.
\end{aligned}\right\} \qquad (7.6)$$

The system of equations can be represented in dimensionless form, if one crosses to new variables and criteria:

$\theta = \frac{T - T_A}{T_н - T_A}$ – temperature simplex;

$Fo = \frac{at}{R_н^2}$ – Fourier criterion;

$Bi = \frac{\alpha R_н}{\lambda}$ – Biot criterion

$M = \frac{R_{вн}}{R_н}$;

$\bar{r} = \frac{r}{R_н}$.

Then

$$\left.\begin{aligned}
&\frac{\partial\theta}{\partial Fo} = \frac{\partial^2\theta}{\partial\bar{r}^2} + \frac{1}{\bar{r}}\frac{\partial\theta}{\partial\bar{r}}, \quad M < \bar{r} < 1;\\
&\theta(\bar{r}, 0) = 1;\\
&\frac{\partial\theta_н}{\partial\bar{r}} = Bi\theta_н;\\
&\frac{\partial\theta_{вн}}{\partial\bar{r}} = 0.
\end{aligned}\right\} \qquad (7.7)$$

The analytic solution of this system of equations, obtained in work [3], has the form

$$\theta = \sum_{i=1}^{\infty} exp(-Fo\delta_i^2)\cdot f_1(M, Bi, \delta_i)\cdot f_2(\bar{r}\delta_i, M\delta_i), \qquad (7.8)$$

where

$$f_1(M, Bi, \delta_i) = \frac{\pi Bi I_1(M\delta_i)\left[\delta_i I_1(\delta_i) - Bi I_0(\delta_i)\right]}{\left[\delta_i I_1(\delta_i) - Bi I_0(\delta_i)\right]^2 - \left(Bi^2 + \delta_i^2\right) I_1^2(M\delta_i)};$$

$$f_2(\bar{r}\delta_i, M\delta_i) = I_0(\bar{r}\delta_i)\, Y_1(M\delta_i) - Y_0(\bar{r}\delta_i)\, I_1(M\delta_i).$$

Here δ_i constitute consecutive positive values of roots (from $i = 1$ to ∞) of the transcendental equation

$$I_1(M\delta)[\delta Y_1(\delta) - BiY_0(\delta)] - Y_1(M\delta)[\delta I_1(\delta) - BiI_0(\delta)] = 0. \qquad (7.9)$$

In the above mentioned expressions I_0 and I_1 – Bessel functions of zero and first orders of the I kind, Y_0 and Y_1 – Bessel functions of the II kind.

Results of calculations by formula (7.8) are given in tables [4]. Tables of values $\Theta = f(Bi, Fo, r)$ are given in the appendix to the present book.

Example. To find the distribution of temperature in a cylindrical charge with assigned dimensions (R_H = 150 mm, R_{BH} = 90 mm) and initial temperature T_H = +20°C in two hours after holding in air with temperature T_A = -30°C when α = 12 kcal/m^{2}h °C.

Propellant properties:

$$\lambda = 0{,}18 \frac{\text{kcal}}{\text{m h °C}};$$

$$a = 0{,}32 \cdot 10^{-6}\ \text{м}^2/\text{ч} \quad [5];$$

$$Bi = \frac{\alpha R_н}{\lambda} = \frac{12 \cdot 0{,}15}{0{,}18} = 10;$$

$$Fo = \frac{at}{R_н^2} = \frac{0{,}32 \cdot 10^{-6} \cdot 2}{0{,}15^2} = 0{,}0284;$$

$$M = \frac{R_{вн}}{R_н} = \frac{0{,}09}{0{,}15} = 0{,}6;$$

$$T = T_A - \Theta(T_A - T_н) = -30 + 50\Theta$$

From tables for $M = 0.6$, $Bi = 10$, interpolating for $Fo = 0.0284$, we obtain values $\Theta = f(r)$ and by it calculate the value $T = f(r)$. Results of calculations are given in Table 7.1.

Table 7.1

$\bar{r}$	Θ	T°C	$r = R_н \bar{r}$, мм
1,0	0,281	−16,0	150
0,9	0,540	− 3,0	135
0,8	0,733	+ 6,7	120
0,7	0,841	+12,1	105
0,6	0,880	+14,0	90

§ 7.3. Influence of Nonuniform Charge Temperature On Ballistic Characteristics of an RDTT

In practice cases are possible when starting of an RDTT is produced before attaining a temperature equilibrium between the charge and environment. As will be shown below, with large dimensions of a charge and an initial drop of temperatures of several tens of degrees for achievement of equality of temperatures, from several hours to several days are required.

During constant hold of a rocket in atmospheric conditions at the starting position or on a launch installation, irregularity of the temperature of the charge can be caused by twenty-four hours oscillations of temperature of the air. The value of these oscillations depends on the season and climatic conditions. As an example we will indicate the fact that for the Soviet Union the daily amplitude of temperature of the air in the summer is changed from 6° in the northern European part (Teriberk) to 11° in Yakutiya and 16°C in the Turan-Kazakh Oblast (Nukus) [6]. In winter the daily oscillations of temperature are less than in the summer. For large charges the time of thermal relaxation (reconstruction of the temperature field) can be larger than the period of oscillations of temperature of atmospheric air, which leads to the appearance of a temperature gradient through the thickness of the arch of the charge.

The irregularity of temperature of a charge, a direct result of which is a change of unit burning rate through the thickness of an arch, changes the progression characteristic of a charge. Let us explain this in an example of a charge with channel of star-shaped section (Fig. 7.1 and 7.2) [7].

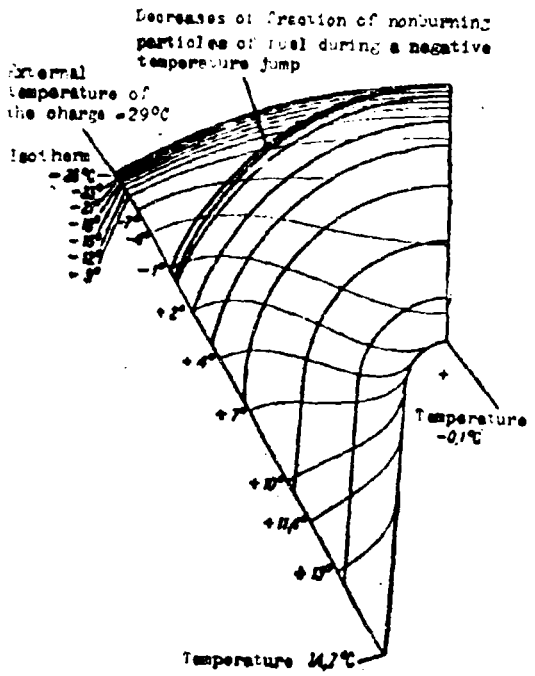

Fig. 7.1. Temperature field of charge with channel of star-shaped section during maximum difference of temperatures through the thickness of the arch.

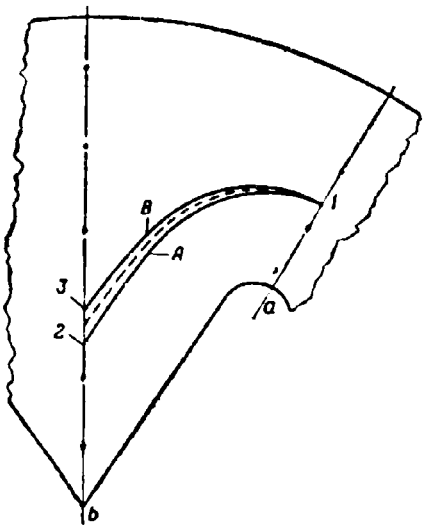

Fig. 7.2. Change of burning front on account of an irregularity of charge temperature.

At a temperature of a charge constant in all its thickness, the surface of burning in a certain arbitrary instant occupies the position depicted by a dotted line. At a temperature diminishing from the periphery to the center of a charge, due to a lag in the burning rate on central sections, the surface of burning after achievement of point 1 will occupy position A.

The surface of burning in this case will be larger than during equal distribution of temperatures, i.e., burning of the charge will become progressive, accompanied by a growth of pressure. Besides, part of degressive remainders of the charge will be increased.

Conversely, at a temperature growing to the center of a charge, burning on sections of the surface located nearer the center, will move ahead of burning on peripheral sections, in consequence of which during passage of the burning front through point 1 it will occupy position B, corresponding to a smaller value of the surface. Burning in this case will be degressive, with a drop of pressure in the engine, but with a decrease in the fraction of degressive remainders.

Calculation of ballistics of an engine with such a charge is complicated by the fact that for every instant the surface of burning must be split into small sections, within limits of which the burning rate is taken constant, corresponding according to expression (5.4) to the average temperature of the fuel on this section. Displacement of the front of burning on each of the sections during a small interval of time is considered to occur at a constant pressure normal to the initial position of this section.

For the end of the interval of time a new value of pressure in the engine is determined in accordance with the attained value of the surface of burning and with a new velocity of distribution of burning

over this surface. The interval of time is selected with the calculation that a change of temperature of the charge through the thickness of an arch during displacement of the front of burning for this interval will be 3÷5°C.

In Table 7.2 calculation data are given obtained for a charge of shown form with a diameter of 152 mm. It was accepted that ambient temperature T_A changes abruptly. Initial distribution of temperature was assumed uniform. Calculations were conducted for a drop of temperatures through the thickness of an arch which was the highest possible during the assigned difference $T_H - T_A$ (Fig. 7.2).

Table 7.2

	$T_A = -29°C$, $T_H = +21°C$		$T_A = +21°C$, $T_H = -29°C$	
	Design pressure of $T_H = +21°C$	Design pressure of $T_H = +21°C$	Design pressure of $T_H = +21°C$	Design pressure of $T_H = +21°C$
	p-70	p-115	p-70	p-115
Change of amount of degressive remainders of charge during a maximum drop of temperatures through the thickness of the arch	+ 7,90	+ 8,28	— 6,36	— 7,32
Change of time of burning in %	+41,5	+45,2	—39,5	—39,2

From the table it follows that the amount of the degressive remainders is increased at $T_H > T_A$ and decreases at $T_H < T_A$.

§ 7.4. Time of Equalization of the Temperature of the Charge and the Surrounding Medium

The process of change of the temperature field of a rocket charge during constancy of temperature of the air and the coefficient of heat transfer can be divided in time into three stages:

- stage of disordered process;
- stage of regular conditions;
- stage of thermal equilibrium.

At the first stage, distribution of heat in a charge carries to a well-known measure an accidental character, not connected with conditions of heat exchange and determined chiefly by the initial thermal state of the body.

At the second stage the influence of the initial thermal state weakens and the change of temperature for all points of the charge in time follows a simple exponential dependence. Here the natural log of excess temperature for any point of the charge will be changed

by a linear law.

At the third stage the temperature in all points of the charge is equal to ambient temperature. A similar regularity is observed during heating and cooling of bodies of different form [8].

In Fig. 7.3 empirical curves are represented for the dependence of θ on time for separate points of a cross-shaped charge MK-13, placed in a rocket engine with a diameter of 82.5 mm [5]. Value θ is in logarithmic scale. As it follows from the graph, upon the expiration of a certain period of time curves of lg θ pass in direct lines, located in parallel to one other, i.e., cooling of the charge follows regular conditions. Inasmuch as the surface layers of the charge in the beginning are cooled faster than the central ones, curves lg θ for them at the first stage are turned with convexity downwards. Conversely, for central points, curves lg θ are turned with convexity upwards. Duration of the initial stage of cooling is small and time of cooling is basically determined by the second stage.

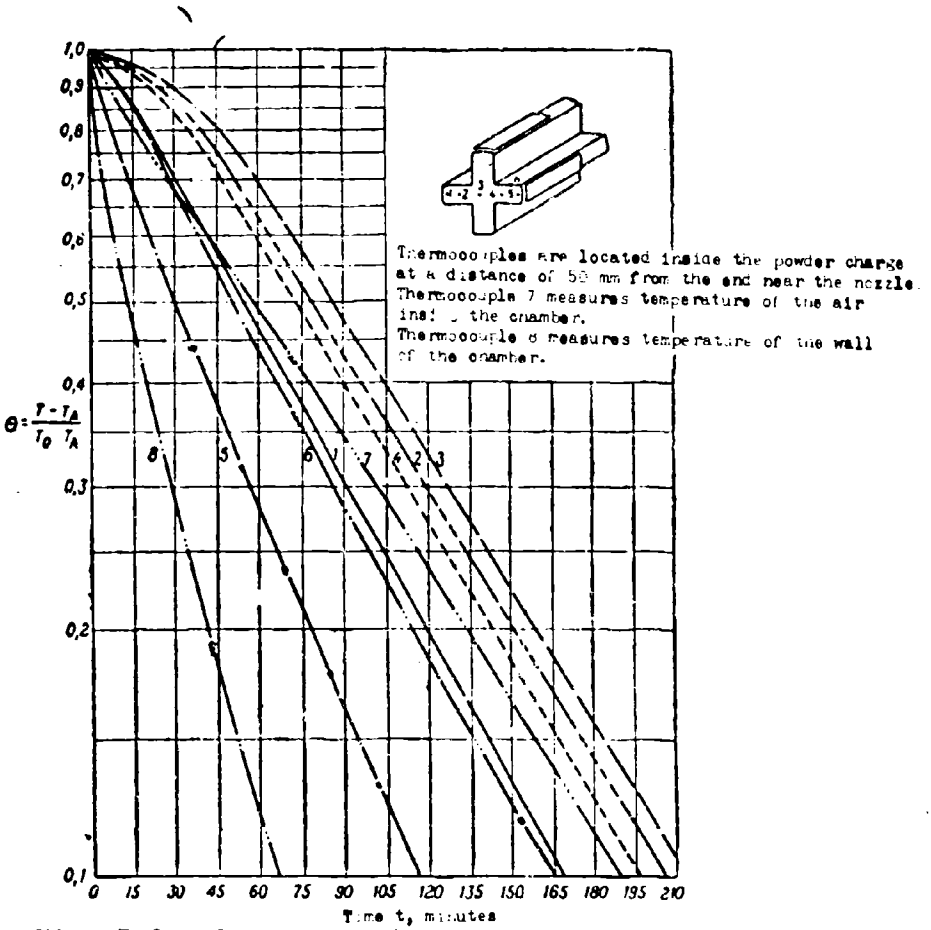

Fig. 7.3. Change of the logarithm of relative excess temperature in separate points of a cross-shaped charge in time.

In the case examined by us this regularity is revealed during analysis of solution (7.8). Inasmuch as every subsequent root of the characteristic transcendental equation (7.9) is considerably larger than the preceding:

$$\delta_1 < \delta_2 < \ldots < \delta_m$$

series (7.8) rapidly converges and, starting from a certain value of criterion Fo_1, value θ is determined by only the first member of the series, as compared to which all remaining members become vanishingly minute. Starting from the instant determined by value Fo_1, the relationship between excess temperature and time will be described simply by the exponential

$$\theta = f_1(M, Bi, \delta_1) f_2(\bar{r}, M, \delta_1) \exp(-Fo_1 \delta_1^2).$$

The angle of inclination of line $\ln \theta = f(t)$ will be determined by value

$$m = \frac{\partial \ln \theta}{\partial t},$$

which in thermotechnics is called the rate of cooling (heating) of an article. During regular conditions this value is identical for all points of the charge, and also for average temperature $\bar{T}$ over the charge.

Value m through average temperature is expressed in the following way:

$$m = \frac{\partial}{\partial t} \ln\left(\frac{T_A - \bar{T}}{T_A - T_H}\right) = -\frac{1}{T_A - \bar{T}} \frac{\partial \bar{T}}{\partial t}. \qquad (7.10)$$

The general equation of heat balance during regular conditions can be recorded in the form

$$c\omega \frac{d\bar{T}}{dt} = \alpha F (T_A - T_n). \qquad (7.11)$$

From equations (7.10) and (7.11) we obtain

$$m = \frac{\alpha F}{c\omega} \frac{T_A - T_n}{T_A - \bar{T}}. \qquad (7.12)$$

We designate

$$\psi = \frac{T_A - T_П}{T_A - \bar{T}}. \tag{7.13}$$

Coefficient ψ is called the criterion of irregularity of the tmperature field. During equal distribution of temperature in the charge $\psi = 1$. During the highest possible irregularity ($T_П = T_A$) $\psi = 0$.

Inasmuch as

$$\alpha = \frac{\lambda Bi}{R_ш}, \quad w = \delta W, \quad \frac{\lambda}{c\delta} = a, \tag{7.14}$$

then

$$m = \frac{aBi}{R_ш} \frac{F}{W} \psi. \tag{7.15}$$

Value ψ for a charge of arbitrary form can be defined by measurements of temperature in several points of a charge for two consecutive instants t_1 and t_2:

$$\psi = \frac{cw}{aF} \frac{\ln\theta_1 - \ln\theta_2}{t_2 - t_1}, \tag{7.16}$$

or, using dependence (7.14):

$$\psi = \frac{1}{aBi} R_ш R_ф \frac{\ln\theta_1 - \ln\theta_2}{t_2 - t_1},$$

where

$$R_ф = \frac{W}{F}.$$

Inasmuch as

$$\frac{at}{R_ш^2} = Fo,$$

then

$$\psi = \frac{1}{Bi} \frac{R_ф}{R_ш} \frac{\ln\theta_1 - \ln\theta_2}{Fo_2 - Fo_1}. \tag{7.17}$$

From the obtained dependence it follows that criterion ψ is determined by criterion Bi and form of the charge $\frac{R_ф}{R_ш}$, but does not depend on its absolute dimensions.

Dependence (7.17) permits one according to the data of a single epceriment to determine value ψ, true at Bi corresponding to the

condition of experiment for any charge of the same form geometrically similar to that with which the experiment was produced. Geometric similarity reduces to constancy of R_V/R_H.

For charges of tubular form

$$\frac{W}{F} = \frac{(1-M^2)R_H}{2}.$$

Consequently:

$$\psi = \frac{\ln\theta_1 - \ln\theta_2}{Fo_2 - Fo_1} \cdot \frac{1-M^2}{2Bi}. \qquad (7.18)$$

On the basis of formula (7.18) according to data of table $\theta = f(Bi, Fo, \bar{r})$ we calculated value ψ for values M represented in the table. Results of calculations are represented on the graph (Fig. 7.4). With an increase of Bi value ψ descend, where the faster it descends, the less the relative diameter of the channel.

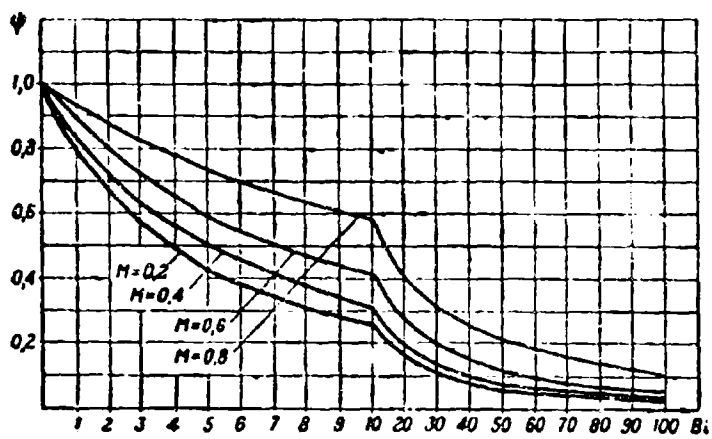

Fig. 7.4. Dependence of the criterion of irregularity of the temperature field ψ for a charge with a cylindrical channel on criterion Bi at M from 0.2 to 0.8.

Calculating by formula (7.15) the cooling rate of the charge, one can determine time τ, during which excess temperature in the point of the charge or average all over the charge) will be changed from θ_1 to θ_2:

$$\tau = \frac{1}{m} \ln \frac{\theta_1}{\theta_2}. \qquad (7.19)$$

Example. To determine the time necessary for setting in a slot charge made from a composite fuel an average temperature -27°C, if initial temperature of the charge is +15°C, and temperature of the ambient air -30°C with wind speed 10 m/s.

Dimensions of charge: D_H = 300 mm, d_{BH} = 60 mm.

Fuel on the basis of a copolymer of polybutadiene and acrylic acid (combustible-binder) and ammonium perchlorate has the following characteristics [9]; λ = 0.355 kcal/mh °C, δ = 1.65 × 10^3 kg/m^3, c = = 0.289 kcal/kg°C; a = 0.743 × 10^{-3} m^2/h.

1. Determination of the coefficient of heat transfer α.

Inasmuch as for the examined article when $d_П = D_H$ $Wd_П$ = 10 × × 0.3 = 3 m^2/s > 0.8, for calculation we use formula (7.4)

$$\alpha_к = 3{,}645\,\frac{10^{0{,}91}}{0{,}3^{0{,}19}} = 20{,}6\,\frac{\text{kcal}}{\text{m}^2\text{h}\,°\text{C}}.$$

The maximum value of the coefficient of radiation heat transfer for the beginning of cooling will be

$$\alpha_р = \frac{45}{15+30}\left[\left(\frac{288}{100}\right)^4 - \left(\frac{243}{100}\right)^4\right] = 3{,}39\,\frac{\text{k/cal}}{\text{m}^2\text{h}\,°\text{C}}.$$

The degree of blackness of full normal radiation is taken for aluminum paint equal to c = 45 [2].

Thus, the initial maximum value α_p does not exceed 15% of value α_K. With a fall of temperature of the surface value α_p sharply drops, therefore in calculations of it, it can be neglected.

Let us take $\alpha = \alpha_K$ = 30 kcal/m^2h °C.

2. Calculation of characteristic criteria:

$$Bi = \frac{\alpha R_п}{\lambda} = \frac{30\cdot 0{,}15}{0{,}355} = 12{,}75;$$

$$\frac{\theta_1}{\theta_2} = \frac{T_A - T_п}{T_A - T_з} = \frac{-30-15}{-30+27} = 15;$$

$$M = \frac{0{,}06}{0{,}30} = 0{,}2.$$

From the graph (Fig. 7.4) for a hollow cylinder at M = 0.2 and Bi = 12.75 we find ψ = 0.23.

3. Calculation of cooling rate.

For a hollow cylinder

$$\psi = \frac{2}{1 - M^2}.$$

Hence according to (7.15)

$$m = \frac{2aBi}{R_m^2 (1 - M^2)} \psi = \frac{2 \cdot 0{,}743 \cdot 10^{-4} \cdot 12{,}75}{0{,}15^2 (1 - 0{,}2^2)} 0{,}23 = 0{,}202 \frac{1}{h}.$$

4. Calculation of necessary time of cooling

$$\tau = \frac{1}{m} \ln \frac{\theta_1}{\theta_2} = \frac{1}{0{,}202} 2{,}303 \lg 15 = 13{,}4 \text{ h}$$

We will examine the change of time of cooling of a charge with an increase of guage with preservation of geometric similarity.

For the conditions accepted in the example, the calculation time of cooling of charges of different diameters is given in Table 7.3.

Table 7.3

d_m, mm	150	300	600	1200
τ, h	4,5	13,4	60,3	229

For one and the same charge, growth of coefficient α leads to an increase of the rate of cooling. However this increase is not infinite inasmuch as what follows from the graph (Fig. 7.4), with a growth of Bi there is a drop of the value of the coefficient ψ. In Fig. 7.5 is shown the dependence of the product $Bi\psi = f(Bi)$, entering in formula (7.15), calculated for a tubular grain at M = = 0.8. From the graph it is clear that, starting with Bi = 60, product Bi ψ remains practically constant. A similar regularity, observed for any form, is explained by the fact that, starting from a certain value α and corresponding to it Bi, the temperature of the surface layers of the charge approaches the temperature of the ambient air and any further increase of coefficient α at insignificant difference of temperatures ($T_A - T_П$) cannot ensure growth of the heat flow directed to the surface of the charge; consequently, an increase of the rate of change of temperature of the charge has its limits. In work [5] it is noted that according to experiment the cooling rate of a charge, 127 mm, of an aircraft rocket remains practically constant during a change of speed of the ambient air from 8 to 130 m/s.

In the same work are given experimentally determined values of the cooling rate for the charge Mk-13 in a rocket engine of diameter

82.5 mm under different conditions of cooling (see Table 7.4). As follows from Table 7.4, a change of wind speed from 0 to 8 m/s leads to growth of the cooling rate by one and a half times. However, application of such a strong cooling influence as submersion in water leads to further increase of the rate of cooling by a total of 14%.

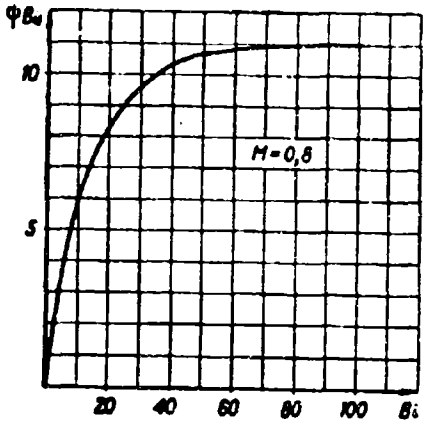

Fig. 7.5. Dependence of value ψBi on criterion Bi.

From a comparison of calculation data for fastened charges of tubular form with experimental data for charges of the same form freely inserted in the engine [5], it follows that under identical external conditions in the second case the cooling rate turns out to be 30-40% lower.

Table 7.4

Condition of cooling	Initial charge temperature T_H, °C	Ambient Temperature T_A, °C	Time corresponding to $\varphi=0,1$, τ, h	Cooling rate m, h^{-1}
Calm air	54	13	2,75	$2,33\cdot10^{-4}$
Wind with speed of 8 m/s	32—56	0—21	1,75*	$3,67\cdot10^{-4}$*
Cooling in water	60	0	1,33	$4,16\cdot10^{-4}$

*Average value

For fastened charges with a channel of complex configuration an approximate calculation of the cooling rate can be carried out by the forementioned graphs and dependences for a charge with cylindrical channel. For this it is necessary to determine the relative value of the internal radius of an equivalent hollow cylinder

$$M_0 = \sqrt{1 - \frac{S_T}{\pi R_H^2}},$$

where S_T – area of cross section of a charge of given form.

§ 7.5. Calculation of the Necessary Power of Electroheating of RDTT

The dependence of intraballistic parameters of an RDTT on temperature of the ambient air can be removed by application of heating devices which keeps the temperature of the charge at a certain constant level. Such a thermal insulation case with electric heaters located on its internal surface is used for regulating the temperature of the military rocket of the army of the United States "Honest John" during its transport on a cart and on the launcher (Fig. 7.6).

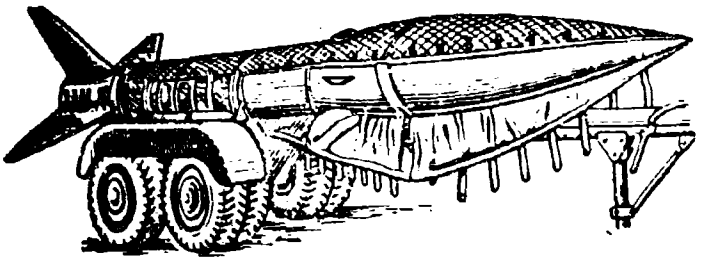

Fig. 7.6. Military rocket "Honest John" with heating case.

The calculation diagram of the electroheating case is represented in Fig. 7.7.

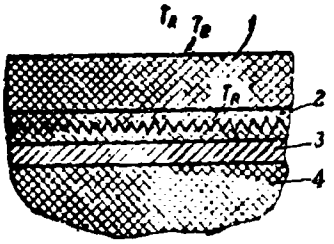

Fig. 7.7. Calculation diagram of electroheating: 1 – thermal insulation layer of case; 2 – heating layer of case; 3 – body of engine; 4 – charge.

During calculation of processes of stationary thermal conduction of cylindrical wall we usually use $q_{пог}$ kcal/mh – linear density of heat flow, inasmuch as q kcal/m^{2}h is a value, which varies in the direction of propagation of heat.

Let us define linear density of heat flow, directed from a heated layer to the external surface of the case. Let us assume that temperature of layer in which electric heaters are disposed is kept equal to T_R. Then

$$q_{пог} = \frac{2\pi\lambda}{\ln\frac{d_n}{d_R}}(T_R - T_n). \qquad (7.20)$$

where $d_П$ – external diameter of engine with case; d_R – diameter of engine with heated layer of case; λ – coefficient of thermal conduction of thermal insulation layer.

The linear thermal resistance of the case

$$r_1 = \frac{1}{2\pi\lambda} \ln \frac{d_П}{d_R}. \tag{7.21}$$

The drop of temperatures in the thermal insulation layer is equal to

$$T_R - T_П = r_1 q_{пог_1}. \tag{7.22}$$

Linear density of heat flow directed from the surface of case to the ambient air

$$q_{пог_2} = \alpha\pi d_2 (T_П - T_A). \tag{7.23}$$

whence external linear thermal resistance is equal to

$$r_2 = \frac{1}{\alpha\pi d_2}. \tag{7.24}$$

The external drop of temperature is equal to

$$T_П - T_A = r_2 q_{пог_2}. \tag{7.25}$$

Adding (7.22) and (7.25), we obtain:

$$T_R - T_A = r_1 q_{пог_1} + r_2 q_{пог_2}. \tag{7.26}$$

Using the condition of equality of heat flow $q_{пог_1} = q_{пог_2}$, we find

$$q_{пог} = \frac{1}{r_1 + r_2} (T_R - T_A), \tag{7.27}$$

or

$$q_{пог} = K_{пог} (T_R - T_A), \tag{7.28}$$

where $K_{пог}$ – linear coefficient of heat transfer, equal to

$$K_{пог} = \frac{\pi}{\frac{1}{\alpha d_п} + \frac{1}{2\lambda} \ln \frac{d_п}{d_R}}, \quad (7.29)$$

Losses of heat to the environment must be compensated by liberation of heat in resistors during passage of electrical current. According to the law of Joule-Lentz the quantity of liberated heat is equal to:

$$Q = 0{,}86IE = 0{,}86I^2R \frac{\text{kcal}}{\text{h}}, \quad (7.30)$$

where I – current intensity in A; E – voltage drop in V; R – total resistance of spirals, disposed on an area of case in 1 m^2, in Ω; 0.86 – thermal equivalent of one watt-hour.

Hence the required power of the source of electrical energy feeding the heating device should be:

$$N = \frac{Lq_{пог}}{0{,}86}, \quad (7.31)$$

where L – length of the engine.

Value N is calculated for the most unfavorable conditions (for the least value of temperature of air during the biggest wind speed).

During dense adjoining of the case to the surface of the engine temperature T_R can be taken equal to the supported temperature of the engine. For approximate determination of coefficient α neglecting radiation by formulas (7.3) and (7.4) it is not necessary to know the temperature on the surface of the case $T_п$.

As analysis shows, with a sufficient thickness of the thermal insulation layer the temperature on the surface of the case turns out to be close to the temperature of the ambient air. Besides, the amount of thermal radiation in total heat flow does not exceed several percent and it is possible to disregard it.

The time necessary for heating all the charge to the temperature of the temperature regulator if from the very beginning it is kept constant in the heated layer, it is determined only by dimensions of the charge and the coefficient of temperature transfer of the fuel. According to data of A. V. Lykov [12] the temperature field in a solid cylinder with constant temperature on its surface is practically leveled at Fo = 0.6-0.8. Hence the necessary time of heating of a fastened charge in the first approximation is defined as

$$\tau_н \approx 0{,}7 \frac{R_н^2}{a}.$$

Example. To determine the required power of the source of electrical energy for heat regulation of an engine of gauge 500 mm and length 6 m at a temperature of +20° C. As calculation conditions we take: $T_A = -40°C$, $W = 15$ m/s.

Dimensions of the case: $d_R = 520$ mm, $d_П = 570$ mm. For the thermal insulation layer (mineral wool) $\lambda = 0.040$ kcal/m × h °C.

1. We determine the coefficient of heat transfer.

Inasmuch as $Wd = 0.57 \times 15 = 8.55$ m/s > 0.8, the calculation is conducted by formula (7.4)

$$\alpha = 3{,}645\,\frac{15^{0.61}}{0{,}57^{0.19}} = 36{,}6 \text{ kcal/h °C}$$

2. External thermal linear resistance

$$r_2 = \frac{1}{36{,}6 \cdot 0{,}57} = 0{,}048 \text{ mh °C/kcal}$$

3. Internal thermal linear resistance

$$r_1 = \frac{1}{2 \cdot 0{,}040} \ln \frac{0{,}57}{0{,}52} = 1{,}145 \text{ mh °C/kcal}$$

4. Coefficient of heat transfer

$$K_{пог} = \frac{1}{0{,}048 + 1{,}145} = 2{,}63 \text{ kcal/mh °C}$$

5. Linear density of heat flow

$$q_{пог} = 2{,}63\,(20 + 40) = 158 \text{ kcal/mh}$$

6. Required power of power supply

$$N = \frac{158 \cdot 6}{0{,}86}\,10^{-3} = 1{,}1 \text{ kW}$$

Literature

1. Shubin Ye. L. Materialy, metody ustroystva i raschet teplovoy izolyatsii truboprovodov (Materials, methods of devices and calculation of thermal insulation of pipelines). Gosenergoizdat, M. L., 1948.

2. Mikheyev M. A. Osnovy teploperedachi (Fundamentals of heat transfer). Gosenergoizdat, M. L., 1949.

3. Garslaw H. S. Jaeger I. C. Conduction of Heat in Solids. Oxford University Press. London, 1948.

4. Geckler R. D. Transient, Radial Heat Conduction in Hollow Cylinders. Jet Propulsion, vol. 25, 1955, No. 1.

5. Uimpress R. N. Vnutrennyaya ballistika porokhovykh raket (Internal ballistics of solid-propellant rockets). Izd. inostr. lit., 1952.

6. Borisov A. A. Klimaty SSSR (Climates of the USSR). Uchpedgiz, M., 1959.

7. Fillips B., Tendzher G. Vliyaniye neravnomernoy temperatury porokhovoy shashki na ballisticheskiye kharakteristiki raketnogo dvigatelya tverdogo topliva (Influence of nonuniform temperature of a powder cartridge on ballistic characteristics of a solid-propellant rocket engine). "Raketnaya tekhnika", t. 32, 1962, No. 6.

8. Kondrat'yev G. M. Regulyarnyy teplovoy rezhim (Regular thermal balance). Gosteortekhizdat, M., 1954.

9. Medford Dzh. Izmereniye koeffitsienta temperaturoprovodnosti tverdykh topliv (Measurement of the coefficient of temperature transfer of solid fuels). "Raketnaya tekhnika", t. 32, 1962, No. 9.

10. Khizhnyakov S. V. Prakticheskiye raschety teplovoy izolyatsii promyshlennogo oborudovaniya i truboprovodov (Practical calculations of thermal insulation of industrial equipment and pipelines). Izd-vo Energiya, M. L., 1964.

11. Veynik A. I. Priblizhennyy raschet protsessov teploprovodnosti (Approximate calculation of processes of thermal conduction). Gosenergoizdat, M. L., 1959.

12. Lykov A. V. Teoriya teploprovodnosti (Theory of thermal conduction). Gostekhteorizdat, M., 1952.

APPENDIX

$\theta = f(Bi, Fo, r)$

$N = 0{,}2$

$\bar{r}$ \ Fo	0,02	0,05	0,10	0,20	0,50	1,0	2,0	5,0	10
					$Bi = 0{,}50$				
1,0	0,920	0,873	0,820	0,740	0,558	0,351	0,138	0,009	—
0,9	0,958	0,913	0,858	0,775	0,585	0,368	0,145	0,009	—
0,8	0,981	0,943	0,891	0,807	0,610	0,383	0,151	0,009	—
0,7	0,993	0,965	0,918	0,834	0,631	0,396	0,156	0,010	—
0,6	0,998	0,980	0,939	0,858	0,649	0,408	0,161	0,010	—
0,5	0,999	0,989	0,956	0,876	0,664	0,417	0,165	0,010	—
0,4	1,000	0,994	0,967	0,891	0,675	0,424	0,167	0,010	—
0,3	1,000	0,997	0,974	0,900	0,683	0,429	0,169	0,010	—
0,2	1,000	0,998	0,997	0,904	0,686	0,431	0,170	0,010	—

$\bar{r}$ \ Fo	0,01	0,02	0,05	0,10	0,20	0,50	1,0	2,0	5,0
					$Bi = 1{,}0$				
1,0	0,858	0,773	0,686	0,569	0,313	0,140	0,023	—	—
0,9	0,929	0,841	0,751	0,621	0,376	0,163	0,031	—	—
0,8	0,971	0,896	0,807	0,673	0,407	0,176	0,033	—	—
0,7	0,990	0,936	0,853	0,717	0,431	0,188	0,035	—	—
0,6	0,995	0,964	0,890	0,755	0,458	0,198	0,037	—	—
0,5	0,999	0,981	0,918	0,786	0,477	0,207	0,039	—	—
0,4	1,000	0,989	0,938	0,809	0,492	0,213	0,040	—	—
0,3	1,000	0,994	0,950	0,825	0,502	0,218	0,041	—	—
0,2	1,000	0,996	0,955	0,830	0,506	0,219	0,041	—	—
					$Bi = 2{,}0$				
1,0	0,801	0,732	0,613	0,501	0,368	0,160	0,041	0,001	—
0,9	0,924	0,856	0,726	0,597	0,440	0,192	0,049	0,001	—
0,8	0,979	0,934	0,817	0,682	0,507	0,221	0,056	0,001	—
0,7	0,995	0,975	0,885	0,756	0,568	0,248	0,063	0,004	—
0,6	1,000	0,992	0,932	0,816	0,621	0,272	0,069	0,004	—
0,5	1,000	0,998	0,962	0,863	0,665	0,292	0,074	0,005	—
0,4	1,000	1,000	0,980	0,897	0,699	0,308	0,078	0,005	—
0,3	1,000	1,000	0,989	0,919	0,721	0,318	0,080	0,005	—
0,2	1,000	1,000	0,992	0,927	0,730	0,322	0,081	0,005	—

ξ \ Fo	0,01	0,02	0,05	0,10	0,20	0,50	1,0	2,0	5,0
					$Bi = 5,0$				
1,0	0,602	0,501	0,360	0,256	0,157	0,042	0,005	—	—
0,9	0,841	0,721	0,531	0,382	0,235	0,063	0,007	—	—
0,8	0,956	0,868	0,677	0,500	0,311	0,084	0,009	—	—
0,7	0,991	0,948	0,792	0,606	0,383	0,103	0,012	—	—
0,6	0,999	0,983	0,874	0,696	0,448	0,121	0,014	—	—
0,5	1,000	0,995	0,929	0,769	0,503	0,136	0,015	—	—
0,4	1,000	0,999	0,962	0,823	0,546	0,148	0,017	—	—
0,3	1,000	1,000	0,979	0,858	0,575	0,156	0,018	—	—
0,2	1,000	1,000	0,985	0,871	0,586	0,159	0,018	—	—
					$Bi = 10$				
1,0	0,408	0,314	0,201	0,132	0,073	0,015	0,001	—	—
0,9	0,753	0,600	0,398	0,264	0,147	0,030	0,002	—	—
0,8	0,928	0,804	0,574	0,393	0,222	0,045	0,003	—	—
0,7	0,986	0,920	0,718	0,513	0,293	0,059	0,004	—	—
0,6	0,998	0,978	0,826	0,618	0,359	0,073	0,005	—	—
0,5	1,000	0,992	0,899	0,704	0,416	0,084	0,006	—	—
0,4	1,000	0,998	0,945	0,769	0,461	0,094	0,007	—	—
0,3	1,000	1,000	0,969	0,812	0,492	0,100	0,007	—	—
0,2	1,000	1,000	0,982	0,827	0,503	0,102	0,007	—	—
					$Bi = 50$				
1,0	0,104	0,071	0,041	0,025	0,013	0,002	—	—	—
0,9	0,372	0,416	0,248	0,154	0,078	0,012	—	—	—
0,8	0,667	0,695	0,447	0,284	0,146	0,022	0,001	—	—
0,7	0,973	0,869	0,621	0,413	0,214	0,032	0,001	—	—
0,6	0,998	0,955	0,757	0,529	0,277	0,041	0,002	—	—
0,5	1,000	0,987	0,854	0,626	0,333	0,050	0,002	—	—
0,4	1,000	0,996	0,917	0,702	0,378	0,057	0,002	—	—
0,3	1,000	0,998	0,952	0,752	0,408	0,061	0,003	—	—
0,2	1,000	1,000	0,963	0,771	0,420	0,063	0,003	—	—
					$Bi = 100$				
1,0	0,052	0,035	0,020	0,012	0,006	0,001	—	—	—
0,9	0,536	0,381	0,226	0,140	0,070	0,010	—	—	—
0,8	0,844	0,668	0,426	0,271	0,137	0,020	0,001	—	—
0,7	0,965	0,853	0,603	0,399	0,204	0,029	0,001	—	—
0,6	0,995	0,947	0,743	0,515	0,266	0,038	0,001	—	—
0,5	0,999	0,984	0,844	0,613	0,321	0,046	0,002	—	—
0,4	1,000	0,996	0,910	0,690	0,365	0,052	0,002	—	—
0,3	1,000	0,999	0,948	0,741	0,395	0,057	0,002	—	—
0,2	1,000	1,000	0,960	0,760	0,407	0,058	0,002	—	—
					$Bi = 0,50$				
1,0	0,944	0,920	0,873	0,819	0,733	0,523	0,307	0,104	0,004
0,9	0,979	0,958	0,912	0,857	0,767	0,554	0,322	0,109	0,004
0,8	0,994	0,981	0,943	0,889	0,795	0,572	0,334	0,113	0,004
0,7	0,999	0,993	0,965	0,915	0,821	0,593	0,344	0,116	0,004
0,6	1,000	0,998	0,979	0,934	0,839	0,605	0,352	0,119	0,005
0,5	1,000	0,999	0,987	0,946	0,851	0,615	0,357	0,121	0,005
0,4	1,000	1,000	0,990	0,950	0,855	0,618	0,359	0,121	0,005

$M = 0{,}4$

$\bar{r}$ \ Fo	0,01	0,02	0,05	0,10	0,20	0,50	1,0	2,0	5,0
					$Bi = 1{,}0$				
1,0	0,892	0,850	0,770	0,683	0,557	0,307	0,113	0,016	—
0,9	0,959	0,921	0,839	0,747	0,609	0,336	0,124	0,017	—
0,8	0,989	0,964	0,894	0,802	0,656	0,361	0,134	0,018	—
0,7	0,998	0,986	0,934	0,847	0,694	0,382	0,141	0,019	—
0,6	1,000	0,996	0,961	0,880	0,723	0,398	0,147	0,020	—
0,5	1,000	0,999	0,976	0,901	0,742	0,409	0,151	0,021	—
0,4	1,000	1,000	0,981	0,909	0,749	0,413	0,153	0,021	—
					$Bi = 2{,}0$				
1,0	0,801	0,732	0,613	0,499	0,352	0,128	0,024	0,001	—
0,9	0,924	0,856	0,726	0,594	0,420	0,152	0,028	0,001	—
0,8	0,979	0,934	0,817	0,677	0,481	0,174	0,032	0,001	—
0,7	0,996	0,975	0,884	0,746	0,532	0,193	0,036	0,001	—
0,6	1,000	0,992	0,930	0,799	0,572	0,207	0,038	0,001	—
0,5	1,000	0,998	0,957	0,832	0,598	0,217	0,040	0,001	—
0,4	1,000	0,999	0,966	0,845	0,607	0,220	0,041	0,001	—
					$Bi = 5{,}0$				
1,0	0,602	0,501	0,360	0,253	0,141	0,025	0,001	—	—
0,9	0,841	0,721	0,531	0,377	0,210	0,038	0,002	—	—
0,8	0,955	0,868	0,677	0,491	0,275	0,049	0,003	—	—
0,7	0,991	0,948	0,791	0,589	0,332	0,059	0,003	—	—
0,6	0,998	0,983	0,870	0,666	0,378	0,068	0,004	—	—
0,5	1,000	0,995	0,918	0,716	0,408	0,074	0,004	—	—
0,4	1,000	0,998	0,934	0,735	0,419	0,076	0,004	—	—
					$Bi = 10$				
1,0	0,412	0,314	0,201	0,129	0,062	0,007	0,000	—	—
0,9	0,753	0,600	0,397	0,258	0,123	0,014	0,000	—	—
0,8	0,928	0,804	0,574	0,381	0,183	0,021	0,001	—	—
0,7	0,986	0,921	0,716	0,490	0,236	0,027	0,001	—	—
0,6	0,998	0,973	0,820	0,578	0,280	0,032	0,001	—	—
0,5	1,000	0,993	0,883	0,636	0,309	0,035	0,001	—	—
0,4	1,000	0,997	0,905	0,657	0,320	0,036	0,001	—	—
					$Bi = 50$				
1,0	0,103	0,070	0,040	0,024	0,010	0,001	—	—	—
0,9	0,573	0,413	0,246	0,147	0,059	0,004	—	—	—
0,8	0,861	0,690	0,444	0,270	0,108	0,007	—	—	—
0,7	0,970	0,865	0,615	0,382	0,154	0,010	—	—	—
0,6	0,996	0,952	0,745	0,475	0,191	0,013	—	—	—
0,5	1,000	0,986	0,828	0,538	0,217	0,014	—	—	—
0,4	1,000	0,994	0,857	0,561	0,227	0,015	—	—	—
					$Bi = 100$				
1,0	0,051	0,035	0,020	0,012	0,005	0,001	—	—	—
0,9	0,535	0,381	0,225	0,133	0,052	0,003	—	—	—
0,8	0,845	0,668	0,425	0,255	0,100	0,006	—	—	—
0,7	0,966	0,853	0,599	0,367	0,144	0,009	—	—	—
0,6	0,993	0,947	0,732	0,460	0,180	0,011	—	—	—
0,5	0,999	0,984	0,817	0,523	0,205	0,012	—	—	—
0,4	1,000	0,993	0,848	0,546	0,215	0,013	—	—	—

$M = 0{,}6$

$\bar{r}$ \ Fo	0,005	0,01	0,02	0,05	0,10	0,20	0,50	1,0	2,0	5,0
					$Bi = 0{,}50$					
1,0	0,960	0,944	0,920	0,872	0,800	0,699	0,450	0,216	0,050	0,001
0,9	0,991	0,979	0,958	0,911	0,850	0,730	0,471	0,226	0,052	0,001
0,8	0,999	0,994	0,981	0,940	0,873	0,754	0,486	0,234	0,054	0,001
0,7	1,000	0,999	0,993	0,957	0,891	0,769	0,496	0,238	0,055	0,001
0,6	1,000	1,000	0,996	0,963	0,897	0,775	0,499	0,240	0,055	0,001
					$Bi = 1{,}0$					
1,0	0,923	0,892	0,850	0,768	0,667	0,506	0,222	0,056	0,004	—
0,9	0,983	0,960	0,921	0,837	0,727	0,552	0,242	0,061	0,004	—
0,8	0,998	0,989	0,964	0,888	0,771	0,587	0,257	0,065	0,004	—
0,7	1,000	0,998	0,985	0,920	0,804	0,610	0,267	0,067	0,004	—
0,6	1,000	0,999	0,991	0,931	0,814	0,618	0,270	0,068	0,004	—
					$Bi = 2{,}0$					
1,0	0,854	0,801	0,732	0,610	0,475	0,291	0,067	0,006	—	—
0,9	0,967	0,924	0,856	0,721	0,562	0,314	0,079	0,007	—	—
0,8	0,996	0,979	0,934	0,805	0,630	0,386	0,089	0,008	—	—
0,7	1,000	0,996	0,973	0,859	0,675	0,413	0,095	0,008	—	—
0,6	1,000	0,999	0,985	0,878	0,691	0,423	0,097	0,008	—	—
					$Bi = 5{,}0$					
1,0	0,690	0,602	0,501	0,355	0,224	0,090	0,006	0,000	—	—
0,9	0,927	0,841	0,721	0,521	0,329	0,133	0,009	0,000	—	—
0,8	0,992	0,955	0,868	0,655	0,416	0,168	0,011	0,000	—	—
0,7	1,000	0,991	0,945	0,744	0,474	0,191	0,013	0,000	—	—
0,6	1,000	0,998	0,968	0,775	0,495	0,200	0,013	0,000	—	—
					$Bi = 10$					
1,0	0,512	0,412	0,314	0,196	0,104	0,030	0,001	—	—	
0,9	0,879	0,751	0,600	0,384	0,205	0,059	0,001	—	—	
0,8	0,985	0,928	0,803	0,543	0,291	0,084	0,002	—	—	
0,7	1,000	0,986	0,915	0,650	0,350	0,101	0,002	—	—	
0,6	1,000	0,996	0,950	0,690	0,372	0,107	0,003	—	—	
					$Bi = 50$					
1,0	0,144	0,103	0,070	0,038	0,016	0,003	0,000	—	—	
0,9	0,746	0,573	0,413	0,228	0,096	0,017	0,000	—	—	
0,8	0,968	0,861	0,688	0,399	0,169	0,030	0,000	—	—	
0,7	0,993	0,970	0,855	0,521	0,221	0,040	0,000	—	—	
0,6	1,000	0,992	0,910	0,566	0,240	0,043	0,000	—	—	
					$Bi = 100$					
1,0		0,050	0,034	0,019	0,008	0,001	—	—	—	
0,9		0,536	0,381	0,206	0,084	0,014	—	—	—	
0,8		0,844	0,666	0,377	0,153	0,025	—	—	—	
0,7		0,965	0,841	0,499	0,203	0,034	—	—	—	
0,6		0,991	0,900	0,515	0,222	0,037	—	—	—	

$M = 0,9$

$\bar{r}$ \ Fo	0,005	0,01	0,02	0,05	0,10	0,20	0,50	1,0	2,0
				$Bi = 0,50$					
1,0		0,943	0,917	0,816	0,730	0,565	0,232	0,066	0,004
0,9		0,978	0,952	0,878	0,768	0,587	0,262	0,068	0,005
0,8		0,989	0,964	0,890	0,778	0,595	0,265	0,069	0,005
				$Bi = 1,00$					
1,0	0,923	0,892	0,844	0,722	0,556	0,331	0,069	0,005	—
0,9	0,983	0,958	0,909	0,778	0,599	0,356	0,075	0,006	—
0,8	0,996	0,979	0,932	0,797	0,615	0,365	0,076	0,006	—
				$Bi = 2,0$					
1,0	0,854	0,800	0,722	0,538	0,330	0,124	0,007	—	—
0,9	0,967	0,921	0,835	0,622	0,382	0,144	0,008	—	—
0,8	0,993	0,960	0,875	0,653	0,400	0,151	0,008	—	—
				$Bi = 5,0$					
1,0	0,691	0,601	0,483	0,261	0,093	0,012	—	—	—
0,9	0,927	0,834	0,678	0,366	0,131	0,017	—	—	—
0,8	0,984	0,914	0,751	0,405	0,145	0,019	—	—	—
				$Bi = 10$					
1,0	0,512	0,410	0,292	0,111	0,022	0,001	—	—	—
0,9	0,878	0,741	0,536	0,204	0,041	0,002	—	—	—
0,8	0,972	0,860	0,630	0,240	0,046	0,002	—	—	—
				$Bi = 50$					
1,0	0,146	0,101	0,057	0,010	0,001	—	—	—	—
0,9	0,745	0,549	0,312	0,058	0,003	—	—	—	—
0,8	0,933	0,732	0,420	0,078	0,005	—	—	—	—
				$Bi = 100$					
1,0	0,075	0,050	0,027	0,004	0,000	—	—	—	—
0,9	0,708	0,507	0,274	0,043	0,002	—	—	—	—
0,8	0,919	0,700	0,380	0,060	0,003	—	—	—	—

U. S. BOARD ON GEOGRAPHIC NAMES TRANSLITERATION SYSTEM

Block	Italic	Transliteration	Block	Italic	Transliteration
А а	*А а*	A, a	Р р	*Р р*	R, r
Б б	*Б б*	B, b	С с	*С с*	S, s
В в	*В в*	V, v	Т т	*Т т*	T, t
Г г	*Г г*	G, g	У у	*У у*	U, u
Д д	*Д д*	D, d	Ф ф	*Ф ф*	F, f
Е е	*Е е*	Ye, ye; E, e*	Х х	*Х х*	Kh, kh
Ж ж	*Ж ж*	Zh, zh	Ц ц	*Ц ц*	Ts, ts
З з	*З з*	Z, z	Ч ч	*Ч ч*	Ch, ch
И и	*И и*	I, i	Ш ш	*Ш ш*	Sh, sh
Й й	*Й й*	Y, y	Щ щ	*Щ щ*	Shch, shch
К к	*К к*	K, k	Ъ ъ	*Ъ ъ*	"
Л л	*Л л*	L, l	Ы ы	*Ы ы*	Y, y
М м	*М м*	M, m	Ь ь	*Ь ь*	'
Н н	*Н н*	N, n	Э э	*Э э*	E, e
О о	*О о*	O, o	Ю ю	*Ю ю*	Yu, yu
П п	*П п*	P, p	Я я	*Я я*	Ya, ya

* ye initially, after vowels, and after ъ, ь; e elsewhere. When written as ё in Russian, transliterate as yё or ё. The use of diacritical marks is preferred, but such marks may be omitted when expediency dictates.

FOLLOWING ARE THE CORRESPONDING RUSSIAN AND ENGLISH

DESIGNATIONS OF THE TRIGONOMETRIC FUNCTIONS

Russian	English
sin	sin
cos	cos
tg	tan
ctg	cot
sec	sec
cosec	csc
sh	sinh
ch	cosh
th	tanh
cth	coth
sch	sech
csch	csch
arc sin	$\sin^{-1}$
arc cos	$\cos^{-1}$
arc tg	$\tan^{-1}$
arc ctg	$\cot^{-1}$
arc sec	$\sec^{-1}$
arc cosec	$\csc^{-1}$
arc sh	$\sinh^{-1}$
arc ch	$\cosh^{-1}$
arc th	$\tanh^{-1}$
arc cth	$\coth^{-1}$
arc sch	sech^{-1}
arc csch	csch^{-1}
rot	curl
lg	log